ResearchOnline@JCU

This file is part of the following reference:

Lewis, Stephen Edward (2005) *Environmental trends in the GBR lagoon and Burdekin River catchment during the mid-Holocene and since European settlement using Porites coral records, Magnetic Island, QLD.* **PhD thesis, James Cook University.**

Access to this file is available from:

http://eprints.jcu.edu.au/1347

JAMES COOK
UNIVERSITY
AUSTRALIA

Environmental trends in the GBR lagoon and Burdekin River catchment during the mid-Holocene and since European settlement using *Porites* coral records, Magnetic Island, QLD.

Volume 1

Thesis submitted by
Stephen Edward Lewis
BSc (Hons) James Cook University
in December 2005

For the degree of Doctor of Philosophy
School of Earth Sciences
James Cook University

Statement of Access

I, the undersigned, author of this work, understand that James Cook University will make this thesis available for use within the University Library and, via the Australian Digital Theses network, for use elsewhere.

I understand that, as an unpublished work, a thesis has significant protection under the Copyright Act and I do not wish to place any further restriction on access to this work.

_____   _____
            Stephen Lewis   *Date*

Statement of Sources

Declaration

I declare that this thesis is my own work and has not been submitted in any form for another degree or diploma at any university or other institution of tertiary education. Information derived from the published or unpublished work of others has been acknowledged in the text and a list of references is given.

_____

Stephen Lewis   *Date*

Statement of the Contribution of Others

Stipend Support: School of Earth Sciences
CRC Reef

Supervision: Dr Graham Shields (JCU)
Dr Janice Lough (AIMS)

Editorial assistance: Dr Graham Shields, Dr Janice Lough, Dr Rosemary Dunn
Dr Jon Brodie, Dr Raphael Wüst

Laboratory assistance: Prof Balz Kamber, Dr Alan Greig

Analytical assistance: Advanced Analytical Centre
James Cook University, Townsville
Dr Kevin Blake, Mr Alan Chappell, Dr Sharon Ness

Australian Institute of Marine Science (AIMS)
Cape Ferguson, Townsville
Dr Janice Lough

ACQUIRE Laboratory
University of Queensland, Brisbane
Prof Balz Kamber, Dr Alan Greig

ANSTO laboratory
Lucas Heights, Sydney
Dr Henk Heinje, Dr Geraldine Jacobson, Dr Alan Williams

QHSS Laboratory
Cooper's Plains, Brisbane

University of Wollongong
David Wheeler

Field assistance: Jonathan Smalley, Barry Brown, Andrew Toy, Aaron Farrell,
Brian Christie, Michael O'Leary, Joanne Muller, Andrea
Sorbello, Michelle Cooper, Anne Gore, Dr Graham Shields

Financial support: CRC Reef
Australian Institute of Nuclear Science and Engineering
Australian Coral Reef Society
JCU Doctoral Research Scheme

Statistical support: David Donald
School of Mathematical and Physical Sciences

James Cook University
Dr. Yvette Everingham
School of Mathematical and Physical Sciences
James Cook University

Approximate project cost: $26,700

Use of infrastructure
external to JCU: Australian Institute of Marine Science

ACQUIRE Laboratory, University of Queensland

ACKNOWLEDGMENTS

Wow-wweeee!! It has been an amazing last 4½ years and now it is finally all over and done with. I still can't quite believe I have made it and I'm sure my family and friends also doubted from time to time (or <u>all</u> the time) if I would get there. Of course none of this work could have been done (*or done good*) without the love and support of my colleagues, family and friends and so here is my dedication to all of you lovely people!

First of all I need to thank my fantastic supervisors for putting up with me over the last few years: Graham Shields and Janice Lough. I have learnt so much from both of you and have treasured your advice, enthusiasm and encouragement throughout my entire project. The thesis (and my writing!) has improved immensely from your discussions and comments on numerous drafts. I'm sure you read these with some agony (some of which were better than others). I have been so very lucky to have two professionals to oversee the project and be so generous with your time. I can only hope that both of you are satisfied with the final product.

Next I have to say a whole-hearted thank you to Balz Kamber who without his analytical genius, loads of enthusiasm and generous laboratory support, it would have been a very different thesis indeed. I would also like to thank Alan Greig who, along with Balz, helped to produce the quality (and big!) dataset that is the cornerstone of this thesis. Thanks also to the Queensland Health Scientific Services (trace element analysis: John Hegarty and Henry Olszwey), the Advanced Analytical Centre (XRD, SEM and sample preparation: Alan Chappell, Kevin Blake, Yi Hu and Sharon Ness), the University of Wollongong (oxygen isotopes: David Wheeler), the Australian Nuclear Science Technology Organisation (C-14 dating: Henk Heinje and Geraldine Jacobson), Jian-Xin Zhao (ACQUIRE laboratory- TIMS U-Th dating), Darren Richardson (Thin sections-JCU) for the analytical support and the quality results. I really appreciated the hospitality, support and funding from AINSE, particularly Ben Thompson and Dennis Mather who made my stay in Sydney a very pleasant experience.

A massive thanks to all the people who read and commented on my thesis. In particular, I am forever indebted to Rosemary Dunn who showed me precise, effective writing and never once complained when I offloaded the big chapters at her office. I feel that my writing has greatly improved since I met Rosemary who showed me the "way with words". Thanks also to Jon Brodie, Raphael Wüst (Raphi) and of course Janice and Graham for their patience and time to read and correct my thesis.

Thanks to Duncan Irvine for letting me out on the site of the Nelly Bay Harbour development and proving me with the scientific and drilling reports. Duncan is also acknowledged for answering my email enquires on where the fossil corals were recovered. I am grateful to Ken Eade and Sonya Bryce from Maunsell for proving me with the earlier McInytre and Associates reports. Geoff Hansen kindly supplied (and scanned) the magnificent first geological map of Magnetic Island.

A sincere thanks to my lady for her patience and understanding when I was working late nights on the thesis and having little time for other more important things such as watching T.V and going to the movies. Seriously Andy- thanks heaps for your support and hopefully I will be able to spend a bit more "quality time at home" in the coming year. I am touched by the hospitality shown by Mario and Claudia Sorbello (and David, Megan and Ella) for letting me stay with Andrea while I was pulling together the final few chapters and letting me come down to the shop to enjoy the best coffee in the world! Thanks also to the girls: Shona, Lilly and Jasmine for keeping me company while I was busy working.

Last but certainly not least, a big thanks to my family and friends for their support and to motivate me through what turned into a "monster-sized" thesis. Also (with the exception of Dad) I appreciate not being regularly asked that bloody annoying question that people doing a PhD commonly receive. Thanks to Mum, Dad, Nana, Tony, Greg, Kristine, Agatha, Kaitlin and Monty. Also a special thanks to my Grandma who I know will be watching over me when I finally get to graduate.

Abstract

The extent of human influence on the Great Barrier Reef (GBR) is controversial but is essential to understand the environmental parameters of "healthy" inshore coral reefs before European settlement and the agriculturally-modified adjacent land catchments. To provide this evidence, core samples were taken from massive *Porites* corals from Magnetic Island and their annual skeletal growth bands were analysed for trace elements and oxygen isotope composition at sub-annual, 2 and 5 yearly sampling resolutions. This geochemical database was exploited to develop proxies of sea surface temperature (SST), seawater salinity, terrestrial runoff, land practices, sedimentation and turbidity. Data were obtained from four long-lived (~100 years) fossil mid-Holocene corals (~6,000 years old) and three modern coral cores, including one with a growth record from 1812-1986, a record which pre-dates European settlement in the region (c. 1850). In addition, the Holocene evolution of the Nelly Bay (Magnetic Island) reef was examined from C-14 dated sediment cores and biological sea-level indicators to construct a stratigraphic model of Nelly Bay. This model helps to investigate cause of the death for the fossil corals.

The mid-Holocene corals died around 5,790-6,150 calibrated (cal) years BP most probably from burial by terrigenous and biogenic sediments (sedimentation) due to a prograding reef flat. The fossil mid-Holocene corals contained sediment trapped within their final growth bands that was evident from elevated Th concentrations (>3 ppb), lower Y/Ho ratios ($<$ 40) and progressively "flatter" rare earth element and Y (REY) distributions. REY distributions indicate that the sediments within the fossil coral's skeleton came from the local (Nelly Bay) area rather than the Burdekin River catchment.

Sea level rapidly transgressed to + 1.0-1.5 m around 7,000-7,500 cal years BP and may have then oscillated up to four times before settling to its current position approximately 1,250 cal years BP. Sea-level in the region was reconstructed from C-14 ages of a fossil oyster bed from Magnetic Island and by compiling previous sea-level data from eastern Australia.

Average climate variability during the mid-Holocene was similar to the 1812-1986 coral record from the coral proxies of SST (Sr/Ca, Mg/Ca, U/Ca ratios and $\delta^{18}O$ composition). The Sr/Ca ratios in the 1812-1986 coral record were significantly correlated with the instrumental dataset from the central GBR at a 2 yearly sampling resolution, while the long-term averages of the other SST proxies agreed with the instrumental record. In addition, there were significant correlations between the coral Sr/Ca ratio and the coral calcification rate (a physical coral SST proxy) at the 2 and 5 yearly sampling resolutions.

Average seawater salinity (coral $\Delta^{18}O$) during the mid-Holocene was also similar to the 1812-1986 coral record. The $\Delta^{18}O$ record for the 1812-1986 coral showed relatively wetter conditions persisted from 1885-1935 and post-1970, while drier conditions prevailed between 1830-1885 and 1935-1970. These long-term trends agreed with the coral luminescence and the rainfall records and coincide with the Pacific Decadal Oscillation. However, correlations between the coral $\Delta^{18}O$ record and luminescence, rainfall and Burdekin River discharge were not significant, although the coral luminescence record was significantly correlated with rainfall in the Burdekin catchment and Burdekin River discharge records. The lack of correlation between coral $\Delta^{18}O$ and luminescence records indicates these proxies are recording different environmental signals. The 5 yearly resolution coral $\Delta^{18}O$ record reveals subtle, long-term variations in seawater salinity, whereas the luminescence record shows large, short-term variations in seawater salinity from rainfall and river discharge events.

The study supports the finding that sediment and colloidal export to the GBR have increased by 4-5 times in the Burdekin River catchment since the arrival of Europeans, based on coral Ba/Ca ratios, Y, Pr, Sm and Ho concentrations as well as REE distribution patterns in the 1812-1986 record. The Ba/Ca ratios and the Y, Pr, Sm and Ho concentrations were significantly correlated with cattle numbers in the Burdekin River catchment. However, previous claims that the additional sediment exported to the inshore GBR has resulted in an increase in turbidity levels are not supported by the coral Y/Ho ratio, a potential proxy of turbidity. In addition, negligible sediment has been trapped within the 1812-1986 coral skeleton, which was evident from low coral Th concentrations.

This finding indicates that the threat of sedimentation to the Magnetic Island's fringing reefs is low.

An excellent record of historical land-use in the adjacent Burdekin River catchment is provided by coral Mn concentrations. Mn levels in the corals record the establishment and growth of the sheep and cattle industries and provide an exceptional historical account of the development of land since European settlement.

This study has helped to establish a record of natural climate and environmental change on inshore coral reefs to provide a baseline of water quality conditions for "healthy" reef ecosystems. From this baseline, the study has been able to separate the natural variability on Magnetic Island's fringing reefs from the human influence and may assist decisions to manage land runoff to inshore reefs of the GBR.

TABLE OF CONTENTS

LIST OF TABLES

CHAPTER 7

CHAPTER 8

LIST OF FIGURES

CHAPTER 1

CHAPTER 2

CHAPTER 3

CHAPTER 4

CHAPTER 5

CHAPTER 6

CHAPTER 7

CHAPTER 8

Chapter 1

Introduction

1.1. Overview

Consensus has been reached that the health of coral reefs around the world is in decline, a concern that is widespread in the global community of reef researchers and those who depend on the reefs riches for their livelihood (e.g. Wilkinson, 2004; Buddemeier et al., 2004). The most recent *Status of coral reefs of the World 2004* reports that 20% of the world's reefs have been completely destroyed by coral bleaching, poor fishing practices and the degradation of landscapes adjacent to the reefs that may result in sedimentation and elevated concentrations of nutrients and pollutants in seawater (Wilkinson, 2004). These parameters, in turn, promote favourable conditions for outbreaks of algae, disease and crown of thorns starfish (Hughes, 1994; Bruno et al., 2003; Brodie et al., 2005a). In addition, a further 50% of reefs are threatened, not only by the aforementioned stresses, but by changes to global climate and the chemical composition of seawater (Wilkinson, 2004).

Of the coral reef ecosystems, the Great Barrier Reef (GBR) is considered to be one of the world's healthiest and best managed (Miller and Sweatman, 2004). However, the GBR is not immune to the local and global stresses that threaten the productivity of reefs worldwide. In fact, some studies have already reported serious degradation to the GBR (Pandolfi et al., 2003; 2005) including a reduction in coral cover (Bellwood et al., 2004), depleted macro-fauna (Miller and Sweatman, 2004), and changes in terrestrial runoff which effects the diversity of the inshore coral reefs (Fabricius et al., 2005). However, historical paleo-reconstructions of coral reef environments are limited, and the nature of the "pristine" GBR before the settlement of Europeans is largely unconstrained. This ignorance poses a significant problem for scientists as, without an established baseline, it is difficult to measure and assess the impact of recent changes to coral reef ecosystems.

Fortunately, growth records from massive corals can provide an independent perspective on environmental parameters that influence coral reefs. Long-lived corals growing in tropical, shallow marine waters can provide excellent proxies of sea surface temperature, seawater salinity, river discharge and sediment export from rivers (McCulloch et al., 1994; Gagan et al., 1998; 2000; McCulloch et al., 2003). Corals constantly secrete calcium carbonate from seawater to form their aragonitic skeleton. Subtle changes in the chemical makeup of this aragonite structure act as a record of the environmental conditions of the surrounding seawater. Coral proxy reconstructions provide a means of establishing a baseline from which changes to these environmental parameters can be quantified. X-ray records of coral slices reveal annual density bands (Knutson et al., 1972) which allow an accurate chronology to be constructed.

This study will reconstruct historical environmental change on the GBR using geochemical and physical proxies in massive, long-lived *Porites* coral records of modern and mid-Holocene age from Magnetic Island, north Queensland. The reliability of these proxies will be assessed and baseline environmental parameters such as sea surface temperature, seawater salinity, seawater chemistry, sedimentation and river runoff will be established using these corals. The Holocene evolution of the fringing reefs of Magnetic Island and the death of the fossil mid-Holocene coral heads will be examined. In addition, changes to these environmental parameters after the arrival of Europeans will also be investigated.

1.2. Climate change and runoff on the Great Barrier Reef

The health of the Great Barrier Reef (GBR) is under increasing pressure due to global warming (Hoegh-Guldberg, 1999), enhanced sediment and nutrient runoff (e.g. Moss, 1992; Fabricius and De'ath, 2001a; Furnas, 2003; Fabricius, 2005), sewage discharge (Bell, 1992; Koskela et al., 2004) and possibly more frequent Crown of Thorns Starfish outbreaks (Keesing et al., 1992; Pandolfi, 1992; Brodie et al., 2005a). Scientists face significant challenges to quantify anthropogenic influences in order to provide direction for future management of the GBR. Here I review the current state of knowledge on interpreted anthropogenic disturbance on the GBR, including rising water temperatures

(global warming), changing seawater chemistry and increased sediment and nutrient pollution as a result of poor land practices.

Rising water temperatures

Increased greenhouse gas concentrations in the atmosphere, associated with the combustion of fossil fuels and the reduction of carbon sinks, has been linked to a rapid and possibly unprecedented rise in global air temperature (Mann and Jones, 2003), which has risen by 0.62° C since 1901 (Jones et al., 1999). In fact, nine of the last ten years have been the warmest ever recorded since reliable instrumental temperature measurements began in 1856 (Fig 1.1; http://www.cru.uea.ac.uk). The warmest year was 1998, which coincided with a worldwide mass coral bleaching event that also significantly affected the GBR (Wilkinson, 1998; 2004; Berkelmans et al., 2004). "Greenhouse" related ocean warming has been observed along the waters of the GBR (Hoegh-Guldberg, 1999; Lough, 2001) and has been accompanied by a slight, but significant rise in global sea level (~ 1-2 mm per year; Houghton et al., 2001). Sea surface temperatures (SST) have increased on the GBR by up to 0.60° C in the southern parts; however, no apparent rise has been reported in the northern zone (Lough, 2001).
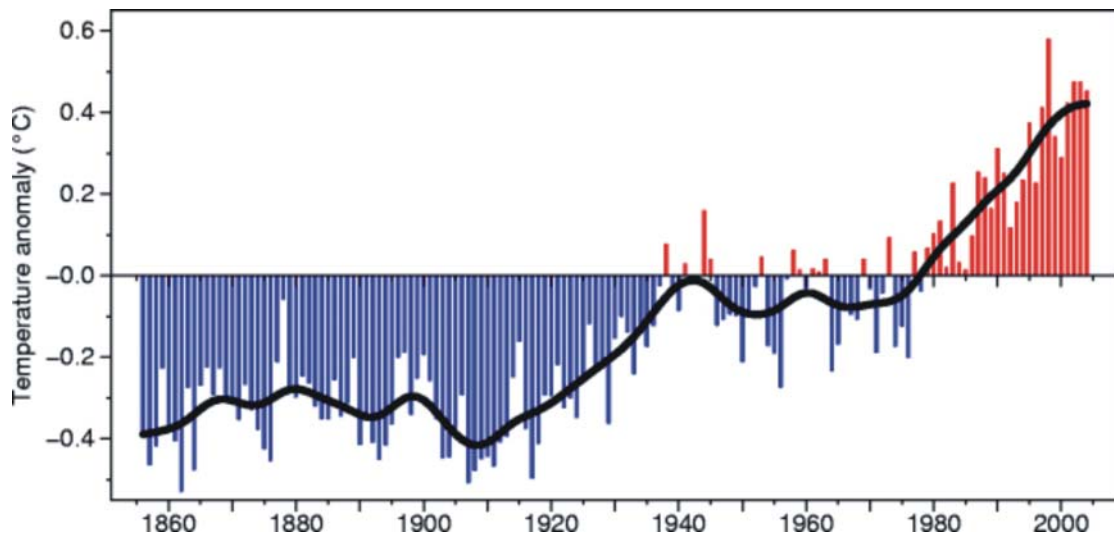
Figure 1.1. A compilation of global air and ocean temperature anomalies from 1856 indicates that a significant warming trend is evident over the last two decades and 9 out of the last 10 years are the warmest on record (from http://www.cru.uea.ac.uk). The rising temperatures have coincided with mass worldwide coral bleaching events and a continuation of this trend could have detrimental impacts on coral reefs (Wilkinson, 2004).

Coral reefs are particularly sensitive to rising water temperatures. Most reefs appear to live within 1-2° C of their upper thermal tolerance limit (e.g. Jokiel, 2004). The predicted increase of 1-3° C in tropical ocean temperatures by the end of this century (Houghton et al., 2001) would increase the frequency of coral bleaching events and significantly alter the makeup of coral reefs (Hoegh-Guldberg, 1999; Lough, 2000; Hughes et al., 2003). The GBR was considerably damaged by the 1998 and 2002 bleaching events, with 74.3% and 72.1% inshore and 20.9% and 41.0% offshore coral reefs affected, respectively (Berkelmans et al., 2004). The GBR corals are at most risk of bleaching during the summer season of warmest SSTs. At this time of year, several days of calm, clear sky conditions and reduced wind speeds can lead a to rapid increase in SST that exceeds the thermal threshold of the corals (Berkelmans and Oliver, 1999). It has been predicted that the GBR will be critically degraded by 2050 as a result of the increased frequency of coral bleaching if corals do not adapt to higher temperatures (Hoegh-Guldberg, 1999; Wooldridge et al., 2005).

Changing water chemistry

Elevated CO_2 levels absorbed into ocean waters as a result of the "Greenhouse effect" may lower seawater alkalinity and reduce the aragonite saturation state which, in turn, could lower coral calcification rates by up to 30% (Kleypas et al., 1999; Hoegh-Guldberg, 2005). However, this model did not consider the accompanying warming seawater temperatures, and a recent study has forecast that coral calcification rates may, in fact, increase by up to 35% by the end of this century (McNeil et al., 2004). Indeed, GBR coral calcification rates have increased in the late 20th century as the oceans warmed (Lough and Barnes, 2000). However, Kleypas et al. (2005) believe that the prediction of a 35% increase in coral calcification rates from warming temperatures by McNeil et al. (2004) is seriously flawed. They argue that the linear relationship between coral calcification and SST of Lough and Barnes (2000) would also be influenced by light and the aragonite saturation state. Moreover, the model of McNeil et al. (2004) does not take into account the effects of coral bleaching and assumes that corals will quickly adapt to the rapidly warming temperatures (Kleypas et al., 2005). McNeil et al.'s (2005) rebuttal argued that there was indeed a significant linear relationship between coral calcification and temperature and while light and the aragonite saturation state did affect calcification, temperature is, by far, the dominant influence on the coral calcification rate. They suggest that the key question is "can

organisms and ecosystems accommodate, acclimatise to, or adapt to rising temperatures faster than ocean temperatures may rise?" (McNeil et al., 2005). There is still much to learn about the impacts of changing ocean chemistry on not just corals but other marine calcifying organisms (The Royal Society, 2005).

A recent coral record from Flinders Reef (GBR) demonstrated that pH varied by up to 0.3 pH units (7.9-8.2) over the last 300 years (Pelejero et al., 2005). The pH fluctuations coincided with the Pacific Decadal Oscillation which occurs on a 50-70 year cycle (Pelejero et al., 2005).

Increased sediment and nutrient runoff

Terrigenious sediment runoff to the GBR is considered a major threat to the health of inshore coral reefs (e.g. Fabricius, 2005). Poor land management practices related to land clearing along coastal river catchments since European settlement have resulted in enhanced sediment erosion which, in turn, is exported to the GBR lagoon (e.g. Furnas, 2003). Models have predicted that sediment runoff to the GBR has increased by as much as 4 to 10 times since 1850 (Moss et al., 1992; Prosser et al., 2001; Neil et al., 2002; Furnas, 2003). It has recently been argued that turbidity levels may have risen along some inshore reefs as a result of this increased runoff (Fabricius and De'ath, 2001a; McCulloch et al., 2003; McCulloch, 2003; Fabricius et al., 2005). However, while most researchers agree that the sediment load from rivers has substantially increased since European settlement, many studies have suggested that this extra sediment would have a negligible effect on inshore turbidity levels due to the amount of sediment already available for resuspension (e.g. Larcombe and Woolfe, 1999a; Larcombe, 2001; Orpin et al., 2004). Suspended sediment concentrations on inshore coral reefs are controlled by the resuspension of bottom sediment from wind-generated wave stress (Larcombe et al., 1995a; Orpin et al., 1999).

Increased nutrient levels are also considered a major cause of deteriorating water quality on the inshore GBR. These nutrients are typically attached to clay particles in suspended sediments (particulate phase), or are in a dissolved phase in agricultural fertiliser runoff and sewage discharge (Furnas, 2003). Nitrogen and phosphorus concentrations have increased in the rivers draining into the GBR lagoon after 1850 (Furnas, 2003), and some nutrient levels may have doubled in the waters surrounding

certain inshore reefs (Moss et al., 1992; Muslim and Jones, 2003). In nutrient-rich waters, suspended sediments are known to aggregate and settle out as a sticky "marine snow", which can suffocate corals (Fabricius and Wolanski, 2000). Marked changes in the make-up of coral reefs have been discovered along water quality gradients (including sedimentation, turbidity and nutrients) from rivers draining into the GBR lagoon (van Woesik et al., 1999; Fabricius, et al., 2005). Enhanced seawater nutrient concentrations can also trigger Crown of Thorns Starfish outbreaks (Brodie et al., 2005a).

A recent paper has suggested that coral cover on the GBR has declined by as much as 50% over the last 40 years because of the "pressures" that have previously been identified (Bellwood et al., 2004). On the other hand, some researchers suggest that a monitoring program since 1986 indicates that the decline of coral cover is considerably lower than that found previously, and that individual reefs have experienced cycles of disturbance and recovery (Sweatman and Delean, 2005).

In summary

There is a range of real, perceived, current and potential threats to the well-being of the GBR. Observational evidence of the GBR ecosystem is limited to the past few decades and there is a need for longer-term records of variability and change on the GBR to assess the impact of current stresses produced by human activity. This study aims to examine the historical record for the central GBR from 5,700 to 6,300 years BP and from 1812 to 1986. A detailed record of climate and river runoff on the GBR which covers "snapshots" of the Holocene Epoch will help improve understanding of these complex systems and will help better predict their response to changes in climate and water quality. Records prior to 1850 are particularly pertinent as these provide an independent measurement of anthropogenically-induced change.

1.3. Previous related studies on Magnetic Island and mid-Holocene climates

Magnetic Island is situated approximately 5 km off the coast of Townsville, north Queensland (Fig. 1.2; 1.3). Townsville-Thuringowa is a major urban centre with a

population of approximately 150,000 (2001 census). The island (population ~3,000; 2001 census), a popular tourist destination, contains appreciable fringing coral reefs in several embayments (Collins, 1987).

The Ross and Burdekin Rivers are the main contributors of terrigenous sediment to Cleveland Bay (Fig 1.2; Carter et al., 1993). The Burdekin River dominates the terrigenous sediment supply to the inner Queensland shelf (Belperio, 1983), and strongly influences salinity conditions in the waters of Magnetic Island/Cleveland Bay (King et al., 2001). The small pocket beaches on Magnetic Island are largely replenished from local catchments draining into the adjacent headlands (Hopley, 1986).

Townsville has a major port, which began operation in 1865 (Pringle, 1996). Dredging is required regularly (~annually) to ensure that the shipping channel remains at an acceptable depth to facilitate large vessels (Hilliard and Raaymakers, 1996). The first record of dredging in the Townsville shipping channel was made in 1883 and, until recently, the dredged spoil has been dumped close to Magnetic Island (Pringle, 1989; 1996). The effect of channel dredging on the fringing reefs off Magnetic Island has aroused controversy for at least three decades. The dredging is believed to be the main contributing factor in the morphological transformation of Cockle Bay (Magnetic Island) from a sandy beach to a muddy mangrove-dominated environment (Pringle, 1996). Dredge spoil dumped to the east of the island may also be resuspended and transported onto the fringing reefs, resulting in significant increases of suspended sediments, nutrients, and heavy metal concentrations (Reichelt, 1993; Muslim, 1995) and ultimately causing reef degradation (Brown, 1972). However, other researchers have measured turbidity in Nelly and Geoffrey Bays and found no significant increase in suspended sediments following dredging activity (Larcombe and Ridd, 1994). The dominant influence on suspended sediment concentrations around Magnetic Island is wind speed and direction, which determines the quantity of sediment particles that become resuspended from the seafloor (Larcombe et al., 1995a).
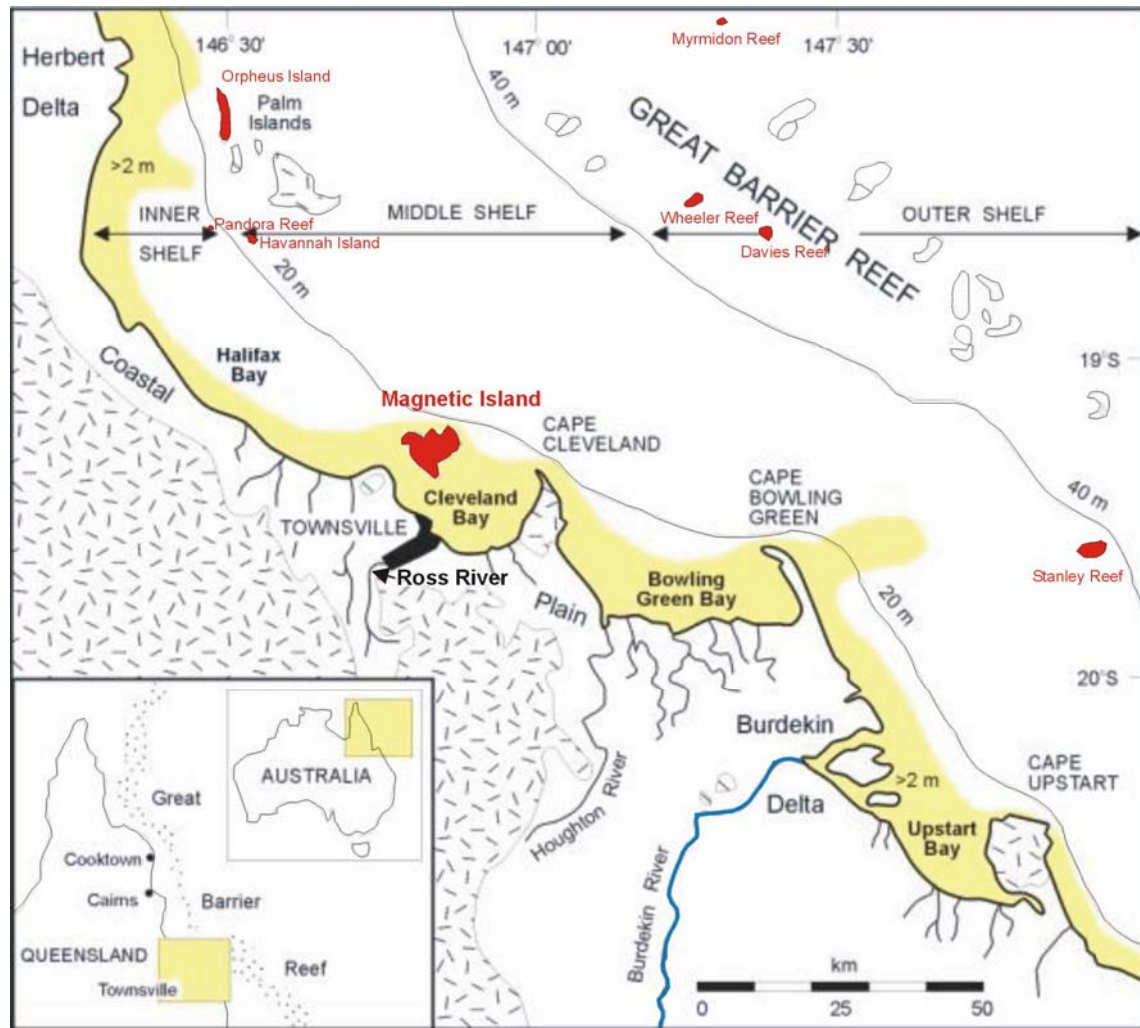
Figure 1.2. Regional map displaying the locations of Magnetic Island, Cleveland Bay and the Burdekin River as well as other islands and reefs of previous studies outlined in red. The shaded yellow region represents the coastal boundary layer of the GBR lagoon (Modified from Carter and Larcombe, 2002).

Water quality in Nelly Bay, located on the eastern side of Magnetic Island, has been studied by Brodie et al. (1992), Muslim (1995; Muslim and Jones, 2003) and Koskela et al. (2004). Nutrient levels have increased considerably over the last two decades (Muslim, 1995; Muslim and Jones, 2003) and have been attributed to sewage discharge into Gustav Creek, which drains into Nelly Bay (Koskela et al., 2004).

A marine harbour has recently been developed at Nelly Bay. Geotechnical reports from two companies involved in the project (McIntyre and Associates, 1986; 1989; Golder Associates, 2000) contain drilling and seismic data. The embayment has been studied from a geomorphological viewpoint (Smith, 1974); however, a detailed stratigraphic account incorporating sea-level fluctuations is lacking.

Previous mid-Holocene sea-level investigations on Magnetic Island include a study of fossil oyster beds (Balding Bay; Fig 1.3) located 1.65 m above the modern living beds. Radiocarbon ages from these fossil beds suggest that sea level was higher about 4-5 thousand years ago (Beaman et al., 1994; Higley, 2000). C-14 dating of fossil coral microatolls (Geoffrey Bay; Fig 1.3) has produced similar estimates for the mid-Holocene highstand (~ +1 m; Chappell et al., 1983; Chappell, 1983). Hopley et al. (1983) and Hopley and Partain (1987) investigated the development of the Geoffrey Bay reef flat from a series of jet probes, although no sediment cores were taken nor was C-14 dating performed to examine the age of this reef. Despite its close proximity to Townsville, James Cook University and other research centres, Magnetic Island still remains relatively unstudied from a paleo-climatic, water quality and sedimentological perspective.

Mid-Holocene paleo-climatic studies for north Queensland are limited and controversial. Studies of sea surface temperatures (SST) and salinities on a fossil coral colony from Orpheus Island (approximately 60 km north of Magnetic Island; Fig. 1.2) show that SSTs were slightly warmer than present about 5,300 years ago (Gagan et al., 1998). Contradictory SST data have been produced for the outer GBR shelf (Stanley Reef) and suggest that SSTs were cooler approximately 6,200 years BP. (Marshall, 2000; Marshall et al., 2000). Interestingly, mid-Holocene waters on the GBR were found to be more saline than today, and this increase has been attributed to the enhanced evaporation of seawater and the transportation to the higher latitudes (Gagan et al., 1998). Land-based records employing geomorphological evidence (Hopley, 1973; 1978) and pollen analyses (Kershaw, 1975a; Shulmeister, 1996) suggest that climates were warmer and wetter between 3000 and 6000 years ago.
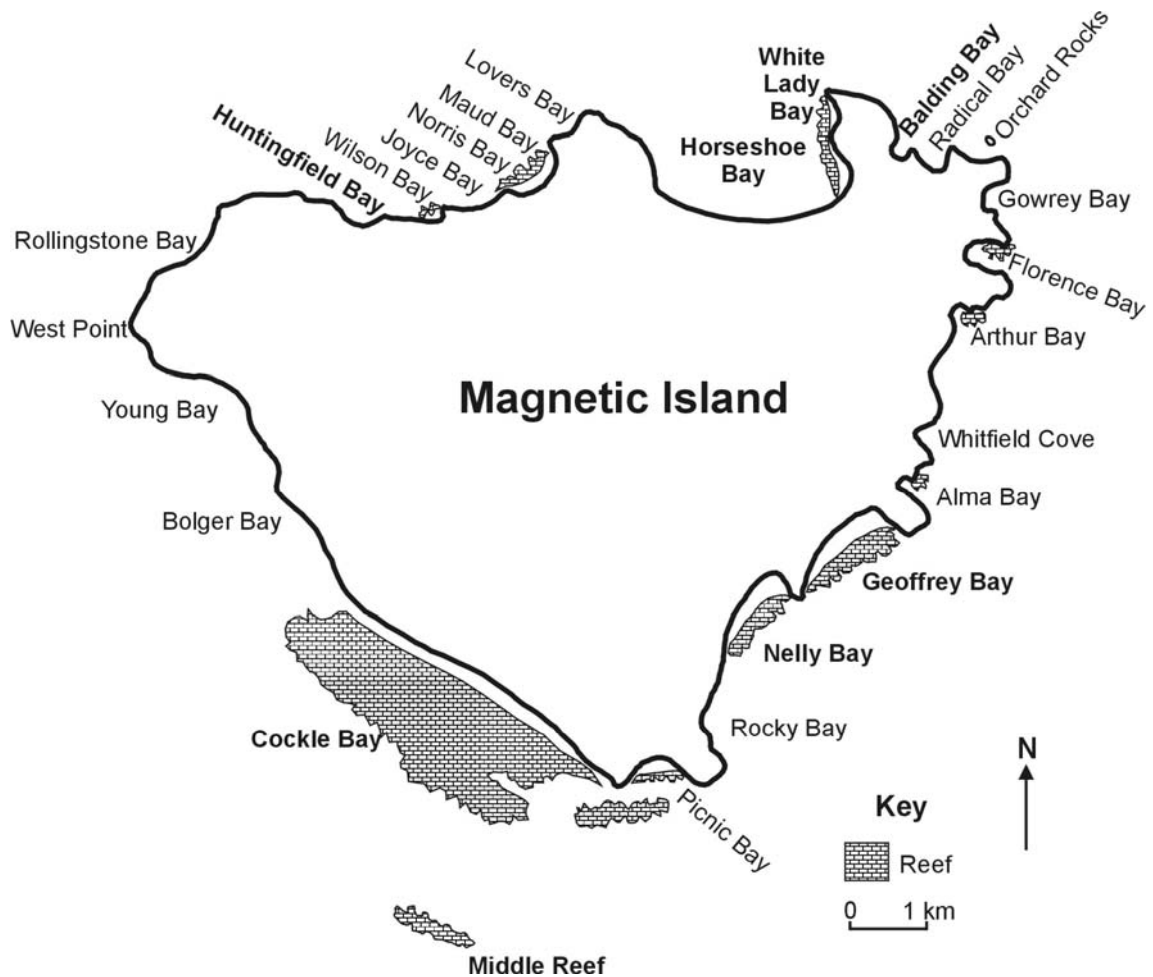
Figure 1.3. Map of Magnetic Island displaying the various embayments (Modified from Collins, 1987). Note in particular the locations of Nelly, Geoffrey, Balding, Huntingfield, Cockle, Horseshoe and White Lady Bays. Also note the location of Middle Reef.

1.4. Thesis outline

A valuable data resource has recently come to light with the recovery of eight large 2-3 m fossil *Porites* coral colonies of mid-Holocene age (Fig. 1.4) in Nelly Bay, Magnetic Island. These corals died around 5,630 and 5,620 ± 90 radiocarbon years BP (J. Chappell, personal communication, 2001) and each contain a growth record spanning about a hundred years. Additional modern coral colonies from Nelly and Geoffrey Bays have been cored. A long growth record (1812-1986) preserved in a modern coral core from Geoffrey Bay is particularly valuable as pre-1850 growth can be analysed to provide an assessment of water quality around the Magnetic Island/Cleveland Bay area prior to European colonisation.

The mid-Holocene and modern day corals enable comparative studies between the two periods. These corals provide the basis for this project which will:

1) Investigate the Holocene evolution of the Nelly Bay fringing reef with a particular focus on the environmental setting of the mid-Holocene corals.

2) Establish the cause of death of the mid-Holocene coral heads.

3) Examine whether the geochemical and physical coral proxies are correlated with instrumental records of SST, rainfall, river discharge and turbidity in the modern coral records.

4) Compare the climate and water quality conditions during the mid-Holocene with the modern coral records.

5) Investigate and quantify the magnitude of change in environmental characteristics using coral proxies after European settlement in the Burdekin River catchment (c. 1850).
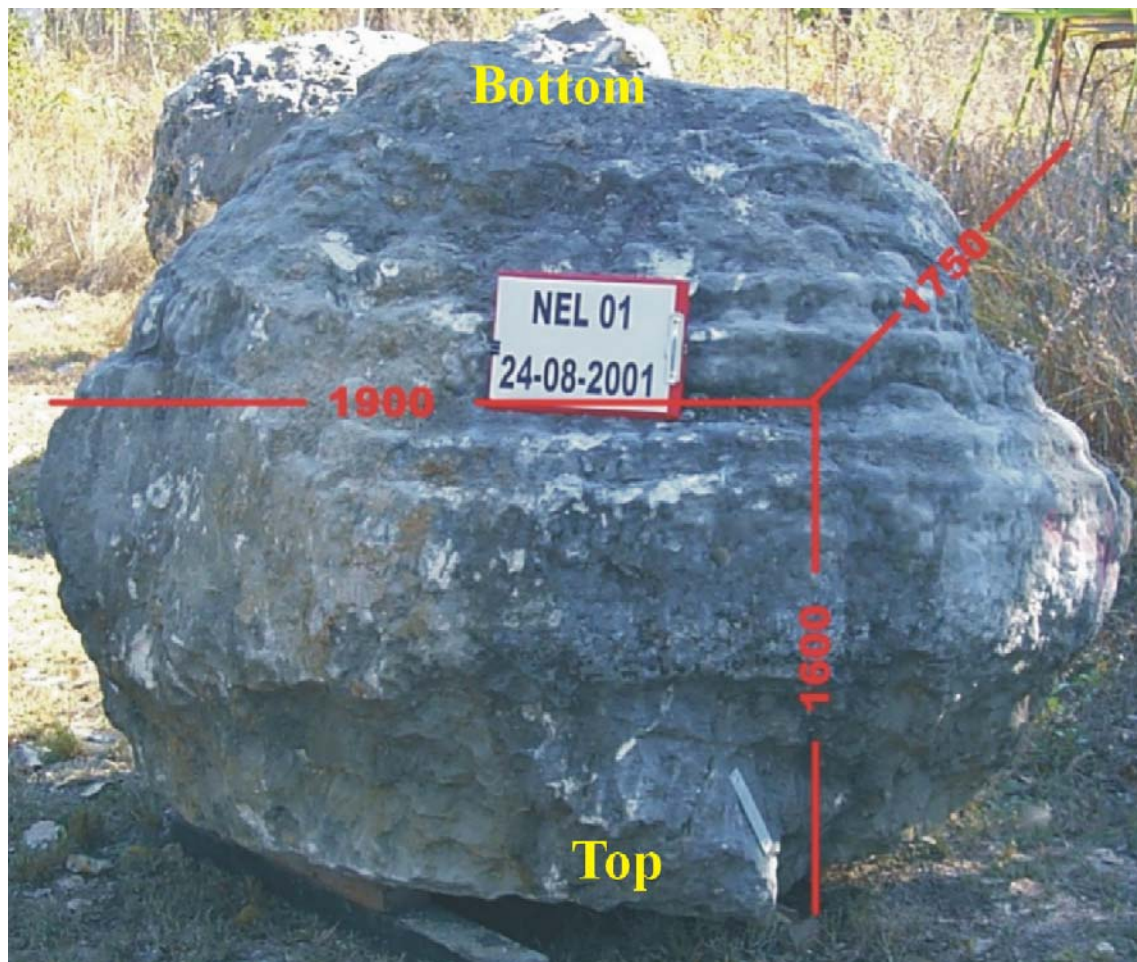
Figure 1.4. One of the 8 fossil *Porites* coral heads recovered from the Nelly Bay Harbour development. The coral grew between 5.70-6.10 thousand years B.P. Note that the coral head is upside down with regards to growth position. Scale is presented in millimetres. (Photo: AIMS).

The outline of this thesis is as follows:

- Chapter 2 reviews the current state of knowledge on the reliability of coral proxies of sea surface temperature (SST), seawater salinity (including rainfall and river discharge) and water quality (terrestrial runoff, nutrients, heavy metals).

- Chapter 3 provides a review of previous studies of the geomorphology and geology of Cleveland Bay, Holocene sea level for eastern Australia, Holocene climate for north Queensland and seawater quality on coral reefs. The local study area (Cleveland Bay) is the particular focus of this chapter, which includes a section on the history of dredging of the shipping (Platypus) channel and its effects on the fringing reefs of Magnetic Island.

- Chapter 4 describes the methodology used in the study, including the sedimentological investigations (e.g. sediment coring, sampling, dating) as well as the coral geochemistry (e.g. sample preparation, analysis).

- Chapter 5 presents new and recalibrated sea-level data and compiles C-14 dates of sediment cores to reconstruct the evolution of the Nelly Bay fringing coral reef and to examine the death of the mid-Holocene fossil coral heads.

- Chapter 6 presents the coral geochemistry proxies of SST, seawater salinity and water quality. In addition, micro-analytical studies of the modern and mid-Holocene corals are presented to investigate any possible diagenetic effects that would compromise the quality of the coral geochemical dataset.

- Chapter 7 discusses the coral geochemistry results from the climate proxies of SST and seawater salinity and discusses the reliability of these coral proxies.

- Chapter 8 examines the coral geochemistry results from the water quality proxies for river discharge, sedimentation, land use and turbidity. The chapter investigates the possible causes for the demise of the mid-Holocene corals and assesses the current threats to the modern fringing reefs of Magnetic Island. Possible environmental changes observed in the coral records since European settlement are also identified.

- Chapter 9 summarises the major findings of the study and discusses the potential for further investigations.

Chapter 2

Proxy climate and environmental records from corals

2.1. Chapter overview

Proxy climate and environmental records are essential to reconstruct high-resolution histories prior to instrumental records and to obtain a better perspective on the dynamics of past climate and environmental variability and change. High-resolution climate proxy tools have proven invaluable in extending the instrumental records and in reconstructing climate around the world over millennia. These include ice core records (for polar and high altitude settings), tree-ring records (temperate settings), documentary records (primarily from Europe and SE Asia) and, more recently, massive coral records (for tropical marine settings; e.g. Cronin, 1999). In particular, instrumental data from tropical environments is scant and, where available, dates only from the late 19th century. The landmark discovery of seasonal density bands in coral X-rays first highlighted the potential of corals to provide high-resolution records from tropical environments and to provide an accurate chronology (Knutson et al., 1972). The development of coral geochemical proxy records, combined with the advances in analytical techniques, has produced a rich archive of climatic information (see reviews in Gagan et al., 2000; Felis and Pätzold, 2003). High-resolution instrumental records of sea surface temperature (SST) for the central GBR and rainfall for north Queensland are only available from the 1870s, while discharge from the Burdekin River (the major plume to affect the fringing reefs of Magnetic Island) has been measured only since 1922. In addition, virtually no long-term instrumental data of water quality exists for the GBR. This chapter reviews the geochemical and physical coral proxies used in this study to reconstruct sea surface temperature, seawater salinity and water quality.

2.2. Sea surface temperature

2.2.1. Overview

The rich archive of geochemical records in massive corals provides several potential sources of information about past variations in SSTs. These include $\delta^{18}O$, Sr/Ca, Mg/Ca, U/Ca and annual calcification rate. Here, I critically evaluate each of these paleothermometers and outline potential problems for their application to the present study.

2.2.2. Oxygen isotopes

Oxygen isotopes are the most commonly used coral proxy in reconstructing long-term climatic records (e.g. Gagan et al., 2000; Felis and Pätzold, 2003). The $\delta^{18}O/\delta^{16}O$ isotopic ratio is influenced by both temperature and salinity and can also be used in combination with other temperature proxies to estimate freshwater influx (e.g. McCulloch et al., 1994; Gagan et al., 1998; see section 2.3.2). Therefore O isotopes, used to measure SST, are best applied on corals living in an area of relatively consistent salinity (Fig 2.1; Gagan et al., 1998; 2000).

The discovery of a significant linear relationship between the composition of $\delta^{18}O$ in inorganic calcite and SST first demonstrated the potential of O isotopes to reconstruct climates (McCrea, 1950) and this relationship also held true when applied to mollusc shells (Epstein et al., 1953). For every 1° C rise in seawater temperature, there is a 0.22‰ decrease in $\delta^{18}O$ in biogenic carbonate (Epstein et al., 1953). A similar relationship exists for coralline aragonite, and calibrations for 44 different coral genera were developed by Weber and Woodhead (1972). Since these early developments, O isotopes have been measured extensively in corals to produce long-term climatic records (reviewed in Gagan et al., 2000 and Felis and Pätzold, 2003). Long $\delta^{18}O$ coral records from around the world over matching timescales display comparable trends (Gagan et al., 2000; Evans et al., 2000). Similar relationships have been observed for several coral cores from the GBR (Hendy et al., submitted). High resolution (weekly to fortnightly) $\delta^{18}O$ measurements also display significant correlations with instrumental

SST in areas where seawater salinities remain constant (Fig 2.1; e.g. McCulloch et al., 1994; Gagan et al., 1998; 2000).

Two competing models have emerged to explain how the $\delta^{18}O$ composition of biogenic carbonate precipitates out of equilibrium from seawater (McConnaughey, 1989; 2003; Adkins et al., 2003). The first model proposes that $\delta^{18}O$ in corals is secreted out of equilibrium with seawater by a kinetic vital effect caused by CO_2 hydration or hydroxylation (McConnaughey, 1989; 2003). There is an incomplete isotopic equilibrium between dissolved inorganic carbonate and seawater. The pH of seawater controls the balance between these two processes and the linear relationship varies for each genus of coral (McConnaughey, 1989; 2003). The second model places emphasis on the role of a thermodynamic vital effect, where pH is thought to strongly influence the carbonate ion concentration and hence the $\delta^{18}O$ of the pool of carbonate species (Adkins et al., 2003).
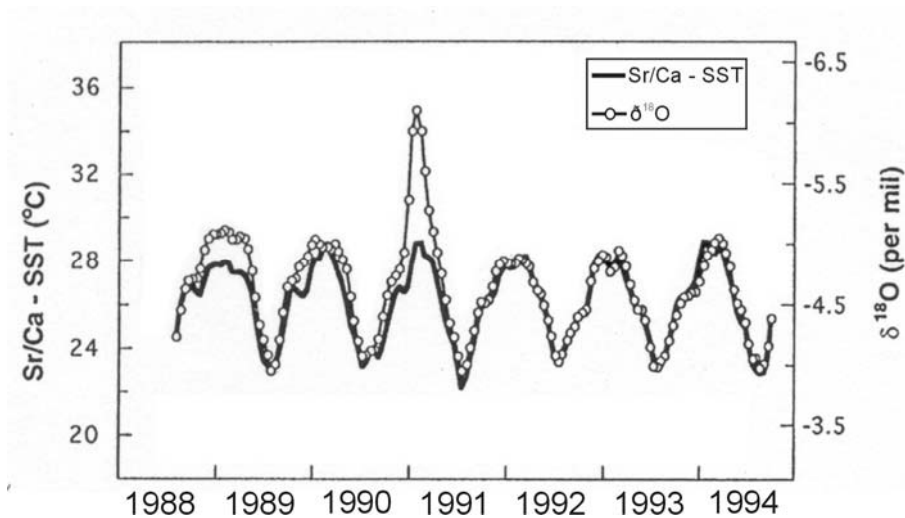
Figure 2.1. O isotopes are a reliable proxy for reconstructing SST. O isotopes closely correlate with Sr/Ca ratios in a coral from Orpheus Island (from Gagan et al., 1998).

A long-term experiment was conducted in the Gulf of Aqaba where several coral colonies living in 6 m of water were transported to a depth of 40 m (Rosenfeld et al., 2003). After 10 years a colony was recovered and $\delta^{18}O$ was measured at high resolution. At the shallow water level, the $\delta^{18}O$ variations were closely correlated to SST; at the deeper water level, extension rates became much lower and a large range in $\delta^{18}O$ was discovered that was not related to SST. This result suggested that a

kinetic/vital effect is much greater at depth where photosynthesis is poorer due to lower light intensities (Rosenfeld et al., 2003). Anomalously high $\delta^{18}O$ values are common in corals that have relatively low extension rates of <0.6 cm per year (Felis et al., 2003). Therefore, corals with extension rates >0.6 cm per year are best for reconstructing SST, and a correction should be applied if coral extension rates are less than 0.6 cm per year (Felis et al., 2003).

The O isotope-SST relationship may break down when corals are exposed to thermal stress. Some corals from the Pacific Ocean did not record the full temperature range during the 1982-83 El Niño/bleaching event and stress bands were found on the corals analysed during this period by Wellington and Dunbar (1995). Therefore, corals that regularly experience stressful conditions should be avoided for climatic reconstructions.

Despite these potential problems, the O isotope is currently the most commonly used climatic proxy and, unlike the trace element SST proxies, is relatively unaffected by calibration and analytical errors, biological effects and calcite replacement (summarised in Table 2.1). In addition, there is little variation in the O isotope-SST calibration curves for corals on a global scale compared to the other geochemical SST proxies (e.g. Evans et al., 2000).

2.2.3. Sr/Ca ratios

Coral Sr/Ca ratios are considered the most reliable proxy for reconstructing SSTs. The technique was first demonstrated by Smith et al. (1979), who discovered that corals incorporate more Sr into their aragonite skeleton as seawater becomes cooler. However, it was not until the development of thermo-ionisation mass spectrometry (TIMS) that small sample sizes could be analysed at the precision required to correlate coral Sr/Ca ratios with instrumental SST (Fig 2.2; Beck et al., 1992). More recently, the development of laser ablation inductively coupled plasma-mass spectrometry (LA-ICP-MS; Sinclair et al., 1998; Fallon et al., 1999) and atomic emission spectrometry (ICP-AES; Schrag, 1999) techniques have also been used to link coral Sr/Ca ratios with SST. To correct for instrumental drift during ICP-AES analysis, a reference solution was analysed between individual samples (Schrag, 1999). This technique significantly improves analytical precision/reproducibility (RSD) within 0.2%. The ICP-AES (or

ICP-MS) technique is beneficial as it is inexpensive to produce large datasets, requires minimal sample preparation and also has the capacity to run large numbers of samples over short timeframes (Schrag, 1999).
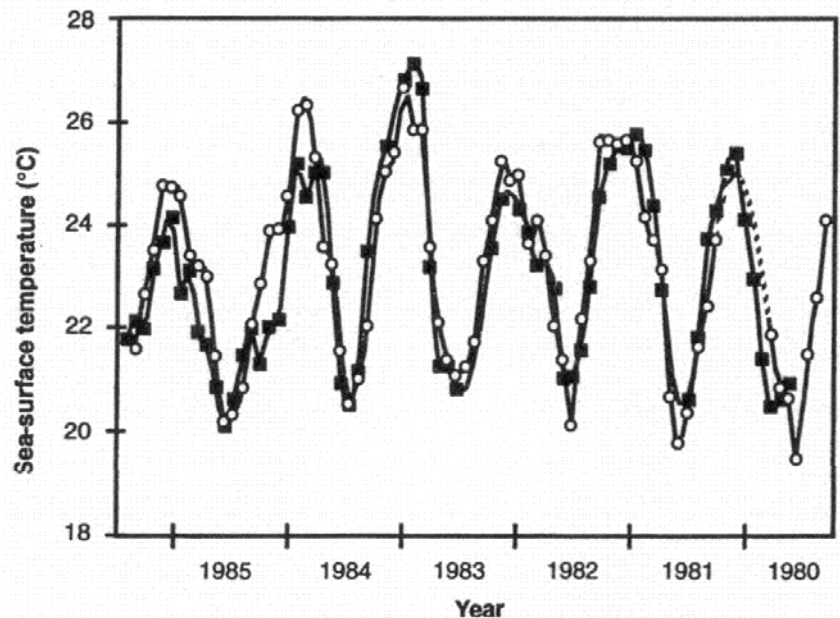
Figure 2.2. Coral Sr/Ca ratios (closed squares) have proven to be a reliable proxy for reconstructing SST in a coral from New Caledonia (instrumental SST- open circles; from Beck et al., 1992).

The slopes of the coral Sr/Ca-SST calibration curves developed around the world are similar for most hard corals, although the intercepts can be considerably offset (Fig 2.3a). This offset may be linked to different environmental influences such as cross-shelf gradients between inshore and offshore corals (Marshall and McCulloch, 2002), different coral genera/species (Smith et al., 1979), different light intensities (Cohen et al., 2001; Reynaud et al., 2004), different photosynthetic activities of symbiotic zooxanthellae (Cohen et al., 2002), and tidal influences (Cohen and Sohn, 2004). In addition, the Sr/Ca-SST calibration may be affected by analytical and sampling techniques. There is a marked difference between the intercepts from a *Porites* coral calibrated from the inshore zone of the GBR (Orpheus Island; Gagan et al., 1998) compared with the calibration curves produced for *Porites* growing on the outer shelf (Davies, Myrmidon and Stanley Reefs; Alibert and McCulloch, 1997; Marshall and McCulloch, 2002; Fig 2.3b). However, a Sr/Ca-SST calibration curve also from an inshore Orpheus Island coral using the LA-ICP-MS technique closely corresponds to the curve intercepts from the outer GBR (Fallon et al., 2003; Fig 2.3b). The slopes of

the calibration curves using TIMS and LA-ICP-MS techniques differ significantly. This offset may reflect the better precision of the TIMS method. Some of the Sr/Ca-SST calibrations may have been produced using juvenile corals, which might respond differently from their mature counterparts (Marshall and McCulloch, 2002).
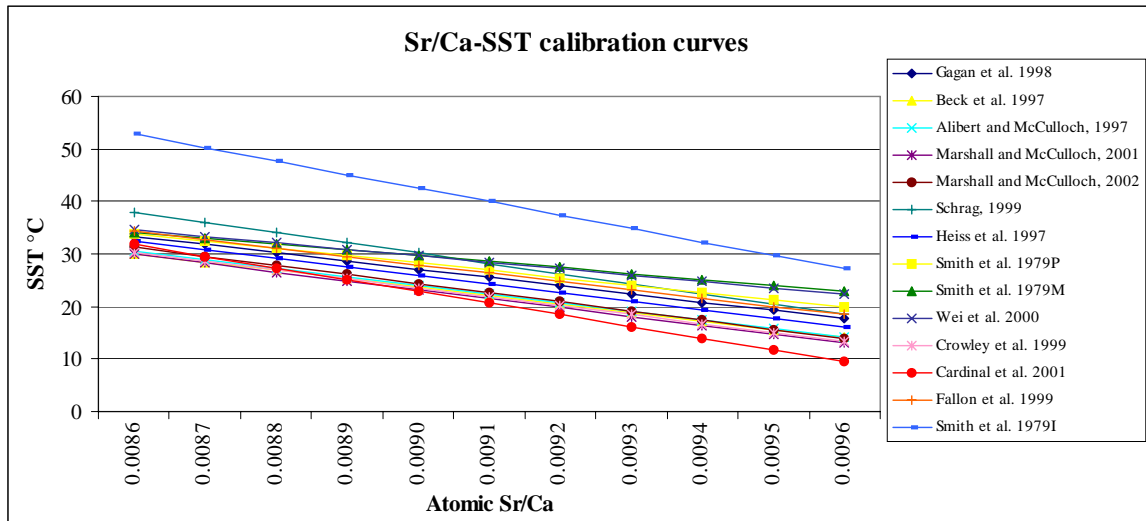
Figure 2.3 (a). The available Sr/Ca-SST calibration curves published in the scientific literature. Most curves follow a similar slope; however, the intercepts may vary. Gagan et al. (Orpheus Island); Beck et al. (New Caledonia); Alibert and McCulloch, (Davies Reef); Marshall and McCulloch, 2001 (Christmas Island); 2002 (Myrmidon Reef); Schrag (Galapagos Islands); Heiss et al. (Indian Ocean); Smith et al. 1979P (*Pocillopora*); M (*Montipora*); I (inorganic aragonite); Wei et al. (Hainan Island); Crowley et al. (New Caledonia); Cardinal et al. (Diploria); Fallon et al. (Japan). Note: all coral genera are *Porites* unless specified.
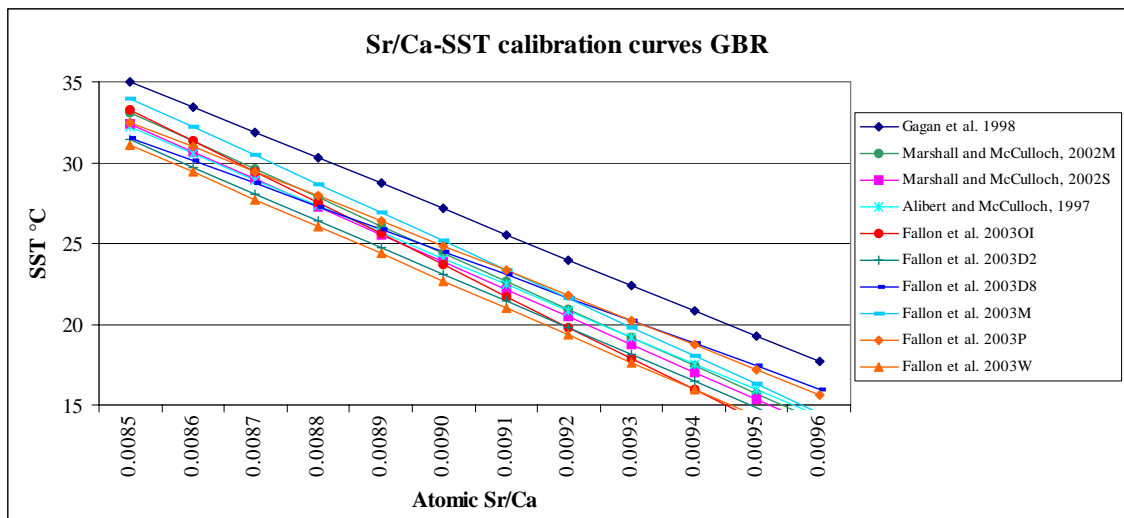
Figure 2.3 (b). Sr/Ca-SST curves produced for *Porites* corals from the GBR. The Sr/Ca calibration curve may be different for corals from the inshore zone (Orpheus Island Gagan et al.) in comparison with the outer GBR (Davies Reef- Alibert and McCulloch; Myrmidon Reef- Marshall and McCulloch, 2002M; Stanley Reef- Marshall and McCulloch, 2002S). However, recent work by Fallon et al. (2003; LA-ICP-MS), suggests that the SST calibrations are similar throughout the GBR. Note Fallon et al. 2003OI (Orpheus Island); 2003D2; D8 (Davies Reef); 2003M (Myrmidon Reef); 2003P (Pandora Reef); 2003W (Wheeler Reef). Also note the difference between the two calibrations produced for Orpheus Island by the TIMS and LA-ICP-MS techniques.

Despite the widespread use of coral Sr/Ca ratios, several potential problems have been identified that may limit the effectiveness of the ratio as a paleothermometer. The Sr/Ca record could be affected by sampling procedures, extension/calcification rates, light/solar radiation, extreme temperatures, fresh water runoff, excess nutrients and diagenesis (summarised in Table 2.1). The incorporation of Sr into the coral skeletal lattice is poorly understood and the Sr/Ca ratio may not provide an independent measurement of SST (Allison et al., 2001; Cohen et al., 2001).

Careful sampling along the major growth axis is required for accurate measurements of the coral Sr/Ca ratio (Fig 2.4). Failure to sample along this axis can result in an underestimation of the Sr/Ca-SST calculation relative to the instrumental record (Alibert and McCulloch, 1997). Microanalyses of the coral's daily growth revealed heterogeneity in the Sr/Ca ratio that cannot be completely attributed to SST (Allison, 1996; Allison et al., 2001; Cohen et al., 2001; Meibom et al., 2003; Allison et al., 2005; Sinclair, 2005a).

Coral Sr/Ca ratios sampled during nighttime growth displayed a significant correlation with SST over a 1 year period. Daytime growth, however, appeared to be strongly influenced by both SST and the photosynthesis of symbiotic zooxanthellae (Cohen et al., 2001). A study involving two cold water symbiont and non-symbiont-bearing corals from New England revealed that the Sr/Ca ratio in the non-symbiont-bearing coral was primarily controlled by SST. However, only 35% of the Sr/Ca ratio could be attributed to temperature in the symbiont-bearing coral (Cohen et al., 2002). A comment on this paper by Schrag and Linsley (2002) acknowledged that the mechanisms involving the fractionation of Sr into the coral lattice are poorly understood. Despite these potential problems, the Sr/Ca ratio is a reliable paleothermometer as previous studies have demonstrated the significant relationship between the coral Sr/Ca ratio and instrumental SST records. The systematics in cold water corals could be different from corals growing in tropical climates (Schrag and Linsley, 2002). There is also doubt about the age of the corals analysed. Juvenile corals should be avoided in SST reconstructions as they are known to produce dubious results (Marshall and McCulloch, 2002). Sr/Ca ratios incorporated in corals are resistant to various chemical leaches which suggest that the ratio is relatively homogenous in the coral skeleton (Watanabe et al., 2001; Mitsuguchi et al., 2001).
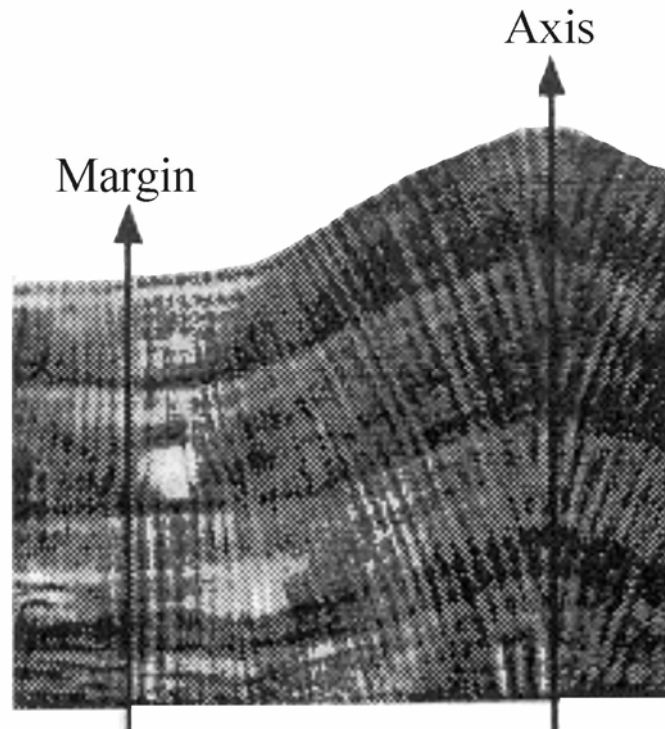
Figure 2.4. It is important that corals are sampled along the major growth axis. Sampling along the margins may produce inaccuracies in SST estimations by as much as -3° C (from Alibert and McCulloch, 1997).

The Sr/Ca ratio varied significantly in corals with changing light intensity in tanks of identical water temperatures (Reynaud et al, 2004). Therefore, corals that receive variable light in environments of relatively high turbidity or depth may not provide reliable estimates of SST or produce different Sr/Ca-SST calibration curves. In addition, the coral Sr/Ca ratio may, in fact, be more closely related to the intensity of solar radiation (Esslemont et al., 2004). However, the Sr/Ca-SST relationship has been significantly correlated with instrumental SST at weekly resolution (e.g. McCulloch et al., 1994; Gagan et al., 1998).

The Sr/Ca ratio may also be affected by extension/calcification rates, biological controls on the uptake of Sr in the coral skeleton, and the Sr/Ca composition of seawater (deVilliers et al., 1994; 1995; Stoll and Schrag, 1998; reviewed in Marshall and McCulloch, 2002). Additional studies reveal that extension/calcification rates have no effect on the Sr/Ca ratios (e.g. Alibert and McCulloch, 1997; Gagan et al., 1998) and that the discrepancies discovered in the studies of deVilliers et al. (1994; 1995) can be

explained simply by failure to sample along the major growth axis (Marshall and McCulloch, 2002).

Sr/Ca ratios incorporated in corals behave differently when subjected to temperature-induced stress (McCulloch et al., 1994). *Porites* corals cease to grow when seawater temperatures drop below 18° C (Fallon et al., 1999) or exceed 32° C (Marshall and McCulloch, 2002). Corals become increasingly stressed as temperatures approach these extremes and the Sr/Ca-SST relationship has been known to break down. One coral from Pandora Reef, central inshore GBR, failed to record the anomalously high temperatures during the El Niño summer of 1997-1998 (Marshall and McCulloch, 2002). However, other corals from the GBR recorded higher than average SST (30-31°C) during the 1998 bleaching event (McCulloch et al., 2000).

Freshwater runoff might also disturb the Sr/Ca-SST relationship (deVilliers et al., 1994; Wei et al., 2000). However, Sr/Ca ratios analysed in corals regularly subjected to freshwater influxes still conform to instrumental measurements of SST (e.g. Gagan et al., 1998).

Another influence on the Sr/Ca-SST relationship may be excessive seawater nutrient concentrations (Marshall and McCulloch, 2002). Elevated nutrient concentrations in seawater can place corals under considerable stress and significantly reduce calcification rates (e.g. Kinsey, 1988; Rasmussen, 1994), but their effect on the Sr/Ca paleothermometer is relatively unknown. Long-lived coral records from Low Isles (Port Douglas) displayed a significant decline in Sr (average of 7550 ppm in 1939 compared with 6650 ppm in 1984) and skeletal density, coinciding with increased seawater phosphorus concentrations related to superphosphate use along the Barron River after the 1950s (Rasmussen, 1988a; 1988b). However, the results were produced using low sampling resolution with relatively low analytical precision, and it is distinctly possible that the decline in Sr concentrations may be an artefact of natural Sr/Ca-SST variations, and not of elevated seawater nutrient concentrations.

Coral diagenesis can produce significant errors in SST estimations obtained from Sr/Ca ratios (Bar-Matthews et al., 1993; Enmar et al., 2000; Müller et al., 2001; McGregor and Gagan, 2003). Secondary aragonite can precipitate into coral pores and produce

errors of up to 2° C lower than the instrumental SST measurements (Enmar et al., 2000). McGregor and Gagan (2003) examined the diagenetic effects of varying amounts of calcite replacement on the Sr/Ca paleothermometer and found that calcite replacement caused a marked decrease in the Sr/Ca ratios equivalent to a 1.1 to 1.5° C rise per percent in calcite.

Table 2.1. The potential problems that have been identified in the literature for the various thermometers.

Potential problem	Sr/Ca ratio	Mg/Ca ratio	U/Ca ratio	O isotopes
Calibration curves	Significant problem- different calibrations can offset SST estimates by up to 3° C (see Fig 7.1). Sr/Ca-SST calibration could vary for different species- but is relatively unstudied for the one location.	Significant problem- calibration curves are significantly different with H_2O_2 treatment procedure. Significant offsets have been observed between inshore and offshore zones (Fallon et al., 2003). Could potentially be offset for different species and is unstudied at the one locality.	Significant problem- calibration curves can vary depending on the analytical technique. Significant offsets have been observed between inshore and offshore zones (Fallon et al., 2003). Could potentially be offset for different species and is relatively unstudied at the one locality.	Calibration curves produced for *Porites* produce similar SST estimates.
Failure to sample along the major growth axis	Significant problem- can offset SST estimates by up to -3° C (Alibert and McCulloch, 1997). Unlikely to be a major problem in this study, but can not be ruled out for some individual samples	Significant problem- more Mg is concentrated towards the centre of calcification (Meibom et al., 2004). Could have a large effect on SST reconstructions if not H_2O_2 treated (Watanabe et al., 2001).	Not studied, but possibly a significant problem	Not identified as a significant problem
Biological/metabolic effects	Significant at microscale (Cohen et al., 2002; Meibom et al., 2003). However the SST relationship seems to work as low as weekly resolutions. Unlikely to pose a significant problem in this study.	Significant problem- organic material in skeleton can produce significant offsets in SST estimates. May be problem for the non-H_2O_2 treated (organics not removed) two-monthly resolution and 2 yearly sampling resolutions employed in this study.	Not studied, but similar problems to the coral Mg/Ca ratio are possible.	Not identified as a significant problem
Analytical error	Problems depend on the technique used. Considered a significant problem for the two-monthly and 2 yearly sampling resolutions in this study (precision= ± 0.65° C compared to ± 0.32° C for 5 yearly resolution).	Problems depend on technique used. Generally considered not as significant a problem compared to the Sr/Ca ratio.	Problems depend on technique used. Generally considered not as significant a problem compared to the Sr/Ca ratio.	Most instruments appear to produce acceptable precisions for SST reconstructions
Sampling resolution	Could potentially contribute to fine-scale analytical uncertainty for the 2 yearly resolution record in this study (e.g. by sampling 1.5 years instead of 2 years produces an error of approx 0.41° C). Minor errors perceived for the 5 yearly sampling resolution. High-resolution sampling may produce bias towards the faster growing summer months.	Could potentially contribute to fine-scale analytical uncertainty for the 2 yearly resolution record in this study (e.g. by sampling 1.5 years instead of 2 years produces an error of approx 0.41° C). Minor errors perceived for the 5 yearly sampling resolution. High-resolution sampling may produce bias towards the faster growing summer months.	Could potentially contribute to fine-scale analytical uncertainty for the 2 yearly resolution record in this study (e.g. by sampling 1.5 years instead of 2 years produces an error of approx 0.41° C). Minor errors perceived for the 5 yearly sampling resolution. High-resolution sampling may produce bias towards the faster growing summer months.	Minor errors are associated with the 5 yearly sampling resolution. High-resolution sampling may produce bias towards the faster growing summer months.
Statistical errors	Identified to potentially produce errors in the calibration curves (Solow and Huppart, 2004). Not perceived as a significant problem in this study	Could potentially produce errors in the development of calibration curves. Not perceived as a significant problem in this study.	Could potentially produce errors in the development of calibration curves. Not perceived as a significant problem in this study.	Could potentially produce errors in the development of calibration curves. Not perceived as a major problem in this study.
Juvenile corals	Identified to potentially produce errors in the calibration curves (Marshall and McCulloch, 2002). Could affect the first ten years of coral growth.	Has the potential to produce errors in the calibration curves. Could affect the first ten years of coral growth.	Has the potential to produce errors in the calibration curves. Could affect the first ten years of coral growth.	Has the potential to produce errors in the calibration curves. Could affect the first ten years of coral growth.

Table 2.1 (continued). The potential problems that have been identified in the literature for the various thermometers.

Potential problem	Sr/Ca ratio	Mg/Ca ratio	U/Ca ratio	O isotopes
Freshwater influx	Not considered a significant problem for the Sr/Ca ratio (e.g. Gagan et al., 1998).	Perceived to be a significant problem by many authors, but largely unstudied.	Perceived problem as U is thought to substitute in the carbonate ion and may be affected by changes in pH related to salinity (Shen and Dunbar, 1995).	Has a significant influence on SST reconstructions in waters of varying salinity (e.g. Gagan et al., 1998). Significant problem in this study.
Diagenetic effects	The presence of secondary aragonite can produce inaccurate SST estimates up to 5 C lower (Mü et al., 2001). Calcite replacement of the coral skeleton can produce considerably higher SST estimates (McGregor and Gagan, 2003).	Perceived to be a significant problem- but unstudied	Perceived to be a significant problem- but unstudied	The presence of secondary aragonite can produce inaccurate SST estimates up to 5 C lower (Mü et al., 2001). Minor calcite replacement of the coral skeleton does not appear to have a large influence on SST estimates (McGregor and Gagan, 2003).

2.2.4. Mg/Ca ratios

Mg/Ca ratios have proven to be reliable indicators of SST (Fig 2.5; Mitsuguchi et al., 1996). The ratio has been significantly correlated with instrumental SST measurements using ICP-AES (Mitsuguchi et al., 1996), and LA- ICP-MS (Sinclair et al., 1998; Fallon et al 1999; 2003) techniques. However, Mg is concentrated heterogeneously within the coral skeleton and is particularly enriched around the centre of calcification (Mitsuguchi et al., 2001; Meibom et al., 2004). Up to 40% of Mg can be incorporated into the coral lattice in organic matter or on crystal surfaces, while the remaining 60% is substituted for Ca in the skeleton (Watanabe et al., 2001). Therefore, a strict preparation procedure is required to remove the organic phase and ensure the accurate measurement of substituted Mg/Ca ratios for SST-based reconstructions (Watanabe et al., 2001).
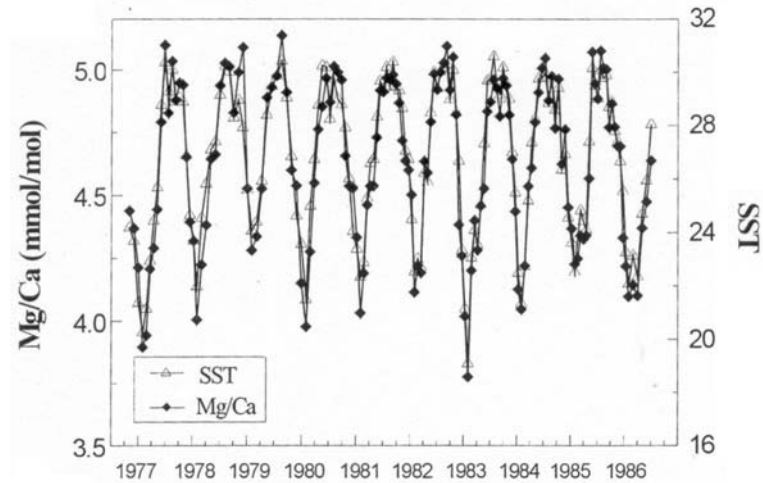
Figure 2.5. Coral Mg/Ca ratios display significant correlations with instrumental SST in a coral from Hainan Island (from Wei et al., 2000).

SST calibrations for the Mg/Ca ratio are influenced by the preparation and analytical procedure (Fig 2.6). The curve produced by Watanabe et al. (2001) was derived from a milli-Q water-H_2O_2-HNO_3 treatment and the slope was subsequently much shallower than the other calibrations derived from untreated coral aragonite (e.g. Sinclair et al., 1998; Fallon et al., 1999; 2003). The calibration curves of Fallon et al. (1999; 2003) and Sinclair et al. (1998) were also produced using the lower-precision technique of LA-ICP-MS.

The coral Mg/Ca ratio has not been applied to SST reconstructions as frequently as has Sr/Ca. The coral Mg/Ca ratio is problematic, particularly because Mg is incorporated heterogeneously into the coral skeleton and is also associated with organic components locked within the coral lattice (e.g. Watanabe et al., 2001; summarised in Table 2.1). Studies have shown that Mg is substituted for Ca into the coral skeleton independent of extension rates, but the Mg/Ca ratio may be influenced by a biological/metabolic effect (Mitsuguchi et al., 2003). The Mg/Ca may also be affected by freshwater runoff (Mitsuguchi et al., 1996) and terrestrial (offshore) gradients (Fallon et al., 2003).
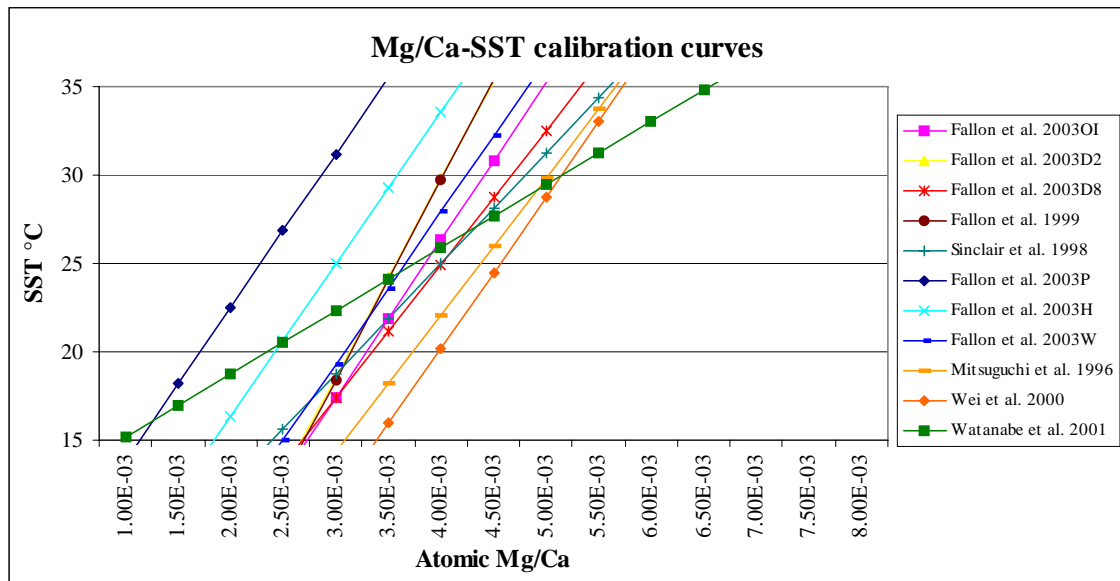
Figure 2.6. Published Mg/Ca-SST calibration curves. The large differences in the slope and intercepts of the curve may reflect the pre-treatment procedures, different analytical techniques or different environment influences such as offshore gradients. Fallon et al. 2003OI (Orpheus Island); 2003D2; D8 (Davies Reef); 2003P (Pandora Reef); 2003H (Havannah Reef); 2003W (Wheeler Reef; LA-ICP-MS); Watanabe et al. (Caribbean Sea; ICP-AES); Mitsuguchi et al. (Ryukyu Islands, Japan; ICP-AES); Wei et al. (Hainan Island; ID ICP-MS); Fallon et al. 1999 (Shirigai Bay, Japan; LA ICP-MS); Sinclair et al. (Davies Reef; LA ICP-MS).

2.2.5. U/Ca ratios

Seasonal variations in coral U/Ca ratios were discovered by Shen and Dunbar (1995) who concluded that U/Ca may be an effective proxy of SST, pH and salinity (Fig 2.7; Shen and Dunbar, 1995; Min et al., 1995). The original calibration of the U/Ca-SST relationship was determined using the TIMS technique employed by Min et al. (1995); it has since been applied to corals from the GBR (Hendy et al., 2002). Other calibrations using LA-ICP-MS (Sinclair et al., 1998; Fallon et al., 1999; 2003) and isotope dilution ICP-MS (Cardinal et al., 2001) have been produced.

Interestingly, the available calibration curves are significantly different for the U/Ca ratios measured by TIMS compared with the LA-ICP-MS technique (Fig 2.8). It is unclear why this is so, but the TIMS method is preferred due to its higher precision measurements of U/Ca compared to LA-ICP-MS.
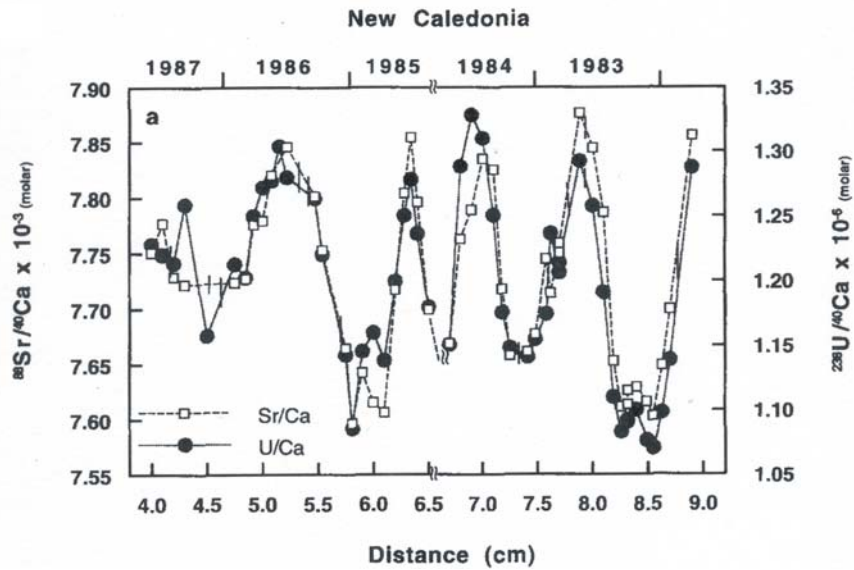
Figure 2.7. U/Ca ratios analysed in corals have shown promise as a reliable SST proxy in corals from New Caledonia (from Min et al., 1995).

The major disadvantage of the coral U/Ca ratio as a paleothermometer is that it may be influenced by other parameters such as pH, salinity/freshwater runoff and terrestrial (offshore) gradients (Shen and Dunbar, 1995; Min et al., 1995; Wei et al., 2000; Cardinal et al., 2001; Fallon et al., 2003; outlined in Table 2.1).
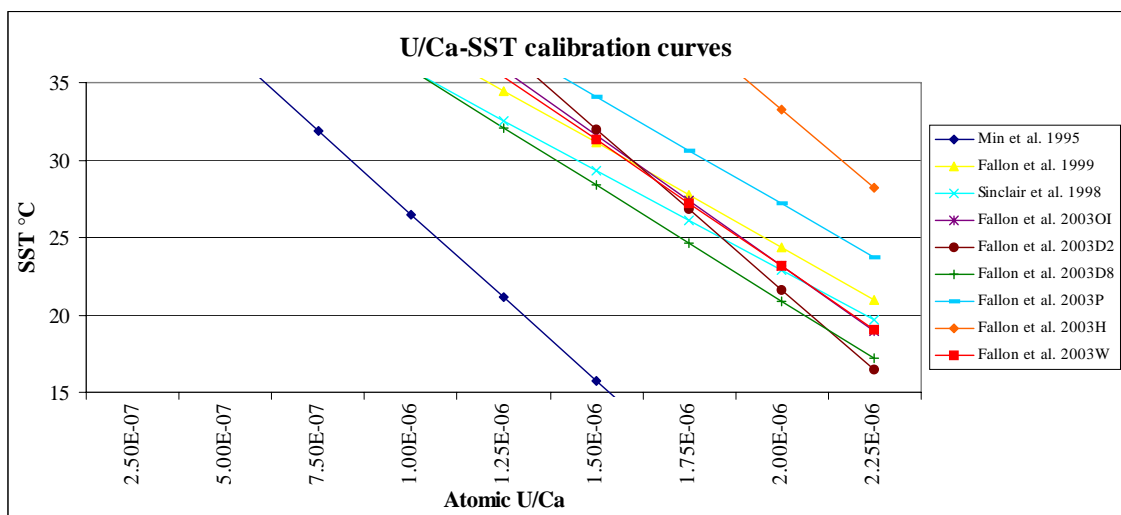
Figure 2.8. Published U/Ca-SST calibration curves. The discrepancies in the curves produced by Min et al. (1995; TIMS) with Fallon et al. (1999; LA ICP-MS) and Sinclair et al. (1998; LA ICP-MS) may reflect the different analytical techniques used. Min et al. (New Caledonia); Fallon et al. (Shirigai Bay, Japan); Sinclair et al. (Davies Reef).

2.2.6. Physical growth/coral calcification rate

Annual coralline density, extension and calcification rates have been studied extensively and provide independent assessments of the coral growth environment (e.g. Lough et al., 1999; Barnes and Lough, 1999; Lough and Barnes, 1997; 2000). Annual coral extension and calcification rates increase significantly northwards along the GBR as SST becomes warmer approaching the equator (Lough et al., 1999). The calcification rate, a combination of coral density and extension, has provided a proxy for SST and coral health (Kinsey, 1988; Lough and Barnes, 1997; 2000; Barnes and Lough, 1999). Averaged 5-yearly calcification rates from 10 long-lived coral cores from the GBR were correlated significantly to the instrumental SST record from the GBR extending back to 1906 (Lough and Barnes, 1997). This significant correlation suggests that the long-term coral calcification rate is related to SST (Lough and Barnes, 1997). For every 1° C rise in temperature on the GBR, average calcification rates increased by approximately 0.33-0.39 g/cm^2 year and coral extension increased by 3.1 mm/year (Lough and Barnes, 2000). These relationships are based on average calcification rates and average mean seawater temperatures and are consistent for shallow water *Porites* corals from a wide range of locations (Fig 2.9; Lough and Barnes, 2000). Outliers from this general relationship may, for example, highlight corals that are not performing as well as they should at the given water temperatures (e.g. Hong Kong Harbour) and this poor performance may be associated with stresses such as poor water quality (J. Lough, personal communication 2004).
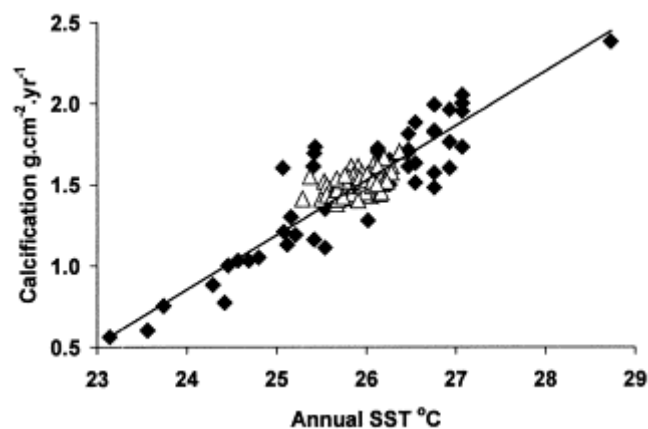
Figure 2.9. Annual coral calcification rates are an excellent indicator of SST and provide a reliable examination of coral health in corals (from Lough and Barnes, 2000).

Average coral calcification rates appear to be an inexpensive and reliable technique to produce long-term historical mean SST (at relatively low resolution). In addition, the calcification rate appears unaffected by many potential problems associated with the geochemical proxies, with the possible exception of diagenesis. Secondary aragonite or calcite replacement within the coral skeleton can interfere with density measurements and produce significant errors in calculating the calcification rate (e.g. Müller et al., 2004).

2.2.7. Summary

The O isotope composition as well as the Sr/Ca, Mg/Ca and U/Ca ratios in corals are proven proxies of SST, provided that the corals are sampled correctly, are of mature age and are free of diagenesis. These elements and isotopes should also be analysed at high precision so that a reliable SST calibration curve can be developed. The annual coral calcification rate also provides reliable reconstructions of long-term SST trends and, with the possible exception of diagenesis, is free of the problems commonly associated with the geochemical proxies.

2.3.   Rainfall/precipitation

2.3.1. Overview

This section will examine previous studies that have investigated the relationship between the coral O isotope composition and river discharge/rainfall. In addition, I review works that have correlated the intensity of luminescent/fluorescent lines in corals with the intensity/volume of river discharge.

2.3.2. Oxygen isotopes

In regions with strong seasonal variations in salinity, oxygen isotopes measured in coral skeletons are better recorders of seawater salinity than SST (e.g. McCulloch et al., 1994; Gagan et al., 1998; 2000). A technique was developed that subtracts the SST component (derived using Sr/Ca, Mg/Ca or U/Ca ratios) from the corresponding $\delta^{18}O$ values so that seawater salinity ($\Delta^{18}O$) could be estimated (McCulloch et al., 1994).

The technique has been applied at various locations (Fig 2.10; Gagan et al., 1998; 2000) and particularly on the GBR where a significant correlation was discovered between the Burdekin River discharge and the corrected $\Delta^{18}O$ measured in a coral from Pandora Reef (Fig 2.11; McCulloch et al., 1994). The Burdekin River discharge is, in turn, significantly correlated with rainfall within its large catchment (Alibert et al., 2003) and the summer monsoonal index for Queensland (Isdale et al., 1998). Therefore, reconstructing river discharge and salinity provides an important climatic record along the north Queensland coast. This subtraction procedure is not required in places with little seasonal variation in SST, and O isotopes have been exclusively measured to investigate monsoonal activity (Tudhope et al., 1996; Klein et al., 1997), river runoff (Swart et al., 1998) and ENSO (Linsley et al., 1994; Dunbar et al., 1994; Tudhope et al., 1995; Wellington and Dunbar, 1995).
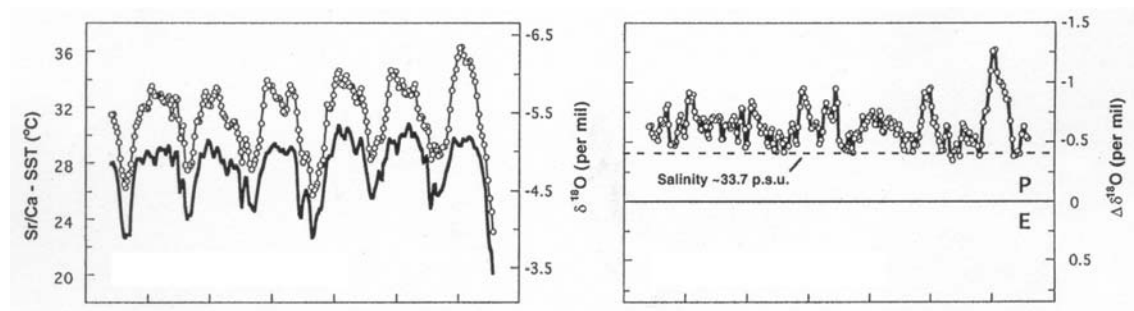
Figure 2.10. By subtracting the SST component from the corresponding O isotopes seawater salinities can be derived. An example from Indonesia (from Gagan et al., 2000).

While it has been demonstrated that a minor addition of secondary aragonite or calcite replacement does not particularly influence the $\delta^{18}O$ composition of the coral (McGregor and Gagan, 2003); diagenesis can strongly affect the other SST proxies and make the correction unreliable for assessing seawater salinity (Enmar et al., 2000).
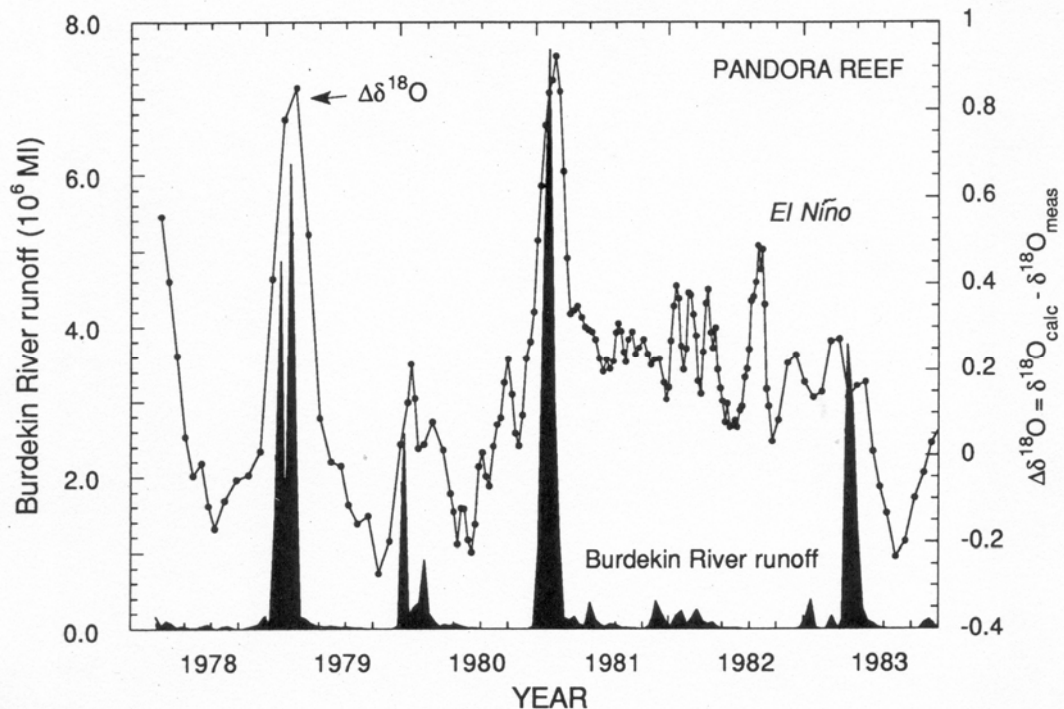
Figure 2.11. The seawater salinity proxy derived from the subtraction of the SST component from the O isotopes is significantly correlated with river discharge. Example from Pandora Reef and the Burdekin River discharge (from McCulloch et al., 1994).

2.3.3. Fluorescent banding/luminescent lines

When a coral slice taken from the inner GBR is illuminated with a UV light source, particular areas of the coral will display distinct yellow/green bands or lines that are related to river runoff (Isdale, 1984; Isdale et al., 1998). These lines were originally called "fluorescent bands" by Isdale (1984), but they are now referred to as "luminescent lines" because coral emits both fluorescence and phosphorescence when illuminated under a UV light (Wild et al., 2000; Barnes and Taylor, 2001). Annual luminescent lines typically occur in corals growing within 20 km of the coastline and are closely correlated with water depth between the particular reef and the mainland (Lough et al., 2002). The varying intensity of the coral luminescent lines is significantly correlated with the strength of the monsoonal rainfall, coastal runoff and the El Niño Southern Oscillation index (Isdale, 1984; Isdale et al., 1998; Lough et al., 2002; Hendy et al., 2003). It was initially proposed that the bands were the result of increased fulvic/humic acids preserved in the coral skeleton (Boto and Isdale, 1985); however, more recently the bands have been linked to changes in the skeletal architecture or coral density associated with lowered salinity, with stress or with altered crystal chemistry (Barnes and Taylor, 2001; 2005). The latter model is preferred as

luminescent lines in corals have been discovered in upwelling zones and in areas that are not influenced by river discharge (Tudhope et al., 1996). Luminescent lines can be measured effectively by eye (Scoffin et al., 1989); the most intense lines are given a value of 3, and no visible lines are valued at 0 (indicative of dry summers; Lough et al., 2002; Hendy et al., 2003). The lines have also been measured quantitatively on a fluormicrodensitometer (Isdale et al., 1998). Recently, a more reliable machine has been developed to provide quantitative measurements of coral luminescence: the Luminometer (Barnes et al., 2003).

Gagan et al. (1994) correlated luminescent lines with $\Delta^{18}O$ measurements recorded in corals from Pandora Reef, GBR. They discovered a 12-18 day delay between the runoff peak from the Burdekin River and the production of luminescent lines. The delay corresponded to the time it takes for the Burdekin plume to reach Pandora Reef. Luminescent lines in corals have shown potential for reconstructing rainfall and river flow variability associated with El Niño Southern Oscillation events and also provide an excellent chronology (Fig 2.12; e.g. Hendy et al., 2003 and references therein). In addition, luminescent lines measured in several long coral cores from the GBR display excellent reproducibility (Fig 2.12; Hendy et al., 2003).
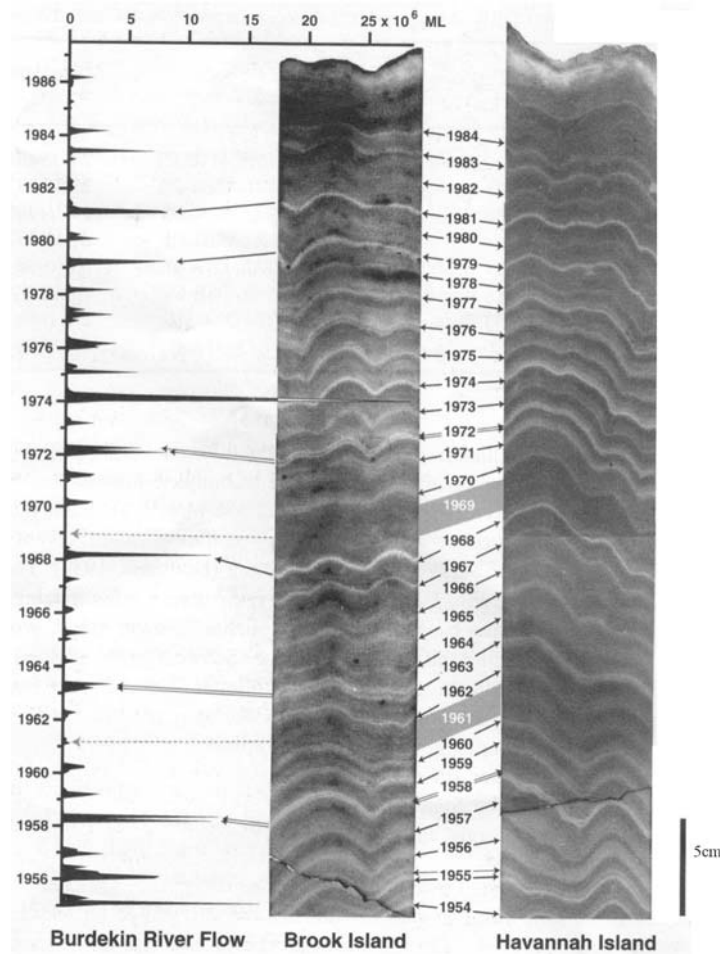
Figure 2.12. Luminescent lines preserved in corals are related to periods of lower salinity and are significantly correlated with river discharge. When several coral records are applied, luminescent lines can be matched to establish a master chronology of wet and dry years on the GBR (from Hendy et al., 2003).

2.3.4. Summary

Subtracting the SST component from the O isotopes produces a reconstruction of seawater salinity ($\Delta^{18}O$). Previous studies discovered significant correlations between coral $\Delta^{18}O$ records from the inshore GBR with Burdekin River discharge and regional rainfall. In addition, the measurement of coral luminescent lines has also proven to be an excellent indicator of river discharge and rainfall.

2.4.   Water Quality

2.4.1. Overview

Sediment and nutrient export from rivers to the inshore GBR has increased substantially since European settlement (c. 1850; Moss et al., 1992; Prosser et al., 2001; Furnas, 2003) and may have significantly altered the makeup of inshore coral reefs (Fabricius, 2005; Fabricius et al., 2005 and references therein). However, there are no long-term instrumental water quality records from the GBR and therefore it is difficult to assess properly the effects of human activity on coral reef ecosystems. Coral geochemistry may provide a more quantitative approach to compare water quality on coral reefs before and after European settlement (c. 1850). This section will review several of the coral proxies that have displayed potential for examining changing water quality on coral reefs. These include Ba/Ca and Mn/Ca ratios, Th concentrations, rare earth elements and their associated anomalies, and heavy metals.

2.4.2. Ba/Ca ratios

Barium is incorporated into the coral skeleton in close equilibrium with the seawater Ba/Ca ratio (Lea et al., 1989; Alibert et al., 2003). The coral Ba/Ca ratio has shown potential as a suitable proxy for river discharge/seawater salinity (Shen and Sanford, 1990; Fallon et al., 1999; Alibert et al., 2003; Sinclair and McCulloch, 2004) or for upwelling events (Lea et al., 1989; Shen et al., 1992a; Fallon et al., 1999). Dissolved Ba concentrations in coastal seawater can have a variety of sources. The dissolved load in river plumes and Ba desorbed from suspended riverine sediment accounts for the dominant supply of Ba to the inshore zone while other minor, but important, sources may include mangrove mud deposits and submarine groundwater seeps (Alibert et al., 2003).

Recently, Ba/Ca ratios have been applied to determine sediment flux to the GBR (McCulloch et al., 2003; Sinclair and McCulloch, 2004). Barium is desorbed from suspended sediments when freshwater plumes become mixed with seawater due to the higher ionic strength of the saline water (Li and Chan, 1979; Coffey et al., 1997; Alibert et al., 2003; McCulloch et al., 2003). Ba/Ca ratios measured in a coral from Havannah

Reef on the GBR increased significantly after 1870 (Fig 2.13; McCulloch et al., 2003). This increase was attributed to increased erosion from cattle and sheep grazing within the Burdekin River catchment. Sediment export to the GBR was estimated to have increased by at least a factor of 5 after European settlement (McCulloch et al., 2003). Although significant correlations between coral Ba/Ca ratios and Burdekin River discharge were observed by McCulloch et al. (2003), the individual dissolved and desorbed Ba components could not be distinguished. Therefore, it was unclear which Ba source provided the dominant signal in the coral record (Sinclair and McCulloch, 2004). Additional high-resolution studies of coral Ba/Ca ratios by Alibert et al. (2003) and Sinclair and McCulloch (2004) indicate that 50-60% of Ba in seawater is derived from the sediment source. The initial coral Ba/Ca "flood" peaks are always sharp; however, in some cases, the Ba/Ca ratios remain elevated for a considerable time before they return to background levels. This return to background levels is much slower when compared with the corresponding baselines of river discharge and seawater salinity (Alibert et al., 2003; Sinclair and McCulloch, 2004). The additional Ba may be released from mangrove mud deposits or submarine groundwater seeps (Alibert et al., 2003; Sinclair and McCulloch, 2004). Coral Ba/Ca ratios are also unusually elevated during flood events following extended periods of drought (McCulloch et al., 2003; Alibert et al., 2003; Sinclair and McCulloch, 2004). Such floods produce severe erosion which may release extra Ba (Alibert et al., 2003). Alternatively, excess mobile Ba may be stored in the river system during periods of low rainfall and then released during the subsequent flood (Sinclair and McCulloch, 2004).

Coral Ba/Ca peaks that do not correspond to river discharge or upwelling have also been discovered in inshore GBR corals (Esslemont et al., 2004; Sinclair, 2005b). These Ba/Ca peaks have been linked to the resuspension of bottom sediments following harbour dredging (Esslemont et al., 2004), *Trichodesmium* blooms or coral spawning (Sinclair, 2005b). These data highlight the difficulties in producing coral Ba/Ca ratios to quantify sediment export to the GBR. However, the majority of inshore coral records from the GBR appear to conform to the previous findings of McCulloch et al. (2003) (e.g. Sinclair and McCulloch, 2004; Alibert et al., 2003).

The Ba flux from the Burdekin River can be reconstructed by calculating the Ba effective river end member (EREM) employing coral Ba/Ca ratios (representing

seawater Ba) and the corresponding seawater salinity values (Sinclair and McCulloch, 2004). The Ba EREM decreased with increasing Burdekin River discharge and this decrease suggests that Ba is diluted during high freshwater runoff and therefore the Ba supply is limited in the Burdekin catchment.
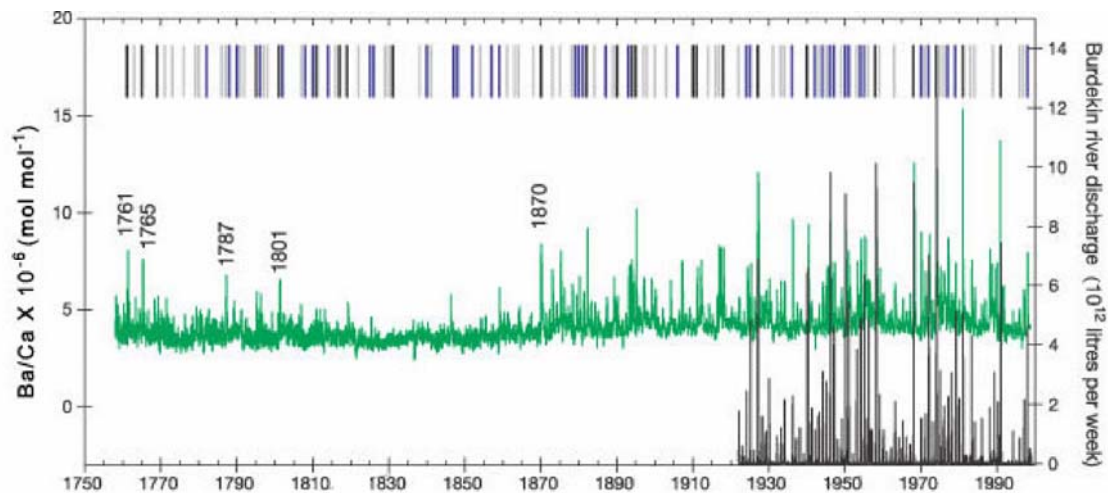
Figure 2.13. Ba/Ca ratios (green line) measured in a coral taken from Havannah Island/Reef, inner GBR. Average Ba/Ca ratios as well as the "flood" values which coincide with Burdekin River discharge (black bars) and the coral luminescence record (top lines: major intensity= black line, average intensity= blue line, small intensity grey line) are significantly higher after 1870. The increase in Ba possibly reflects enhanced sediment supply to the GBR following European settlement (from McCulloch et al., 2003).

The data of McCulloch et al. (2003) require replication at other inshore coral reefs along the GBR. Presumably, inshore coral reefs in the path of the Burdekin River plume would be more susceptible to seasonal influxes of Ba because of the intense land-use in the Burdekin catchment and because of the sheer volume of discharge from the Burdekin River. Other sources of Ba may include upwelling and groundwater influxes, but these are considered minor compared to river-exported Ba into the GBR lagoon (McCulloch et al., 2003; Alibert et al., 2003).

2.4.3. Mn/Ca ratios

The coral Mn/Ca ratio has also been suggested as a potential proxy for river discharge and as an upwelling indicator (Shen and Sanford, 1990; Shen et al., 1992; a, b). High resolution studies have revealed, however, that coral Mn/Ca ratios do not correlate with the corresponding Ba/Ca counterparts that increase after flood events and during the spring and summer seasons (Alibert et al., 2003; Wyndham et al., 2004). Most probably, increased Mn/Ca ratios in corals result from the decay of organic matter and

therefore are a potential proxy of primary productivity or biological activity in coastal seawater (Alibert et al., 2003; Wyndham et al., 2004). Calmer and warmer conditions during the summer months are favourable to increased seawater chlorophyll concentrations (Alibert et al., 2003; Wyndham et al., 2004). The main source of Mn to the inshore central GBR is river particulate matter in the oxyhydroxide form, which is released into seawater by reductive dissolution. Once this Mn enters the marine environment, it is rapidly consumed by phytoplankton or absorbed onto sediments. Two possible mechanisms have been proposed for the re-release of Mn into seawater from the marine sediments and organic material, both of which depend on the oxidation of organic matter. Muddy sediments on the seafloor provide the suboxic conditions necessary for the accumulation and degradation of organic matter, which may promote benthic fluxes of Mn at the sediment-seawater interface (Alibert et al., 2003). Another possible Mn reservoir comes from algal blooms following flood events, where organics flocculate with fine suspended sediments that sink to the seafloor (Alibert et al., 2003). Organic matter could scavenge Mn from suspended sediments and Mn would then be released as solar radiation increases during the spring season (Alibert et al., 2003). Manganese is enriched by a factor of 5 in the inshore corals of the GBR (Alibert et al., 2003) and is thought to substitute for Ca in the coral lattice, but could also be incorporated as an oxide or organic phase (Shen et al., 1991).

Mn/Ca ratios may also be related to the dissolved oxygen levels in seawater, where higher ratios reflect lower oxygen quantities below a critical redox state (Abram et al., 2003). This finding is supported by the significantly elevated Mn concentrations recorded in Indonesian corals during an oxygen consuming "red tide" (algal bloom) which resulted in widespread coral mortality. This "red tide" was a result of wild fires in Indonesia that provided the nutrients required for an algal bloom (Abram et al., 2003). Therefore, coral Mn concentrations may be a reliable proxy to assess oxygen levels in seawater and may record significant algal outbreaks. Mn/Ca ratios are significantly correlated with SST during the winter months; however, they are not correlated with SST or river discharge during the summer months, which suggests that other parameters are influencing the coral Mn/Ca ratio (Alibert et al., 2003; Wyndham et al., 2004).

Mn/Ca ratios were found to increase in corals from Misima Island, Papua New Guinea, (PNG) after gold mining began on the island (Fallon et al., 2002). This increase suggests that coral Mn levels may also be influenced by land disturbance.

2.4.4. Thorium concentrations

Coral Th concentrations have, typically, only been measured for U-Th dating purposes (e.g. Cobb et al., 2003) and to ensure that there is no contamination of coral records from detrital material (Wyndham et al., 2004). The measurement of Th concentrations in corals could, therefore, be used as an indicator of sediment incorporated into the coral skeleton (sedimentation) provided that the coral slice has not been contaminated and the surface area is removed before samples are taken. The potential of coral Th concentrations as a proxy for sedimentation has not yet been studied but will be developed in this thesis.

2.4.5. Rare earth elements

Rare earth element (REE) distributions in corals closely reflect the REE distribution in ambient seawater (Fig 2.14; Sholkovitz and Shen, 1995; Wyndham et al., 2004). REEs in corals have potential as climatic indicators, weathering proxies (Sholkovitz and Shen, 1995) and may show changes to the biological activity of seawater (Wyndham et al., 2004). Corals growing in the coastal zone have significantly higher (up to 10 times) REE concentrations than reefs located on the mid and outer shelf of the GBR (Fig 2.14; Alibert et al., 2003; Wyndham et al., 2004; Akagi et al., 2004). The REE concentrations are higher near the coast because of terrestrial influences (Wyndham et al., 2004) as there are few changes in the distribution coefficients controlling the REE incorporation into corals between the inshore and offshore zones (Akagi et al., 2004). Elevated REE concentrations in corals are most probably linked to increased suspended sediments delivered from river catchments. Coral REE concentrations increased after a gold mine began operation in PNG; this increase was linked to the elevated sediment export from the gold mine to the nearby coral reef (Fallon et al., 2002).

REE ratios such as the neodymium/ytterbium (Nd/Yb) ratio, the cerium (Ce) anomaly and yttrium (Y) concentrations have also shown potential as proxies for biological

activity, nutrient levels and terrestrial runoff, respectively (Alibert et al., 2003; Wyndham et al., 2004; Sinclair, 2005b). The Nd/Yb ratio displays a positive correlation with Mn/Ca ratios during the summer and spring seasons, and it has been proposed that the ratio is largely controlled by the scavenging of the heavy REEs (Yb) by organic ligands (Wyndham et al., 2004). This finding explains the tight correlation with Mn/Ca ratios so, although the mechanisms controlling their release into seawater are different, both ratios respond to episodes of enhanced primary productivity (Wyndham et al., 2004). The coral Ce anomaly is significantly elevated in coastal corals compared to corals growing at offshore sites as the anomaly is strongly dependent on the abundance of Ce oxidising bacteria. The Ce anomaly has potential as a proxy of biological activity as well as for monitoring nutrient levels in seawater (Wyndham et al., 2004). Y concentrations are 6 times higher in the terrestrially-influenced inshore corals than in offshore corals of the GBR (Alibert et al., 2003). Coral Y concentrations were initially thought to be a less sensitive indicator of sediment export from rivers compared with the more established Ba/Ca and Mn/Ca ratios (Alibert et al., 2003); however, a recent study found that in some corals Y may actually be a better recorder of river discharge than the Ba/Ca ratio (Sinclair, 2005b).
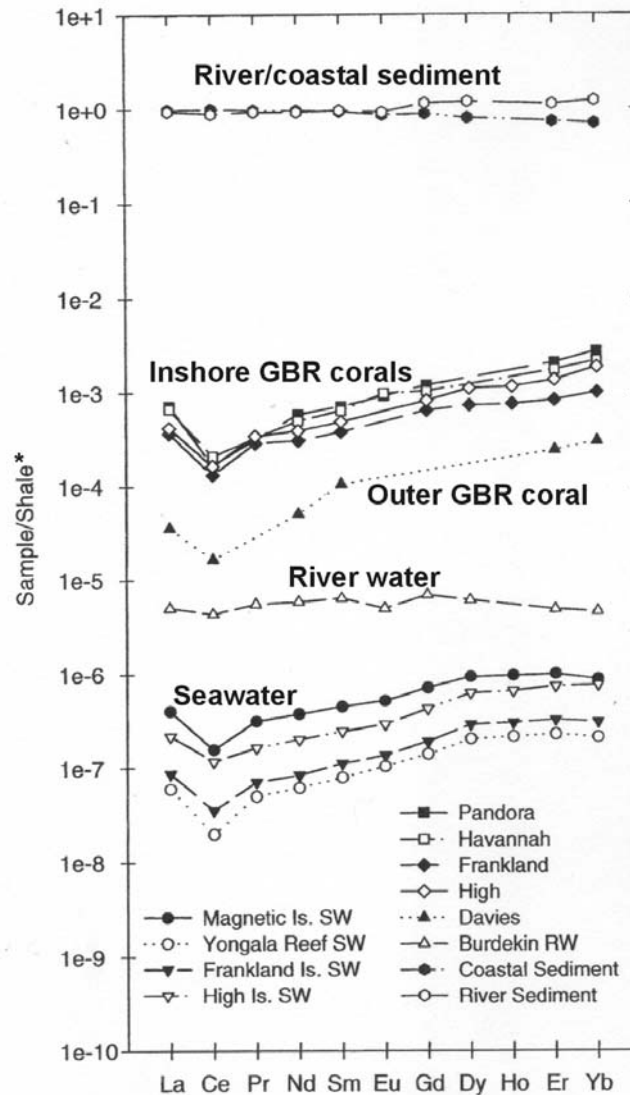
Figure 2.14. Rare earth elements preserved in corals closely follow seawater trends. In comparison, sediment and river water display relatively flat trends. Corals from the inshore GBR (e.g. Pandora Reef, Havannah, Frankland and High Islands) have higher REE concentrations than corals from the outer reef (e.g. Davies Reef; from Wyndham et al., 2004). Note: *reference shale from Byrne and Sholkovitz, 1996.

2.4.6. Heavy metals

The measurement of heavy metals in long-lived corals of the GBR allows assessment of the terrestrial and environmental contamination of coral reef ecosystems. Enhanced heavy metal concentrations in corals result from either mining activity or industrial fallout. Exceptionally high heavy metal concentrations of copper (Cu), lead (Pb), zinc (Zn) and tin (Sn) were discovered in corals growing near a rum refinery outlet pipe discharging effluent (Runnalls and Coleman, 2003). Corals closer to the outlet pipe had died and heavy metal concentrations in their outer growth layers are thought to have

been toxic enough to have initiated coral death (Runnalls and Coleman, 2003). Extremely high levels of heavy metal pollution are known to destroy coral reefs (Runnalls and Coleman, 2003) and also inhibit coral reproduction. Massive increases in Pb and particularly in Zn were recorded in corals that were influenced by a polluted river system draining a catchment containing a gold mine on Misima Island, PNG (Fallon et al., 2002). Heavy metal concentrations may also be higher in corals growing near shipping ports (e.g. Esslemont, 2000; Reichelt-Brushett and McOrist, 2003).

2.4.7. Summary

Ba/Ca ratios in inshore corals of the GBR may provide a proxy to quantify the amount of fine sediment particles exported from rivers. However, elevated Ba/Ca ratios may also be linked to *Trichodesmium* blooms, coral spawning and harbour dredging. Coral Mn/Ca ratios may be used to reconstruct environmental parameters such as upwelling, release from bottom sediments, the decay of plankton and changes in land-use. Coral Th concentrations may provide a proxy for sedimentation. Rare earth elements and the associated anomalies have also proved useful in examining the biological activity of seawater and terrestrial influences. The heavy metal concentrations in corals provide a means of assessing contamination levels on coral reefs.

2.5.   Chapter summary

➢ In locations where there is little variation in salinity, oxygen isotopes measured in corals provide reliable reconstructions of SST.

➢ Sr/Ca ratios are widely considered to be the best coral paleothermometer, while Mg/Ca and U/Ca ratios have also displayed promise in reconstructing historical SST.

➢ The coral calcification rate, a combination of density and extension measurements, has proven a reliable proxy to reconstruct (low-resolution) average SST. In addition, the annual coral calcification rate can be used as an indicator of coral health.

➢ A number of potential problems with coral thermometers including sampling errors, biological effects and diagenesis may affect the reliability of SST reconstructions.

➢ Oxygen isotopes can also be used to reconstruct seawater salinity ($\Delta^{18}O$) provided that a SST proxy (Sr/Ca, Mg/Ca, U/Ca) can be applied to subtract this component from the isotopes.

➢ The measurement of the intensity of coral luminescent lines provides a reliable proxy for river discharge, rainfall and the El Niño Southern Oscillation index.

➢ The coral Ba/Ca ratio has demonstrated potential to quantify sediment export to the GBR lagoon.

➢ Coral Mn/Ca ratios have been applied to reconstruct environmental changes accompanying river discharge, upwelling, primary productivity/phytoplankton outbreaks and seawater oxygen levels.

➢ The concentration of Th in the coral skeleton may be used as an indicator of sedimentation.

➢ REE concentrations/distributions and the associated anomalies have shown potential as a proxy for biological activity, terrestrial influences and dissolved seawater nutrient levels.

➢ Coral heavy metal concentrations provide an assessment of contamination levels on coral reefs.

Chapter 3

Background

3.1. Chapter overview

In this chapter, I review previous studies that have investigated Cleveland Bay and Magnetic Island from a geomorphological, geological, climatic, historical and environmental perspective. This chapter has five sections:

1) The geomorphology and geology of Cleveland Bay/Magnetic Island and surrounds (section 3.2)
2) The Holocene sea levels of eastern Australia (section 3.3)
3) The Holocene climate archives (section 3.4)
4) The history of settlement in the Burdekin region (section 3.5)
5) The water quality on coral reefs (section 3.6)

3.2. The geomorphology and geology of Cleveland Bay/Magnetic Island and surrounds

3.2.1. Overview

This section will examine previous studies on the geomorphology, geology and stratigraphy of Cleveland Bay and Magnetic Island. The geomorphology section will describe the size and setting of Cleveland Bay, the influence of nearby rivers, the sediment supply to the bay and the fringing reefs of Magnetic Island. The composition and ages of the rocks in Cleveland Bay and Magnetic Island are also discussed. The stratigraphy of Cleveland Bay and Magnetic Island (Nelly Bay) is described from sediment cores and seismic data.

3.2.2. Geomorphology

Cleveland Bay is a shallow (max depth 15 m) north-facing embayment located between 19° and 20° S and 146° and 147° E, and covers an area of approximately 400 km^2 (Fig 1.2; Carter et al., 1993). The bay is protected from the dominant southeast trade winds,

although it can be exposed to northerly winds and the occasional tropical cyclone. Rocky headlands such as Cape Cleveland, Magnetic Island, Cape Pallarenda, and Mt Stuart surround the embayment. The Burdekin River month is currently approximately 50 km south of Cleveland Bay, and is believed to have once flowed further northwards, possibly along Barratta Creek or the current Haughton River channel during the early Holocene/Pleistocene Epochs (Hopley, 1970a; Fielding et al., 2003; 2005a; Fig 3.1). It was thought that the river turned further south approximately 3000 years ago (Hopley, 1970a; Orpin et al., 2004). Around this time, a tombolo was formed linking Mt Stuart and Cape Cleveland, and circulation and energy conditions within the bay were significantly reduced (Fig 3.2; Carter et al., 1993; Orpin et al., 2004). However, detailed studies on the evolution of the Burdekin River delta show a more complex history with up to 13 sub-delta "lobes" recognised in the sedimentary record (Fielding et al., 2005b; 2006). These data suggest that that Burdekin River has avulsed back and forth along both Bowling Green Bay and Upstart Bay over the last 8-10 thousand years (Fielding et al., 2006). The Burdekin River, as well as the Ross and Haughton Rivers, supply the majority of the sediment to Cleveland Bay. Sand-sized grains replenish the beaches concentrated to the western end of Cleveland Bay towards Cape Pallarenda while mud-sized particles are deposited in the tidal flats on the coastal plain east of Ross River (Carter et al., 1993; Fig 3.2). The majority of sediment exported from the Burdekin River is retained within Bowling Green Bay (80-90%) and only small amounts of sediment are deposited in both Upstart and Cleveland Bays (5-10%; Orpin et al., 2004). The sediments in Cleveland Bay are extensively reworked, resuspended and redeposited in northward embayments; this finding is supported by the low sediment accumulation rates (<1 mm per year) that have been calculated for the bay (Orpin et al., 2004).
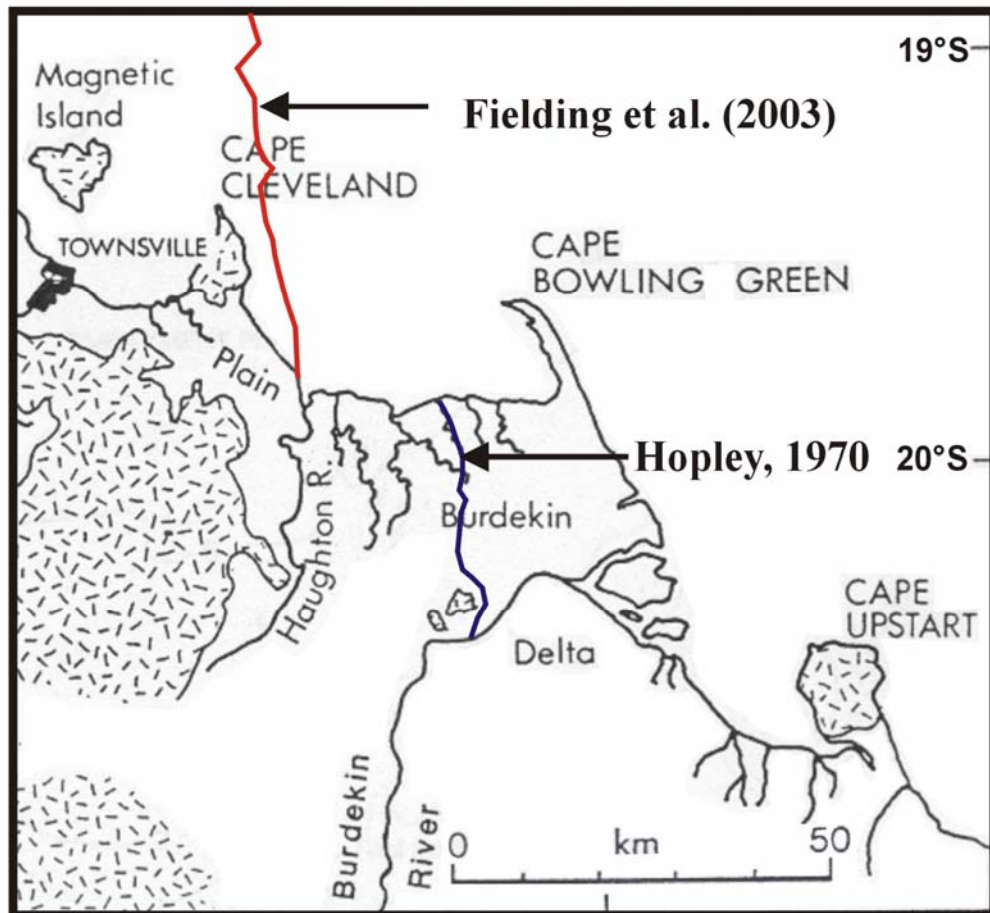
Figure 3.1. The Burdekin River is thought to have once flowed further northwards during the early and mid-Holocene. Hopley (1970a) believed the paleo-Burdekin channel may have been near the Barratta Creek system, but Fielding et al.'s (2003) seismic investigation discovered the channel may have flowed along the current Haughton River during the last glacial period (map modified from Carter and Johnson, 1987). Recently Fielding et al. (2005b; 2006) has interpreted a more complex history of the Burdekin delta over the Holocene with up to 13 delta lobes recognised in both Bowling Green and Upstart Bays.

Fringing reefs are situated in Cleveland Bay off Magnetic Island, an inshore continental island of the GBR (Collins, 1987). The living biology and geomorphology of these reefs have been well studied (Morrissey, 1980; Mapstone et al., 1992; Collins, 1987). Magnetic Island has a diverse (over 100 species) range of corals which exist in conditions of varying levels of wind and wave exposure, which range from very protected (calm conditions) to moderately exposed (Collins, 1987). The relative proportions of coral species, however, change over time (decade-century scale timeframes) due to the stresses imposed from bleaching and tropical cyclone events, which allows the more robust corals to temporarily flourish. Evidence from sedimentary cores and seismic data indicate that the majority of inshore fringing reefs of north Queensland developed on unconsolidated Pleistocene sediments (Hopley et al., 1983; Johnson and Risk, 1987; Smithers and Larcombe, 2003).
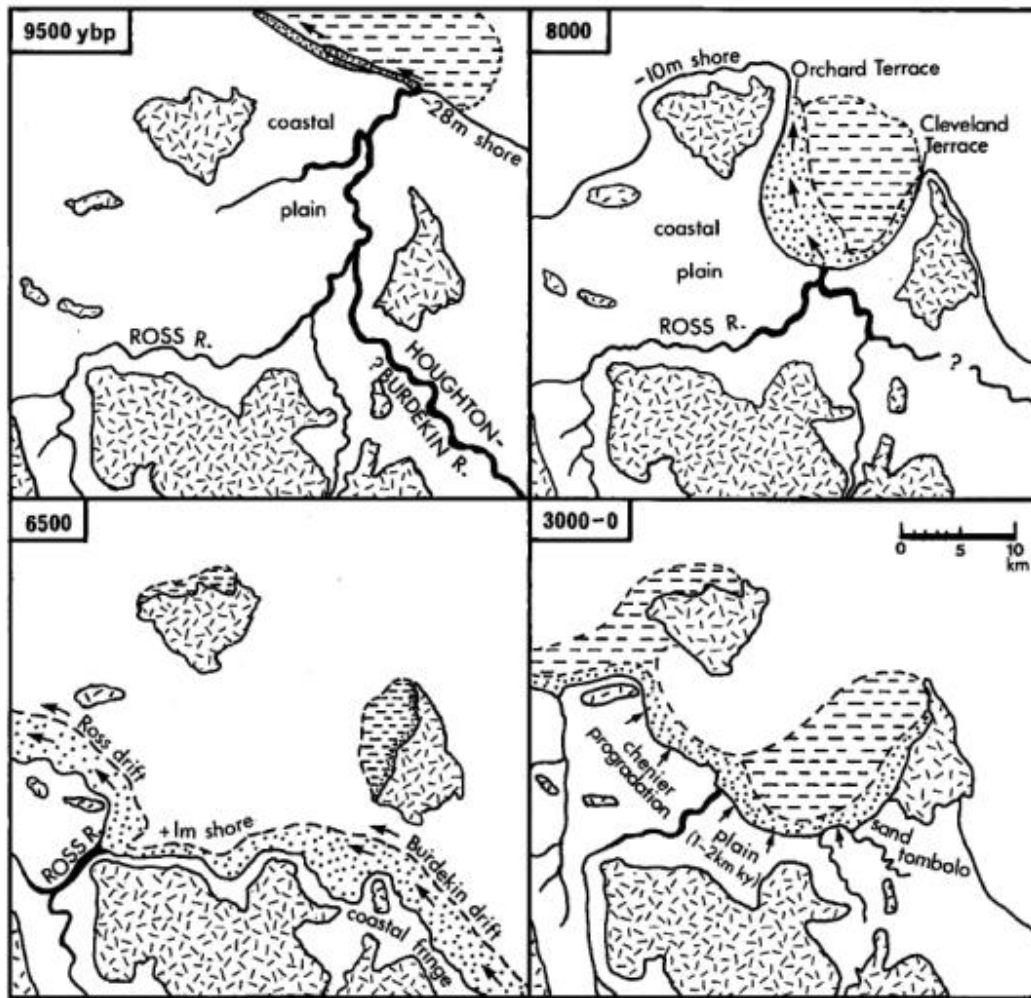
Figure 3.2. Sea level model for the Cleveland Bay area (from Carter et al., 1993). Note the predicted flow from the Burdekin and Haughton Rivers and the coastal progradation over the last 3,000 years, causing a tombolo to link Cape Cleveland to the mainland.

The fringing reefs of Magnetic Island bleached during the summers of 1979-80, 1981-82, 1986-87, 1991-92, 1993-94 (Jones et al., 1997), 1997-1998 and 2001-2002 (Berkelmans et al., 2004). These bleaching events were correlated with anomalously high air temperatures (used as a proxy for SST) not experienced in the local area since the 1930s. Numerous coral colonies from Magnetic Island bleached when seawater temperatures exceeded 31.5° C (Jones et al., 1997).

3.2.3. Geology

The rocks of the Cleveland Bay area are made up of the Permo-Carboniferous "Julago Volcanics" and Permian granitoids (Trezise and Stephenson, 1990). The Julago Volcanics consist of lava and pyroclastic deposits of rhyolitic and andesitic

composition, and sedimentary sandstones, conglomerates, and shales (Trezise and Stephenson, 1990). These rocks are found around Mt Stuart, Many Peaks Range, and Liver Point (Magnetic Island). The Permian granitoid intrusions have a stronger resistance to weathering than the Julago Volcanics and are now topographic highs emerging over the landscape (Mt Stuart, Castle Hill, Mt St John, Magnetic Island; Trezise and Stephenson, 1990).

The first detailed survey of Magnetic Island was conducted by J. G. O'Connell in 1886 (Fig. 3.3). The majority of the embayments were named after members of the Pearce family living in Townsville (Porter, 1983). A. Gibb Maitland completed the first geological map in 1892 (Fig. 3.4) and reported that the island was made up of three major geological units, including superficial deposits, altered volcanic rocks of Permo-Carboniferous age, and granite and felsite. Of particular interest in Maitland's (1892) report is a description of "coral rock occurring on the sea beach best seen at low water mark" (Maitland, 1892; p 2). The age of the "coral rock" is unknown, and was used to construct some of the early buildings in Townsville and Magnetic Island (Porter, 1983). Maitland (1892) also observed "a considerable quantity of stranded pumice [mainly in the bays] exposed to the open sea… nothing above 12 feet [3.72 m] above high water mark." These deposits were presumably formed during storm events.
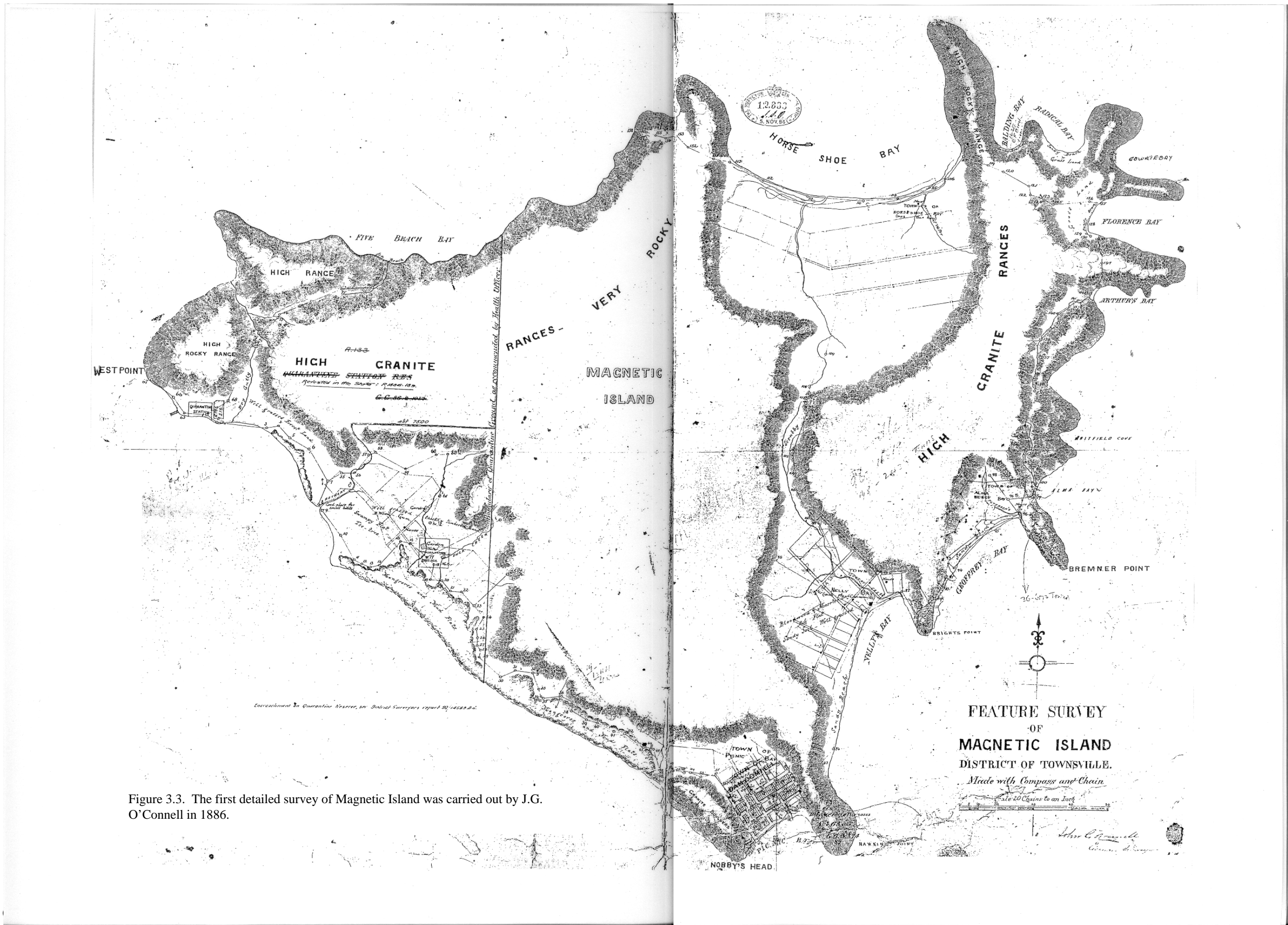
Figure 3.3. The first detailed survey of Magnetic Island was carried out by J.G. O'Connell in 1886.
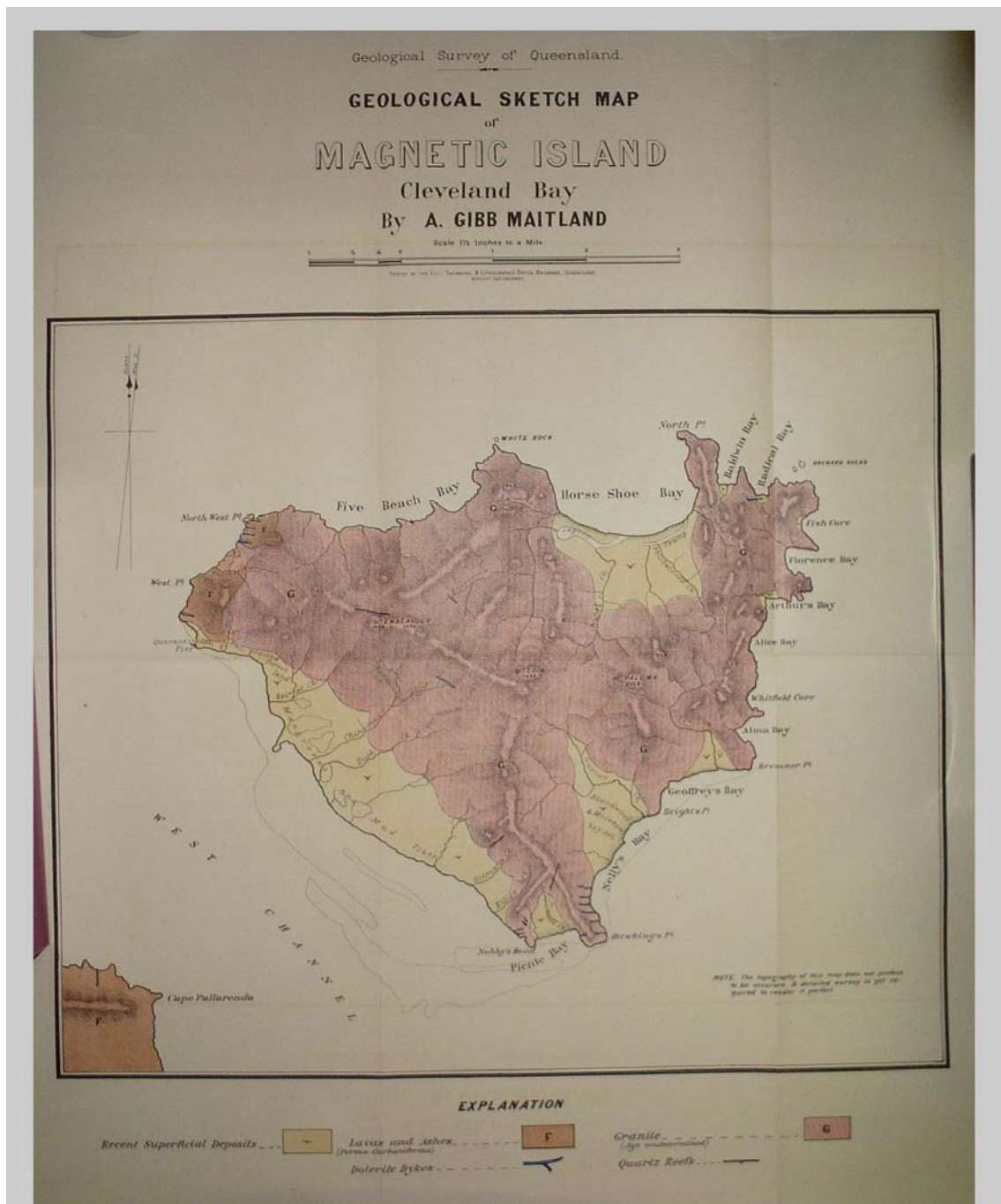
Figure 3.4. The first geological map of Magnetic Island completed in 1892 by A. Gibb Maitland.

3.2.4. Stratigraphy of sedimentary units in Cleveland Bay

Three common Holocene stratigraphic units were recognised in seismic and core data taken from Cleveland Bay (Fig 3.5; Carter et al., 1993) resting on reflector "A", a tough compacted oxidised clay thought to represent the Pleistocene-Holocene boundary (Orme et al., 1978; Johnson et al., 1982; Johnson and Searle, 1984). The main

Holocene units have been labelled units A, B, and C respectively and were described by Carter et al. (1993). Unit A is "transgressive beach sand" grading up into a bioturbated offshore muddy-sand believed to represent a rapid sea-level rise during the early-mid Holocene. Unit B is composed of massive mangrove mud underlying unit A. This unit is short lived (7.7-8.5 ka) and thought to have been a "back beach" zone before being overcome by the rapid sea-level transgression. Unit C is cross-bedded sand which has infilled paleo-river channels active in the last glacial period (Fig 3.5; Carter et al., 1993).

A regional study on the central GBR was conducted by collecting a transect of sediment cores from the inner to the outer central shelf east of Townsville (Harris et al., 1990). One core (V45) was collected on the 18 m isobath in Cleveland Bay, approximately 5 kms northeast of Magnetic Island. About 2 m of core was recovered; the lower portion was described as a "transgressive sand" overlayed by a "stillstand" mud-dominated unit. Radiocarbon dating of the contact between the two units provided an age of 7,550 years BP (Harris et al., 1990).
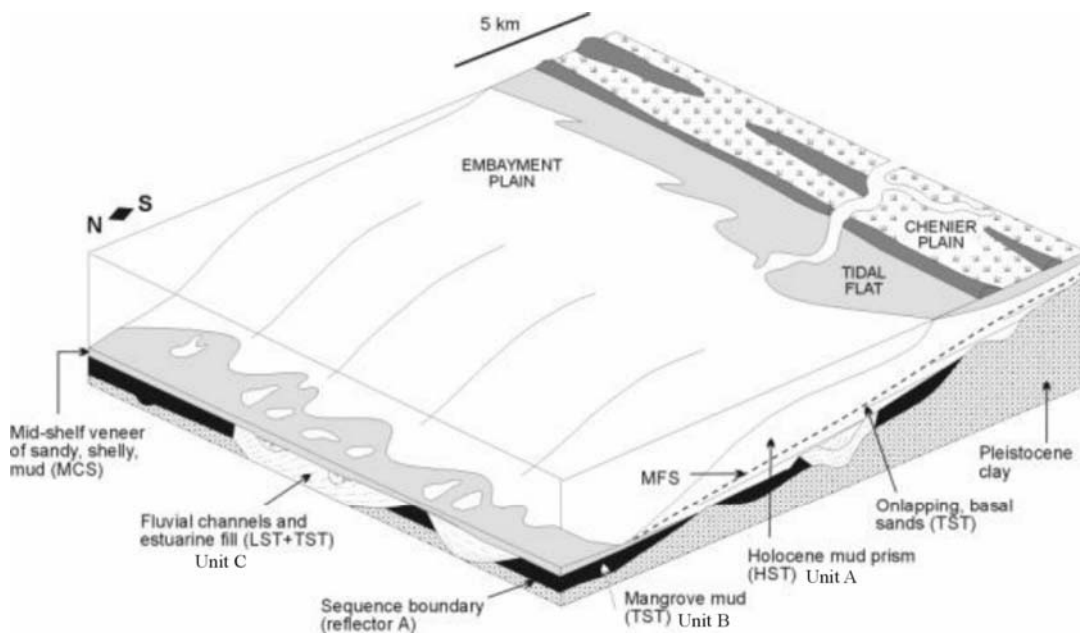
Figure 3.5. A stratigraphic model of Cleveland Bay (from Carter et al., 1993). Three major units (A-C) can be recognised from seismic data and sediment coring.

3.2.5.   Stratigraphy of Magnetic Island and Nelly Bay

Spencley (1980) extracted 19 sediment cores to depths of up to 4.5 m from the southern end of Magnetic Island (Cockle Bay). Intervals of coarse sand, mangrove mud and shell-dominated layers were intercepted. "Granite basement" was struck in 5 cores ranging in depth from 0.75 m to 4 m. A 2-3 m thick mangrove layer overlies fan deposits produced from the weathering and erosion of the granite on Magnetic Island. The base of this deposit was radiocarbon dated to 7,230 ± 500 C-14 years BP (Spencley, 1980).

Numerous jet probes revealed that the reef in Geoffrey Bay is largely comprised of sand and coral shingle (Hopley et al., 1983). An older ridge that appeared to run parallel to the shoreline was discovered near the current reef front. This ridge may have provided the foundation structure for the present reef (Hopley et al., 1983). A similar feature was also discovered in Nelly Bay (Hopley, 1986), although additional seismic surveys in the embayment have failed to reveal this "structure" (Carter and Johnson, 1989; Sinclair Knight Merz, 1998). The base of the Nelly Bay reef flat is approximately 7,000 years old (Hopley, 1986).

Nelly Bay is a "closed system" as coarse sediments are derived from catchments draining into the adjacent headland. Negligible sediment transport occurs within the embayment except during storm/cyclonic events. Aerial photographs of the embayment over 50 years reveal few changes in this highly stable environment (Hopley, 1986). Three major geomorphogical units have been identified within the bay, including the upper beach, the lower beach and the reef flat (Smith, 1974). The upper beach is characterised by good-to-moderately-sorted medium sands with a low carbonate fraction and a symmetrical distribution. The lower beach has sand similar to the upper beach; however, this sand has a negatively-skewed distribution curve and higher carbonate content. The reef flat deposits are poorly sorted coarse-grained sediments that are high in carbonate and have a positively-skewed distribution (Smith, 1974).

A seismic reflection survey of the Nelly Bay Harbour site by Douglas Partners Pty Ltd for Sinclair Knight Merz (1998) showed the Pleistocene-Holocene boundary to lie between 2.0-4.5 m from the surface (Sinclair Knight Merz, 1998). Another reflector,

between 10-13m, was interpreted as granitic basement. No clear evidence of "hard coral" was evident; however, "obscured zones" in the northeastern quarter of the survey area may be associated with hard, dense coral or partially cemented sands (Sinclair Knight Merz, 1998). Carter and Johnson (1989) also conducted seismic investigations of the area and discovered that the Pleistocene-Holocene boundary was between 2.5-5.5 m below the superficial sediments in Nelly Bay. Hard areas in the bay were interpreted as individuals or groups of patch reefs growing on the hard Pleistocene substrate.

Three main sedimentary units have been identified from drilling records in the Nelly Bay Harbour site (McIntyre and Associates, 1986; 1989). These units include marine sand and coral (1.4-3.2 m thick), clayey sand (1.6-5.9 m thick), and sandy clay (~2.4 m thick). The clayey sand and sandy clay units may have been deposited during the Pleistocene (McIntyre and Associates, 1986; 1989). Golder Associates Pty Ltd (2000) drilled 17 boreholes in Nelly Bay Harbour to a maximum depth of 10.63 m. The sedimentary units included medium sand with traces of coral, coarse sand with trace coral, sandy clay and clayey sand, sand coral and coral sand, gravely sand, peaty clayey sand, and coral.

3.2.6. Summary

Cleveland Bay is a shallow, protected north-facing embayment that contains the study area of Magnetic Island. The Burdekin River dominates the terrigenous sediment supply to Cleveland Bay and the Burdekin plume influences the fringing reefs of Magnetic Island annually. The Burdekin River delta was once further northwards and discharged into Bowling Green Bay during the early-mid Holocene. Three distinct Holocene sedimentary units make up the stratigraphy of Cleveland Bay including a transgressive beach sand which grades into a bioturbated offshore muddy sand (unit A), a "back-beach" mangrove mud (unit B) and a cross-bedded sand which has infilled former paleo-river channels (unit C). Three morphological zones have been identified in Nelly Bay including the upper beach, the lower beach and the reef flat. The modern Nelly Bay reef formed approximately 7,000 years ago. Seismic surveys from Nelly Bay suggest that granite basement is 10-13 m below the surface and is overlain by Pleistocene alluvial sediments (clayey sand and sandy clay) and a marine sand and coral

Holocene unit. The boundary between the Holocene and Pleistocene units is thought to be between 2.0 and 4.5 m below the surface.

3.3. Holocene sea levels

3.3.1. Overview

Holocene sea levels have been widely studied for north Queensland and the surrounding areas. Sea level strongly influences coral reef growth and sedimentary processes. Therefore, reconstructions of past sea levels are invaluable to understand the evolution of the GBR. Numerous parameters have been used to reconstruct past sea levels including: sequence stratigraphy of sediment cores and seismic data, fossil oyster beds, tubeworms, barnacles, coral microatolls, mangrove mud and beach rock. This section will review the previous work on Holocene sea levels with a particular focus on the early Holocene transgression and the mid-Holocene highstand and will also examine the reliability of the sea-level indicators that were applied to measure the Holocene sea levels.

3.3.2. The early Holocene transgression

The early Holocene transgression marked a time when sea levels rose rapidly following climate warming and the melting of large ice caps that were particularly prominent during the last glacial period. Seismic investigations, sediment cores, and radiocarbon dates from the GBR (sequence stratigraphy) were compiled to produce a detailed account of sea levels from the past glacial age to the present interglacial period (Carter et al., 1986; Carter and Johnson, 1986). Ten migrating shorelines were identified and dated. Paleo-shorelines were discovered at –113 m 18 thousand years ago (18 ka), -88 m at 17 ka, -75 m at 15 ka, -56 m at 12 ka, -46 at 11 ka, -28 m at 9.5 ka, -24 m at 9 ka, -9 m at 7.5 ka, 0 m at 6.5 ka, and +2-3 m at 6 ka. The data indicate that, during some stages, sea level rose as rapidly as 12 m per thousand years. Some of the shorelines, however, may have remained stable for up to 1-2 thousand years (Carter et al., 1986; Carter and Johnson, 1986). Larcombe et al. (1995b) and Larcombe and Carter (1998) discovered that sea-level oscillations during the early Holocene were more

complex then previously thought and that sea level fell by as much as 5-6 m at around 8.5 ka. They concluded that higher resolution dating techniques would be required to measure sea level more accurately. Larcombe et al. (1995b) compiled 364 radiocarbon dates to produce a sea-level reconstruction for north Queensland during the Holocene (Fig 3.6). A 5-6 m fall in sea level at 8 ka, postulated by Larcombe et al. (1995b; Larcombe and Carter, 1998), was criticised by Harris (1999) who suggested that a sea-level oscillation of this magnitude would be complemented by a pronounced shift in O isotopes which was not evident in the Greenland ice core record (Fig 3.7). This "sea level fall" could also be explained by a decline in the rate of sea-level transgression (Harris, 1999).
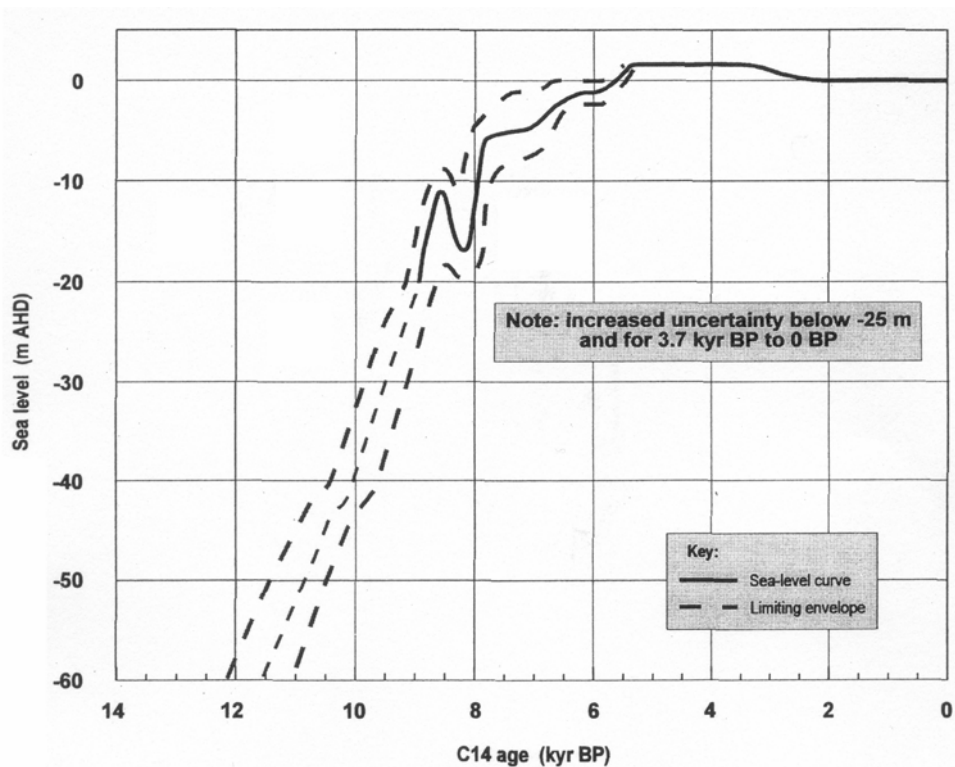
Figure 3.6. Sea-level curve produced for north Queensland was developed from a number of different indicators including mangrove mud, fixed biological indicators (FBIs) and coral microatolls (from Larcombe et al., 1995b)
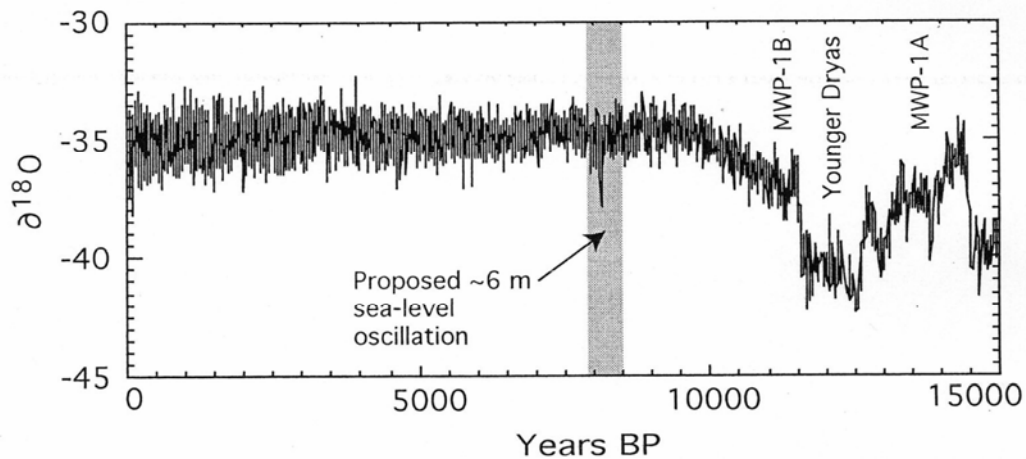
Figure 3.7. Oxygen isotope record from the Greenland ice core (Harris, 1999). The 5-6 m oscillation in sea level as proposed by Larcombe et al. (1995b) should have a pronounced shift in the $\delta^{18}O$ isotopes which is not displayed in the Greenland ice core record.

3.3.3. The mid-Holocene sea-level highstand

Sea-level indicators, such as coral microatolls, oyster beds, barnacles, tubeworms, beach rock and mangrove mud, provide conflicting evidence of the timing and magnitude of the mid-Holocene sea-level highstand(s) along the eastern Australian coastline. In addition, these indicators have been subject to various interpretations and two competing models have emerged to explain the cause of the mid-Holocene highstand and the recent sea-level fall. These include the hydro-isostatic deformation model and the oscillating, global eustatic model.

The hydro-isostatic deformation model was first used to explain the spatial variations of Holocene sea levels along the Australian coastline (Chappell et al., 1982; Lambeck and Nakada, 1990). The model proposes that the mass of seawater loaded onto the continental crust during the rapid early Holocene transgression caused the outer part of the shelf to downwarp while the shoreline became uplifted (Woodroffe, 2003). This flexure of the crust, therefore, produced a relatively higher sea level without the need for a change in global ice volumes (global eustatic). The crust then gradually settled to produce a smoothly falling sea level.

Support for a single, smooth sea-level fall was provided by measuring the height and age of fossil coral microatolls from continental islands off the north Queensland coast, including Magnetic Island (Chappell, 1983; Chappell et al., 1983). Microatolls are

among the most reliable sea-level indicators as their vertical growth range is commonly within 10 cm of the mean low water spring tide in the open marine environment (Chappell et al., 1983). The microatolls provided evidence for a smoothly falling sea level from about +1 m around 6,000 years BP (Chappell et al., 1983); although Blake (1994) found evidence for a +1 m sea level at 2,500 C-14 years from fossil coral microatolls from the Whitsunday Island Group. This finding indicates that sea level may have remained at a higher elevation for longer than the original estimates of Chappell et al. (1983).

Evidence for considerably higher sea levels has been reported by Hopley (1970b; 1971; 1983) from cemented beach rock deposits. Elevated beach rock within sand spits, attached to continental islands off the north Queensland coast, is considered an indicator of paleo-beaches during the mid-Holocene; the radiocarbon dating of carbonate fragments incorporated in this beach rock may provide reliable estimates of the timing and magnitude of sea level (Hopley, 1970b; 1971; 1980; Gill and Hopley, 1972). The dating of these deposits suggests that sea levels were approximately 3.4 m higher than present around 3.5-4.5 ka (Hopley, 1970b; 1971). This finding is supported from beach rock deposits about 2.5 m above the present high tide mark near Darwin; shell samples from these deposits were radiocarbon dated at 2,050-3,390 years (Nott 1996). The evidence for a +2.5-3.5 m sea level from beach rock deposits contradicts the findings from the coral microatoll indicators (Chappell et al., 1983); however, the sea-level estimates from beach rock concur with regional mid-Holocene estimates from the South China Sea (range from 2.4 to 5 m) and from the Pacific Ocean using coral terraces and oyster beds (+1-2.6 m; Davis et al., 2000; Zhao and Yu, 2002; Dickinson, 2004).

Belperio (1978; 1979) has warned against the use of beach rock as a sea-level indicator as it is formed from recrystallised material and may not provide an accurate age or sea level position due to local tectonic influences. Also, what is considered a former "beach" deposit may, in fact, be a cemented chenier ridge produced by storms. Belperio (1979) also argued that there was no evidence of mid-Holocene sea levels higher than +1 m from the dating of mangrove mud deposits in Cleveland Bay. Both mangrove mud and beach rock are considered to be less precise sea-level indicators in comparison to microatolls and fixed biological indicators (FBIs: oyster beds, barnacles, tubeworms) (e.g. Larcombe et al., 1995b).

More recently, Baker and Haworth (2000a) have reinterpreted the microatoll dataset of Chappell et al. (1983) and have produced new evidence that supports an oscillating eustatic sea-level model for the mid-late Holocene. The evidence for this alternative model is preserved in FBI assemblages from the New South Wales coastline. Fixed biological indicators, such as oyster beds, tubeworms and barnacles, confined to the intertidal zone, are common along the rocky shorelines of eastern Australia (e.g. Endean et al., 1956a; 1956b) and, along with coral microatolls, are the most precise indicators of sea levels (estimates typically within ± 0.25 m). The vertical range of these organisms is typically within 1.5 m although this is subject to exposure conditions (Baker and Haworth, 1997; 2000b). Hiatuses in the growth of fossil barnacles and tubeworms that once grew in the intertidal zone up to 1.7 m above their living counterparts suggest that sea levels may have fallen between 3,500 and 3,400 years BP and briefly rose again approximately 1,900 years ago (Fig. 3.8; Baker and Haworth, 2000a; 2000b).

These findings complement data from other FBIs from north Queensland (oyster beds; Beaman et al., 1994; Higley, 2000) as well as other parts of the world (e.g. Angulo et al., 1999). At Balding Bay (Magnetic Island), fossil oyster beds at 1.65 m above their living counterparts were dated between 4,040 and 5,860 ± 50 C-14 years (Beaman et al., 1994; Higley, 2000) which suggests the maximum mid-Holocene highstand occurred no earlier than the oldest date (5,860 uncorrected C-14 years) and remained at this level until at least 4,040 C-14 years ago (Beaman et al., 1994; Higley, 2000). Higley (2000) found evidence of growth hiatuses in oyster beds from Balding Bay and Bathurst Heads at similar ages. These hiatuses may be due to storm events; however, the age range is similar to the time-breaks for the FBI data of Baker and Haworth (2000a; b).

If the less precise sea-level indicators, such as beach rock and mangrove mud, are ignored, the precise indicators (microatolls and FBIs) suggest that the mid-Holocene sea level(s) was approximately 1.0-1.7 m higher than present although the timing of the higher sea level(s) is disputed. The microatolls appear to support a smoothly falling sea level and thus provide support for the hydro-isostatic model but, on the other hand, the FBI data appear to have grown to this 1.0-1.7 m level within the last 2,000 years and seem to support the oscillating global eustatic sea-level model.
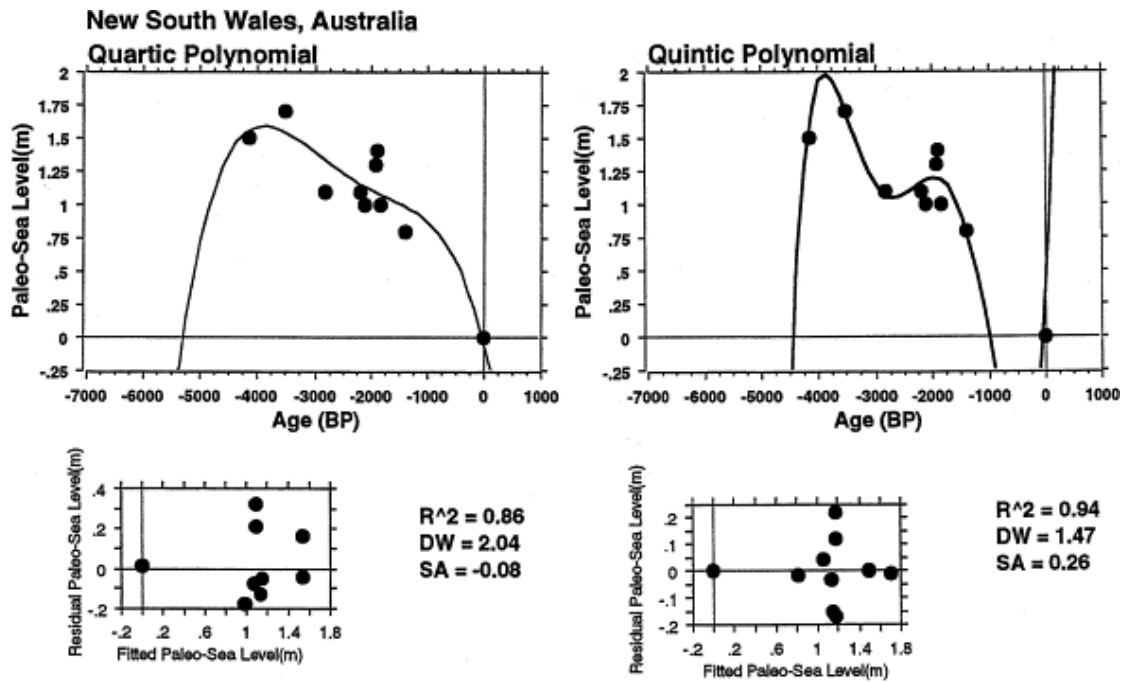
Figure 3.8. Modelled sea levels for the New South Wales coastline during the Holocene (from Baker and Haworth, 2000b). The better regression in the Quintic Polynomial model suggests a possible sea-level oscillation around 1,900 years ago. The sea-level curve has been produced using FBI from New South Wales and shows a strong correlation with the data from northern Queensland and suggests a global eustatic change in sea level, rather than the previous model of hydro-isostatic deformation.

3.3.4. Summary

Holocene sea levels on the GBR transgressed rapidly from -88 m approximately 17,000 years BP to +1-3 m about 6,000 years ago. The dynamics of sea level after this time are controversial and some researchers believe that sea level fell smoothly from +1-3 m, while others have found evidence for an oscillating sea level over the last 6,000 years.

3.4. Holocene climate archives

3.4.1. Overview

High-resolution climate records for tropical north Queensland and the immediate surrounds are sparse due to a lack of adequate proxies available and the scarcity of instrumental data. This section describes the current climate in Cleveland Bay/Magnetic Island and reviews the available instrumental and proxy data for the area

over the Holocene, including records of air temperature, sea surface temperature (SST), precipitation (including seawater salinity, rainfall) and storm events.

3.4.2. Current climate in Cleveland Bay

Average air temperatures in Cleveland Bay are highest in January and December (31.4° C) and lowest in July (25.0° C). Air temperatures have ranged as high as 44.3° C and as low as 1.1° C (BOM, 2004). High-resolution SST records, taken from Nelly and Geoffrey Bays since 1994, are highest in February (average 29.36° C), and lowest in July, on average 21.91° C (Appendix 3; GBRMPA, 2003). Historically, they have soared to 34.74° C (February 1998) and dropped to 17.28° (August 1995).

Rainfall in Cleveland Bay is highly variable and is largely influenced by the El Niño Southern Oscillation (ENSO) and tropical cyclones (Lough, 1994). Townsville receives an average rainfall of 1135 mm per year and has a range from 464.2 mm (1969) to 2399.8 mm (2000; Appendix 4). Rainfall is particularly concentrated in the summer months and January, February, March, and December all average over 125 mm; February is the wettest month. June, July, August, and September receive, on average, less than 20 mm of rain, and September is the driest month (Appendix 4).

North Queensland climates are particularly influenced by cycles of ENSO and anti-ENSO events which affect rainfall, river runoff, and temperature (Lough, 1994). Anti-ENSO periods, when the Southern Oscillation index (SOI; surface pressure difference between Tahiti and Darwin) is positive, produce more intense summer monsoons which result in higher rainfall, higher land runoff (lowered salinity) and higher turbidity conditions on the inshore reefs of the GBR. ENSO events, where the SOI is negative, are characterised by fine "winter like" conditions with little rainfall and high solar radiation from scant cloud cover (Lough, 1994). The correlation between rainfall and ENSO in Queensland (1891-1986) varies with season, region and over time (Lough, 1991). Annual rainfall was relatively constant for the period between 1920 and 1950 and coincided with a weakening of SOI-climate teleconnections (Lough, 1991). A significant increase in Queensland's summer rainfall average and variability was identified after 1949 and particularly high rainfall was recorded during the 1950s and the 1970s (Lough, 1991).

3.4.3.   Holocene SST records

Coral proxy records have provided some, albeit incomplete, insights into changing SSTs on the GBR and surroundings during the Holocene. These short "snap-shots" of SST appear to produce conflicting evidence and it is unclear if the SST records reflect a genuine spatial or temporal change or are an artefact of coral sampling, diagenesis or SST-calibration. In addition, the early-mid Holocene coral proxy records only cover short periods (< 15 years) and so some SST reconstructions may be from juvenile corals which are unsuitable for reconstructions of SST (Marshall and McCulloch, 2002). The following section provides a chronological overview of SST and is presented with a particular focus on coral reconstructions from the early-mid Holocene, the Little Ice Age and the recent period. In addition, instrumental SST trends over the last 100 years are described.

Coral Sr/Ca ratios indicate that SSTs were 2-3° C cooler in the Huon Peninsula (Papua New Guinea) around 7,000-9,000 years ago (7-9 ka) (Table 3.1; McCulloch et al., 1996). SSTs may have increased rapidly at this location soon after a eustatic sea-level rise led to the opening of Torres Strait (~7 ka; McCulloch et al., 1996). Similar evidence of mid-Holocene (ages range from 7.60-8.00 and 6.20-6.35 ka) SST cooling by up to 2° C on the GBR (Myrmidon and Stanley Reefs) was also discovered using coral Sr/Ca reconstructions (Marshall, 2000). On the other hand, Sr/Ca-SST estimates also provide evidence of early-Holocene warming. A *Porites* coral from Myrmidon Reef shows SSTs similar to, or 1° C warmer than, the present (carbon dated at 8.02 ± 0.05 ka; McCulloch et al., 1998). Gagan et al. (1998) found supporting evidence of mid-Holocene (5.3 ka) warming of approximately 1° C from Orpheus Island using coral Sr/Ca ratios and $\delta^{18}O$ composition.

However, Marshall et al. (2000; also Marshall, 2000) recalibrated Gagan et al.'s (1998) SST estimates by applying an alternative Sr/Ca-SST equation that was developed for corals from the outer GBR. The Sr/Ca-SST estimates of this Orpheus Island coral were up to 1.8° C cooler by applying this alternative calibration. This finding suggests that all the available Sr/Ca-SST reconstructions need to be thoroughly assessed to determine whether correct sampling techniques were applied, coral diagenesis was avoided and a reliable calibration was developed for each record.

Table 3.1. Differences in early-mid-Holocene sea surface temperature (°C compared to modern SST) reconstructions from corals for the GBR and surrounds. Age in thousand of years before present.

Coral location	Age (ka)	°C from present	Reference
Huon Peninsula	8.92	- 2.0-3.0	McCulloch et al. 1996
Huon Peninsula	7.37	- 2.0-3.0	McCulloch et al. 1996
Myrmidon Reef	8.02	+ 1.0	McCulloch et al. 1998
Myrmidon Reef	7.60-8.00	- 2.0	Marshall, 2000
Stanley Reef	6.20-6.35	- 2.0	Marshall, 2000
Orpheus Island	5.35	+ 1.0	Gagan et al. 1998
Orpheus Island*	5.35	-1.8	Marshall et al. 2000

* Marshall at al.'s (2000) recalibration of the Gagan et al (1998) data.

Lower than average SSTs (-0.2-0.3° C; derived from Sr/Ca, U/Ca) during the time of the Little Ice Age (LIA; ~ from 1565-1700 AD) were estimated from 8 long *Porites* coral cores from the GBR (Hendy et al., 2002). SSTs then warmed by up to 0.4° C by 1700 AD, and these temperatures persisted, until slight cooling occurred in the early 20th century (Hendy et al., 2002).

SSTs have increased by as much as 0.60° C on the GBR since 1903 (Fig 3.9; Lough, 2001). The 1998 ENSO event coincided with the highest annual SST in the 95-year instrumental record (Lough, 1999) and coral proxy archives also record a significant warming trend towards the end of the 20th century by as much as 1.3° C since 1979 (Alibert and McCulloch, 1997; McCulloch et al., 1998). A warming SST trend during the late 20th century was also discovered in the coral proxy records of Hendy et al. (2002), although this rise was not as large as that found in previous studies.

Sea surface temperatures 1903-2000
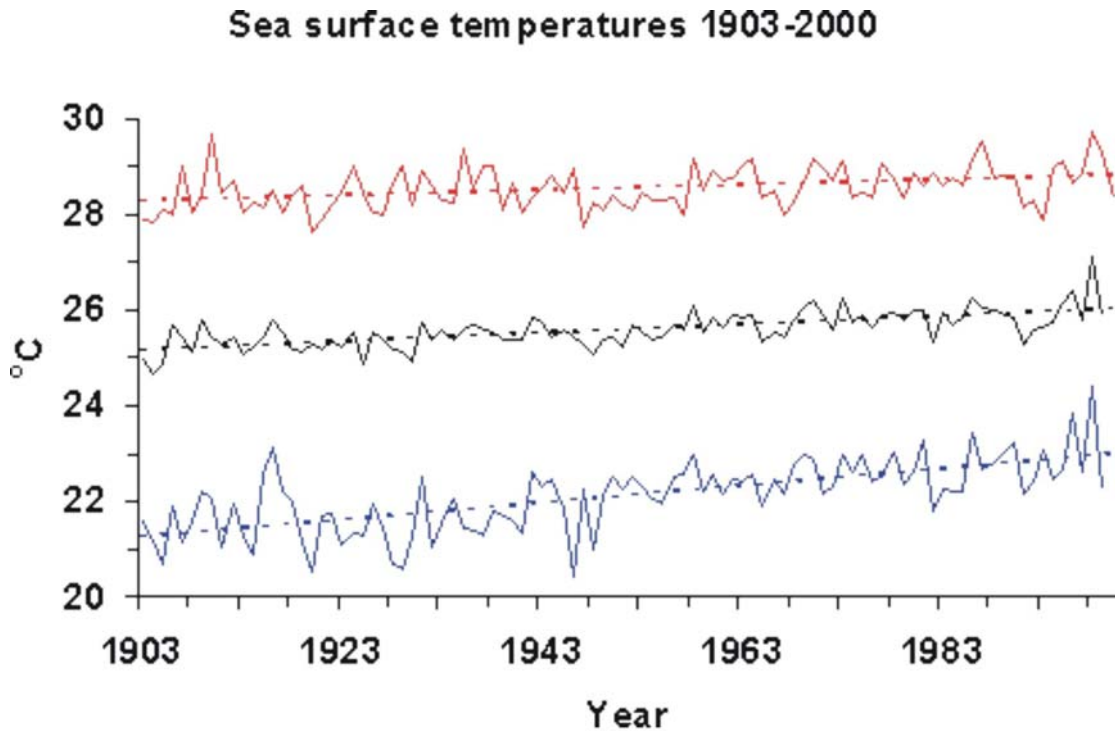
Figure 3.9. Instrumental sea surface temperatures measured in Cleveland Bay from 1903-2001. Minimum (blue), average (black) and maximum (red) SST have significantly increased over this timeframe consistent with the onset of global warming (from Lough, 2001).

3.4.4. Holocene precipitation records (seawater salinity, rainfall, El Niño Southern Oscillation)

Precipitation reconstructions, from geomorphic interpretations, pollen analysis, coral $\Delta^{18}O$ and luminescent lines, provide evidence of climate changes throughout the Holocene and the influence of important drivers such as ENSO on the climates of north Queensland. Geomorphic and pollen records only allow a relative assessment of changes in precipitation (wetter and drier) at coarse resolutions (10^2-10^3 years), while coral and instrumental records provide a much higher resolution (sub-annual) archive of climate. These four precipitation indicators are combined to produce a chronological review of precipitation changes for north Queensland over the Holocene.

Coarse alluvial fan deposits in the Townsville region are thought to indicate a drier climate approximately 15 ka (Hopley, 1970b; 1973; 1978). These fans stabilised during the mid-Holocene, possibly because extra water effectively cemented these deposits; therefore, this feature was indicative of a change to "warmer and wetter" conditions (Hopley, 1970b; 1973; 1978). This finding is supported by other geomorphic evidence from waterfall plunge pools in the Northern Territory. An increase in the size of these

pools between 10 and 5 ka indicates a shift towards wetter climates (Nott and Price, 1994). In addition, pollen records from Lake Euramoo (Kershaw, 1970), Quincan Crater (Kershaw, 1971), Bromfield Swamp (Kershaw, 1975a), and Lynch's Crater (Kershaw, 1974; 1976) on the Atherton Tablelands (north Queensland) suggest that the area was covered by extensive rainforests between 9,500 and 6,000 years BP and that wetter conditions persisted during the early-mid Holocene (Kershaw, 1975b). Evidence of aridity during the early-mid Holocene in the north Queensland region has, however, also been recorded. Dune activation in the Gulf of Carpentaria occurred between 8.2 and 5.9 ka, which is consistent with periods of aridity from other parts of the world (Nott et al., 1999). These brief "events" may not have been recorded by other proxy records (Nott et al., 1999).

Precipitation levels can also be inferred from coral salinity records (see section 2.3.2). A coral record from Orpheus Island suggests that waters of the GBR were slightly more saline (a 0.50 ‰ enrichment in the $\Delta^{18}O$ values) during the mid-Holocene (Gagan et al., 1998). This finding was not interpreted to indicate that precipitation during the mid-Holocene was lower than present, but rather was related to higher evaporation levels and the transport of relatively enriched O-16 to the southern latitudes (Gagan et al., 1998). The transport of O-16 would result in a relative enrichment of the O-18 isotope in seawater (Gagan et al., 1998). However, in order to produce accurate seawater salinity reconstructions, the SST reconstruction must be reliable. As previously discussed, Gagan et al.'s (1998) SST estimate has been disputed by Marshall et al. (2000; Marshall, 2000). The recalibrated SST estimates by Marshall et al. (2000) may, in fact, provide evidence of lower seawater salinity during the mid-Holocene.

A climatic change to drier conditions occurred approximately 3,000 years ago in northern Australia. This change was interpreted from pollen records in sediment cores from the Atherton Tablelands; rainforest pollen became partially replaced by eucalypt vegetation in the sediment cores after this time, which signified a shift to drier conditions (Kershaw, 1975b). Similarly, Shulmeister (1996) reported evidence of a sharp decline in effective precipitation around 3,700 years BP using pollen records in sediment cores from the Northern Territory and the Atherton Tablelands. This change has been interpreted to indicate the onset of a more intense ENSO dominated climate.

That the north Queensland climate was drier during the LIA is highlighted by slightly positive $\Delta^{18}O$ signals in several coral records from the GBR (Hendy et al., 2002). The coral $\Delta^{18}O$ values decreased significantly after 1870, which suggests a return to wetter conditions and that the GBR lagoon had "freshened" (Hendy et al., 2002). Lough (1991) found that luminescent lines in a coral from Pandora Reef were significantly correlated with Burdekin River discharge and the statewide rainfall index. This coral luminescence record revealed anomalously low rainfall between 1770 and 1860, coinciding with the LIA, and above average rainfall between 1870 and 1899, corresponding to the time of early European settlement (Lough, 1991). A clear shift towards warmer and wetter conditions towards the end of the LIA is also supported by coral records of $\Delta^{18}O$, taken from various tropical locations, including the GBR (reviewed in Gagan et al., 2000).

Luminescent lines in long-lived *Porites* lutea and *Porites* lobata corals from Pandora Reef and Havannah Island were measured to reconstruct Burdekin River discharge from 1644 to 1986 (Isdale et al., 1998). A significant regression ($r^2 = 0.83$) was calculated when correlating the predicted river discharge using the luminescent lines and the measured Burdekin River discharge. Evidence of increased runoff (wetter conditions) was discovered during the late 17th century to the mid 18th century and during the early 19th century, while drier conditions prevailed in the late 18th to mid 19th centuries (Isdale et al., 1998). Dendrochronological techniques were employed to match and date luminescent lines from 8 coral cores from different localities in the GBR (Hendy et al., 2003; e.g. Fig 2.12). A 373 year record of Burdekin river runoff was generated and a significant correlation with ENSO was discovered. An inverse correlation between Burdekin discharge and ENSO was identified for the "wetter" period between the 1650s and 1800, while positive correlations were found during the dry 1760-80s (Hendy et al., 2003). This finding provides further evidence that the climate of north Queensland is strongly influenced by ENSO.

3.4.5. Holocene tropical cyclone/storm records

Tropical cyclones and storms can cause coral mortality and significantly alter the short-term makeup of coral reefs by four different processes (Hopley, 1974a):

1) Physical structural damage of corals such as breaking of the coral framework or the overturning of colonies.

2) Burial of corals by coarse sand and shingle deposited during the high energy conditions.

3) Suffocation of corals from a layer of mud which settles out following a return to calmer conditions after intense stream runoff and increased turbidity.

4) Bleaching of corals from a drop in seawater salinity following high freshwater influx.

One of the most severe tropical cyclones to affect the north Queensland coastline in 150 years, "Althea," crossed the coast 38 km north of Townsville in 1971 and was accompanied by a 2.85 m storm surge (Hopley, 1974a; 1974b). Severe structural damage to the fringing reefs of the Palm Island Group was documented, but negligible physical damage to the reefs of Magnetic Island was observed (Hopley, 1974a; 1974b). Several weeks after the cyclone, silt began to accumulate over some of the Magnetic Island fringing reefs (Hopley, 1974a), and coral mortality in Nelly Bay was observed in the wet season following the cyclone (Smith, 1978). The cyclone also caused severe coastal erosion in Cleveland Bay. The foredunes of The Strand and Pallarenda retreated by 11.6 and 15.8 m (Hopley, 1974a), while the dunes in Nelly and Geoffrey Bays eroded by 12 m (Smith, 1974). Nevertheless, significant sand accumulation did occur on the coasts north of Pallarenda and northwest of Magnetic Island (Hopley, 1974a) including a new berm, about 1 m high, deposited in the western half of Horseshoe Bay (Smith, 1978).

The hard corals of Pandora Reef (inshore GBR) were severely damaged by Tropical Cyclone Althea in 1971 and an algal dominated community emerged (T. Done, personal communication 2005). The coral reef recovered to pre-1971 conditions during the 1980s and flourished until the severe 1998 bleaching event which resulted in widespread coral mortality. The reef remained lifeless until 2003, when new coral recruits began to resettle the reef (T. Done, personal communication 2005).

Elevated seawater concentrations of NO_2, NH_4, NO_3, SiO_4 and suspended solids (relative to an average non-cyclone wet season) were measured shortly after Tropical Cyclone Aivu (1989) at fringing reefs surrounding the Whitsunday Island Group

(Blake, 1994). PO_4 levels, however, remained normal and were attributed to rapid phytoplankton uptake and sedimentation. Phytoplankton blooms were observed by Furnas (1989; 1991) after Tropical Cyclone Winifred (1986).

Evidence of past cyclonic events and their effect on coral reefs has been discovered in the sedimentary record. Four different stages of coral growth were identified in a sediment core from Rattlesnake Island, about 10 km north-west of Magnetic Island (Hopley et al., 1983). Each growth stage, radiocarbon dated at $7,010 \pm 180$, $6,860 \pm 140$, $6,480 \pm 170$, and $5,380 \pm 120$ years, were overlain by units of coarse sand, coral rubble and shingle deposits (Fig 3.10). These coarse-grained deposits represent periods of rapid accumulation that may be associated with large storm events, and similar deposits have been found in sediment cores from Hayman Island, Orpheus Island, and Great Palm Island (Hopley et al., 1983).

Twenty-two stratified coral shingle deposits from Curacoa Island, a member of the Palm Island Group, were dated to estimate tropical cyclone frequency since the mid-Holocene (Hayne and Chappell, 2001). These deposits are thought to have formed from the combination of heavy seas and cyclonic storm surges. The frequency of large cyclones has been statistically constant over the last 5000 years (Hayne and Chappell, 2001). Nott and Hayne (2001) dated storm surge deposits along the north Queensland coastline and inshore continental islands. The heights of these deposits were applied to a numerical model which calculated the central pressure (intensity) of the cyclone (Nott and Hayne, 2001). Category 5 cyclones have occurred, on average, once every 200-300 years over the last 6,000 years (Nott and Hayne, 2001); however, it is unclear if sea level and coastal progradation over this time were incorporated into this model. In particular, the calculation of the central pressure for the mid-Holocene shingle deposits would be significantly affected if the +1.5 m sea level was overlooked.

Rattlesnake Island
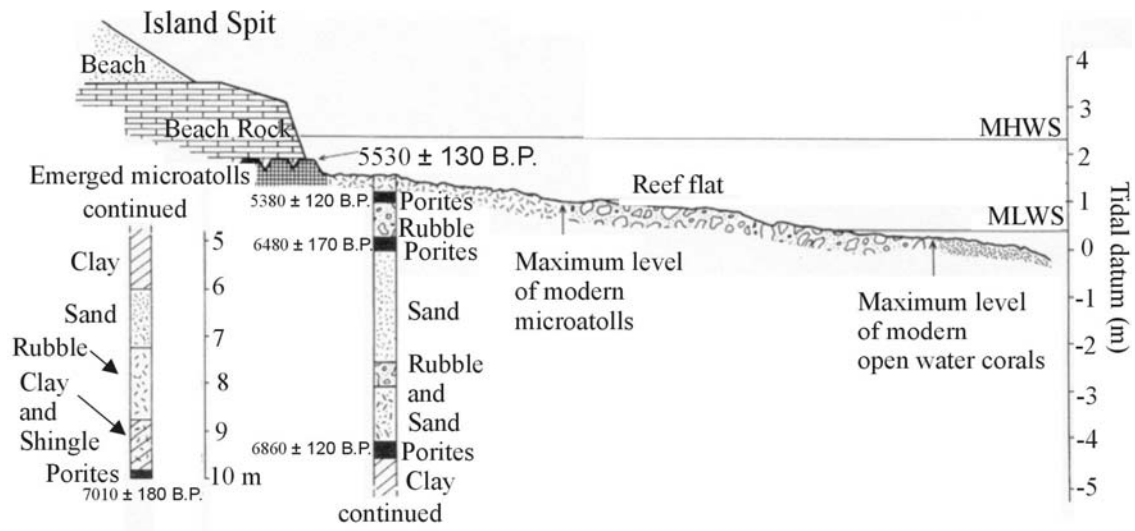
Figure 3.10. A sedimentary core from Rattlesnake Island, approximately 10 km northwest of Magnetic Island, has provided evidence of high energy storms that have occurred during the mid-Holocene (from Hopley et al., 1983). These storms have deposited coarse sediment (rubble, coral shingle and sand) which has buried *Porites* coral heads.

3.4.6. Summary

The SST reconstructions of the early-mid Holocene from coral proxy records on the GBR provide conflicting evidence. Coral proxy records suggest that SSTs were cooler during the LIA and have warmed in the 20th century. Instrumental records from the GBR also suggest that SSTs have increased, in some parts, by 0.6° C in the last 100 years. Holocene climates have been reconstructed using geomorphological investigations, pollen and coral records. Pollen and geomorphic evidence suggests that a relatively wetter environment persisted from 9,500 to 3,000 years BP which was followed by a change to drier conditions in the region over the last 3,000 years; this change coincided with the onset of a greater ENSO influence in the region. Large tropical cyclones (category 5) appear every 100-200 years in the region which can significantly alter the short-term makeup of coral reefs by removing and damaging hard coral communities.

3.5.   The history of European settlement in the Burdekin region

3.5.1. Overview

Sediment and nutrient runoff to the GBR lagoon has increased significantly since European settlement in north Queensland (e.g. Furnas, 2003; McCulloch et al., 2003) and may have affected the makeup of coral reef ecosystems (e.g. Fabricius et al., 2005). The Burdekin River plume influences the coral reefs of Magnetic Island annually and, therefore, this section will review the history of land settlement in the Burdekin River catchment with a particular focus on the sheep and cattle industries.

3.5.2. European settlement and land use in Queensland

The Burdekin and neighbouring river catchments, bar their coastal fringe, remained unexplored by Europeans until 1844 (Fig 3.11). Only three explorers (Leichardt, Mitchell and Kennedy) have left detailed accounts (Leichardt, 1847; Mitchell, 1848; Beale, 1970) of their expeditions inland before the arrival of European grazing animals. While Kennedy's 1848 exploration of the tropical and mountainous Cape York (Fig 3.11) met with great logistical difficulties (Beale, 1970), Leichhardt's epic 4,500 km journey across the state (Fig 3.11) was facilitated by easier topography but, more importantly, by a terrain largely free of undergrowth. The frequency with which Leichhardt's journal comments on the 'openly timbered', 'open well-grassed' forest land (Leichardt, 1847) is remarkable and in stark contrast to the scrubby, dense underwood vegetation encountered today (Bowman, 1998). The rapid transformation from an openly treed, grassy landscape to denser, woodier undergrowth since European settlement can also be reconstructed from the accounts of early sea-based explorers (Flannery, 1994) and is commonly attributed to the cessation of the Aboriginal inhabitant's back-burning practice: 'fire-stick farming' (Jones, 1969; Fensham et al., 2003). As early as 1848, the astute observer Thomas Mitchell (Mitchell, 1848) concluded that fire, grass, kangaroos and human inhabitants formed an inter-dependent existence.

Nowhere was the impact of sheep grazing on the Australian landscape more dramatic than in eastern Queensland. The initial sheep-grazing efforts of the early 1840s focused on the state's extreme SE (Fig 3.11) in the Darling Downs and Logan areas (Campbell, 1936; Knight, 1895; Fox, 1919-1923). From this restricted area, squatters rapidly moved northwards with flocks of sheep brought from the already-established colonies in the south. New ports were opened along the coast in 1854 at Port Curtis (Gladstone), in 1861 at Port Denison (Bowen) and in 1865 at Townsville (Fig 3.11) to export wool and to supply the rapidly growing grazing industry with new stock as well as to support the gold prospectors. The great speed with which new districts were settled between 1851 and 1865 reflects the reliance of the newly-formed colony on wool exports and the English textile industry's demand for wool, especially after 1861 when the vital North American raw cotton supply was halted as a result of the Yankee naval blockade during the American Civil War (Fox, 1919-1923; Menghetti, 1992).

By 1859, Queensland's sheep population had reached 3,166,802 and more than doubled to 7,278,778 by 1866 (Statistics of the Colony/State of Queensland). However, by the end of the American Civil War in 1865, the wool industry along the coast had already begun to collapse due to a drop in demand, various sheep afflictions and, most importantly, the disappearance of suitable feeding grasses, accompanied by the proliferation of unwelcome coarse vegetation (Menghetti, 1992). Spear grass (*Stipa* spp.), in particular, was notorious in reducing the quality of sheep fleeces and damaging the health of the animals (Menghetti, 1992; Bolton, 1963). Sheep had been a short-lived, but disastrous, experiment and cattle were to become increasingly important to coastal catchments (Fig. 3.13) and the Queensland economy after 1880 (Thorpe, 1996). Other major agricultural industries in the region included sugar cane and tobacco (Kerr, 1994); however, cattle were the predominant users of land in the large Burdekin River catchment (Furnas, 2003).
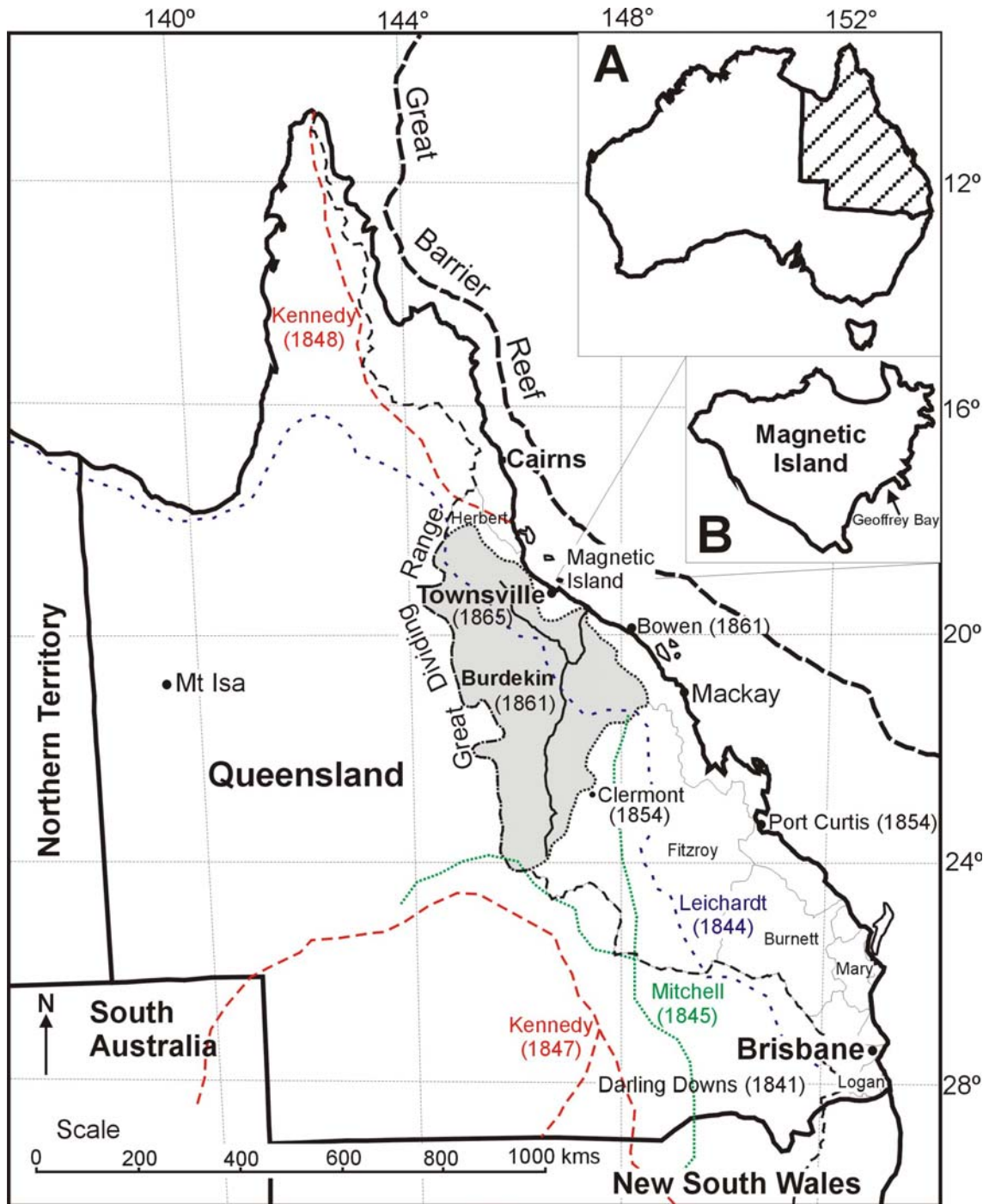
Figure 3.11. Map of Queensland (location within Australia: Inset A). A massive *Porites* coral was cored in Geoffrey Bay, Magnetic Island (Inset B), approximately 5 km off the coast near Townsville. The major coastal river catchments east of the Great Dividing Range are outlined, including the Burdekin (shaded). Detailed descriptions of the pre-European settlement landscapes were documented by Leichardt (blue line, 1844), Mitchell (green line, 1845) and Kennedy (red line, 1847; 1848). The first sheep run in the Burdekin catchment occurred in 1854 west of the present day Clermont Township (shown on map). British demand for wool during the American Civil War in the 1860s prompted rapid settlement in both the Burdekin and Fitzroy River catchments. Suitable sheep and cattle pastures in the Burdekin catchment were sub-divided in 1861. Port Curtis (1854; Gladstone), Port Denison (1861; Bowen) and Townsville (1865) rapidly emerged to supply the sheep industry and to export wool produced from these areas. Sheep grazing in the *coastal* area was an environmental disaster and the major sustainable wool districts are now to the *west* of the Great Dividing Range.

Figure 3.12. The Burdekin River catchment and immediate surroundings. The Burdekin River has been divided into six sub-catchments including the Belyando, Bowen, Suttor, Cape, upper Burdekin, and lower Burdekin. The police districts in the vicinity of the Burdekin River catchment from where cattle and sheep numbers were recorded are highlighted. The statistics from the Rockhampton (until 1865), Emerald, Springsure, Alpha, Clermont and Belyando districts were included in the Belyando sub-catchment. The Suttor and Bowen sub-catchments were combined due to the spare districts in this area; the statistics from the Peak Downs, Fort Cooper, Mackay and Bowen districts were used for this location. The Charters Towers and Cape River district was placed in the Cape River sub-catchment. The Ravenswood, Townsville, Cardwell and Kennedy districts were incorporated into the upper Burdekin, while the Ayr district was included in the lower Burdekin sub-catchment. Note the Aramac, Barcaldine and Blackall districts which are all located to the west of the Great Dividing Range. These districts are among the most successful sheep grazing areas in Queensland. The outcropping mafic volcanic rocks within the Burdekin River catchment are also shown.

3.5.3.   Land-use changes in the Burdekin catchment

Sheep and cattle numbers reported from police districts within or adjacent to the Burdekin River catchment have been compiled from the annual statistical records for the Colony/State of Queensland (where available). The Burdekin River catchment was subdivided into five sub-catchments that relate to the major rivers of the Burdekin system, i.e. the Belyando, Bowen and Suttor, Cape, upper Burdekin, and lower Burdekin sub-catchments (Fig 3.12). The police district in closest proximity was assigned to that particular sub-catchment (Fig 3.12), e.g. the Alpha, Belyando, Springsure, Clermont, Emerald and Rockhampton (1860-1865) police districts were assigned to the Belyando sub-catchment, while the Bowen and Suttor River sub-catchment included the districts of Bowen, Mackay, Fort Cooper and Peak Downs.

Prime grazing land in NE Queensland was first identified by Leichardt in 1844 and described by him in two letters to Charles and William Archer, two pastoralist explorer brothers who set out in 1853 in search of suitable pastures (O'Donnell, 1989). In 1854 they identified Clermont, part of which lies within the Burdekin catchment (Belyando and Suttor sub-catchments), as a suitable location and returned in 1856-7 with several thousand sheep, by which time others had already moved in. The first sheep grazed in the Burdekin River catchment were brought in by Jeremiah Rolfe in 1854 to Mistake Creek (O'Donnell, 1989), which is within the Belyando sub-catchment but also borders the Suttor sub-catchment (Fig 3.12). Sheep numbers were prominent in the Belyando and Suttor sub-catchments from this time and rose dramatically during the 1860s and remained elevated until the 1940s (Fig 3.13). The initial boom of the sheep industry in the Belyando sub-catchments peaked in the year 1872 (approx 1.5 million sheep). Following this period sheep numbers significantly declined to a low of ~450,000 in 1886 before rising again gradually to a new peak in 1914 (~1.7 million) and remaining at relatively consistent numbers until the early 1940s, when the sheep industry in the Belyando sub-catchment collapsed (Fig 3.13). This period coincided with a major drought during WW-II (Young, 2000). With the exception of the Belyando and Suttor sub-catchments, the sheep industry was never particularly prominent in the rest of the Burdekin catchment.

Cattle numbers increased significantly in the Burdekin catchment after the late 1870s to the 1890s, particularly in the Bowen and Suttor, Belyando, and Cape River catchments (Fig 3.13). Cattle numbers dropped considerably during the late 1890s to the early 1900s coinciding with the Federation Drought, but the industry had completely recovered by 1910. More recently (post World War II), the cattle industry became particularly prominent in the upper Burdekin, Bowen and Suttor sub-catchments (Fig 3.13).
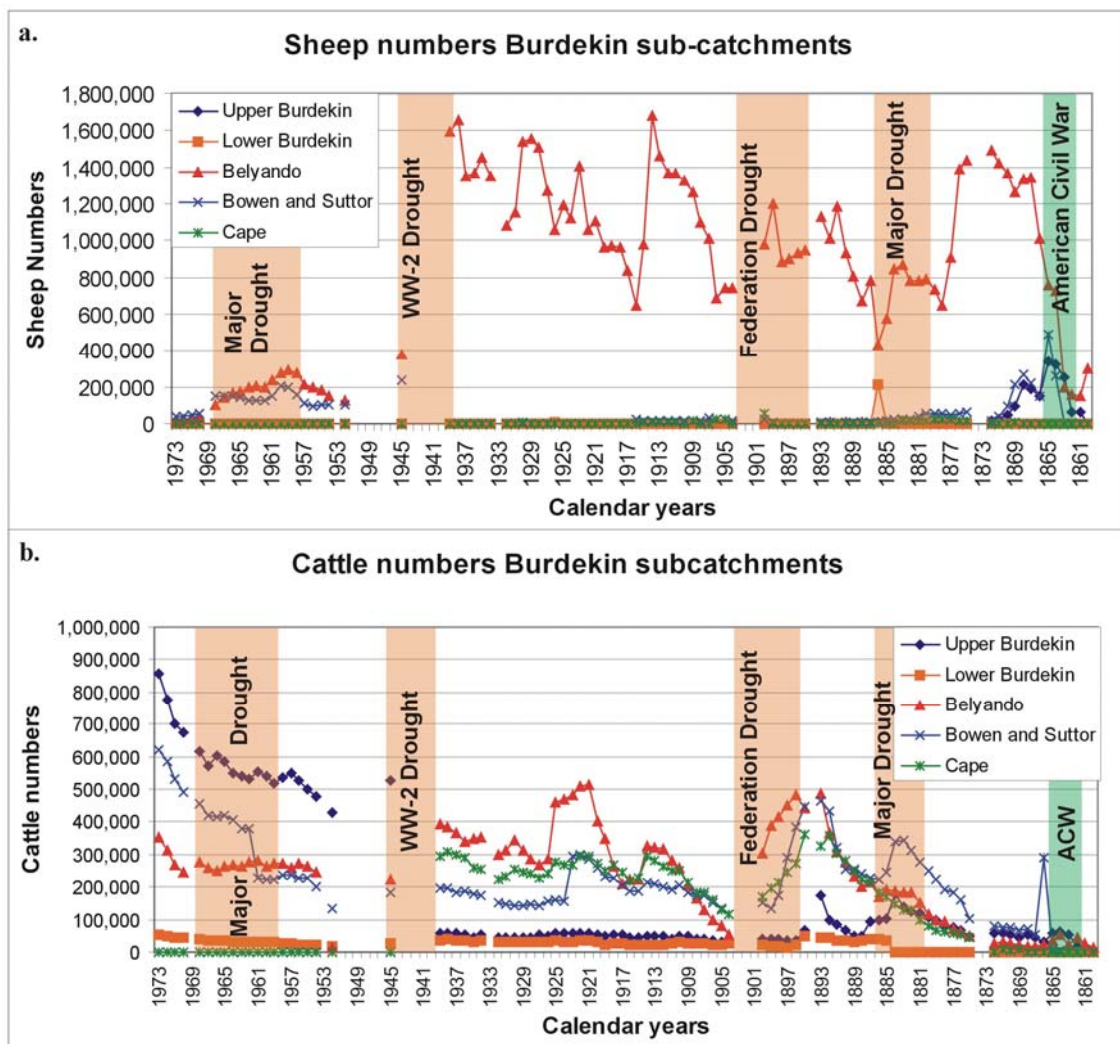
Figure 3.13 (a-b). Sheep numbers for the Burdekin River sub-catchments (a). The statistics indicate that the sheep industry was only prominent in Belyando sub-catchment. Major droughts typically coincided with declining sheep numbers; while the increased demand for wool by the British during the American Civil War (ACW) was linked to the initial expansion of the sheep industry in the Burdekin River catchment. Cattle numbers in the Burdekin River sub-catchments (b). Cattle are the most prominent industry in the Burdekin River catchment and use the most land. Cattle numbers increased particularly in the Bowen, Suttor, Cape and Belyando sub-catchments during the 1870s-1880s until significantly declining during the Federation Drought between 1895 and 1903. The cattle industry significantly increased in the Bowen, Suttor and upper Burdekin sub-catchments after World War II.

3.5.4. Summary

The Burdekin River catchment was first settled by Europeans in 1854 around the Clermont Township (Belyando and Suttor River sub-catchments). The land was initially used for sheep grazing and this industry boomed during the early 1860s, mainly because of the British demand for wool. Sheep farming in the Burdekin collapsed in the mid-1860s and cattle emerged as the prominent industry, which expanded in the 1870s particularly in the Belyando, Bowen and Suttor, and Cape River sub-catchments. Major droughts coincided with declines in both the sheep and cattle industries and the Federation Drought, in particular, severely affected these industries. Cattle numbers significantly increased in the upper Burdekin and Bowen and Suttor sub-catchments following World War II.

3.6. Characterisation of seawater quality on coral reefs

3.6.1. Overview

Changing water quality is considered one of the major factors affecting the health of the GBR (Devlin et al., 2001). Yet, water quality on coral reefs is a complex subject and involves many parameters such as SST, seawater salinity, nutrients and turbidity. In addition, "acceptable" water quality conditions are not well defined for coral reefs. This section will focus on changes to sediment and nutrient runoff since European settlement on the GBR and will examine the effect of increased nutrients and turbidity on the health of coral reefs using examples from Kaneohe Bay, Hawaii and from the GBR. Instrumental records of nutrient and turbidity levels from Cleveland Bay/Magnetic Island will also be discussed as will a case study which investigates the impact and history of dredging in Cleveland Bay on Magnetic Island's fringing reefs.

3.6.2. Accepted water quality conditions on coral reefs

Tropical coral reefs flourish at seawater temperatures between 25-29° C and salinities between 34 and 36‰ (Kinsman, 1964). Some tropical corals can, nevertheless, tolerate temperatures as low as 16-17° C and as high as 36-38° C, and salinities between 27 and

45‰ (Kinsman, 1964). The *Acropora* genus is thought to be the most sensitive to these parameters, while *Porites* is considered to be the most robust (Kinsman, 1964). Accepted nutrient and turbidity levels on coral reefs have long been debated in the scientific literature (e.g. Walker, 1991; Bell, 1991, Bell and Gabric, 1991; Kinsey, 1991a; Hopley et al., 1991). Some scientists consider that parts of the GBR have already been damaged by excess nutrients and by higher turbidity caused from human activity (Bell, 1992; Bell and Gabric, 1991; Fabricius, 2005; Fabricius et al., 2005). However, other researchers believe that the coral reefs of the inshore GBR have adapted to naturally high nutrient and turbidity levels over millennia (e.g. Larcombe et al., 2001; Smithers and Larcombe, 2003) and that any extra nutrients that may have entered the GBR lagoon since European settlement would be significantly diluted by the time they reach inshore reefs (Walker, 1991; Larcombe, 2001).

3.6.3. Seawater nutrient levels on the GBR and Cleveland Bay

Total nitrogen export to the GBR has doubled since 1850, while total phosphorus concentrations have tripled (Moss et al., 1992; Furnas, 2003). Nitrogen (N) and phosphorus (P) are largely exported to the GBR in particulate form, incorporated in sediments/soils, biomass and organic material. Dissolved inorganic N and P (DIN; DIP) and dissolved organic N and P (DON; DOP) make up the remaining sources of N and P flushed into the GBR (Furnas, 2003). The particulate nitrogen and phosphorus phases are released slowly into the inshore waters of the GBR through sediment reworking/resuspension processes. The controlling factor for elevated concentrations of chlorophyll a, nitrate, and phosphate, in Cleveland Bay, is bottom resuspension from wind-generated waves (Walker, 1981a; Walker and O'Donnell, 1981). Seawater silicate levels are mainly influenced by river runoff (Walker and O'Donnell, 1981). The dissolved inorganic components are consumed rapidly by marine organisms such as phytoplankton (Furnas, 2003; Furnas et al., 2005).

Seawater DIN and nitrite levels were reported to be above those considered by some authorities to promote healthy reef growth on the southeast fringing reefs of Magnetic Island (Brodie et al., 1992). Phosphorus and silicate concentrations were considered at "normal" levels; however, copper measurements were anomalously high.

Dissolved nutrients, chlorophyll a and suspended sediments in seawater were measured on the Nelly Bay fringing reef (Muslim, 1995; Muslim and Jones, 2003). Elevated chlorophyll a (a proxy for primary productivity) levels occurred after sediment resuspension, high temperatures, and rainfall (Muslim, 1995). The overwhelming control on dissolved nutrients and chlorophyll a in Nelly Bay is the resuspension of sediment driven by wind strength and direction (Muslim, 1995); this finding supports the previous works by Walker (1981a) and Walker and O'Donnell (1981). Bacterial blooms coincided with increased levels of inorganic phosphorus, chlorophyll a, and suspended sediment concentrations. Muslim's (1995) study found that chlorophyll a levels had more than doubled compared to the measurements by Brodie et al. (1992) and Walker (unpublished data) from the early 1980s and 1990s, respectively.

Dissolved ammonia and DON concentrations were also significantly higher than these previous studies. These findings may indicate that Nelly Bay has become eutrophic (Muslim and Jones, 2003) as nutrient and suspended sediment levels exceeded those found to cause a 20% decrease in coral calcification on coral reefs (Muslim, 1995). However, this dataset was produced during one of the driest years of the 20th century (1993-1994), and a corresponding study is required to substantiate these claims. Koskela et al. (2004) measured nutrient concentrations in Nelly Bay before and after the construction of the Nelly Bay Harbour in 2001 and 2003, respectively. Ammonia, phosphate and total phosphorus levels were substantially higher compared to the work of Brodie et al. (1992); these increased values were attributed to sewage discharge into Gustav Creek that flows into Nelly Bay. In between the study periods, the sewage was diverted to Picnic Bay, where a tertiary treatment plant was constructed. This diversion coincided with significantly lower seawater nutrient levels measured in 2003 (Koskela et al., 2004).

3.6.4. The effect of elevated nutrients on coral reefs and coral reef recovery from stress

Enhanced nutrient input over prolonged intervals encourages phytoplankton and hence zooplankton production and provides ideal conditions for communities such as barnacles and sponges, which gradually cause the demise of coral reefs (Kinsey, 1991b). Kinsey (1988) developed two categories of "abnormal stresses" in corals. Acute "natural" stresses are the result of storm events, freshwater inundation, and crown

of thorns starfish outbreaks; chronic "human induced" stresses are due to excess sediment input, elevated sewage discharge, increased nutrients, and tourism. Coral recovery is relatively rapid if only one type of stress is inflicted (Kinsey, 1991b); however, the combined effects of chronic and acute stresses can cause serious long-term damage to coral reefs.

Kaneohe Bay, in the Hawaiian Islands, illustrates how the combined effects of sewage, tourism, freshwater inundation and sedimentation resulted in the severe degradation of the coral reef ecosystem and lead to the overgrowth of particle feeding epifauna and infauna. The diversion of the sewage discharge pipes from Kaneohe Bay significantly decreased the nutrient input, and resulted in the disappearance of the filter feeders and formation of an algal-dominated community. The algae community eventually declined and was followed by the recolonisation by new coral recruits and subsequent coral recovery (Kinsey, 1991b; Maragos et al., 1985).

Increased nutrients were added to a reef from One Tree Island in the southern GBR over 8 months to maintain seawater nitrogen and phosphate levels at 20 μM and 2 μM, respectively (Kinsey, 1988). The community structure was scarcely affected but coral calcification decreased by as much as 50-60%. Another experiment on One Tree Island (ENCORE) was performed over a 2 year period which investigated the separate effects of nitrogen and phosphorus on coral reefs (Koop et al., 2001). Interestingly, the high loading of nitrogen in the second year of the experiment (mean dose= 36.2 μM) resulted in a number of significant biotic responses in corals including stunted growth and declines in coral reproduction (Koop et al., 2001). The addition of phosphorus also hindered coral reproduction, although coral extension and calcification rates increased. However, average coral density declined which made the corals more susceptible to breakage (Koop et al., 2001).

Elevated nutrients on coral reefs from changes in terrestrial runoff may initiate Crown of Thorns Starfish (COTS) outbreaks which, in turn, can severely damage the hard coral communities (Birkeland, 1982; Brodie et al., 2005a). Walbran et al. (1989) measured skeletal remains of the COTS in C-14 dated sediment cores taken along individual reefs of the GBR, and discovered COTS outbreaks had occurred over the last 8,000 years. This research was criticised by some scientists who cited the mobility of the COTS and

the apparent lack of stratigraphic control in the cores from bioturbation as potential flaws in this study (Keesing et al., 1992; Pandolfi, 1992). However, the sediment cores displayed a reliable age structure and the presence of contemporary COTS skeletal remains were discovered in modern superficial sediments, where outbreaks had occurred after the 1960s (Henderson and Walbran, 1992). A correlation between COTS outbreaks and increased terrestrial runoff was discovered by Brodie et al. (2005a); the enhanced terrestrial runoff since European settlement may have contributed to an increase in the frequency of COTS outbreaks at inshore coral reefs (Brodie et al., 2005a). Increased seawater nutrient levels have also been linked to outbreaks of coral disease in reefs from the Caribbean (Bruno et al., 2003).

Elevated nutrient and suspended sediment concentrations in seawater also provide ideal conditions for sediments to aggregate and settle out as "marine snow" which can have detrimental effects on coral reefs (Fabricius and Wolanski, 2000). Evidence of marine snow has been reported near Cairns which may have considerably affected coral reefs at this location (Wolanski and Spagnol, 2000). Additional evidence of the effects of enhanced nutrient input to the inshore GBR was reported by Blake (1994) in the coral reefs of the Whitsunday Island Group. A phase shift from a coral to an algal-dominated community occurred in a coral reef from Repulse Bay and this shift coincided with the highest measured dissolved inorganic nutrients and suspended solid concentrations in the Whitsunday Island Group (Blake, 1994; van Woesik et al., 1999).

3.6.5.   Sediment runoff and turbidity levels on the GBR

Moss et al. (1992) modelled sediment input to the GBR and concluded that sediment input had increased by 3-5 times since European settlement. This model has been developed by Prosser et al. (2001), Neil et al. (2002), Furnas (2003) and Brodie et al. (2003). Prosser et al. (2001) applied the "*Sed Net*" modelling program to the catchments of the GBR and particularly examined parameters for sediment erosion such as topography, vegetation cover, rainfall, soil type and land-use. This model estimated that sediment export to the GBR had increased by a factor of 10 since 1850 (Prosser et al., 2001). Neil et al. (2002) and Furnas (2003) have suggested that sediment export has increased by a factor of 4, which better corresponds to the earlier study by Moss et al. (1992).

A significant increase in coral Ba/Ca ratios from Havannah Island after 1870 coincided with the expansion of the cattle industry in the Burdekin River catchment (Fig 2.13; McCulloch et al., 2003). This significant rise is thought to reflect increased sediment runoff as a result of riverbank erosion from cattle and sheep farming (McCulloch et al., 2003). The magnitude of the coral Ba/Ca rise is thought to represent a 5-10 fold increase in sediment exported to the GBR and matches the estimates produced by the models. This increase in sediment may have resulted in enhanced turbidity along the inshore coral reefs (McCulloch, 2003; 2004; Fabricius and De'ath, 2001a; Fabricius, 2005; Wolanski and Spagnol, 2000). Yet this hypothesis of increased turbidity is disputed in the literature as turbidity levels are controlled by resuspension of bottom sediments (Larcombe et al., 1995a; Larcombe and Woolfe, 1999a; Larcombe, 2001). A typical river plume extending 45 km along the coastline and 10 km wide is estimated to contain approximately 2,700-9,000 tonnes of sediment, which is significantly less than can be held in suspension from swell waves (Larcombe and Woolfe, 1999a; Larcombe, 2001). River plumes only occupy the top 2-3 m of the water column and, on average, contain suspended sediment concentrations of up to 3 mg/L away from the river mouth (Taylor, 1995). This result is negligible when compared to depth-average readings of up to 50 mg/L measured at some inshore coral reefs in water depths up to 10 m (Larcombe et al., 1995a; Woolfe and Larcombe, 1999). In addition, sediments on the seafloor at depths of less then 10 m become resuspended, on average, more than 110 days per year (Orpin et al., 1999).

Suspended sediment concentrations (SSC) were measured by nephelometers deployed in Geoffrey and Arthur Bays to investigate turbidity levels on inshore coral reefs (Magnetic Island; Larcombe et al., 1995a). SSC exceeded 5 mg/L on 30-40% during the time-measured series; although SSC were rarely higher than 40 mg/L. In some cases, SSC that had exceeded 20 mg/L were recorded over 24 hour periods. These conditions probably have been consistent for the last 6,000 years and inshore coral reefs are well adapted to the relatively high turbidity levels (Larcombe et al., 1995a). Significantly elevated turbidity concentrations were measured on living coral reefs of the Paluma Shoals, north of Townsville (Larcombe et al., 2001). SSC exceeded 40 mg/L over 40 days per year and reached as high as 175 mg/L. However, negligible net sediment accumulation has been reported on the inshore fringing reefs of the GBR despite the relatively high turbidity levels and an increased sediment supply since

European settlement (Woolfe and Larcombe, 1999; Larcombe and Woolfe, 1999b; Larcombe et al., 2001). Suspended sediment concentrations were found to be correlated with wind speed and direction (Larcombe et al., 1995a). South-easterly trade winds transport suspended sediment northwards along the coast (Orpin et al., 1999) and, in turn, sediment particles display a greater maturity (mineralogy, sorting and roundness) further northwards (Lambeck and Woolfe, 2000). The location of near-shore coral reefs are primarily controlled by substrate availability (Woolfe and Larcombe, 1998). Corals can potentially withstand relatively high SSC, but cannot grow without a hard, stable substrate. It has been hypothesised that the erosion of nearshore unconsolidated sediments may have exposed consolidated Pleistocene sediments and this exposure of a hard substrate may be related to the timing of first reef growth during the Holocene (Larcombe and Woolfe, 1999b).

3.6.6. Dredging in Cleveland Bay and the impacts on Magnetic Island's fringing reefs

The history of channel dredging and the dumping of spoil for shipping in the Townsville Port have been reviewed by Pringle (1989; 1996). Historical documents indicate that the dredge spoil was dumped in Cockle Bay from 1883-1893. Spoil was dumped near Middle Reef (Fig 1.3) before the mid-1960s, while both shallow and deep draft dump sites southeast of Magnetic Island have been exploited since the 1960-70s (Pringle, 1989). Dredging of Platypus Channel is necessary 1-2 times per year in order to maintain navigable depths in Townsville harbour (Hilliard and Raaymakers, 1996). Typical dredging quantities are approximately 170,000 m^3 per year; however, emergency dredging after a flood or tropical cyclone may be required. For instance, 460,000 m^3 of spoil was dredged from the channel after Tropical Cyclone Althea (Hilliard and Raaymakers, 1996). Under calm conditions, the dumped spoil compacts to about 8% of its original volume within 4 days of dumping, but in moderate to rough inshore conditions, suspended solids may drift away with wind generated currents (Wolanski et al., 1991; 1992). Evidence of spoil dumping east of Magnetic Island has been found in seismic profiles and vibrocores reported by Carter et al. (1993; Fig 3.14).
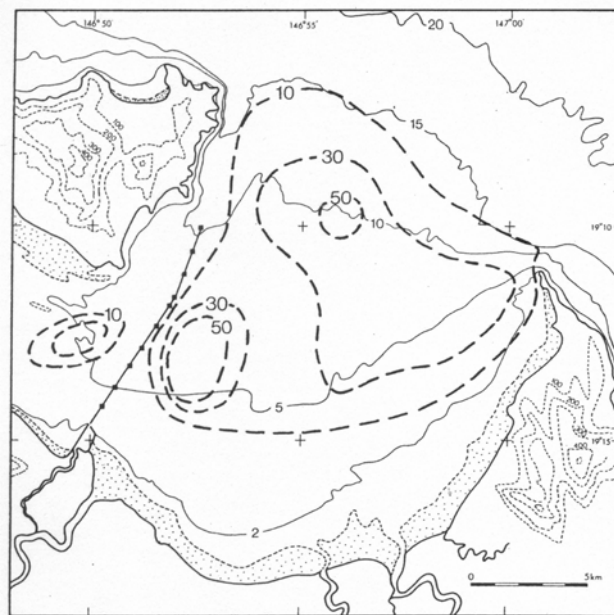
Figure 3.14. Isobath map (in cm) displaying the dumping sites of the dredged spoil taken from Platypus Channel (from Carter et al., 1993).

Fringing reefs on Magnetic Island were documented by Brown (1972) as having "lush coral development," particularly on the eastern side of the island when his study commenced in 1961. An extensive coral reef on the southern end of the island (Cockle Bay) was interpreted to have succumbed to siltation following the dumping of dredged spoil. Waters in this area were observed to be extremely turbid, but waters on the eastern side of the island, including Nelly Bay, were clear. Between 1961 and 1965 fine sediment destroyed most of the coral colonies in the Cockle Bay reef complex. Brown returned to the island in 1969 and discovered turbid water conditions in Nelly Bay. Observations of the fringing reefs were regularly conducted during 1970-72. Over this period severe disturbance was observed: coral colonies became pale and encrusted with algal growth forms (Fig 3.15) and *Acropora* and *Montipora* corals were particularly affected by the elevated turbidity. By 1971, siltation had destroyed about 60% of the tabular and branching corals. Regrowth occurred by mid-1972 but coral diversity was severely affected and only some species displayed signs of regeneration (Brown, 1972). However, Collins (1987) believes that there is no substantial evidence of siltation during this period. He considered that freshwater dilution from heavy rainfall, generated from Tropical Cyclones Althea (1971) and Bronwyn (1972) caused the coral mortality. Long-term residents of Magnetic Island also have contradictory views about the effects of channel dredging on the island's fringing coral reefs (Appendix 1).

Particulate matter on coral colonies was collected before and after 2 dredging periods in Cleveland Bay and analysed for heavy metal concentrations (Reichelt, 1993; Reichelt and Jones, 1994). Significant increases in Cu, Zn and Pb were recorded in sites from Middle Reef shortly after dredging but little change was recorded in Picnic and Geoffrey Bays. Analyses of sediment samples collected in Cleveland Bay revealed that some inshore sites were contaminated with Cu, Zn, Pb, Ni, and Fe (Reichelt, 1993). This contamination was attributed to port activities, sewage discharge, and urbanisation. Enhanced metal concentrations recorded at some coral reef sites may not only be the result of dredging activities, but may arise from the release and transport of contaminated sediments within the port area. Nevertheless, the heavy metal concentrations are still well below their respective sediment quality recommended limits (Reichelt and Jones, 1994). Aerial photography revealed that suspended sediment drifted towards Magnetic Island during the channel dredging operation (Fig 3.16). Dissolved inorganic phosphate, total dissolved phosphate, dissolved ammonium levels, chlorophyll a, and SSC in Nelly Bay were significantly elevated in Nelly Bay during the 1994 intensive capital dredging of Platypus Channel (Muslim, 1995; Muslim and Jones, 2003). Nephelometer data, however, from Middle Reef, Nelly, Geoffrey, Florence, and Arthur Bays before, during, and after the dredging reveal that no detectable fluctuations in turbidity could be attributed to the dredging activity (Larcombe and Ridd, 1994). Turbidity was found to be highly variable around the embayments and was significantly correlated with wind strength and direction (Larcombe and Ridd, 1994; Larcombe et al., 1995a).
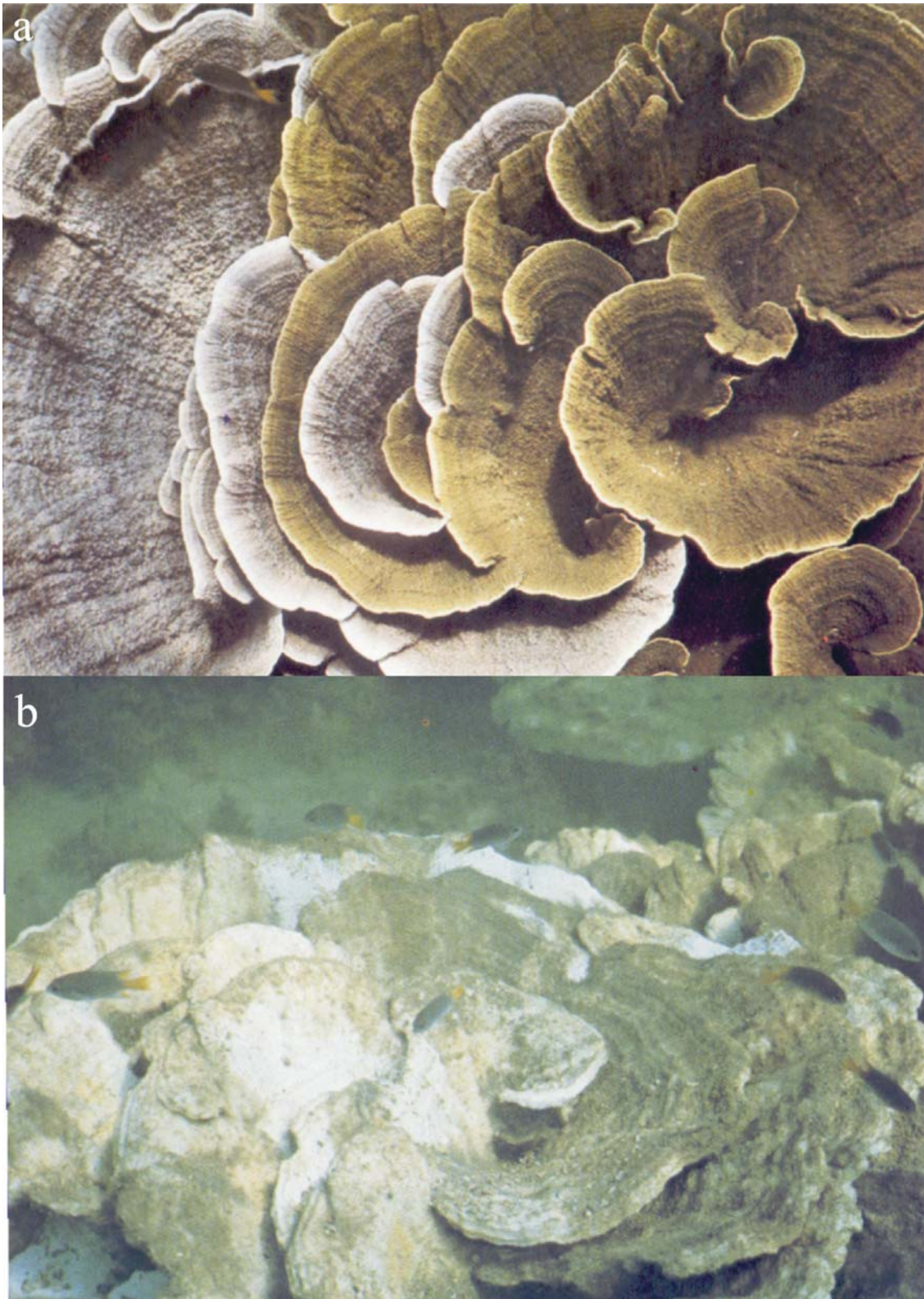
Figure 3.15. *Montipora* coral in Nelly Bay a) coral in 1969; b) the same coral in 1971. Plate corals appear to have been severely affected by siltation due to the 1970 dredging of the shipping channel (from Brown, 1979).

Figure 3.16. The dredge in operation causing turbid water to drift in towards Nelly Bay (Photo: Sinclair Knight Merz; taken from Reichelt, 1993).

3.6.7. Summary

The amount of sediments and nutrients exported from rivers has increased significantly since European settlement and it appears that seawater nutrient levels have risen significantly in the Cleveland Bay/Magnetic Island area. In addition, turbidity levels may be higher since European settlement. A decline in water quality is known to have

deleterious effects on coral reef ecosystems; however, accepted water quality conditions for coral reefs are not well defined and instrumental measurements of turbidity and nutrients on coral reefs are restricted to only the last two decades. The degree of damage to the fringing reefs of Magnetic Island from dredging in Cleveland Bay remains controversial.

3.7. Chapter summary

➢ Cleveland Bay is a low energy, north facing embayment that contains Magnetic Island. In turn, Magnetic Island has a number of fringing coral reefs.

➢ The Nelly Bay fringing reef is thought to have initiated approximately 7,000 years ago.

➢ The Burdekin River dominates the terrigenous sediment supply to Cleveland Bay and switched to a southerly course approximately 3,000 years ago.

➢ The timing, magnitude and mechanisms relating to Holocene sea level for north Queensland is disputed in the literature.

➢ It is thought that sea level reached its present elevation around 6,500 years ago and has remained more or less (within 2-3 m) at this height.

➢ Cleveland Bay experiences highly variable annual rainfall which is related to ENSO events.

➢ Holocene proxy climate records for north Queensland and the GBR are sparse.

➢ It is thought that SSTs on the GBR have warmed from the early Holocene by approximately 2-3° C; however, it appears that climate during the mid-late Holocene may have been variable.

➢ The SST record for the mid-Holocene is controversial and coral proxy records only cover periods of less than 15 years.

➢ The mid-Holocene climate in north Queensland was wetter, and a change to more "drier" conditions occurred about 3,000 years ago which may have coincided with the onset of a more ENSO-dominated climate.

➢ Large cyclonic events occur every 100-200 years which can significantly alter the short-term makeup of coral reefs by damaging hard coral communities.

➢ The Burdekin River catchment was settled by Europeans in 1854 and quickly became sub-divided for sheep and cattle grazing.

> ➢ Cattle became the desired industry after sheep farming in the Burdekin catchment collapsed. Cattle numbers in the Belyando, Bowen, Suttor and Cape River sub-catchments rose significantly in the 1870s-1880s, and also increased after World War II in the upper Burdekin, Bowen and Suttor sub-catchments.

> ➢ The "accepted limits" for water quality parameters on the GBR are not well defined.

> ➢ Nutrient levels in Cleveland Bay/Magnetic Island appear to have increased significantly over the last two decades; however, there are no long-term instrumental measurements of nutrient levels on the GBR.

> ➢ Relatively high seawater turbidity levels (compared to the outer GBR) occur in Cleveland Bay, which most scientists consider to be a natural phenomenon; however, as with nutrient levels, there are no available long-term instrumental turbidity measurements.

> ➢ The impact of channel dredging in Cleveland Bay on the fringing reefs of Magnetic Island is controversial.

Chapter 4

Methods

4.1.   Chapter overview

This chapter summarises the methods used in this study including the construction of the sedimentary evolution/stratigraphy of Nelly Bay, to the geochemical and physical proxies of SST, salinity and water quality. The chapter is presented in three sections:

1) Section 4.2 examines the scientific methodology used to construct the stratigraphy and stratigraphic model of Nelly Bay including topographic profiling, the collection of sediment cores, the sampling of oyster beds, carbon dating and the geochemical analysis of the sediments.

2) Section 4.3 describes sampling and geochemical analyses of the Magnetic Island corals including coral collection, coral dating, microanalytical procedures, the sampling of coral slices and the sample preparation procedure for the geochemical analyses. In addition, the analytical techniques and the calibrations that were used to reconstruct SST are detailed.

3) Section 4.4 describes the sources and techniques used for the compilation of the instrumental datasets. These include rainfall records, Burdekin River discharge data, coral luminescence and calcification data, and instrumental sea surface temperature and turbidity data.

4.2.   Construction of the stratigraphy in Nelly Bay

4.2.1. Overview

In order to construct the stratigraphy and produce a stratigraphic model of Nelly Bay for the Holocene, a number of tasks were performed. These included a review of previous investigations, topographic profiling as well as the collection of sediment cores for dating, geochemical and mineralogical analyses. A fossil oyster bed was sampled and dated to contribute to the construction of a new Holocene sea-level curve for eastern Australia. This section will present the methodology undertaken to understand the age

of the fossil corals, the origin of the terrigenous sediments in Nelly Bay, the Holocene sea levels, the development and evolution of the Nelly Bay fringing reef, and ultimately, the stratigraphy of the embayment.

4.2.2. Overview of previous data and techniques

Planning for the Nelly Bay Harbour development evolved over 20 years and involved a number of surveys. This study has compiled data from these previous surveys and from additional sources. In order to develop a stratigraphic profile of Nelly Bay with an accurate age control, sediment coring, carbon dating and topographical profiling were completed to complement these previous datasets. The coring did not penetrate into the Pleistocene sediments; therefore, seismic profiles from Carter and Johnson (1989) and Sinclair Knight Merz (1998) were used to define this boundary. Drill logs from McIntyre and Associates Pty Ltd (7 rotary boreholes and 28 excavation pits; 1986; 1989) and Golder Associates Pty Ltd (17 rotary boreholes; 2000) were compared with the sediment cores from Nelly Bay.

4.2.3. Topographic profiles

Topographic surveys were performed along three transects in Nelly Bay where sediment cores were also taken (Fig 4.1). The surveys were conducted using a theodolite (Fig 4.2) and levels were corrected to sea-level datum by measuring the previous high tide mark. The tidal level was also measured at the time of each survey in order to cross-check the sea-level datum. Geomorphological characteristics along these transects were also documented.
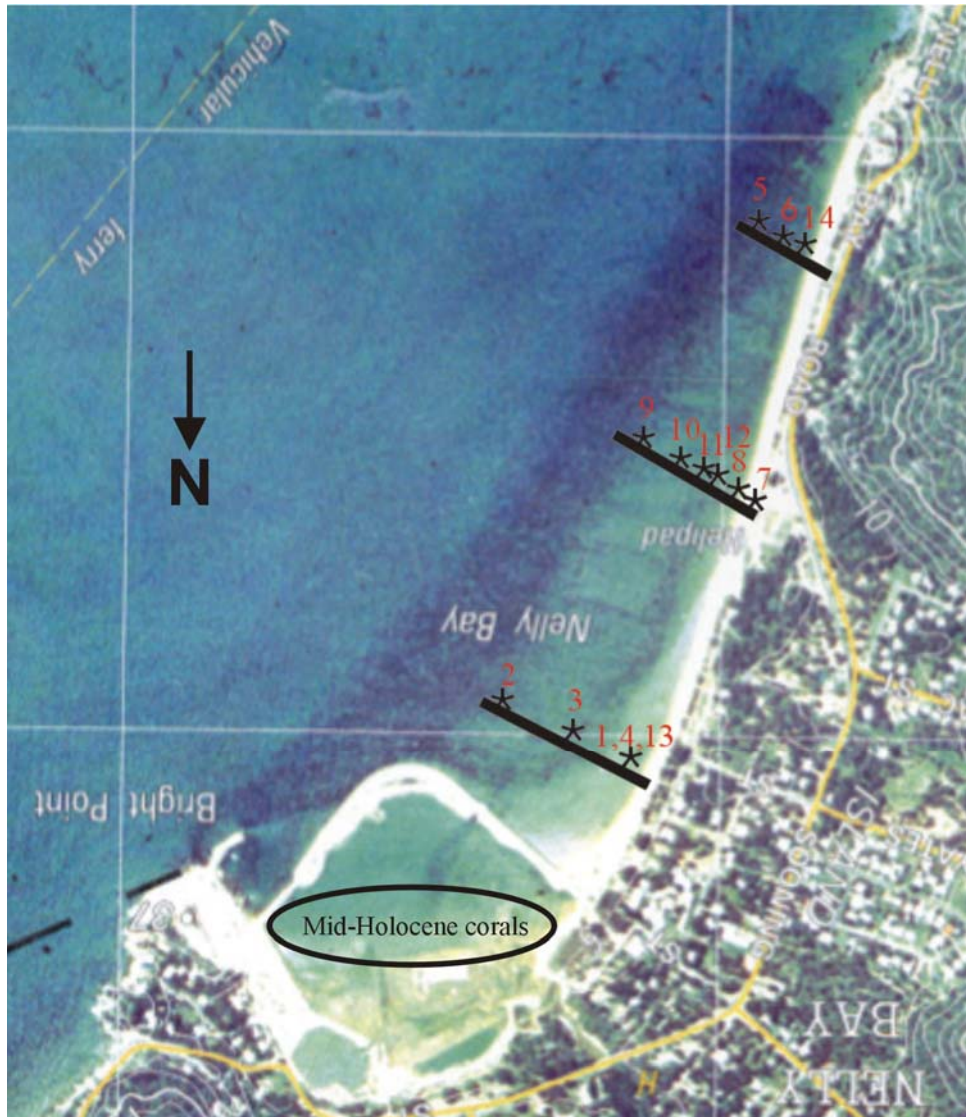
Figure 4.1. Three transects were surveyed in Nelly Bay using a theodolite. Sediment cores were taken along these transects to develop the stratigraphy. The present reef flat is the dark shaded area located seawards of the present harbour site. Note the location where the mid-Holocene corals were recovered.

Figure 4.2. Topographical surveying in Nelly Bay using a theodolite.

4.2.4. Sediment cores

Fourteen sediment cores were taken along the three transects in Nelly Bay to gain a perspective of the Holocene stratigraphic units within the embayment (Fig 4.1). Aluminium pipes, up to 4 m in length and 7.5 cm in diameter, were driven into the ground surface with a star-picket driver. A 2 m stepladder added extra height for maximum penetration of the sediment cores (Fig 4.3a). On average, the cores were driven 2 m into the ground surface with a maximum penetration of 3 m for core 13. Each core was terminated when the pipe could no longer be driven into the ground or when the length of the pipe ran out. The core was filled with water and sealed with a rubber plug. The cores were then winched to the surface with a tripod (Fig 4.3b). Typical core recovery was approximately 1.5 m with a maximum of 2 m for core 13. This result indicates that, on average, about 25-30% of sediment was compacted during the coring process.

Figure 4.3a. Sediment coring in Nelly Bay. Aluminium pipes were driven into the ground surface with a star picket driver. To gain extra height a 2 m stepladder was used. Average penetration was about 2 m.

Figure 4.3b. The sediment cores were retrieved using a tripod. The cores were filled with water and sealed with a rubber plug. Typical recovery was approximately 1.5 m.

The sediment cores were logged by examining changes in grainsize distribution and composition. Six stratigraphic units were characterised according to the ratio of coral fragments to terrigenous sediments and to the grainsize distribution of the sediments. Each unit was then corrected uniformly for compaction although different sedimentary layers would compact differently. Thus, a uniform compaction may introduce a slight error in the corrected thickness of the sedimentary layers.

The mineralogical composition of six samples from core 13 were analysed using a *D5000 Siemens X-ray Diffractometer* (XRD) at the Advanced Analytical Centre (AAC) at James Cook University (JCU). To represent the stratigraphic succession, samples were taken at increments of 3 cm, 36 cm, 93 cm, 106 cm, 175 cm and 195 cm from the top of the core. The samples were then pulverised in a zirconia mill. The pulverised powders were mixed to a paste with water, smeared onto a glass disc and submitted to XRD analysis. XRD data was quantified using a "Rietvel" synthesis from the software package *Siroquant™*.

Cores 13, 2 and 8 were sampled for AMS radiocarbon analysis to establish an age control for the stratigraphy in Nelly Bay. Seven shell and six coral fragments were selected at various increments in these cores to best represent the sedimentary layers in Nelly Bay. Core 13 was sampled at 27-30 cm (shell), 72-76 cm (shell), 107-111 (shell and coral), 146-150 cm (shell), 177-180 cm (coral) and 194-198 cm (coral) from the top of the core. Core 2 was sampled at 16-19 cm (coral), 53-57 cm (shell), 80-84 cm (coral) and 122-126 cm (coral) from the core top while core 8 was sampled at 70-73 cm (shell) and 103-107 cm (shell) increments from the top of the core.

4.2.5. Oyster beds

A fossil oyster bed (*Saccostrea cuccullata*: J. Collins personal communication, 2005) in Huntingfield Bay, Magnetic Island (Fig 1.3), was 1.75 m (± 0.05; splash zone), 1.55-1.35 m (main bed), and 0.95 m (lower oyster colony) above the living beds (Fig 4.4). Five samples were taken from the splash zone (1), the main oyster bed (3; inner, middle and outer zone) and 1 sample from the lower colony for AMS carbon dating.
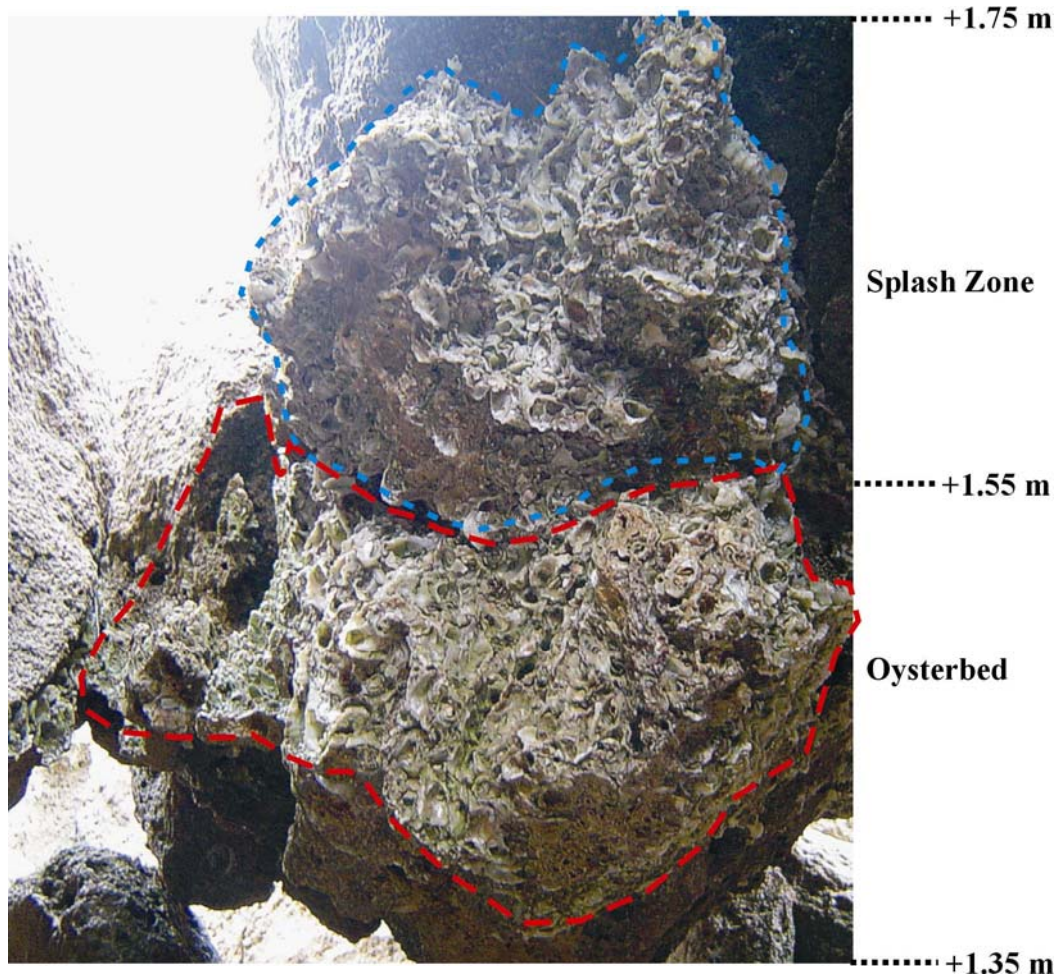
Figure 4.4. A fossil oyster bed in Huntingfield Bay, Magnetic Island, was sampled for AMS radiocarbon dating to constrain sea level during the mid-Holocene. The measurements were calculated to the height above the living oyster bed.

4.2.6. Carbon dating of the sediment cores, oyster beds and corals

Twenty samples were prepared for AMS C-14 dating at the Australian Nuclear Science and Technology Organisation (ANSTO) in Lucas Heights, Sydney. The samples included the 13 coral and shell fragments from the sediment cores, the 5 oyster bed samples and the 2 coral samples from the NEL03D coral core. The samples were cleaned with a stainless steel drill and wheel cutter, and etched with 0.5 M HCl acid for approximately 1 min and then thoroughly rinsed with milli-Q water to remove any surface contamination. The samples were then placed in a 60° C oven for 2 days to dry. Samples were reduced to 20-30 mg pieces and dissolved in 2 ml of 85% phosphoric acid. The CO_2 released in this process was captured and converted to graphite (Fink et al., 2004). The graphite was pressed in a tin cup and analysed at the ANTARES AMS centre (Fink et al., 2004).

4.2.7.   Sediment samples

Sediment samples from the wider region around Nelly Bay were analysed for their trace element compositions to discover the provenance of the Nelly Bay sediments. Grab samples were collected from the Burdekin Falls Dam (2; Lake Dalrymple), Ross River Dam (2), the Townsville Port Shipping Channel (1), and from the outer reef slope in Nelly Bay (1). The sediments were collected in a small (225×180 mm) stainless steel *Van Veen* grab sampler. One sediment sample was also hand-scooped from the freshwater section of Gustav Creek which discharges into Nelly Bay. Five sediment samples from core 13 (at 40 cm, 88-90 cm, 110 cm, 180 cm, and 198 cm increments from the top of the core) and 1 sample from core 2 (107 cm from the top of the core) were sampled for the trace element analyses to match the regional geochemical signatures with the sediment cores. The thirteen sediment samples were all washed through an 80 μm sieve as the fine fraction is considered the most reliable to establish a distinctive geochemical fingerprint.

4.2.8.   Geochemistry- sediment samples

The geochemical analyses of the sediment samples were undertaken at the Advanced Centre for Queensland University Isotope Research Excellence (ACQUIRE) laboratory at the University of Queensland (UQ). The sediment samples were bombed digested with a mixture of double distilled hydrofluoric and nitric acids and analysed by ICP-MS for Li, Be, Sc, Ti, V, Cr, Co, Ni, Cu, Zn, Ga, As, Rb, Sr, Y, Zr, Nb, Mo, Cd, Sn, Sb, Cs, Ba, La, Ce, Pr, Nd, Sm, Eu, Tb, Gd, Dy, Ho, Er, Tm, Yb, Lu, Hf, Ta, W, Tl, Pb, Th and U (e.g. Kamber et al., 2005).

4.2.9.   Summary

This study drew on information from drilling logs and seismic data taken during the construction of the Nelly Bay Harbour. In addition, three topographic profiles and 14 sediment cores were taken along transects within Nelly Bay. The cores were logged and the sediment layers were identified according to grainsize and composition. Samples from selected cores were submitted to three forms of analyses: XRD, trace element geochemistry and C-14 analysis. These analyses allowed the sedimentary

layers in Nelly Bay to be characterised by their mineralogy, chemistry and age. Sea level during the Holocene was assessed by radiocarbon analysis of samples from fossil oyster beds at 1.55 m above their nearest living counterparts.

4.3.   Coral geochemistry

4.3.1. Overview

Several geochemical techniques were used to analyse the Magnetic Island corals for trace elements, isotopic composition and radiocarbon levels (age). This section describes the sampling, preparation and analytical procedures for these geochemical analyses. In addition, this section outlines the methods of coral collection, coring, slabbing and cleaning in order to prepare the corals for sampling as well as the microanalytical analyses to ensure that the corals were free of diagenesis. The SST calibrations for the coral Sr/Ca, Mg/Ca and U/Ca ratios that were applied to the data are also discussed.

4.3.2. *Porites* coral collection and preparation

Eight large (2-3 m in diameter; Fig 1.4) fossil mid-Holocene *Porites* coral heads, recovered during the construction of the Nelly Bay Harbour in early 2001, were transported to the Australian Institute of Marine Science (AIMS). The corals were cored at AIMS using an aluminium frame with a hydraulic drill and pump (Fig 4.5). The cores were recovered using core barrels, approximately 900 mm long with a diameter of 75-80 mm and containing a tungsten tip. The cores were then cut into 7 mm thick slices with a diamond saw. The slices were cleaned in an ultrasonic bath with milli-Q water and dried (as described in Hendy et al., 2002; Isdale at al., 1998). Three additional living *Porites* coral cores were collected, following the technique of Isdale and Daniel (1989). The cores were gathered in 1987, 2001 and 2004 by AIMS from Geoffrey Bay (MAG01) and Nelly Bay (NEL09; NEL21). X-ray records (Fig 4.6-4.12; courtesy of AIMS) were viewed to determine which coral cores contained the best growth axes to sample for trace element geochemistry. Four of the mid-Holocene corals (NEL01D, NEL03D, NEL06A, and NEL07C) contained growth axes suitable for coral geochemistry. The coral cores from Geoffrey Bay (MAG01D) and Nelly Bay

(NEL21A) also displayed ideal growth records (Fig 4.10; 4.12), but the other modern coral from Nelly Bay (NEL09D) contained a poor growth record (Fig 4.11). A coral colony taken from Pandora Reef was homogenised and used as a standard.

Figure 4.5. The mid-Holocene corals were cored using a hydraulic drill and pump with an aluminium frame (Photo: AIMS).
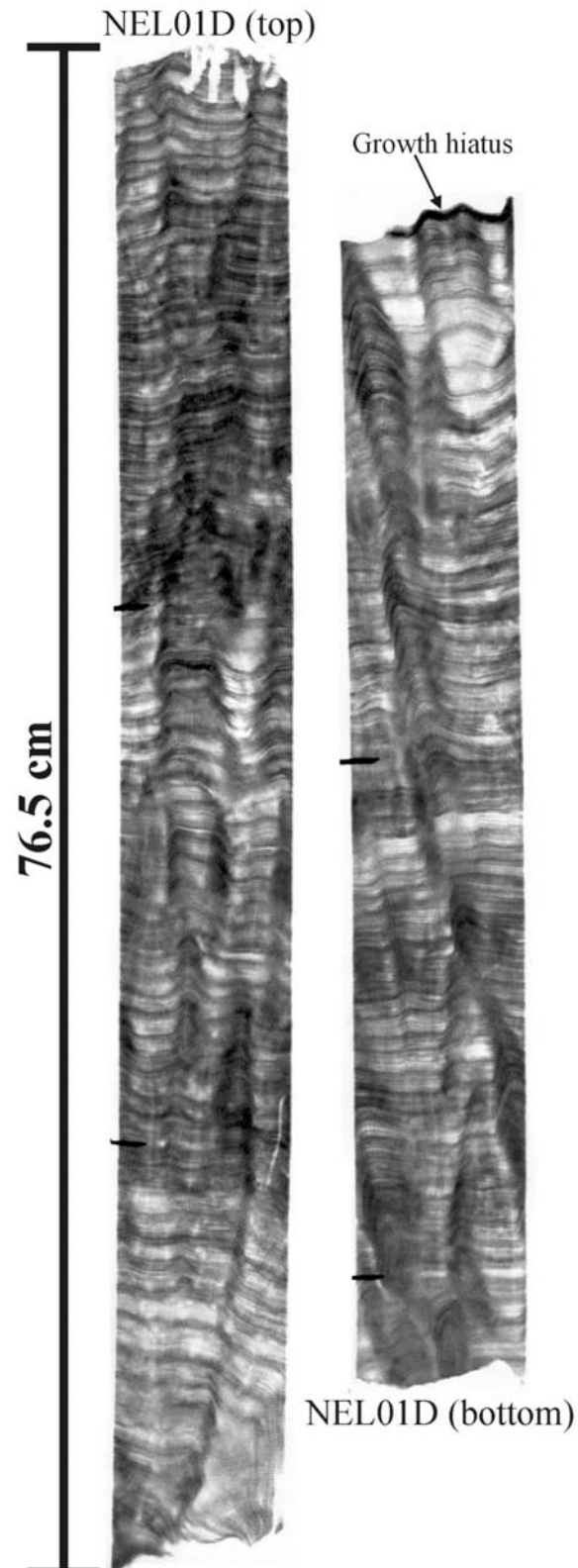
Figure 4.6. Coral x-ray positive print of NEL01D. Note the annual growth banding; the high density dark bands are characteristic of winter growth. Also note the top of the "bottom" slice is a distinct growth hiatus where the coral has died and then regenerated.
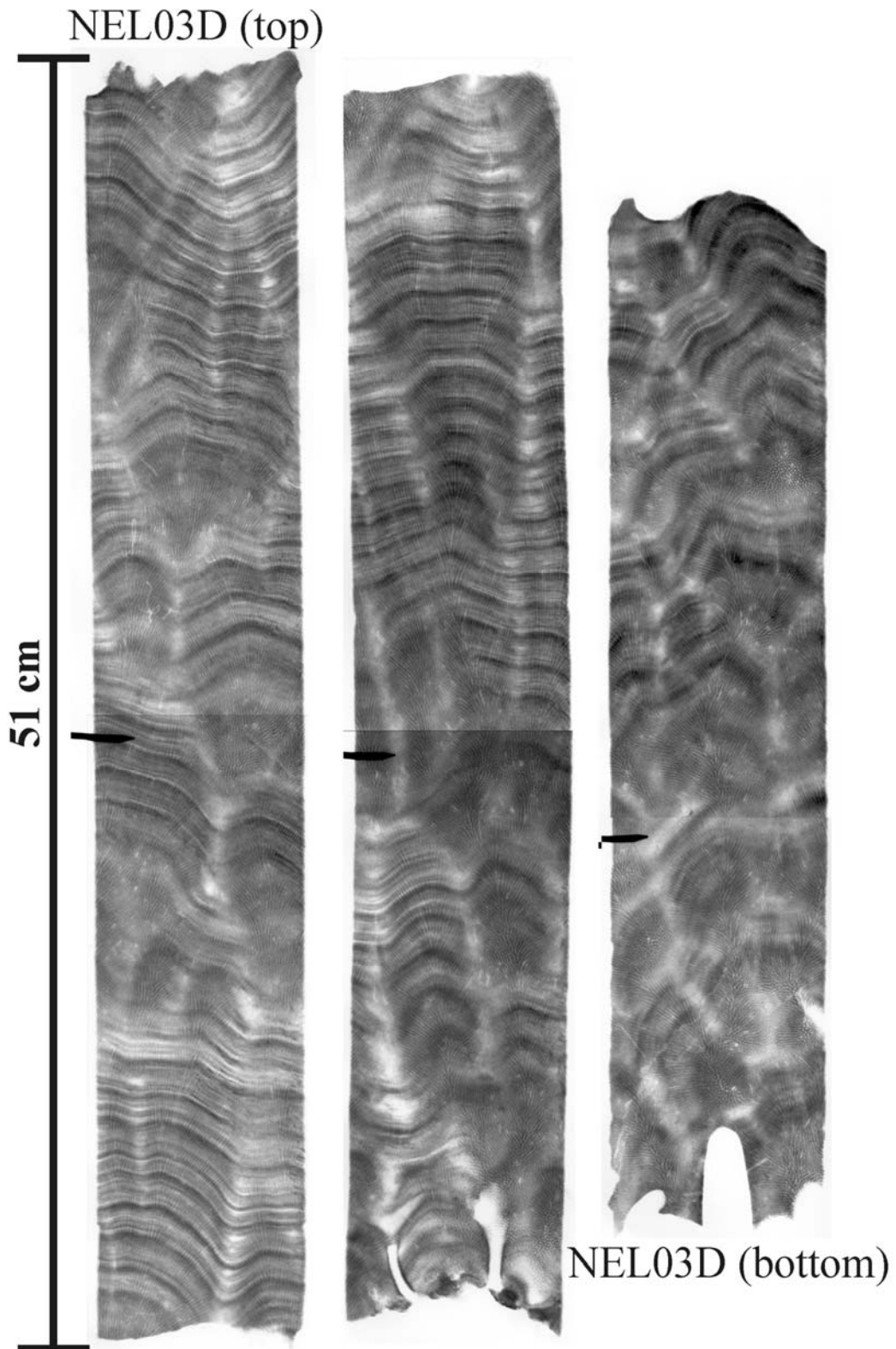
Figure 4.7. X-ray positive print of NEL03D. Note the poor growth record at the bottom of the coral slice which was discarded during sampling. There is a growth hiatus at the top of the "bottom" slice, as in NEL01D.
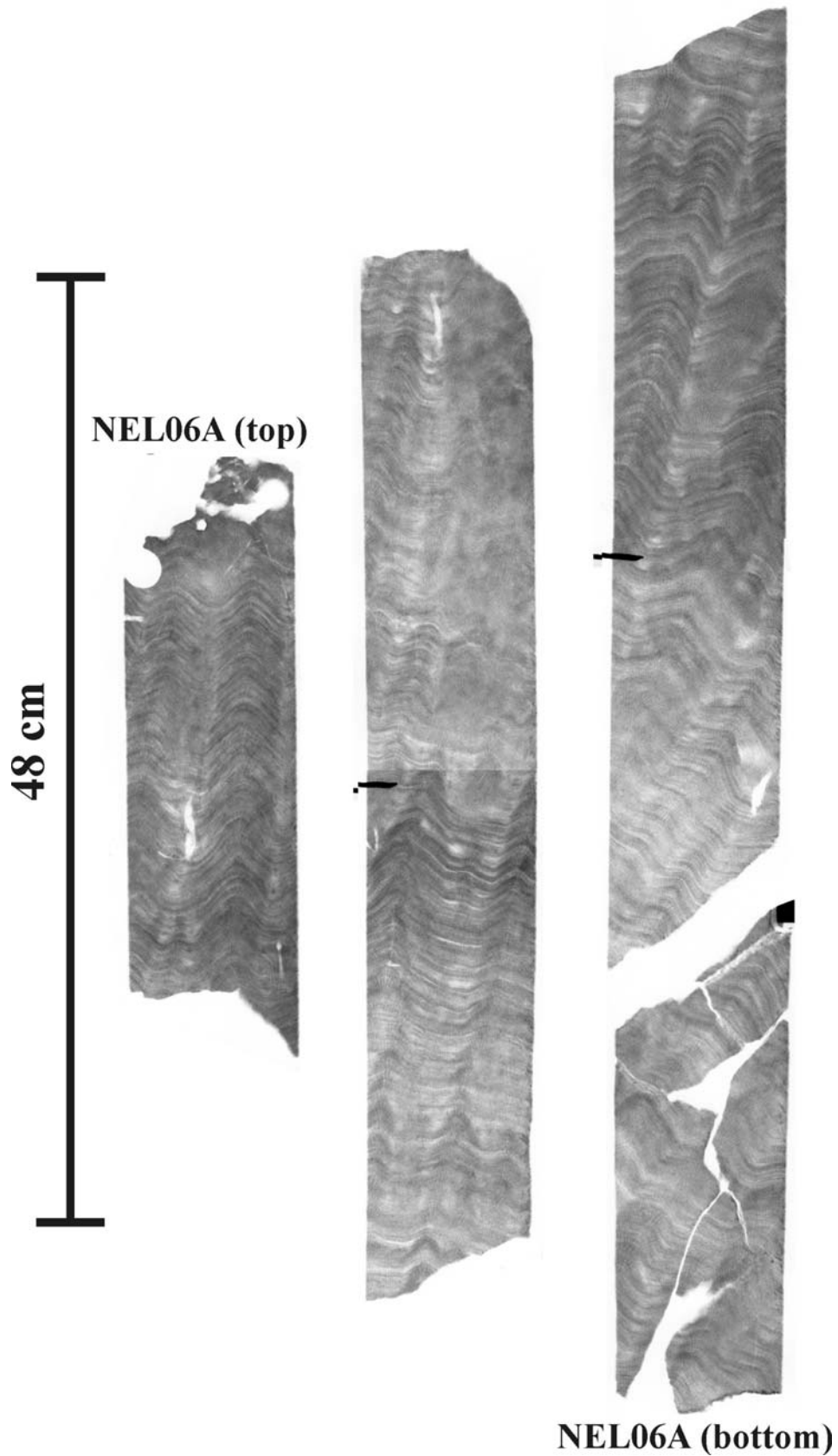
Figure 4.8. X-ray positive print for NEL06A. Ten samples were extracted at two yearly resolution (20 years of growth) from both the early and the final growth bands to investigate the cause of death of the mid-Holocene corals.
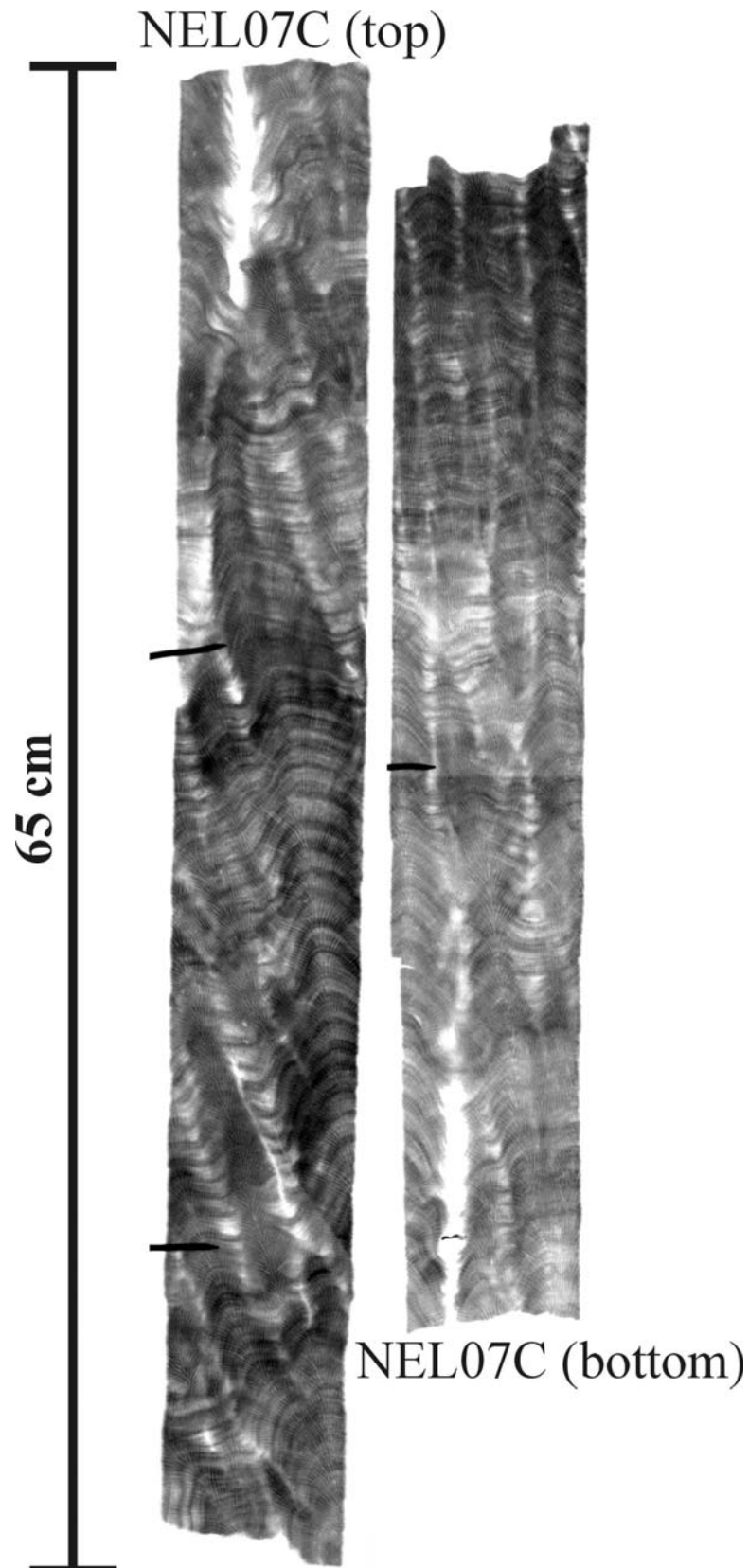
Figure 4.9. X-ray positive print of the NEL07C coral slice. Ten samples were extracted at two yearly resolution (20 years of growth) from both the early and the final growth bands to investigate the cause of death of the mid-Holocene corals.
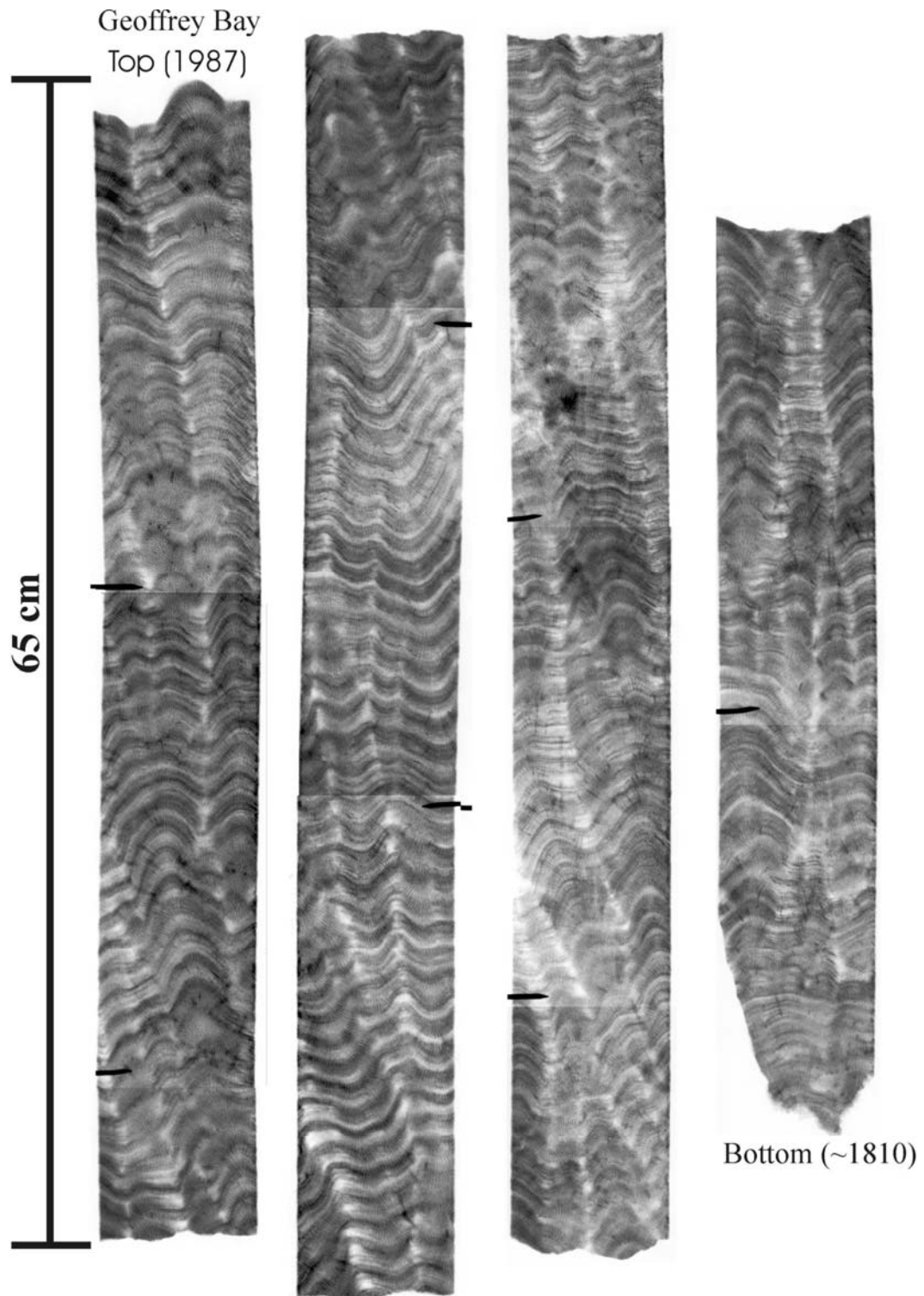
Figure 4.10. X-ray positive image of the modern coral taken in Geoffrey Bay in 1987 (MAG01D). Luminescent lines in the coral, as well as the well-preserved annual growth bands indicate that the coral began growing in 1812.
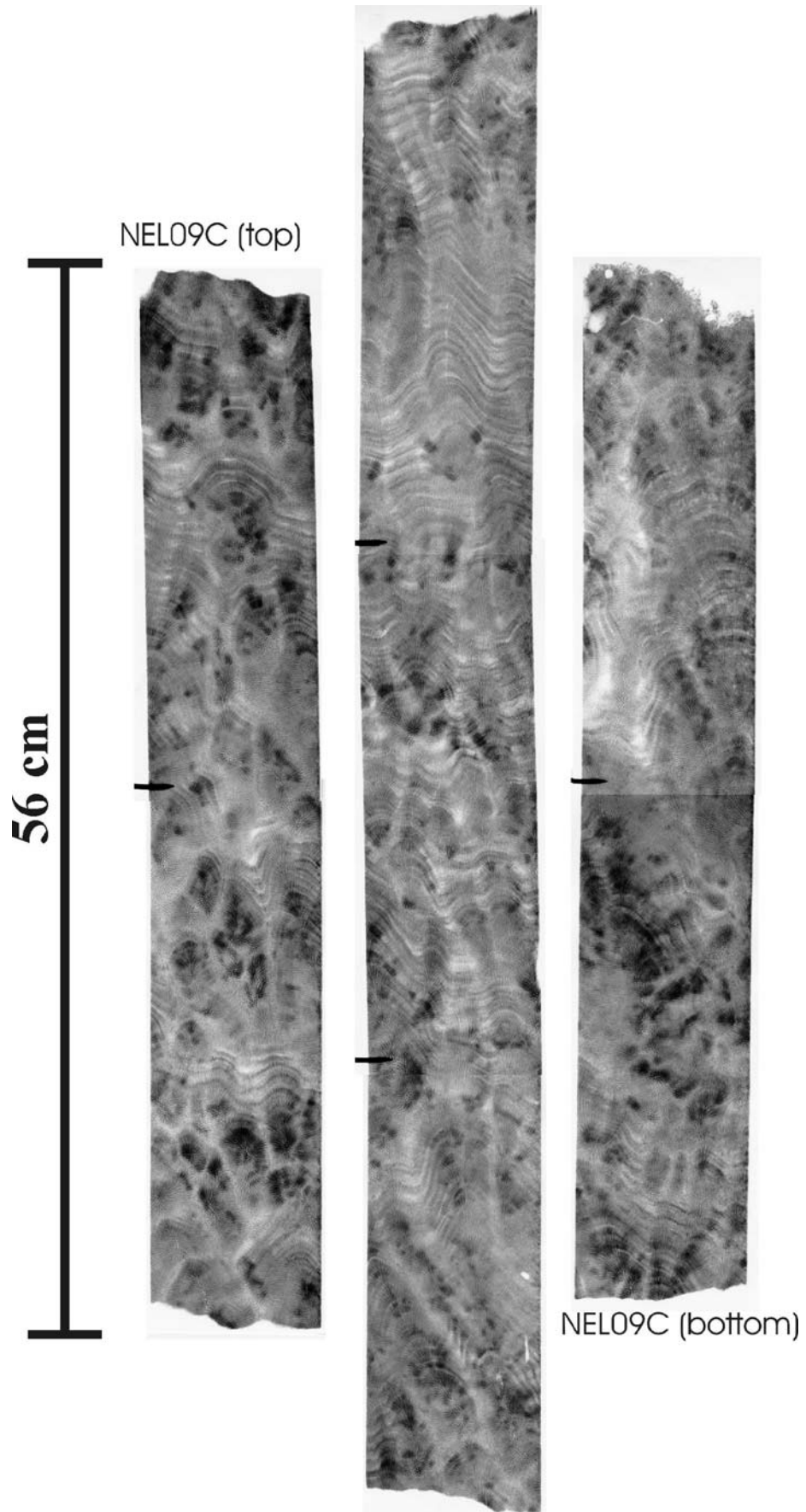
Figure 4.11. X-ray positive print of NEL09C. In contrast to the MAG01D coral, the core was not cut to the growth axis and it was very difficult to sample for trace element analyses or to establish an accurate age chronology.
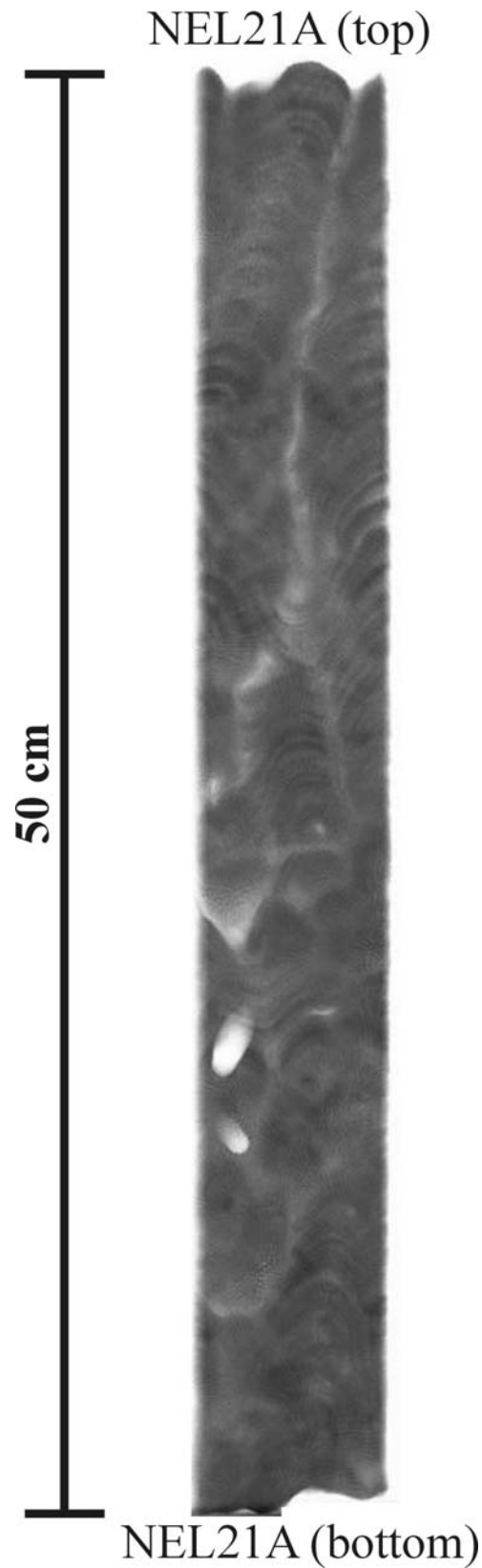
Figure 4.12. X-ray positive print of NEL21A coral slice. Samples were taken from 1968-1973 and 2000-2003 coral growth as well as from the 1991 and 1974 luminescent lines.

4.3.3. Coral age determination

The outer growth layers of two mid-Holocene corals (NEL07, NEL08) were carbon dated at The Australian National University (ANU) Radiocarbon Dating Laboratory which provided conventional uncorrected C-14 ages of 5,630 ± 90 years before the present (BP; NEL07; ANU-11580 G) and 5,620 ± 90 years BP (NEL08; ANU-11581 G; J. Chappell personal communication, 2001: Appendix 13). In addition, four samples from the top and bottom growth bands from the NEL01D and NEL03D coral slices were drilled using a stainless steel drill tip on a moveable stage. The coral powders were stored in 5 mL vials and U-Th dated at the ACQUIRE laboratory at UQ by thermo-ionisation mass spectrometry. Splits from the outer and basal growth sections of NEL03D were taken for AMS radiocarbon analysis (see section 4.2.6) to compare with the corresponding U-Th ages and to investigate the marine carbon reservoir effect for the Townsville/north Queensland region.

X-ray records and luminescent lines helped to develop an accurate chronology of the modern corals. Luminescence data from Hendy et al. (2003) as well as the annual growth bands exposed in the coral X-rays provided a date of 1812 at the base of the Geoffrey Bay coral (MAG01D). A chronology for the modern Nelly Bay corals (NEL09D; NEL21A) was established by matching the major luminescent lines with local (Townsville) rainfall (Appendix 4) and the Burdekin River discharge (Appendix 5) records.

4.3.4. Scanning Electron Microscopy and coral thin-sections

Microscopic analyses were used to determine whether the corals were free of diagenesis and thus suitable for trace element geochemistry (Bar-Matthews et al., 1993; Enmar et al., 2000; McGregor and Gagan, 2003; Müller et al., 2001; Müller et al., 2004; Hendy et al., submitted). The presence of secondary aragonite or calcite replacement can strongly influence sea surface temperature reconstructions (see section 2.2.3; Enmar et al., 2000; Müller et al., 2001; McGregor and Gagan, 2003). The first signs of diagenesis typically occur in the basal section (Enmar et al., 2000) or towards the top (Hendy et al., submitted) of the coral and thus these areas received particular attention.

Eight coral fragments were analysed for secondary aragonite or calcite replacement by a *JEOL JSM-5410LV Scanning Electron Microscope* (SEM) at the AAC at JCU. 2×2cm samples were taken from the bottom sections of NEL01D, NEL03D, NEL06A, NEL07C and MAG01D and from the top of NEL01D, NEL03D and MAG01D. The samples were platinum-coated, to divert the negative charge, and placed in the SEM. The images were taken at $100 \times$ and $2000 \times$ magnifications and photographed.

Twelve thin sections were prepared to evaluate further the possibility of coral diagenesis. Three samples each from the NEL01D and MAG01D coral slices were removed from the bottom, middle and top sections; while 2 samples each from NEL03D and NEL07C were extracted from the bottom and top of these coral slices. One coral thin section from the bottom of NEL06A and one from a Pandora Reef coral were also prepared. The samples were impregnated with a blue-dye resin, so the coral pores could be identified and discriminated from the skeleton. The samples were then glued onto frosted glass and ground down to approximately 60-100 µm. The thin sections were placed under a *Leica IM50* microscope and photographed with a mounted *Leica* digital camera at $2.5 \times$, $5 \times$, $10 \times$ and $20 \times$ magnification.

4.3.5.   Trace element analyses (Queensland Health Scientific Services Laboratory)

A coral colony from Pandora Reef was pulverised with a tungsten carbide mill. Ten samples from this homogenised coral were H_2O_2 treated and analysed for Sr, Mg, Ba and Ca at the Queensland Health Scientific Services (QHSS) laboratory to ensure that the facility was capable of producing the precision required for coral SST and environmental reconstructions. The samples were dissolved in 10% hydrochloric acid (HCl) and analysed on a *Varian Vista* (with an axial view) ICP-AES at the QHSS laboratory in Brisbane employing the technique of Schrag (1999). The results were then corrected for instrumental drift and precisions (RSD) were calculated by dividing the standard deviation (1σ) and the average. The precisions obtained during the analysis were found to be acceptable for coral SST reconstructions using the Sr/Ca and Mg/Ca ratios (Appendix 8).

Four corals were selected for geochemical analyses at the QHSS laboratory (NEL01D, NEL03D, NEL09D and MAG01D). Three of the core slices (NEL01D; NEL03D;

MAG01D) were sampled by homogenising 5-yearly growth increments with a stainless steel drill tip mounted on a moveable stage (Fig 4.13). The top 1 mm of the sampled area was shaved off to remove any possible surface contamination before sampling. The drill was then set to sample an additional 3 mm into the slice, along the major growth axis; the samples were then recovered and stored in sterile 5 mL vials. Any residual powder on the coral slice was then removed with pressurised air. The drill tip was cleaned in between samples with a steel wire bush and also wiped with a paper towel.

Figure 4.13. Sampling the coral slices. The corals slices were mounted on a moveable stage and, using a stainless steel drill, sampled to 2-5-yearly homogenised increments. The samples were recovered and stored in sterile 5 mL vials. Any residual powder on the slice was removed with pressurised air between samples.

The NEL09D coral slice was sampled at sub-annual resolution (4 samples per year), using a dental drill with a fine stainless steel drill tip, to cover a 5-year period of coral growth (1992-1996). The drill tip was cleaned in between samples with a steel brush and with ethanol and acetone, while any residual coral powder on the coral slice was removed with pressurised air.

The samples were all homogenised using an agate mortar and pestle, which was cleaned thoroughly with ethanol and acetone between samples. One hundred and ten samples were prepared for analysis including 4 blanks, 5 homogenised samples from Pandora Reef, 25 samples from NEL01D, 13 from NEL03D, 35 from MAG01D, 20 from NEL09D, and 8 duplicates.

The samples were then chemically pre-treated to remove any organic matter incorporated into the coral skeleton following a technique similar to that of Watanabe et al. (2001). Approximately 3 mL of milli-Q water was added to each vial which held the coral samples, which was then placed in an ultrasonic bath for 15 min and centrifuged for 15 min at 3000 RPM. The water was decanted from the samples and 3 mL of 10% hydrogen peroxide (H_2O_2) was added to each sample. The samples were placed in an ultrasonic bath for 15 min and centrifuged. The samples were decanted and rinsed three times with milli-Q water and centrifuged after shaking. The samples were then frozen and freeze-dried for at least 24 hours or until completely dry.

The samples were dissolved in 10% HCl and analysed for Sr, Mg, Ba, Mn and Ca by a *Varian Vista* (with an axial view) ICP-AES at the QHSS laboratory. The coral samples were analysed according to Schrag's (1999) method, where an internal standard is run between each sample, so results could be corrected for instrumental drift. The results were converted to atomic Sr/Ca, Mg/Ca and Ba/Ca ratios (Appendix 9). The analysis produced reproducibilities (RSDs) of 0.22% (Sr/Ca), 0.75% (Mg/Ca), 4.64% (Ba/Ca) and 44.72% (Mn). From a thermometry perspective, this precision equates to $\pm 0.35°$ C for the Sr/Ca ratio and $\pm 0.75°$ C for Mg/Ca (1σ standard deviation).

4.3.6.   Trace element analyses (ACQUIRE laboratory)

Five coral slices were selected for additional trace element analyses (NEL01D, NEL03D, NEL06A, NEL07C and MAG01D) which were prepared and analysed at the ACQUIRE laboratory (Appendix 10). The corals were sampled identically to the QHSS samples; however, this time 2-yearly increments of coral-growth along the major growth axis were sampled and homogenised. Two of the corals (NEL01D and MAG01D) were sampled throughout their entire slice. Forty years of growth (first and last 20 years of growth) were sampled in the remaining 3 coral slices (NEL03D,

NEL06A and NEL07C) to investigate the demise of the fossil corals. Five years of growth were sampled at a two-monthly resolution with a stainless steel dental drill (6 samples per year) in the MAG01D (1980-1984) and the NEL03D coral slices to compare seasonal fluctuations between the modern and mid-Holocene corals. All the samples were homogenised with an agate mortar and pestle and thoroughly cleaned with ethanol and acetone in between the crushing. Two hundred and eighty-seven samples were prepared for analysis including 30 samples each at two-monthly resolution from NEL03D and MAG01D, 88 2-yearly resolution samples from MAG01D, 63 from NEL01D, 20 samples each from NEL03D, NEL06C and NEL07A, and a further 16 (spilt) samples from MAG01D (1958-1986) with the inclusion of a pre-treatment step.

The 16 pre-treated samples were rinsed in 3 mL of milli-Q water, shaken and placed in an ultrasonic bath for 15 min. Each of the samples were centrifuged and decanted, and then 3 mL of ultra-pure H_2O_2 was added. The samples were again placed in an ultrasonic bath for 15 min, centrifuged, decanted and rinsed 3 times with milli-Q water before being dried in a 40° C oven for 24 hours.

The two-monthly resolution and pre-treated samples were the first to be analysed at the ACQUIRE laboratory. Between 0.44 and 2.2 mg of sample were weighed and placed into 14 mL sterile polystyrene centrifuge tubes. The additional samples (untreated 2-yearly NEL01D, NEL06A, NEL07C and MAG01D) were weighed out between 9.55 and 10.36 mg and placed into the polystyrene tubes. All the samples were then digested in 10 mL of 2.5% HNO_3 (double sub-boiling distilled). From this stock solution, an aliquot was taken into a new pre-cleaned 14 mL polystyrene tube and diluted to a factor of 5,000 with 2% HNO_3 and a nominal internal standard concentration of 6 ppb. Internal standards used were ^{6}Li, ^{61}Ni, ^{115}In, and ^{235}U (see Eggins et al., 1997). Samples were analysed by ICP-MS at ACQUIRE in three consecutive batches (two-monthly resolution and pre-treated, 2-yearly resolution modern [MAG01D] coral, and 2-yearly resolution mid-Holocene corals) of 60-80 samples on a Thermo Electron X-Series instrument with the Xi interface (preferred over the high-performance interface due to the high Ca concentrations). External drift of <3% was monitored and corrected for by repeated analyses of a mixed coral solution judiciously spiked with some dolerite solution. Instrumental response for the trace elements were calibrated against dilute

(5,000 – 20,000x) solutions of the U.S.G.S. dolerite standard W2. Calcium was calibrated against the G.S.J. coral standard JCp-1 (Okai et al., 2002), which was run as an unknown for the other elements, the precisions of which were better than 2% from multiple analyses.

The two-monthly resolution and pre-treated samples were analysed for Li, Mg, Ca, Mn, Ni, Sr, Ba and U. The remaining 2-yearly resolution modern and mid-Holocene samples were analysed for Li, Mg, Ca, Mn, Ni, Zn, Sr, Y, Ba, Pr, Sm, Ho, Pb, Th and U. Twenty-one samples selected from this dataset to investigate the behaviour of the rare earth elements (REE) were reanalysed on the high-performance interface for Li, Be, Sc, Ti, Ga, Rb, Y, Zr, Nb, Cd, Ba, La, Ce, Pr, Nd, Sm, Eu, Tb, Gd, Dy, Ho, Er, Tm, Yb, Lu and W.

The coral paleothermometer (Sr/Ca, Mg/Ca and U/Ca) and environmental (Ba/Ca) proxies were converted to atomic ratios. The RSDs of the ratios were 0.46% (Sr/Ca), 0.90% (Mg/Ca), 0.81% (U/Ca) and 11.20% (Ba/Ca), respectively. From a thermometry perspective, these results equated to $\pm\,0.65°$ C (Sr/Ca), $\pm\,0.35°$ C (Mg/Ca) and $\pm\,0.25°$ C (U/Ca; 1σ standard deviation).

Sixty additional samples were prepared and analysed at the ACQUIRE laboratory to examine the behaviour of REE, Ba and Mn at higher resolution time intervals. Twenty-seven samples from the years 2000-2004 (>6 samples per year), 21 samples from 1968-1972 and 3 samples from the 1973, 1974 and 1991 luminescent lines were extracted from the NEL21A coral slice with a dental drill. In addition, 7 samples were taken from the NEL01D coral slice surrounding the distinct growth hiatus (Fig 4.6) to investigate the demise of the fossil coral. The 1831 and 1870 flood bands were also sampled from MAG01D coral slice by a dental drill. The samples were prepared and analysed by ICP-MS this time using the high-performance interface.

4.3.7. Oxygen and carbon isotope analyses

Oxygen and carbon isotopes were analysed in two separate batches. The first sample batch was splits from the homogenised 5-yearly samples from the QHSS trace element analysis; these sub-samples were not pre-treated with H_2O_2. Eighty-three samples were

analysed including 25 from NEL01D, 13 from NEL03D, 35 from MAG01D, 5 duplicates and 5 homogenised samples from a Pandora Reef coral colony. The second sample batch was splits from the two-monthly resolution analyses carried out at the ACQUIRE laboratory, including 30 samples each from NEL03D and MAG01D (For carbon isotopes results and write-up see Appendix 16; raw O and C isotope data: Appendix 11).

The samples were prepared and analysed on a Micromass PRISM III stable-isotope mass spectrometer at the University of Wollongong which followed this procedure:

> "Samples were loaded into 1 mL Weaton V-vials which were sealed with Kel-F and silicone septa and placed in a heated block maintained at 90° C. A double-bore needle was pushed through the septa and into the vial, the vial was evacuated and then pure phosphoric acid (103%) was dispensed onto the sample. The evolved CO_2 was passed through the water trap and cryogenically collected in the external cold finger. After all the gas was collected, it was released into the sample side of the dual inlet and was analysed against the working gas. Calibration was performed against an internal laboratory standard, NBS18 and NBS19" (http://www.uow.edu.au/science/eesc/facilities/stableisotope.html).

The results were calibrated to Pee Dee Belemnite for both the O and C isotopes.

4.3.8. SST calibrations

Since it was not possible to produce accurate SST calibration curves for the coral Sr/Ca, Mg/Ca and U/Ca ratios in this study because of the relatively low sampling resolutions, previous calibration curves were adopted. The SST calibration curves for O isotopes and the Sr/Ca ratio from Gagan et al. (1998) were chosen, as these calibrations were produced from a coral from Orpheus Island, located approximately 60 km north of Magnetic Island (Fig 1.2). However, the intercept of this Sr/Ca-SST calibration curve was adjusted (using the coral Sr/Ca ratios from the 2-monthly resolution 1980-1984 record) to fit with the two-monthly instrumental SST record from Cleveland Bay (Fig 4.14; Appendix 3; Table 4.1). Fallon et al. (2003) also produced a Sr/Ca-SST calibration from Orpheus Island using the LA-ICP-MS technique. Nevertheless, while the intercept of this curve closely matched the adjusted calibration of Gagan et al. (1998), the slope of the curve was considerably different to those produced using the TIMS technique (Fig 4.14). Two separate calibration curves for the Mg/Ca data were used to account for both the H_2O_2 treated and the untreated samples. An intercept

adjustment was also applied to the calibration curves of Mitsuguchi et al. (1996; Mg/Ca; Fig 4.15; untreated samples; Table 4.1), Watanabe et al. (2001; Mg/Ca; Fig 4.15; H_2O_2 treated samples; Table 4.1) and Min et al. (1995; U/Ca; Fig 4.16; Table 4.1) to establish a better correlation with the instrumental SST record from Cleveland Bay.
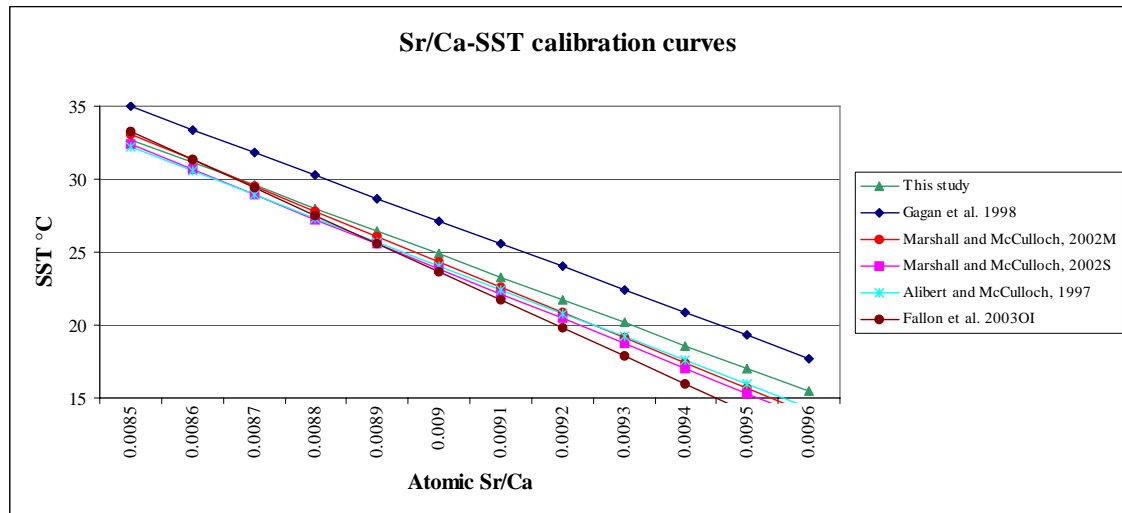
Figure 4.14. The adjusted calibration curve from Gagan et al. (1998) used for this study (green) compared to published curves from the GBR. This calibration curve was derived by adjusting the intercept value from the Gagan et al. (1998) equation from Orpheus Island to match the SST range measured in Cleveland Bay/Magnetic Island. Note the curve is in close agreement with published curves from the outer GBR using the TIMS technique. In addition, the slope of the Fallon et al. (2003) curve from Orpheus Island (OI) using LA-ICP-MS is offset from the published curves of Marshall and McCulloch, 2002M (Myrmidon Reef); 2002S (Stanley Reef) and Alibert and McCulloch, 1997 using TIMS.
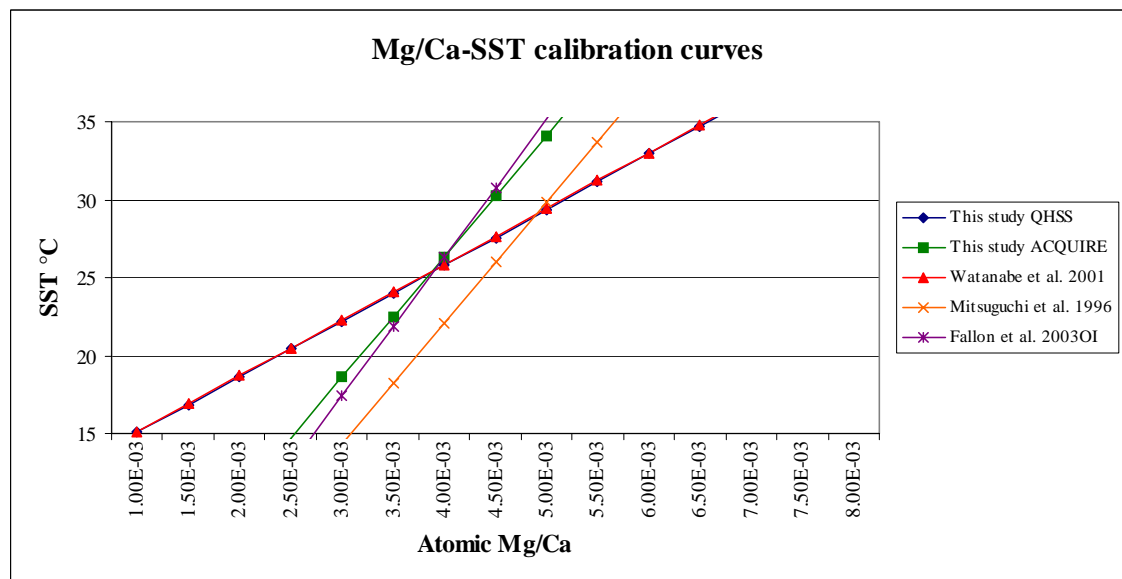
Figure 4.15. The Mg/Ca-SST calibration curves for this study (blue and green) were derived by adjusting the intercepts of the Mitsuguchi et al. (1996; for the ACQUIRE dataset) and the Watanabe et al. (2001; for the QHSS dataset) equations to fit with the instrumental SST data measured in Cleveland Bay/Magnetic Island. Note that the Fallon et al. (2003) calibration curve is similar to the one used for the ACQUIRE samples in this study by adjusting the Mitsuguchi et al. (2001) curve.
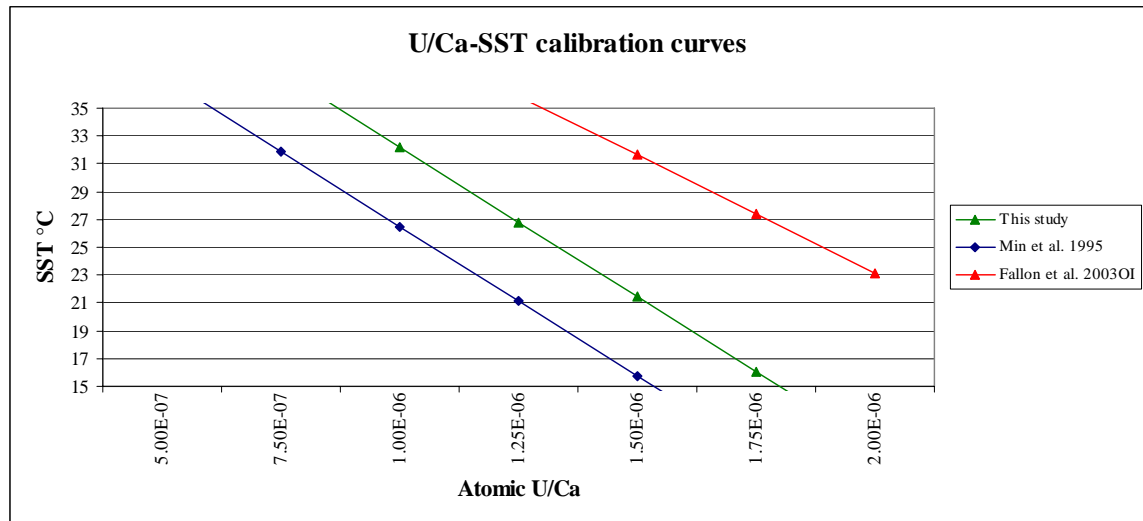
Figure 4.16. The intercept of the Min et al. (1995) U/Ca calibration was adjusted, so the coral U/Ca values closely matched the instrumental SST measurements from Cleveland Bay/Magnetic Island. Note that the U/Ca calibration curve of Fallon et al. (2003) for Orpheus Island is significantly different to the equation using the TIMS technique.

Table 4.1. Summary of the equations used to calibrate the geochemical coral proxies to SST for the Magnetic Island corals. The coefficient of each published curve was adjusted to fit the expected SST range for Magnetic Island for each particular proxy.

Coral proxy	Equation	Location	Reference
Sr/Ca	SST (°C)= [(atomic Sr/Ca × 1000)/0.0638 - (10.731/0.0638)] × -1	Orpheus Island	Gagan et al. (1998)
Sr/Ca	SST (°C)= [(atomic Sr/Ca × 1000)/0.0638 - (10.5869/0.0638)] × -1	Magnetic Island	This study
Mg/Ca	SST (°C)= [(atomic Mg/Ca × 1000)/0.28 + (3.24/0.28)]	Caribbean Sea	Watanabe et al. 2001
Mg/Ca	SST (°C)= [(atomic Mg/Ca × 1000)/0.28 + (3.221/0.28)]	Magnetic Island*	This study
Mg/Ca	SST (°C)= [(atomic Mg/Ca × 1000)/0.129 + (1.15/0.129)]	Ryukyu Islands	Mitsuguchi et al. 1996
Mg/Ca	SST (°C)= [(atomic Mg/Ca × 1000)/0.129 + (0.60/0.129)]	Magnetic Island**	This study
U/Ca	SST (°C)= 48.00 - (21.5 × 1000000) × atomic U/Ca	New Caledonia	Min et al. 1995
U/Ca	SST (°C)= 53.69 - (21.5 × 1000000) × atomic U/Ca	Magnetic Island	This study

* H$_2$O$_2$ treated sample; ** untreated sample

4.3.9. Summary

Eight large fossil *Porites* coral heads were recovered during the construction of Nelly Bay Harbour and transported to AIMS where they were cored, sliced and prepared for analysis. In addition, three living *Porites* corals were cored in Nelly and Geoffrey Bays to compare the physical and geochemical characteristics between the modern and fossil corals. Four samples were taken from the basal and top growth layers from the NEL01D and NEL03D for U-Th dating. In addition, the basal and top growth layers from NEL03D were sampled for AMS C-14 dating to investigate the marine 14-C

reservoir effect in the local area. Microanalytical techniques, including scanning electron microscopy and thin sections, were employed on the corals to examine any possible effects of diagenesis and to ensure that the corals were suitable for geochemistry. One modern (Geoffrey Bay 1812-1986) and two mid-Holocene corals (NEL01D and NEL03D) were sampled at 5-yearly resolution and analysed by ICP-AES at the QHSS laboratory for Sr, Mg, Ba, Mn and Ca. Another coral was sampled at sub-annual resolution (NEL09C; 4 samples per year). Prior to the analysis at QHSS, the samples were treated with H_2O_2 to remove the organic component. Untreated split-samples from the 5-yearly resolution dataset were analysed for O and C isotope composition at the University of Wollongong. Trace elements of the 2-yearly resolution samples from Geoffrey Bay (MAG01D) and NEL01D corals were analysed at the ACQUIRE laboratory. In addition, the NEL03D, NEL06A and NEL07C coral slices were sampled at 2-yearly resolution to investigate the demise of the fossil mid-Holocene corals. Selected sections were sampled at two-monthly resolution to examine seasonal variations in the coral proxies. Split-samples from the two-monthly resolution records for 1980-1984 and the NEL03D corals were also analysed for O and C isotopic composition. The most reliable SST calibrations for the Sr/Ca, Mg/Ca and U/Ca ratios were selected from previous studies based on the precision of the analysis and sampling location. The intercepts of these curves were adjusted to match the observed SST range measured in Nelly and Geoffrey Bays.

4.4.   Additional data

4.4.1. Overview

This section reviews the sources for the instrumental datasets that were used to examine the correlations with the physical and geochemical coral proxies including rainfall records, Burdekin River discharge, coral luminescence and calcification, sea surface temperature and seawater turbidity.

4.4.2.   Rainfall data

Rainfall data were provided by the Australian Bureau of Meteorology (BOM; http://www.bom.gov.au). Long-term rainfall records were compiled from areas that would influence Magnetic Island. The Townsville rainfall data (Station 032040) was selected as the local runoff proxy, as this station is close to Magnetic Island. The Burdekin River catchment was divided into six sub-catchments including the upper Burdekin, lower Burdekin, Cape River, Belyando River, Suttor River and Bowen River (Fig 4.17). Long-term rainfall data were collated to cover all these sub-catchments. In the upper Burdekin sub-catchment, 6 rainfall stations were chosen including Gleneagle (Station 032018), Valley of Lagoons (032044), Christmas Creek Station (032104), Clarke River Telecom (032008), Charters Towers Airport, Post Office (034002; 034084) and Mount McConnell (034007); while Woodhouse (033073) and Kalamia Estate (033035) stations represented the lower Burdekin sub-catchment. Rainfall data from Balfe's Creek Post Office (034000), Pentland Post Office (030040) and Torren's Creek Post Office (030051) were selected to characterise the Cape River sub-catchment, while Moray Downs (036071), Surbiton Station (036139) and Alpha Post Office (035000) represented the Belyando River section. Only 2 stations covered the Suttor River (Avon Downs: 034081; Twin Hills Post Office: 036047) and Bowen River (Strathmore: 033082; Bowen: 33007, 33257) sub-catchments. The local Townsville rainfall data stretches back to 1871. Combining the average rainfall records for all the Burdekin River sub-catchments provides data back to 1906. However, the rainfall record for most of the sub-catchments stretches back to the early 1880s (Appendix 4).
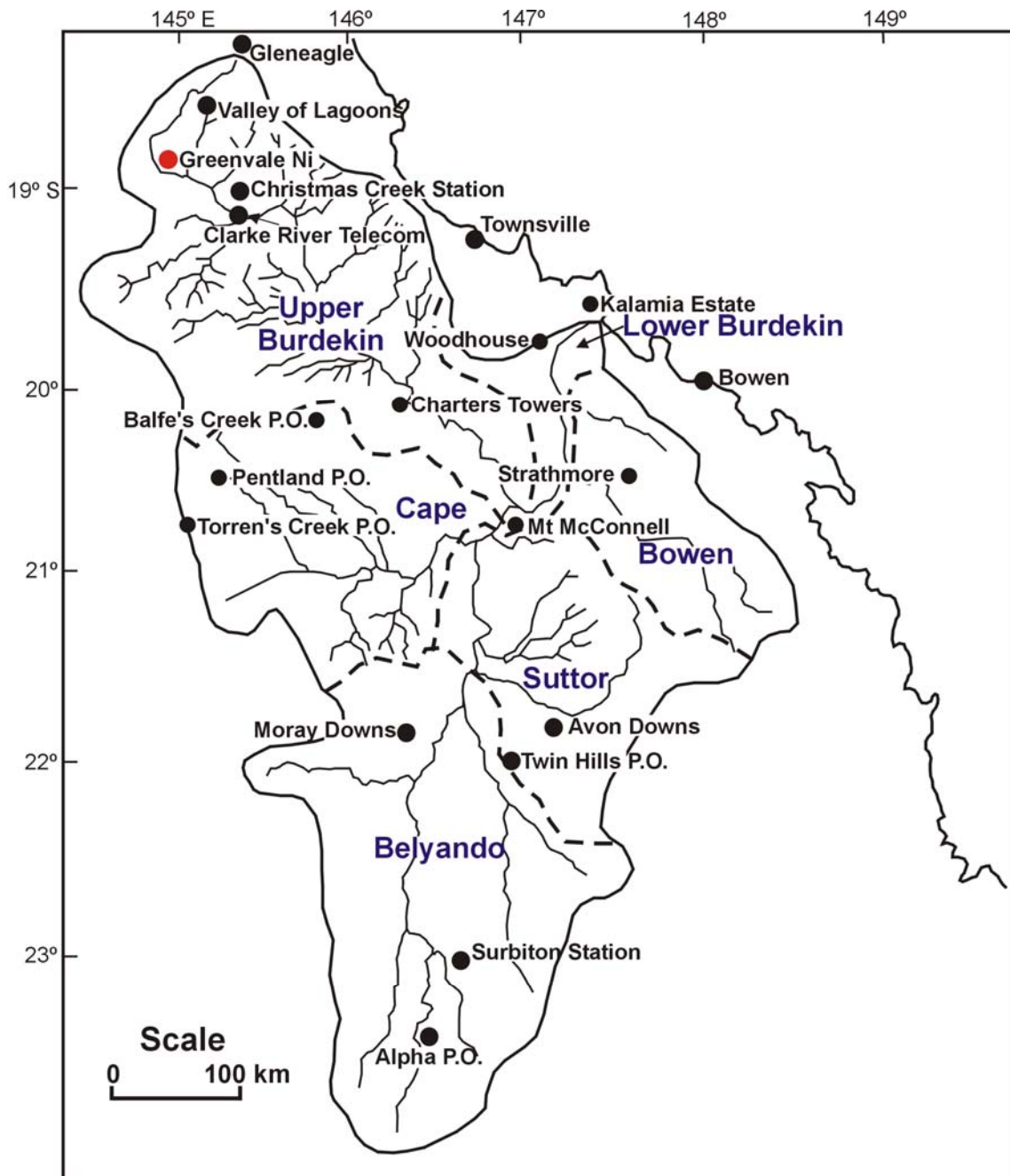
Figure 4.17. Map of the Burdekin River catchment. The catchment was divided into six sub-catchments and rainfall data has been obtained from the BOM to use as a proxy for river flow for each sub-catchment. Note the location of the Greenvale Ni mine in the northern section (Figure adapted from Amos et al., 2004).

4.4.3. Burdekin discharge data

The Burdekin discharge data, supplied by Queensland Department of Natural Resources and Mines, extends back to 1922 (Appendix 5; http://www.nrm.qld.gov.au). The daily river flow for the lower Burdekin River has been measured at gauging stations located at Home Hill (1922-1953) and Claire (since 1951).

4.4.4. Luminescence data

Luminescence data, provided by Dr Janice Lough (AIMS), were analysed annually on all the corals sampled for trace element geochemistry. The intensity of the luminescent lines in the coral slices was measured using a Luminometer as described in Barnes et al. (2003; Appendix 7). Luminescent lines, as well as X-ray records, were used to establish an accurate chronology for the modern corals.

4.4.5. Calcification data

The annual coral calcification data were also supplied by Dr Lough. The annual density (measured by a densimeter) and extension were combined to provide a measure of how much calcium carbonate was precipitated by the coral during each particular year, termed the annual calcification rate (Lough and Barnes 2000; Appendix 6).

4.4.6. Sea surface temperature data

Sea surface temperature (SST) data from Cleveland Bay/Magnetic Island are sparse and were collated from a variety of sources. Preliminary measurements in Cleveland Bay from the 1960s and 1970s were conducted by Kenny (1974) and Walker (1981b). Data for the early 1980s, corresponding to the two-monthly resolution measurements in MAG01D, were measured by Willis (1987). These data were collected opportunistically, during the day-time, so it is expected that these results would be slightly biased towards higher SSTs. Recent high resolution measurements (every 30 min) from Magnetic Island in Nelly and Geoffrey Bays have been taken by the Great Barrier Reef Marine Park Authority (GBRMPA; http://www.gbrmpa.gov.au) from 1992 and 1996, respectively (all data presented and summarised in Appendix 3; Fig A-3.1).

4.4.7. Turbidity data

Turbidity data from Nelly and Geoffrey Bays have been taken at high resolution by the School of Physics at JCU since the year 2000. The data were collected using 4 nephelometers (e.g. Ridd and Larcombe, 1994) placed at various locations in the two embayments (Fig 4.18). The nephelometers were designed to measure suspended solid

concentrations every 10 minutes. These data were converted to real time and were averaged over weekly and monthly resolutions to smooth the dataset (Appendix 12).
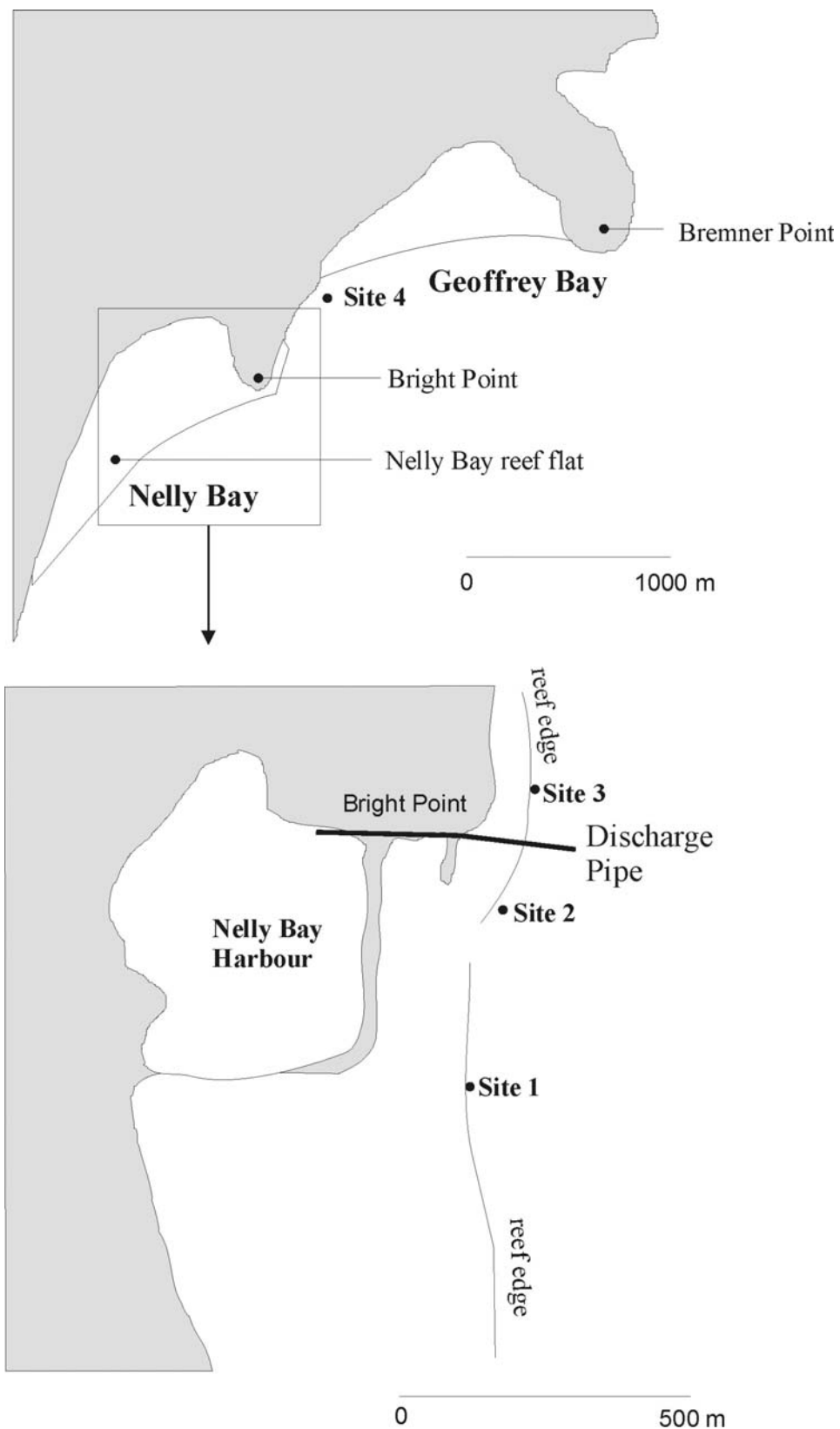
Figure 4.18. Four nephelometers were deployed in Nelly and Geoffrey Bays to measure the concentration of suspended solids in the water column.

4.4.8. Summary

Instrumental records of SST, rainfall in the Burdekin river catchment, Burdekin River discharge data and turbidity measurements were compiled to investigate correlations with the geochemical and physical coral proxies. In addition, the annual coral calcification rate and luminescence data for the modern and mid-Holocene corals were compiled to examine correlations with the trace element SST and salinity reconstructions, respectively.

4.5. Chapter summary

- All available data from the investigations carried out for the construction of the Nelly Bay Harbour were compiled.
- Topographic profiles were performed along three transects in Nelly Bay using a theodolite.
- A total of 14 sediment cores were taken along these transects.
- The cores were logged and sedimentary layers were identified from the grainsize and composition of the sediments.
- Selected cores were sampled for AMS C-14 dating, XRD mineralogy analysis and trace element geochemistry.
- Grab samples were taken from the Burdekin River, Ross River, Gustav Creek, the shipping channel and the Nelly Bay reef slope for trace element geochemistry, to understand the provenance of the sediments in Nelly Bay.
- Eight fossil *Porites* coral heads of mid-Holocene age were recovered during the construction of the Nelly Bay Harbour.
- The corals were cored and sliced at AIMS.
- Additional "modern" *Porites* coral colonies were cored in Nelly and Geoffrey Bays for comparative analysis with the fossil corals.
- Selected mid-Holocene corals were dated by C-14 and U-Th techniques.
- Microanalytical work to examine the corals for diagenesis was carried out by scanning electron microscopy and coral thin sections.
- The corals were sampled at two-monthly as well as 2 and 5-yearly resolutions.
- The 5-yearly resolution samples were pre-treated with milli-Q water and H_2O_2 prior to trace element analysis on ICP-AES at the QHSS laboratory while the

remaining two-monthly and 2-yearly resolution samples were analysed untreated at the ACQUIRE laboratory.

➢ Splits from the 5-yearly and two-monthly resolution samples were analysed for O and C isotope composition.

➢ The most reliable calibration curves available in the literature for coral Sr/Ca, Mg/Ca and U/Ca ratios were used to reconstruct SST.

➢ All available instrumental rainfall, Burdekin discharge, coral luminescence, calcification, SST and turbidity data were compiled to examine correlations between these parameters and the coral trace element and isotope data.

Chapter 5

Local setting and stratigraphy

5.1. Chapter overview

This chapter examines the sedimentological context of the study area for a stratigraphic model of Nelly Bay and to reconstruct the evolution and demise of the fossil corals. This chapter is divided into 5 sections:

1) Section 5.2 reviews calibrated carbon-14 (C-14) and U-Th ages of the fossil corals to place them within the stratigraphy of Nelly Bay and to describe the evolution of the Nelly Bay reef.

2) Section 5.3 examines the calibrated C-14 ages of a fossil oyster bed from Magnetic Island to understand the position of sea level during the Holocene. Additional sea-level data from the east coast of Australia have been compiled, reviewed and recalibrated to produce a reliable reconstruction of the timing and magnitude of Holocene sea levels.

3) Section 5.4 presents topographic profiles from Nelly Bay to investigate the morphological zones within the embayment and thus place the sea-level data in perspective.

4) Section 5.5 uses sediment cores to examine the sedimentary layers within Nelly Bay. Each sedimentary layer in Nelly Bay has been described in terms of composition (including mineralogy and geochemistry), grainsize, age structure (using calibrated C-14 dates), sorting and the lateral and vertical extent of each layer.

5) Section 5.6 is a synthesis of the sea-level data, the topographic profiles, the sediment cores, the age structure of the sedimentary layers and previous investigations to construct a stratigraphic model for Nelly Bay. This final model describes a possible scenario of the palaeoenvironment for the fossil corals and a historical evolution of Nelly Bay based on the sediment core records.

5.2. Ages of mid-Holocene corals

5.2.1. Overview

The fossil corals were dated at three laboratories using conventional C-14 (ANU), AMS C-14 (ANSTO) and TIMS U-Th (ACQUIRE) techniques. The radiocarbon ages were calibrated using the *IntCal04 Marine04* C-14 "global" marine calibration dataset (Hughen et al., 2004) in the Calib 5.0 program (Stuiver et al., 2005). This program uses a global C-14 marine reservoir effect value of 400 years and the data was combined with a local correction (ΔR) of 12 ± 6 years for marine carbonates from the central Great Barrier Reef (Hughen et al., 2004). U-Th ages were calibrated using the Isoplot Excel program at the ACQUIRE laboratory. This section will discuss the ages of the fossil corals.

5.2.2. Age data and discussion

The outer and basal layers of the NEL03D coral slice were dated by both the C-14 and the U-Th techniques to evaluate the reliability of the C-14 calibration program and the local ΔR correction. The calibrated C-14 ages for NEL03 coral (6,290 ± 110; 6,130 ± 150 years BP) corresponded (within error) with the U-Th dates (6,180 ± 40; 6,060 ± 90 years BP for the basal and outer layers, respectively; Table 5.1), which suggests that the marine C-14 reservoir effect and the *Marine04* C-14 calibration are within the errors inherent to both analyses. However, the U-Th ages were systematically younger than the calibrated C-14 dates, an average difference 70 (outer layer) and 110 (basal layer) years respectively. Since the *Marine04* C-14 calibration program is reliable up to 10,000 years BP (Stuiver et al., 2005; Bard et al., 2004), a local reservoir correction (ΔR) for Magnetic Island has been calculated at 95 ± 15 years. This estimation is based on the average age difference between the U-Th ages and the calibrated C-14 ages, instead of the 12 ± 6 years estimate for east central Australia. Estimation of the local reservoir effect (ΔR), however, varies widely from site to site on the GBR (Stuiver et al., 2005) and 12 ± 6 years has been retained for the calibrated C-14 ages in this study. The age difference between the basal and outer layers of the NEL03 coral for the U-Th and C-14 dates is 120 and 160 years, respectively. The

annual density banding record for the NEL03D coral slice suggests that the coral lived for approximately 100 years (Fig 4.7) and, therefore, the U-Th dates may be more precise. However, the uncorrected radiocarbon ages provided a range of 130 years, which was closer to the U-Th estimate (Table 5.1).

The U-Th dates for the NEL01 coral was 6,090 ± 40 (basal layer) and 5,790 ± 30 (outer layer) years BP. The annual density bands of the NEL01D coral slice (Fig 4.6) indicated an age span for the coral of approximately 130 years, which was significantly lower than the U-Th age range (230-370 years using 2σ standard deviation). There is a distinct growth hiatus in the NEL01 coral which is located near the centre of coral growth (~60-65 years of growth from the base of the coral; Fig 4.6) which may account for this discrepancy if the coral died and then started to grow again.

All the outer growth layers of the dated corals (NEL03, NEL06, NEL07) contain ages which cluster around 6,000-6,150 years BP, with the exception of the U-Th age of the NEL01 coral (5,790 ± 30 years BP; Table 5.1). The NEL01 coral may have died around the same time as the other coral heads, but possibly regenerated around 100-200 years later. Another possibility is that this U-Th date is incorrect. Nonetheless, the majority of the fossil mid-Holocene corals all died within a 150-year period.

Table 5.1. Ages, in years BP, for the fossil mid-Holocene corals.

Lab code	Sample ID	Description	Method	Uncorrected age	±	Calibrated age	± (2σ)
ANU-11580	Nel07	Outer layer NEL07	Standard 14-C	5630	90	6040	210
ANU-11581	Nel08	Outer layer NEL08	Standard 14-C	5620	90	6000	210
OZH574	Coral 15	Basal layer NEL03	AMS 14-C	5870	50	6290	110
OZH575	Coral 16	Outer layer NEL03	AMS 14-C	5740	60	6130	150
ACQUIRE	NEL04D02	Basal layer NEL03	U-Th	6210	30	6180	40
ACQUIRE	NEL03D02	Outer layer NEL03	U-Th	6200	60	6060	90
ACQUIRE	NEL01D02	Basal layer NEL01	U-Th	6100	40	6090	40
ACQUIRE	NEL02D02	Outer layer NEL01	U-Th	5830	30	5790	30

5.2.3. Summary

The calibrated C-14 ages corresponded with the U-Th dates for the NEL03 coral which indicated that the estimate of the marine reservoir effect and the C-14 *Marine04* calibration were both reasonable. The coral ages suggested that the fossil mid-Holocene corals ceased growing between 6,000-6,150 years BP. An appreciation of the stratigraphy in Nelly Bay and sea level during the mid-Holocene should shed more light on the death of these fossil corals.

5.3. Sea level during the Holocene

5.3.1. Overview

Despite numerous Holocene sea-level data published for the Great Barrier Reef and eastern Australia (most recently summarised by Larcombe et al., 1995b), there is no clear agreement about the timing, elevation and controlling mechanism(s) of the "mid-Holocene" sea-level highstand. The limitation of most previous studies has been that the radiocarbon

data were corrected for the marine reservoir effect (-450 years; Gillespie and Polach, 1979), but not for secular atmospheric variations in C-14 (e.g. Bard et al., 2004). Production of C-14 in the atmosphere has not been constant over time (de Vries, 1958) and a calibration program has been developed to correct for the activity of atmospheric C-14 (Stuiver et al., 2005). Moreover, application of less precise sea-level indicators has produced estimates for the mid-Holocene highstand that vary from > 3 m (Hopley, 1971; Hopley and Thom, 1983) to 0 m (Belperio, 1979) above present sea level. Recent studies on the New South Wales (NSW) coastline suggest that sea level over the last 6,000 years oscillated up to three times and that global eustacy may have been the dominant influence on Holocene sea level (Baker and Haworth, 2000b; Baker et al., 2001). The data, however, contradicts the previous hydro-isostatic model that proposes a smoothly falling sea level after reaching a peak approximately 6-7,000 years BP (Chappell et al., 1982; Lambeck and Nakada, 1990; Lambeck and Chappell, 2001). A revised sea-level history for eastern Australia is presented here and draws on new and recalibrated radiocarbon ages of fossil oyster beds, barnacles, tubeworms and coral microatoll data taken relative to their highest living counterparts from the same location. These precise sea-level markers for the eastern Australian coastline have been compiled from the Torres Strait to Port Hacking (NSW; Table 5.2; Fig 5.1).

5.3.2. Sea-level data

Fixed biological indicators (FBIs: oyster beds, tubeworms and barnacles) and coral microatolls are the most precise indicators of sea level (typically within ± 0.25 m; Baker and Haworth, 2000a; Larcombe et al., 1995b; Beaman et al., 1994). These indicators have been used to reconstruct sea level for eastern Australia over the last 8,000 years (summarised in Table 5.2). Radiocarbon ages of "transgressive" mangrove mud from Cleveland Bay (Belperio, 1979; Carter et al., 1993) and Halifax Bay (R. Wüst, unpublished data) have also been used to extend the dataset to encompass the entire Holocene Epoch (Table 5.2). Two separate C-14 calibrations were applied to the samples including the *Marine04* C-14 "global" marine calibration dataset (for marine shell and coral material; Hughen et al., 2004) and the terrestrial Southern Hemisphere dataset (for the mangrove

mud; *SHCal04*; McCormac et al., 2004). In addition, the nearest regional reservoir correction (ΔR) was applied for the marine samples including 52 ± 31 years (regional average NE Australia) for the sites north of Cairns, 3 ± 70 years (regional average SE Australia) for the NSW samples and 12 ± 6 years (regional average E central Australia) for the data between Cairns and Mackay (Fig 5.1; Stuvier et al., 2005). The calibrated C-14 ages were all rounded to the nearest decade and presented with a 2σ error (Table 5.2). The sample elevations, where possible, were taken to the highest living organism of the same genus or species from that particular location. The elevation errors were taken from those cited in each study; however, 30 cm has been subtracted from the reported levels for the barnacle samples in Beaman et al. (1994) and Higley (2000). The elevation of barnacles is notoriously difficult to calculate as they commonly form in high-energy swash zones (Flood and Frankel, 1989). In addition, they can grow up to 30 cm above oyster beds in modern environments (Beaman et al., 1994). A ± 5 m maximum error of elevation was estimated for the mangrove mud samples by Beaman et al. (1994) and Bunt et al. (1985). These studies suggested a number of potential inaccuracies in confining the elevation of mangrove mud including post depositional compaction, contamination/reworking (by younger/ higher mangrove rootlets) and coring effects.
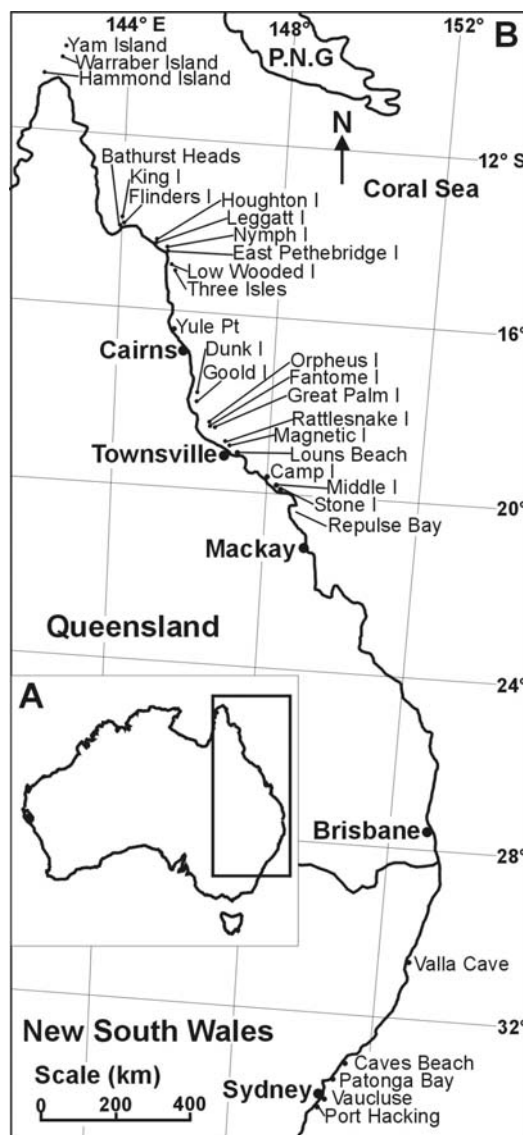
Figure 5.1. Locations of data used to reconstruct Holocene
sea level for eastern Australia.

5.3.3. Holocene sea level of eastern Australia

The sea-level reconstruction using the FBI, microatoll and mangrove mud data (Fig 5.3) is similar to that of Larcombe et al. (1995b; Fig 3.2), with a few notable exceptions. The early Holocene transgression (10,000-7,500 cal years BP) is difficult to interpret in this reconstruction due to the sparse and variable data points of the mangrove mud data. This "transgressive" mangrove mud unit needs to be more accurately and consistently measured, particularly the sea-level elevation and the material selected for radiocarbon dating.

The Holocene sea-level reconstruction indicates that sea level was higher around 7,000-7,500 cal years BP (Fig 5.3). This finding contradicts the work of Larcombe et al. (1995b), which suggests that sea level in this region first reached this elevation only by 5,000-5,500 C-14 years (Fig 3.1). This result is presumably an artefact of the C-14 ages used by Larcombe et al. (1995b) which were only corrected for the marine reservoir effect and not for atmospheric C-14 variability. For example, one of Beaman et al.'s (1994) C-14 ages for a fossil oyster bed from Magnetic Island provided a radiocarbon age of 5,660 ± 50 years. The "environmentally corrected C-14" age applied for this sample by Larcombe et al. (1995b) was 5,210 ± 50 years, while the calibrated C-14 calendar age, which incorporates the marine reservoir effect, is 6,050 ± 130 cal years BP, an offset of 840 years.

A fossil barnacle from Balding Bay (+ 1.35 m), Magnetic Island, was dated by Higley (2000) to a calibrated C-14 age of 7,390 ± 140 years BP. This age places the timing of the mid-Holocene sea level highstand approximately 500-1,000 years earlier than the previous earliest dated sea-level indicator by Chappell et al. (1983; 6,870 ± 280 cal years BP). However, this datum needs to be verified with more data from this period before it can be accepted as a reliable indicator.

This sea-level reconstruction (Fig 5.3) also contradicts Larcombe et al.'s (1995b) finding that sea level fell to its present position approximately 2,500-3,000 C-14 years BP. Based on *Porites* microatoll data from Yule Point and Camp Island (Chappell et al., 1983), and FBI data from New South Wales (NSW; Flood and Frankel, 1989; Baker and Haworth, 2000b; Baker et al., 2001), the sea-level curve suggests that sea level may not have fallen to its current position until 1,000-1,500 cal years BP. This timing is also supported by the maximum calibrated C-14 age for the present Nelly Bay beach of 1830 ± 130 years BP (see Section 5.5.2), as well as by similar C-14 and thermoluminescence ages for the modern beaches surrounding Sandon Point, NSW (Bryant et al., 1992).

Elevations for the coral microatoll data are systematically lower than the FBIs at similar timeframes (Fig 5.3b). FBIs are known to grow to higher elevations in swash zones compared to calmer environments and the relative elevations of these indicators may have

been overestimated. Fossil oyster beds from Louns Beach (+ 1.96 m Australian height datum; AHD) were found at a similar elevation to the fossil beds from Balding Bay (+ 2.07 m AHD; Higley, 2000). However, the fossil oyster beds from Louns Beach were 1.26 ± 0.11 m above the highest living bed (Fig 5.2) while only the nearest living oyster beds were measured at Balding and Huntingfield Bays which showed a 1.65 m and 1.55 m difference in elevation, respectively. Further measurements of living oyster beds from Magnetic Island may reveal similar elevations to the Louns Beach samples. The fossil oyster beds at Bathurst Heads were lower compared to other sites (+ 1.46 AHD); however, the highest living beds are also at a lower elevation and produce an identical relative sea-level estimate to the Louns Beach oyster beds (+ 1.21 ± 0.11 m). A + 1.20-1.30 m elevation places the oyster beds at a similar height to the highest measured fossil microatoll.
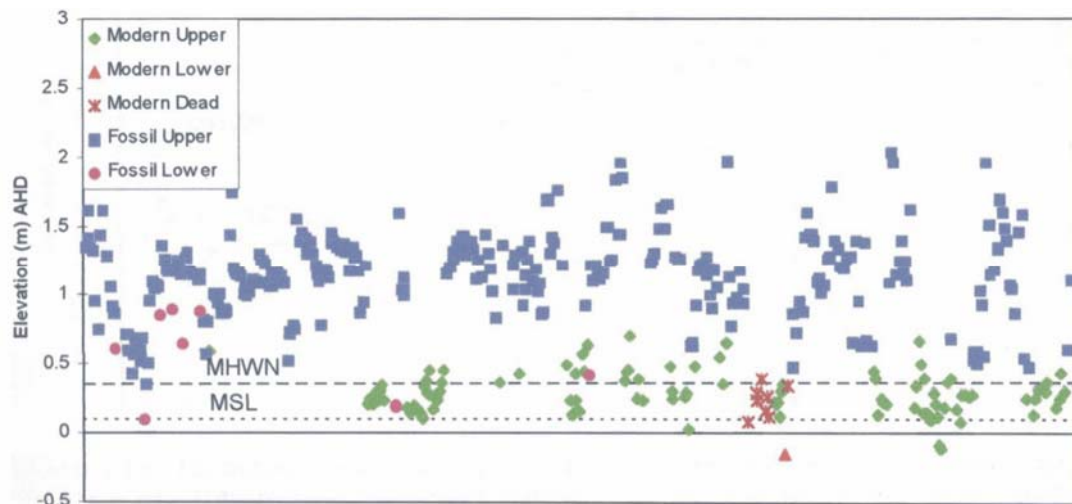
Figure 5.2. Oyster bed elevation data for Louns Beach, Cleveland Bay (from Higley, 2000). The living oyster beds have a variable elevation range exceeding 0.5 m, which places some doubt on the accuracy of the Balding Bay data where only 1 living oyster bed was measured. The highest fossil oyster bed in Louns Beach is 1.26 m above the highest living beds.

Elevation measurements of coral microatolls can also produce higher sea-level estimates if their geomorphology is not well understood; they can grow to a level as high as 1.1 m above mean low water springs in "moated" localities (Scoffin and Stoddart, 1978). Chappell et al. (1983) reported fossil "moated" microatolls from Magnetic Island at 1.7-1.9 m above modern living microatolls. This elevation is similar to the FBI data from Magnetic Island and is of similar age (calibrated C-14 ages of 5700 ± 250 and 5620 ± 200 years BP respectively). Beaman et al. (1994) argued that the difference in elevation

between the oyster bed and microatoll data may be due to either lack of suitable conditions (e.g. available substrate; higher energy) for the corals to preserve the higher elevation, or that the fossil microatolls may have been buried by beach deposits during the recent sea-level regression. Another possible explanation, although unlikely, is that the tidal range has changed, as the oyster beds record the high water neap tides while the microatolls grow to the low mean water spring elevation (Larcombe et al., 1995b).

The Holocene sea-level reconstruction (Fig 5.3) suggests that there may have been up to four sea-level oscillations upwards of 1 m during the mid-to-late-Holocene at approximately 5,080-4,030, 3,580-2,510, 2,510-1,940 and <1,250 cal years B.P. These oscillations are all supported by palaeoenvironmental data from Baker et al. (2001) who found changes in the $\delta^{18}O$ composition and species assemblages of FBIs in NSW around 5,200, 3,800 and 2,400 cal years BP with distinct growth hiatuses between $3,080 \pm 60$ and $2,310 \pm 80$ years BP. Hiatuses in oyster growth at Balding Bay (5,770-4,290 cal years BP) and at Bathurst Heads (5,970-3,740 and 3,740 and 3,210 cal years BP) further support an oscillating sea level during these periods (Higley, 2000). These hiatuses have, however, also been interpreted as possible higher energy cyclonic events (Higley, 2000). The sea-level reconstruction of this study (Fig 5.3) provides evidence for an oscillating sea level during the periods of no oyster growth; there is limited other FBI evidence around these timeframes for the east coast of Australia. It should be noted, though, that the sea-level reconstruction is complex and there is contradictory FBI evidence over some of the "oscillation" periods.

The evidence for Holocene sea-level fluctuations and the similarities in elevation between NSW and Queensland FBI data place considerable doubt on the hydro-isostatic sea-level model for the eastern Australian coastline developed by Chappell et al. (1982) and Lambeck and Nakada (1990; Fig 5.4) that predicts a smoothly falling sea level. The present sea-level curve and recent research (Baker and Haworth, 2000a; Baker et al., 2001) suggests that a global eustatic influence may have had a major influence on the Holocene sea levels of eastern Australia.

Chapter 5

Stephen E Lewis

- 130 -

Environmental trends in the GBR lagoon and Burdekin River catchment during the mid-Holocene and since European settlement using Porites coral records, Magnetic Island, QLD.

Table 5.2. Calibrated C-14 sea level data for eastern Australia using fixed biological indicators (FBI), coral microatolls and mangrove mud.

Lab code	Sample ID	Material	Location	Method	Uncorrected age	±	Calibrated age	± (2σ)	Sea level (m)	±	Reference
OZH576	Oyster shell 17	Oyster	Huntingfield Bay*	AMS 14-C	5360	50	5730	130	1.55	0.10	This study
OZH577	Oyster shell 18	Oyster	Huntingfield Bay*	AMS 14-C	5400	60	5760	140	1.55	0.10	This study
OZH578	Oyster shell 19	Oyster	Huntingfield Bay*	AMS 14-C	3330	40	3180	140	0.95	0.10	This study
OZH579	Oyster shell 20	Oyster (swash)	Huntingfield Bay*	AMS 14-C	4640	50	4860	150	1.55	0.10	This study
OZH580	Oyster shell 21	Oyster	Huntingfield Bay*	AMS 14-C	4260	50	4360	160	1.55	0.10	This study
Wk2917	BBAY1a	Oyster	Balding Bay*	Standard 14-C	4040	50	4050	160	1.65	0.15	Beaman et al. 1994
Wk2918	BBAY1b	Oyster	Balding Bay*	Standard 14-C	4600	60	4790	180	1.65	0.15	Beaman et al. 1994
Wk2919	BBAY1c	Oyster	Balding Bay*	Standard 14-C	5660	50	6050	130	1.65	0.15	Beaman et al. 1994
Wk2920	BBAY4	Barnacle	Balding Bay*	Standard 14-C	5000	60	5360	170	1.35	0.15	Beaman et al. 1994
Wk2921	BBAY2	Oyster	Balding Bay*	Standard 14-C	5010	50	5360	120	1.65	0.15	Beaman et al. 1994
OZE422	BBAY01-1	Oyster	Balding Bay*	AMS 14-C	5860	50	6280	110	1.65	0.15	Higley, 2000
OZE423	BBAY01-2	Oyster	Balding Bay*	AMS 14-C	5690	50	6080	140	1.65	0.15	Higley, 2000
OZE424	BBAY01-3	Oyster	Balding Bay*	AMS 14-C	4940	50	5250	180	1.65	0.15	Higley, 2000
WK7710	BBAY01-4	Oyster	Balding Bay*	AMS 14-C	5040	50	5400	130	1.65	0.15	Higley, 2000
WK7711	BBAY01-5	Oyster	Balding Bay*	AMS 14-C	4120	60	4170	190	1.65	0.15	Higley, 2000
WK7712	BBAY01-6	Barnacle	Balding Bay*	AMS 14-C	6890	130	7390	140	1.35	0.15	Higley, 2000
Wk7490	CM2	Oyster	Bathurst Heads	Standard 14-C	4640	60	4780	200	1.21	0.11	Higley, 2000
Wk7491	CM3	Oyster	Bathurst Heads	Standard 14-C	5180	60	5460	150	1.21	0.11	Higley, 2000
OZE419	CM3-1	Oyster	Bathurst Heads	AMS 14-C	5090	50	5420	140	1.21	0.11	Higley, 2000
OZE420	CM3-2	Oyster	Bathurst Heads	AMS 14-C	5200	50	5480	150	1.21	0.11	Higley, 2000
OZE421	CM3-3	Oyster	Bathurst Heads	AMS 14-C	5190	50	5460	140	1.21	0.11	Higley, 2000
WK7713	CM3-4	Oyster	Bathurst Heads	AMS 14-C	3820	70	3700	210	1.21	0.11	Higley, 2000
WK7714	CM3-5	Oyster	Bathurst Heads	AMS 14-C	3420	60	3210	180	1.21	0.11	Higley, 2000
WK7715	CM3-6	Oyster	Bathurst Heads	AMS 14-C	3310	60	3090	200	1.21	0.11	Higley, 2000
WK7716	CM3-1W	Oyster	Bathurst Heads	AMS 14-C	5220	60	5490	160	1.21	0.11	Higley, 2000
Wk7493	LB602	Oyster	Louns Beach	Standard 14-C	5740	60	6130	150	1.26	0.11	Higley, 2000
Wk7494	LB416	Oyster	Louns Beach	Standard 14-C	4800	110	5070	270	1.26	0.11	Higley, 2000

Chapter 5

- 131 -

Stephen E Lewis

Environmental trends in the GBR lagoon and Burdekin River catchment during the mid-Holocene and since
European settlement using Porites coral records, Magnetic Island, QLD.

Table 5.2 (continued). Calibrated C-14 sea level data for eastern Australia using fixed biological indicators (FBI), coral microatolls and mangrove mud.

Lab code	Sample ID	Material	Location	Method	Uncorrected age	±	Calibrated age	± (2σ)	Sea level (m)	±	Reference
OZC279	Site 1Aa	Tubeworms	Port Hacking, NSW	AMS 14-C	4600	90	4820	320	1.50	0.25	Baker and Haworth, 1997
OZC280	Site 2B	Barnacle	Port Hacking, NSW	AMS 14-C	3790	90	3740	300	1.50	0.25	Baker and Haworth, 1997
ANU-2321	KI/5	microatoll	King Island	Standard 14-C	4410	90	4520	270	0.45	0.25	Chappell et al. 1983
ANU-2322	KI/6	microatoll	King Island	Standard 14-C	4400	90	4510	270	0.55	0.25	Chappell et al. 1983
ANU-2323	KI/7	microatoll	King Island	Standard 14-C	5560	100	5910	260	0.75	0.25	Chappell et al. 1983
ANU-2324	KI/8	microatoll	King Island	Standard 14-C	5500	130	5870	300	0.75	0.25	Chappell et al. 1983
ANU-2319	FI/1	microatoll	Flinders Island	Standard 14-C	6110	200	6490	470	0.95	0.25	Chappell et al. 1983
ANU-2320	FI/2	microatoll	Flinders Island	Standard 14-C	6050	100	6430	220	0.55	0.25	Chappell et al. 1983
	EWY-1	microatoll	Yule Point	Standard 14-C	4870	95	5080	250	1.20	0.20	Chappell et al. 1983
	EWY-2	microatoll	Yule Point	Standard 14-C	4055	90	4030	280	1.05	0.20	Chappell et al. 1983
	EWY-3	microatoll	Yule Point	Standard 14-C	4925	120	5150	310	0.70	0.20	Chappell et al. 1983
	EWY-6	microatoll	Yule Point	Standard 14-C	1755	60	1250	150	0.55	0.20	Chappell et al. 1983
	EWY-4	microatoll	Yule Point	Standard 14-C	1600	55	1100	140	0.35	0.20	Chappell et al. 1983
	EWD-1	microatoll	Dunk Island	Standard 14-C	6175	100	6610	240	0.85	0.25	Chappell et al. 1983
	EWD-3	microatoll	Dunk Island	Standard 14-C	5745	90	6120	200	0.70	0.25	Chappell et al. 1983
	EWD-5	microatoll	Dunk Island	Standard 14-C	5805	70	6190	180	0.35	0.25	Chappell et al. 1983
	EWD-4	microatoll	Dunk Island	Standard 14-C	5095	95	5440	210	0.45	0.25	Chappell et al. 1983
	EWG-1	microatoll	Goold Island	Standard 14-C	6305	140	6770	340	1.25	0.25	Chappell et al. 1983
	EWG-2	microatoll	Goold Island	Standard 14-C	5665	110	6050	240	0.95	0.25	Chappell et al. 1983
	EWG-3	microatoll	Goold Island	Standard 14-C	3500	70	3380	180	0.55	0.25	Chappell et al. 1983
ANU-2471	EWO/4	microatoll	Orpheus Island	Standard 14-C	5310	80	5690	180	0.95	0.20	Chappell et al. 1983
ANU-2476	EWO/3	microatoll	Orpheus Island	Standard 14-C	4750	70	5030	200	0.65	0.20	Chappell et al. 1983
ANU-2473	EWO/2	microatoll	Orpheus Island	Standard 14-C	3470	70	3330	180	0.40	0.20	Chappell et al. 1983
ANU-2470	EWO/1	microatoll	Orpheus Island	Standard 14-C	2910	70	2630	190	0.20	0.15	Chappell et al. 1983
ANU-2477	FA/5	microatoll	Fantome Island	Standard 14-C	5790	70	6160	170	1.00	0.20	Chappell et al. 1983
ANU-2464	FA/4	microatoll	Fantome Island	Standard 14-C	5970	90	6400	200	0.90	0.20	Chappell et al. 1983

Table 5.2 (continued). Calibrated C-14 sea level data for eastern Australia using fixed biological indicators (FBI), coral microatolls and mangrove mud.

Lab code	Sample ID	Material	Location	Method	Uncorrected age	±	Calibrated age	± (2σ)	Sea level (m)	±	Reference
ANU-2478	FA/3	microatoll	Fantome Island	Standard 14-C	4770	80	5050	220	0.65	0.20	Chappell et al. 1983
ANU-2463	FA/1	microatoll	Fantome Island	Standard 14-C	3000	80	2750	220	0.45	0.20	Chappell et al. 1983
ANU-2469	FA/2	microatoll	Fantome Island	Standard 14-C	2990	80	2740	220	0.35	0.20	Chappell et al. 1983
ANU-2466	GP/5	microatoll	Great Palm Island	Standard 14-C	5440	110	5820	250	0.85	0.20	Chappell et al. 1983
ANU-2474	GP/4	microatoll	Great Palm Island	Standard 14-C	4840	80	5090	220	0.85	0.20	Chappell et al. 1983
ANU-2465	GP/3	microatoll	Great Palm Island	Standard 14-C	5940	90	6370	200	0.80	0.20	Chappell et al. 1983
	EWM/4	microatoll	Geoffrey Bay*	Standard 14-C	5775	70	6150	170	1.20	0.20	Chappell et al. 1983
	EWM/5	microatoll	Geoffrey Bay*	Standard 14-C	5220	70	5580	170	1.00	0.20	Chappell et al. 1983
	EWM/6	microatoll	Geoffrey Bay*	Standard 14-C	4980	100	5290	270	0.50	0.20	Chappell et al. 1983
	EWM/7	microatoll	Geoffrey Bay*	Standard 14-C	5215	110	5560	250	0.70	0.20	Chappell et al. 1983
	EWM/8	microatoll	Geoffrey Bay*	Standard 14-C	810	60	410	110	0.15	0.05	Chappell et al. 1983
	EWC/1	microatoll	Camp Island	Standard 14-C	6270	110	6710	270	0.90	0.20	Chappell et al. 1983
	EWC/2	microatoll	Camp Island	Standard 14-C	5470	95	5830	230	0.70	0.20	Chappell et al. 1983
	EWC/3	microatoll	Camp Island	Standard 14-C	1730	95	1270	210	0.50	0.20	Chappell et al. 1983
	EWS/1	microatoll	Stone Island	Standard 14-C	6375	110	6870	280	1.08	0.18	Chappell et al. 1983
	EWS/2	microatoll	Stone Island	Standard 14-C	5735	130	6130	280	1.08	0.18	Chappell et al. 1983
	EWS/3	microatoll	Stone Island	Standard 14-C	6205	100	6640	240	0.98	0.18	Chappell et al. 1983
	EWS/4	microatoll	Stone Island	Standard 14-C	5700	90	6090	190	0.63	0.18	Chappell et al. 1983
Beta-30959		Tubeworms	Valla Beach, NSW	Standard 14-C	3870	70	3840	270	1.02	0.10	Flood and Frankel, 1989
Beta-30960		Barnacle	Valla Beach, NSW	Standard 14-C	2230	140	1860	390	0.70	0.10	Flood and Frankel, 1989
Beta-113733	Site 1Ab	Tubeworms	Port Hacking, NSW	Standard 14-C	3950	100	3950	340	1.70	0.20	Baker and Haworth, 2000b
Beta-116617	Site 1Ca	Tubeworms	Port Hacking, NSW	Standard 14-C	3260	60	3090	240	1.10	0.25	Baker and Haworth, 2000b
Beta-116618	Site 1Cb	Tubeworms	Port Hacking, NSW	Standard 14-C	2630	80	2360	310	1.10	0.25	Baker and Haworth, 2000b
Beta-116616	Site 1Cc	Barnacle	Port Hacking, NSW	Standard 14-C	4800	90	5080	270	1.00	0.20	Baker and Haworth, 2000b
Beta-125965	Site 1Cd	Mollusc	Port Hacking, NSW	Standard 14-C	4880	40	5190	230	1.20	0.20	Baker and Haworth, 2000b

Table 5.2 (continued). Calibrated C-14 sea level data for eastern Australia using fixed biological indicators (FBI), coral microatolls and mangrove mud.

Lab code	Sample ID	Material	Location	Method	Uncorrected age	±	Calibrated age	± (2σ)	Sea level (m)	±	Reference
Beta-111205	Site 2A	Tubeworms	Port Hacking, NSW	Standard 14-C	2560	70	2220	270	1.00	0.10	Baker and Haworth, 2000b
Beta-116620	Site 3	Tubeworms	Port Hacking, NSW	Standard 14-C	1820	50	1380	180	0.80	0.25	Baker and Haworth, 2000b
Beta-111204	Site 4A	Tubeworms	Port Hacking, NSW	Standard 14-C	2280	60	1900	240	1.00	0.25	Baker and Haworth, 2000b
Beta-111206	Site 4B	Tubeworms	Port Hacking, NSW	Standard 14-C	2370	60	2030	240	1.30	0.10	Baker and Haworth, 2000b
Beta-111203	Site 5	Tubeworms	Port Hacking, NSW	Standard 14-C	2330	70	1960	260	1.40	0.25	Baker and Haworth, 2000b
Wk8234	Site 1B	Tubeworms	Vaucluse, NSW	Standard 14-C	3390	90	3240	300	1.10	0.25	Baker et al. 2001
Beta-132994	Site 1A	Barnacle	Vaucluse, NSW	Standard 14-C	5120	40	5470	170	1.40	0.50	Baker et al. 2001
Wk8495	Site Pat 1	Tubeworms	Patonga Bay, NSW	Standard 14-C	3750	65	3680	250	1.00	0.25	Baker et al. 2001
Wk8236	CSIRO-CB2	Tubeworms	Caves Beach, NSW	Standard 14-C	2590	70	2270	280	1.20	0.20	Baker et al. 2001
Wk8492	VAL6C flood	Tubeworms	Valla Beach, NSW	Standard 14-C	3570	70	3470	250	1.00	0.10	Baker et al. 2001
GaK-7688		microatoll	Rattlesnake Island	Standard 14-C	5530	130	5900	290	1.00	0.25	Hopley et al. 1983
Gak-5215		microatoll	Middle Island	Standard 14-C	5210	115	5570	270	1.00	0.25	Hopley, 1975
ANU-1604		microatoll	Low Wooded Isle	Standard 14-C	6060	90	6450	200	0.60	0.20	McLean et al. 1978
ANU-1287		microatoll	Houghton Island	Standard 14-C	5850	170	6230	390	1.10	0.25	McLean et al. 1978
ANU-1286		microatoll	Leggatt Island	Standard 14-C	5800	130	6160	290	1.00	0.25	McLean et al. 1978
ANU-1380		microatoll	Three Isles	Standard 14-C	3750	110	3630	280	0.80	0.25	McLean et al. 1978
ANU-1285		microatoll	Nymph Island	Standard 14-C	3700	90	3580	230	1.30	0.25	McLean et al. 1978
ANU-1384		microatoll	East Pethebridge	Standard 14-C	2370	70	1940	200	0.60	0.20	McLean et al. 1978
Wk7760	YM1	microatoll	Yam Island	Standard 14-C	6340	80	6750	220	0.30	0.10	Woodroffe et al. 2000
Wk7775	YM2	microatoll	Yam Island	Standard 14-C	5820	80	6170	200	0.50	0.10	Woodroffe et al. 2000
Wk7772	YM3	microatoll	Yam Island	Standard 14-C	4200	80	4200	240	0.00	0.10	Woodroffe et al. 2000
Wk7763	YM4	microatoll	Yam Island	Standard 14-C	2740	60	2450	210	-0.30	0.10	Woodroffe et al. 2000
Wk7757	YM5	microatoll	Yam Island	Standard 14-C	6300	90	6700	230	0.70	0.10	Woodroffe et al. 2000
Wk7773	YM6	microatoll	Yam Island	Standard 14-C	5070	70	5380	190	0.50	0.20	Woodroffe et al. 2000

Table 5.2 (continued). Calibrated C-14 sea level data for eastern Australia using fixed biological indicators (FBI), coral microatolls and mangrove mud.

Lab code	Sample ID	Material	Location	Method	Uncorrected age	±	Calibrated age	± (2σ)	Sea level (m)	±	Reference
Wk7774	W12	microatoll	Warraber Island	Standard 14-C	5770	70	6110	170	0.70	0.20	Woodroffe et al. 2000
Wk7771	W13	microatoll	Warraber Island	Standard 14-C	5660	70	6030	180	0.80	0.20	Woodroffe et al. 2000
Wk7794	W18	microatoll	Warraber Island	Standard 14-C	5150	70	5450	160	1.00	0.20	Woodroffe et al. 2000
Wk7769	HI5a	microatoll	Hammond Island	Standard 14-C	6340	80	6750	220	1.00	0.20	Woodroffe et al. 2000
ANU-8822		microatoll	Repulse Island	Standard 14-C	2320	70	1930	180	1.00	0.25	Blake, 1994
ANU-8823		microatoll	Repulse Island	Standard 14-C	2770	70	2510	190	1.00	0.25	Blake, 1994
GAK/6719		Mangrove mud	Cleveland Bay	Standard 14-C	7730	170	8580	410	-11.00	5.00	Belperio, 1979
GAK/6720		Mangrove mud	Cleveland Bay	Standard 14-C	8540	170	9470	450	-10.00	5.00	Belperio, 1979
GAK/7223		Mangrove mud	Cleveland Bay	Standard 14-C	7970	200	8840	480	-9.00	5.00	Belperio, 1979
Wk794	V2/433	Mangrove mud	Cleveland Bay	Standard 14-C	7820	280	8660	640	-20.00	5.00	Carter et al. 1993
Wk793	V2/383	Mangrove mud	Cleveland Bay	Standard 14-C	7520	260	8300	510	-19.50	5.00	Carter et al. 1993
Wk792	V2/300	Mangrove mud	Cleveland Bay	Standard 14-C	7950	300	8830	660	-18.50	5.00	Carter et al. 1993
Wk795	V3/175	Mangrove mud	Cleveland Bay	Standard 14-C	6910	240	7730	440	-7.00	5.00	Carter et al. 1993
Wk865	85B/S	Mangrove mud	Cleveland Bay	Standard 14-C	7110	90	7860	180	-5.00	5.00	Carter et al. 1993
Wk16749	OI-2-04 (193-195)	Mangrove mud	Halifax Bay	Standard 14-C	9065	60	10090	180	-21.00	5.00	Wüst, unpublished
Wk16750	OI-2-04 (293-295)	Mangrove mud	Halifax Bay	Standard 14-C	9515	60	10710	160	-22.50	5.00	Wüst, unpublished

* samples from Magnetic Island
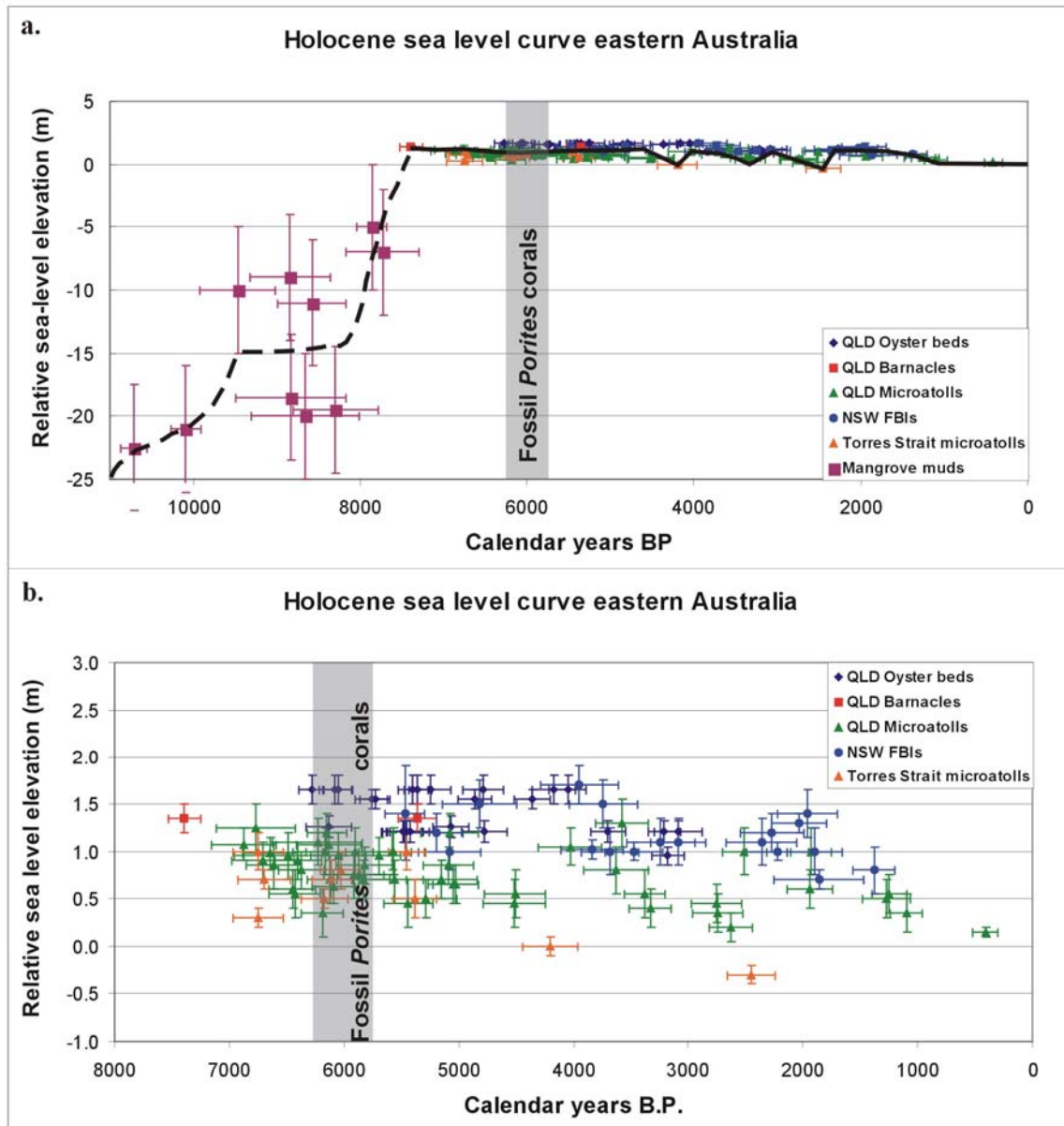
Figure 5.3 (a-b). Holocene sea level curves for eastern Australia using the calibrated C-14 dataset listed in Table 5.2 (note: shaded area corresponds to the calibrated C-14 ages for the fossil mid-Holocene corals). The reconstruction (a) suggests that sea level rose to a height of 1.0-1.5 m above the present about 7,000-7,500 cal years BP. Sea level remained more or less at this position (small oscillations identified at 5080-4030, 3580-2510 and 2510-1940 cal years BP) until approximately 1,000-1,500 cal years BP when it fell to its current elevation. The Holocene sea level curve, excluding the mangrove mud indicators (b), suggests that the FBI data (oyster beds, barnacles and NSW samples) appear to be higher than the coral microatolls during similar timeframes. This finding suggests that there may be some systematic errors in these sea-level indicators.

The fossil mid-Holocene corals lived during a period of relatively stable sea level (shaded area; Fig 5.3). The FBIs are, however, consistently at higher elevations compared to the coral microatoll data during this period (Fig 5.3b). Microatolls provide the more accurate account of sea level as their vertical growth range is much less (<20 cm) compared to FBI (~1 m); however, it is possible that there were minor sea-level fluctuations during this period.
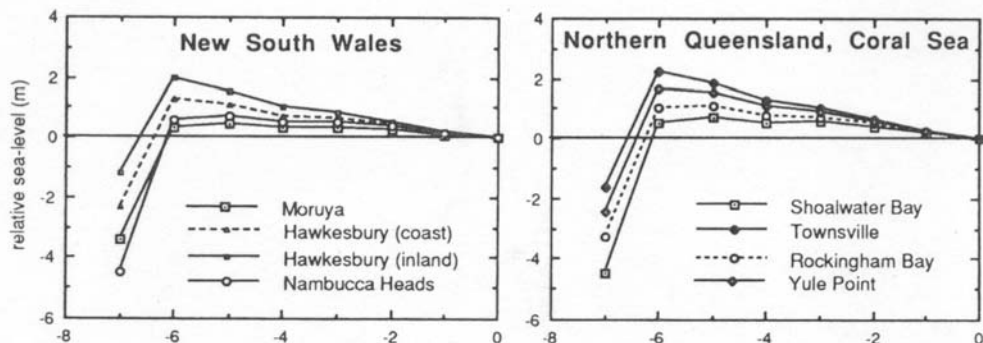
Figure 5.4. Holocene sea level models for north Queensland and New South Wales from Lambeck and Nakada (1990). These models suggest that sea level fell smoothly from 6 ka and reached its present position about 1.5-2.0 ka. This model does not agree with the sea level curve developed in this study, which suggests sea level remained at a similar elevation from approximately 7.5 to 2.0 ka, with minor changes throughout that period.

5.3.4. Summary

A new Holocene sea-level curve was developed for eastern Australia using coral microatoll, FBI and mangrove mud data. These indicators are considered to provide the most accurate measurements of sea level. There are, nevertheless, differences in the relative elevations between coral microatolls and FBIs at identical timeframes. It is unclear why these differences occur in the sea-level reconstruction. Sea level reached a height approximately 1.0-1.5 m above present sea level about 7,000-7,500 cal years BP and remained more or less at this level (~1 m) until approximately 1,000-1,500 cal years BP, when sea level fell to its current position. The fossil mid-Holocene corals may have grown at a time of relatively stable sea level but the temporal resolution of the data (including both elevation and C-14 ages) is too coarse to determine precisely any minor sea-level fluctuations that may have occurred during the growth of the mid-Holocene corals.

5.4. Topographic profiles

5.4.1. Overview

Topographic profiles taken along three transects in Nelly Bay are presented. The locations and the depths of penetration for 14 sediment cores taken along these transects are displayed and the morphological boundaries discussed. The surface sediments in Nelly Bay are compared to the previous work carried out by Smith (1974; 1978).

5.4.2. Topographic surveys and surface sediments

Three transects were taken along the southern (X-base section; Fig 5.5), middle (Fig 5.6), and northern (harbour section; Fig 5.7) areas in Nelly Bay from the beach to the reef flat (the locations for the sediment cores are given in Fig 4.1). Three major morphological boundaries were identified in all the topographic profiles including the beach, tidal flat and reef flat. The beach material is composed of medium to coarse well-sorted sand, similar to that described by Smith (1974; 1978). The tidal flat is made up of a mixture of coarse sand and coral fragments, while the reef flat is composed of live corals, microatolls and coral shingle. The tidal flat and reef flat zones in this study are identical to the description of the reef flat by Smith (1974; 1978). This study divides this zone, classified by Smith, into two morphologies separated by the presence/absence of living corals. During the elevated Holocene sea level (~1.5-7.5 ka), it is likely that live coral growth extended to the present beach. Therefore, the tidal flat could represent the remnants of a prograding reef flat. The modern foredune in the X-base section (Fig 5.5) is composed of well-sorted, fine to medium quartz-feldspathic sand and is present (but not surveyed) in the other profiles. A significant sand body, composed of well-sorted medium sand, was observed landward of the current Nelly Bay road in the X-base section (Fig 5.5). This deposit is interpreted to be the former beach ridge/foredune active during the mid-Holocene sea level highstand. The base of this feature is approximately 1 m above the base of the present Nelly Bay foredune and its peak is about 1.8 m higher than the top of the active foredune. The elevation of this sand body is, therefore, consistent with sea level from 7,500-1,500 cal years BP (Fig 5.3).
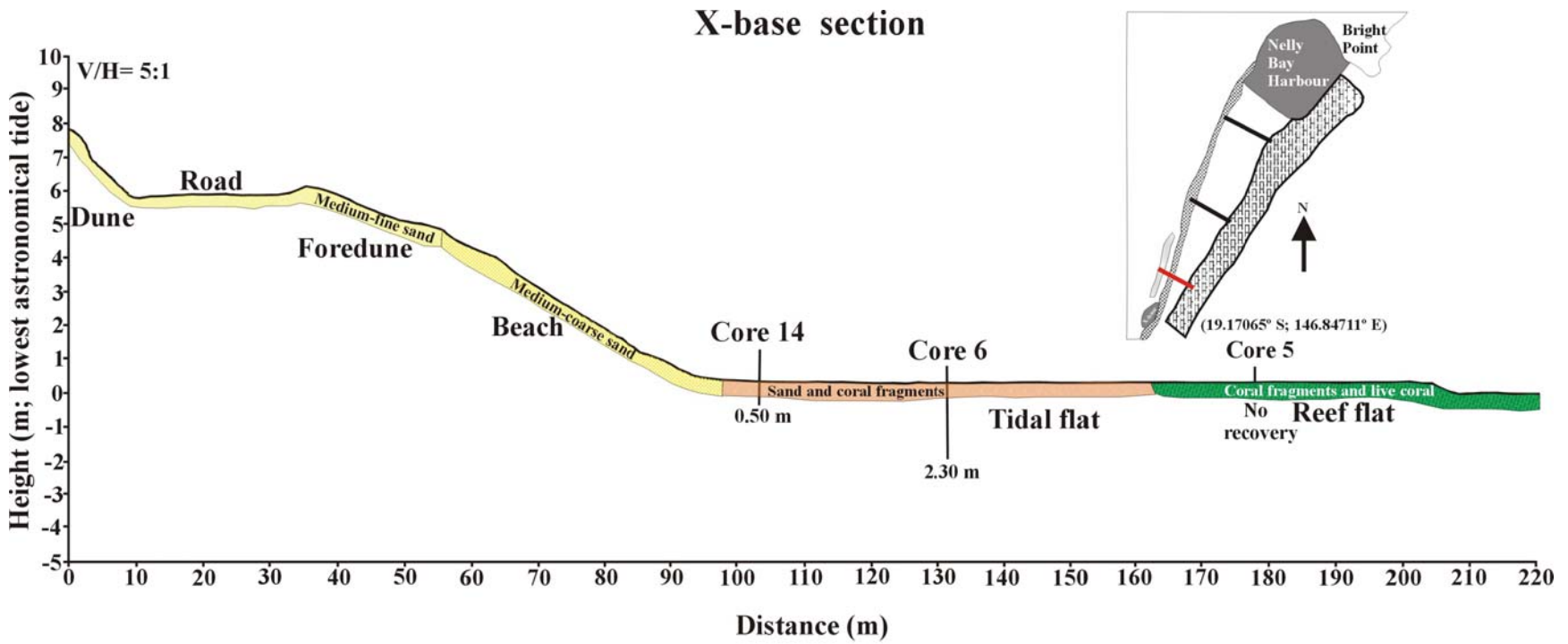
X-base section

Figure 5.5. Topographic profile of the X-base section Nelly Bay. Note the locations and penetration depth of the sediment cores.
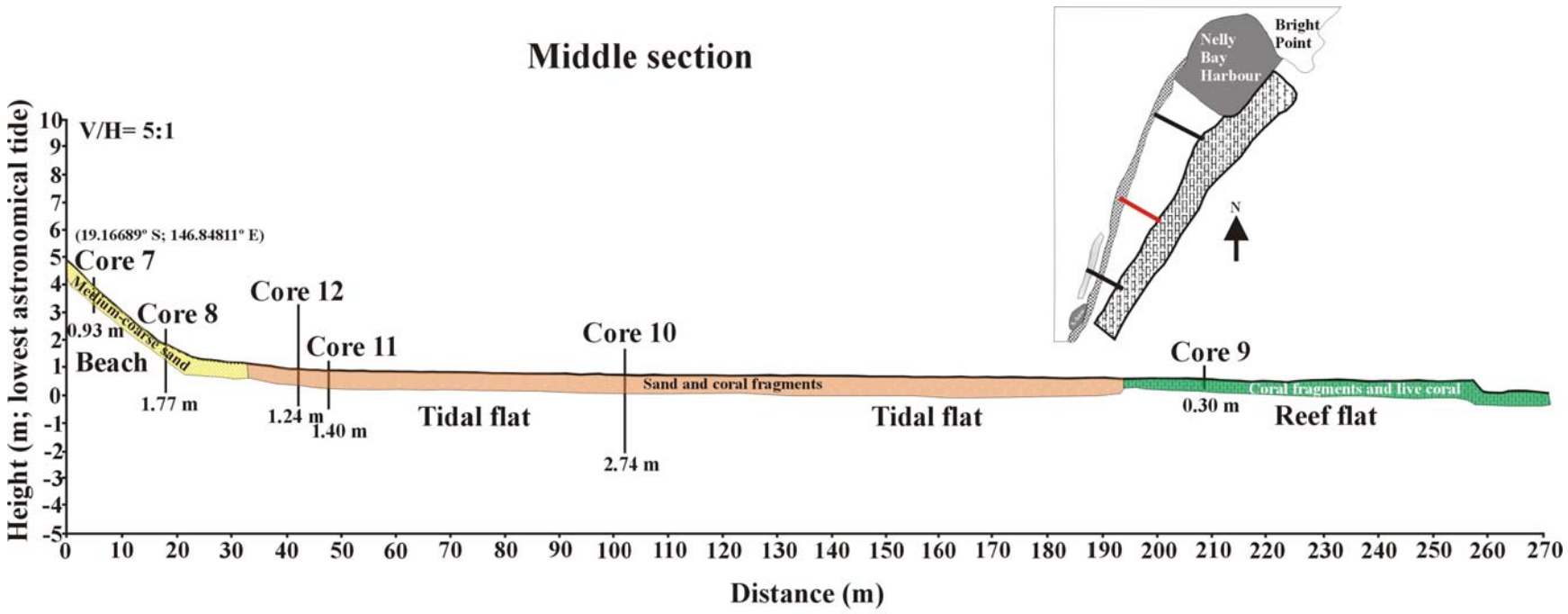
Figure 5.6. Topographic profile of the middle section Nelly Bay. Note the locations and penetration depth of the sediment cores.
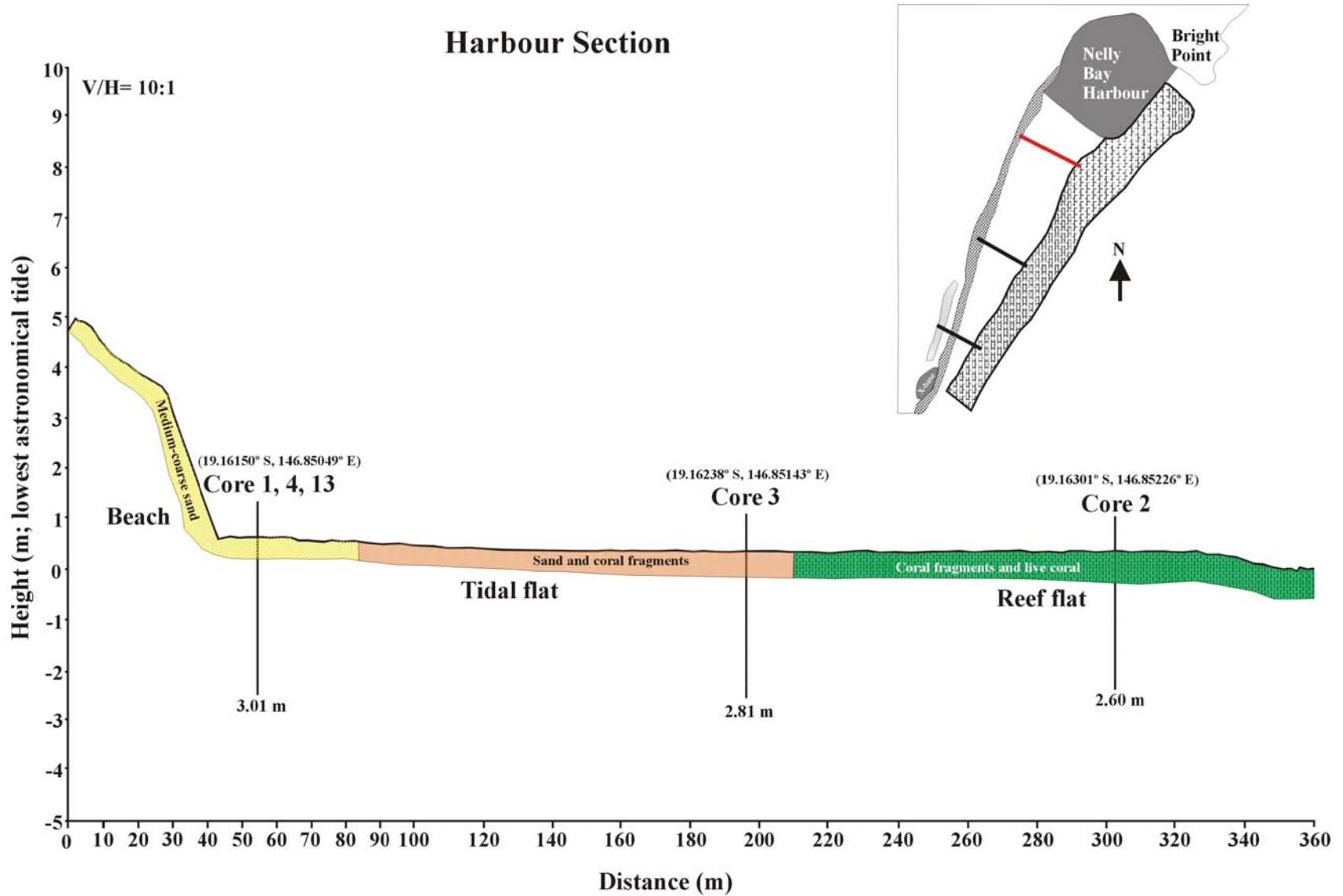
Figure 5.7. Topographic profile of the harbour section Nelly Bay. Note the locations and penetration depth of the sediment cores.

5.4.3. Summary

Four major morphological zones were identified in three topographic surveys along the southern, middle and northern sections of Nelly Bay. These included dune, beach, tidal flat and reef flat and are consistent with the zones described by Smith (1974; 1978). An extensive sand body was observed on the southern (X-base section) transect landward of the Nelly Bay road which is interpreted to be the former beach ridge active during the mid-Holocene sea level highstand.

5.5. Sedimentary units in Nelly Bay

5.5.1. Overview

The sedimentary units classified in the cores from Nelly Bay were determined by grainsize and composition of the sediments. Six sedimentary units were identified in the fourteen sediment cores taken along the three transects in Nelly Bay:

1.   sand unit (ranging from medium, medium-coarse to coarse grained),
2.   coral fragments unit,
3.   medium sand with coral fragments unit,
4.   muddy sand with coral fragments unit,
5.   sandy mud with coral fragments unit, and
6.   mud with minor coral fragments unit.

This section discusses the lateral and vertical extent, composition, sediment sorting, age, mineralogy and geochemistry of each unit and compares these units with previous work.

5.5.2.   Sand unit

The sand unit is composed of sand-sized terrigenous grains with minor shell and shell hash material (typically <10%). The beach sediments in Nelly Bay are entirely composed of this unit and range from moderately sorted, medium-coarse and coarse-grained sand in the upper beach (i.e. core 7) to well-sorted, medium-grained sand in the lower beach (core 8;

Fig 5.9). The thickness of this unit was not determined in this study, but the sand unit was up to 4-5 m thick in excavation pits dug during the planning for the Nelly Bay Harbour (McIntyre and Associates, 1989). This unit has not been age-dated but the maximum age of the beach in Nelly Bay is thought to be less than $1,830 \pm 130$ cal years old (i.e. the age of the medium sand with coral fragments unit found directly below this deposit in core 8; Fig 5.9). The sand unit probably formed when sea level fell to its present position around 1.0-1.5 thousand years ago. This unit is largely composed of quartz (52%) and plagioclase/microcline feldspar (45%) with a minor lithic/clay component (5%; Table 5.3).

5.5.3. Coral fragments unit

The coral fragments unit is a superficial deposit occurring along the Nelly Bay reef flat (see the topographic profiles Figs 5.5-5.7). The unit is entirely composed of reworked staghorn and branching coral fragments and is typically less than 20 cm thick. The unit has not been dated but the material is thought to have been either reworked from the medium sand with coral fragments unit (modern to 1830 years in age) or derived from the current fore reef.

Table 5.3. Mineralogy of the various units in core 13 as determined by the *Siroquant*™ program (see Fig 5.10 for sampling locations).

Unit	Quartz	Calcium plagioclase	Microcline	Expanding clay	Aragonite	Calcite	High Magnesium calcite	Muscovite/ Illite	Garnet phase	Sodium Chloride
Sand unit	52%	20%	25%	Trace	0%	0%	0%	0%	0%	0%
Medium sand/coral frags	23%	10%	0%	Trace	45%	4%	15%	Trace	0%	0%
Muddy sand/coral frags	10%	0%	0%	0%	50%	Trace	23%	0%	15%	0%
Mud/some coral frags	20%	9%	16%	0%	40%	Trace	13%	0%	0%	Trace
Mud/some coral frags	38%	18%	18%	0%	22%	0%	4%	0%	Trace	0%
Mud/some coral frags	10%	9%	8%	0%	42%	Trace	28%	0%	Trace	0%

5.5.4. Medium sand with coral fragments unit

The medium sand with coral fragments unit is a laterally extensive deposit present in all three transects (Figs 5.8-5.10). It varies in thickness from about 0.51 m in core 13 to 1.75 m (corrected thickness) in core 3 (Fig 5.10). The compaction-corrected thickness in core 3 and some of the other cores (e.g. core 6 and 10) may have been over estimated due

to the relatively high compaction (Table 5.4) and preferential compression of the "muddy" units. The unit is composed of a poorly-sorted 50-50% mixture of medium to coarse terrigenous sand and coral fragments. The medium sand is comprised of quartz (62%), plagioclase feldspar (27%), expanding clays (8%) and muscovite (3%; removing the carbonate component). The coral fragments in this unit are up to 7 cm long and are dominantly branching corals. The age of this unit ranges from modern to 1830 cal years BP (calibrated C-14) and probably formed after sea level fell to its present position (Table 5.5). The geochemistry of this unit (ICP-13e; Figs 5.10-5.11 for sampling location) is slightly different to the lower "muddier" unit with a relative enrichment towards the heavy rare earth elements (see section 5.5.9 for sediment provenance). In addition, elements such as Nb, Ta and Hf are relatively abundant in this unit compared to the other sedimentary layers (for a discussion on the provenance of this unit see section 5.5.9).

Table 5.4. Sediment cores penetration, recovery and % compaction.

Sediment core	Core length (cm)	Penetration (cm)	Compaction
1	176.5	281.5	37%
2	127	260	51%
3	56	281	80%
4	177	295	40%
5	0	0	N/A
6	95	230	59%
7	83	93	11%
8	110	177	38%
9	24	30	20%
10	93	274	66%
11	45	140	68%
12	67	124	46%
13	200	300	33%
14	32	50	36%

Sediment cores Nelly Bay X-base section
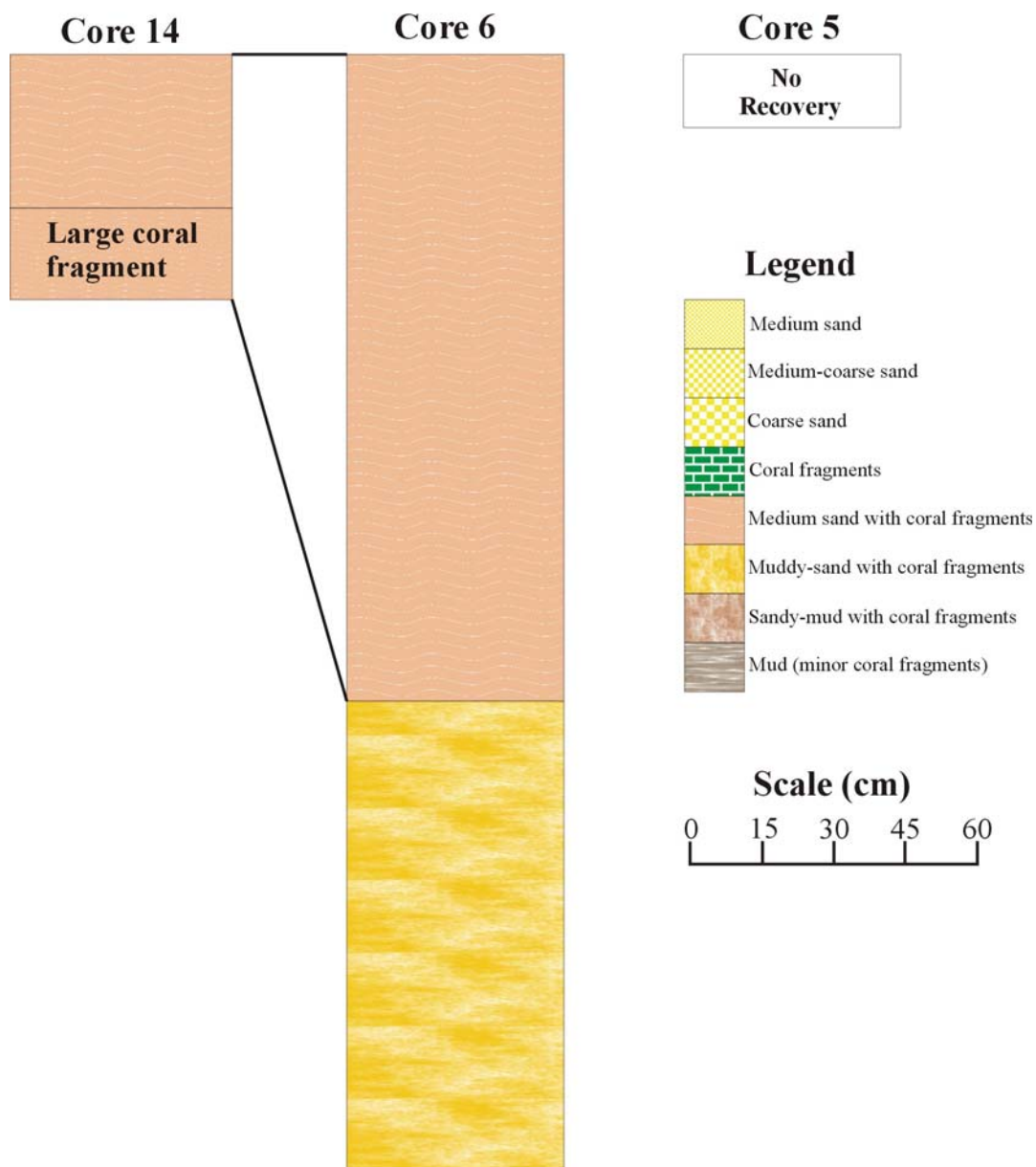
Figure 5.8. Sediment cores taken along the X-base section. Unfortunately, coring was particularly difficult along this transect. Core 5 was not recovered and a large coral fragment became wedged in core 14 and prevented any further penetration. Core 6, however, demonstrates that the medium sand with coral fragments and the muddy sand with coral fragments units were laterally continuous throughout Nelly Bay.

Sediment cores Nelly Bay Middle section

1830 ± 130 cal yrs BP

2150 ± 150 cal yrs BP

Large coral fragment

Legend

Medium sand
Medium-coarse sand
Coarse sand
Coral fragments
Medium sand with coral fragments
Muddy-sand with coral fragments
Sandy-mud with coral fragments
Mud (minor coral fragments)

Scale (cm)
0   15   30   45   60
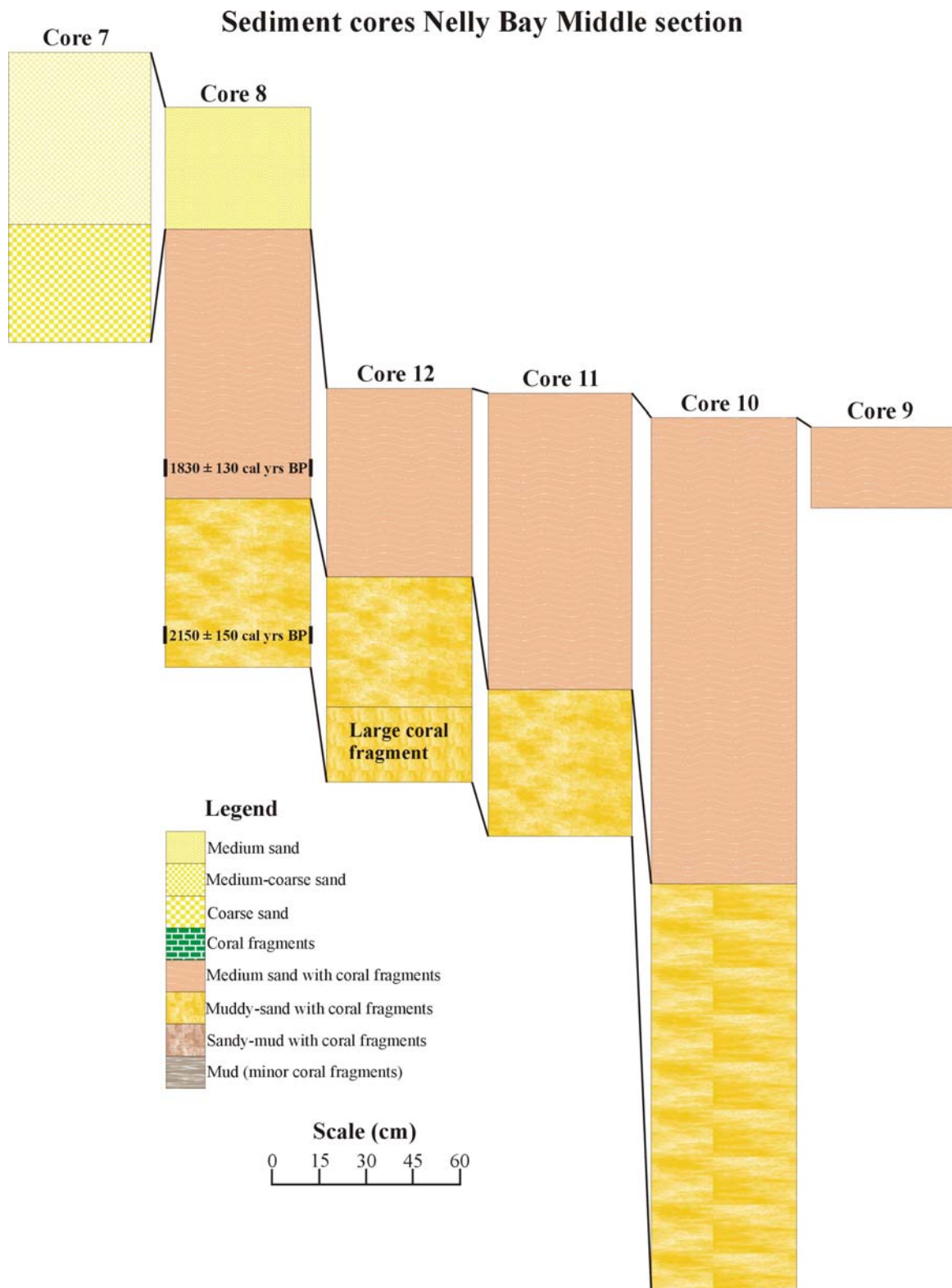
Figure 5.9. Sediment cores taken along the middle section (note the location of the calibrated C-14 ages for core 8). The medium sand with coral fragments unit was dated in core 8 at 1830 ± 130 years BP, placing a maximum age on the beach sediments in Nelly Bay. This is in agreement with the sea-level reconstruction (Fig 5.3) which estimates that it fell to its present position around 1.0-1.5 ka.

Sediment cores Nelly Bay Harbour section
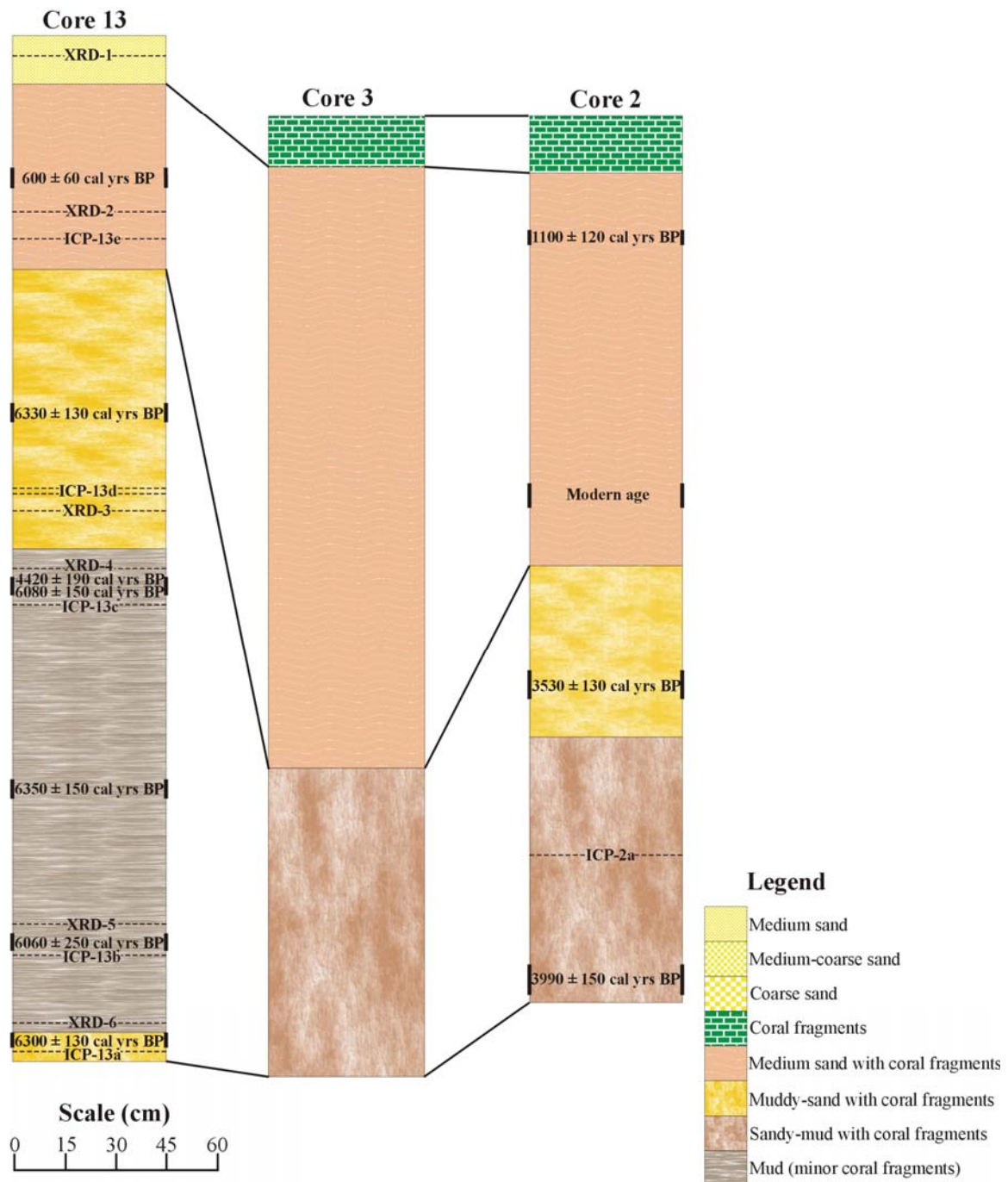
Figure 5.10. Sediment cores from the Nelly Bay Harbour section (note the location of the calibrated C-14 ages, the XRD samples taken in core 13 and the ICP analysis sampled in cores 13 and 2). The cores indicate that the medium sand with coral fragments unit is laterally continuous across Nelly Bay, while the muddy sand with coral fragments, sandy mud with coral fragments, and the mud with minor coral fragments units were of similar age and appear to be the same sedimentary layer.

5.5.5. Muddy sand with coral fragments unit

The muddy sand with coral fragments unit is composed of poorly-sorted, medium-coarse sand and coral fragments with some mud-sized material (~5-10%). The unit can be traced laterally throughout the embayment and may be positioned directly above Pleistocene sediments. No sediment core completely penetrated this unit, so its thickness cannot be accurately determined; however, sediment cores taken in previous studies estimated this unit to be 2.5-3.0 m thick in most parts of the embayment (e.g. McIntyre and Associates, 1989; Golder Associates, 2000). The calibrated C-14 age of this unit varies from 2,150-6,330 cal years BP which suggests that it has accumulated over a relatively long timeframe (Table 5.5). In addition, these ages were identical to the sandy mud with coral fragments (3,990 cal years BP) and mud with minor coral fragments (4,420-6,350 cal years BP) units; these units may all be the same laterally continuous sedimentary layer. The XRD mineralogy of the terrigenous mud-sand component was 40% quartz and 60% of a "garnet phase" (Table 5.3). The presence of garnet was unusual and this mineral phase may have been incorrectly interpreted by the XRD and Siroquant™ software (M. Rubenach personal communication, 2005). This mud-sand component is most probably similar to the XRD analysis of the mud with minor coral fragments unit (see section 5.5.7). The geochemistry of this unit (with the exception of ICP-13a) is very similar to the sandy mud with coral fragments unit and to the mud with minor coral fragments unit, which further indicates that these units are the same (Fig 5.10; see section 5.5.9 for sediment provenance). The muddy sand with coral fragments unit at the base of core 13 has a similar geochemical signature (ICP-13a; Fig 5.10) to Gustav Creek. This sample may sit directly above the Pleistocene alluvial sediments and may have become mixed with these non-marine Pleistocene sediments.

Table 5.5. Calibrated C-14 ages of the sediment cores

Lab code	Sample ID	Material	Core	Depth (m)	Corrected depth	Unit	Uncorrected age	±	Calibrated age	± (2σ)
OZH561	Shell 2	Shell	13	0.27-0.30	0.40-0.45	Medium sand/coral frags	1040	40	600	60
OZH562	Shell 3	Shell	13	0.72-0.76	1.08-1.14	Muddy sand/coral frags	5930	60	6330	130
OZH563	Shell 4a	Shell	13	1.07-1.11	1.60-1.66	Mud/some coral frags	4280	70	4420	190
OZH564	Coral 4b	Coral	13	1.07-1.11	1.60-1.66	Mud/some coral frags	5670	60	6080	150
OZH565	Shell 5	Shell	13	1.46-1.50	2.19-2.25	Mud/some coral frags	5940	70	6350	150
OZH566	Coral 6	Coral	13	1.77-1.80	2.65-2.70	Mud/some coral frags	5640	110	6060	250
OZH567	Coral 7	Coral	13	1.94-1.98	2.91-2.97	Muddy sand/coral frags	5880	60	6300	130
OZH568	Coral 8	Coral	2	0.16-0.19	0.33-0.39	Medium sand/coral frags	1530	40	1100	120
OZH569	Shell 9	Shell	2	0.53-0.57	1.08-1.17	Medium sand/coral frags	Modern		Modern	
OZH570	Coral 10	Coral	2	0.80-0.84	1.64-1.72	Muddy sand/coral frags	3630	50	3530	130
OZH571	Coral 11	Coral	2	1.22-1.26	2.50-2.58	Sandy muddy coral	3960	50	3990	150
OZH572	Shell 13	Shell	8	0.70-0.73	1.13-1.18	Medium sand/coral frags	2250	50	1830	130
OZH573	Shell 14	Shell	8	1.03-1.07	1.66-1.72	Muddy sand/coral frags	2450	50	2150	150

5.5.6. Sandy mud with coral fragments unit

The sandy mud with coral fragments unit is composed of poorly-sorted coral (~50%), mud (~40%) and medium sand (~10%) particles and was only intersected in sediment cores 2 and 3 (Fig 5.10). The coral fragments were up to 5 cm long and were dominantly branching corals. The unit was 78 cm and 90 cm thick in the two cores, respectively; however, the unit was not completely penetrated. As previously discussed, this unit is probably the stratigraphic equivalent to the muddy sand with coral fragments unit as it is of similar age (3990 cal years BP; Fig 5.9; Table 5.5). XRD analysis was not performed on this unit, but the mineralogy is probably similar to the muddy sand with coral fragments and mud with minor coral fragments units. The geochemistry of this unit is identical to the muddy sand with coral fragments unit (Fig 5.11).

5.5.7. Mud with minor coral fragments unit

The mud with minor coral fragments unit is composed of well-sorted mud with some sparse coral fragments (branching form) up to 7 cm long. This unit was only intersected in sediment core 13 where it is 130 cm thick (Fig 5.10). The average terrigenous component is 43% quartz, 54% feldspar (25% plagioclase; 29% microcline) and 3% of a "garnet phase". The age of this unit ranges from 4,420 to 6,250 cal years BP (Table 5.5), similar to

the muddy sand with coral fragments unit. The geochemistry (Fig 5.11) and mineralogy (Table 5.4) were also similar to the muddy sand with coral fragments unit which further indicates that these units are a continuous sedimentary layer. This unit will, therefore, be combined with the muddy sand with coral fragments and sandy mud with coral fragments units for the construction of the stratigraphic profile in Nelly Bay. The convoluted age structure in core 13 (Fig 5.10) suggests that this layer has been extensively reworked and mixed over a considerable period of time.

5.5.8. Previous work

A series of excavation pits, boreholes and Rotary drill holes were undertaken in Nelly Bay during investigations for the construction of the marine harbour by McIntyre and Associates (1986; 1989) and Golder Associates (2000). These reports document three major sedimentary units in Nelly Bay including a marine sand and coral unit (with traces of silt), a clayey sand unit and a sandy clay unit. The marine sand and coral unit averages 3 m in thickness and is considered to represent both the medium sand with coral fragments and muddy sand with coral fragments units identified in this study. These earlier investigations probably used water to lubricate the drilling equipment which would have effectively removed any mud-sized material before the sediments could be logged. The muddy sand with coral fragments unit would, therefore, have been reported as a sand with coral fragments layer. The clayey sand and sandy clay units are interpreted as alluvial Pleistocene deposits as no shell or coral material was reported in these sedimentary layers. In addition, the descriptions of these units frequently refer to colours of "mottled orange", "pale grey" and "white" which are consistent with oxidised sediments. These units were also classified as stiff clays and in many cases the boreholes were terminated due to difficulty in penetration.

5.5.9. Application of rare earth elements and Y (REY) to determine the provenance of sediments

To investigate the origin of the fine-grained sediments in Nelly Bay, the rare earth element and Y (REY) abundances were examined from possible sources including the Burdekin

Dam, Ross River Dam, Gustav Creek and the Nelly Bay reef slope (grab samples; Fig 5.12a). Sediments in Nelly Bay can only be derived from these particular sources and, to ensure sampling consistency, all sediment samples were washed through an 80 μm sieve. The medium sand with coral fragments unit (ICP-13e) and the muddy sand with coral fragments unit (average of ICP2a, 13b-d) were analysed for REY composition and the normalised patterns (to MUQ sediment; Kamber et al., 2005) were compared to the possible sediment sources.

Sediments from Nelly Bay all contained consistently lower REY concentrations compared to sediments from the Burdekin River, Ross River and Gustav Creek (Fig 5.12a). This finding suggests that a considerable fraction of REY has been removed from the sediments in the marine environment. This may pose some problems for determining the sediment provenance, particularly if REE distributions were fractionated.

The provenance of the medium sand with coral fragments unit (ICP-13e) was difficult to assess. The light REY pattern was distinctive of a Burdekin River source, whereas the steep pattern observed in the heavy REY group was more consistent with sediments from Gustav Creek (Fig 5.12b). The best possible mixing plot was a 70%-30% mix of Gustav Creek and Burdekin River sediments, respectively (Fig 5.12b). The sediments that make up this unit were significantly coarser than the other units and previous studies on the evolution of fringing reefs suggest that the relatively coarse-grained sediments are derived from a local origin (e.g. Johnson and Risk, 1987).

The REY pattern for the muddy sand with coral fragments unit suggests it was dominated by Burdekin and/or Ross River sediments. The unit was consistent with a mixture of 85% Burdekin River and 15% Gustav Creek sediment (Fig 5.12c). This composition is considered the maximum possible influence from Gustav Creek for the muddy sand with coral fragments unit. The notable shift from a dominant Burdekin River signature in the muddy sand with coral fragments unit to a Gustav Creek signature in the younger medium sand with coral fragments unit suggests that there may have been a considerable change in the sediment provenance within Nelly Bay in the last 2,000 years. However, the REY

pattern from the grab sample taken from the modern Nelly Bay reef slope has a similar provenance to the muddy sand with coral fragments unit (Fig 5.12a); therefore, the Burdekin River (and/or Ross River) may still supply the majority of the mud-sized material to Nelly Bay, while the sand-sized particles are derived from the local area (Gustav Creek). This interpretation would explain why the medium sand with coral fragments unit displayed a Gustav Creek signature as the composition of this unit was composed of sand-sized terrigenous particles. The majority of suspended sediments that are discharged from the Burdekin River are derived from the Bowen River sub-catchment (Brodie et al., 2005b), which links with the main Burdekin system below the Burdekin Dam. Therefore, without sediment samples which cover the entire Burdekin River catchment (and other regions) a precise assessment of the source of the sediments in Nelly Bay was not possible.
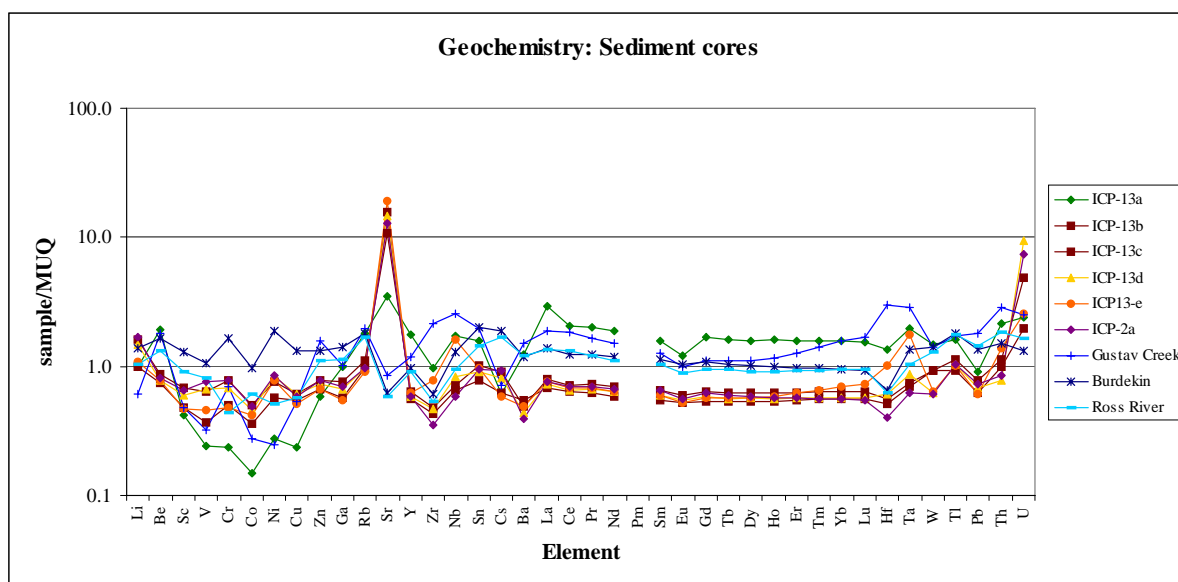
Figure 5.11. Trace element geochemistry of the sedimentary units in Nelly Bay (normalised to mud from Queensland MUQ sediments). Medium sand coral unit (ICP-13e); Muddy sandy coral unit (ICP-13a, 13d); Mud with minor coral fragments unit (ICP-13b, 13c); Sandy muddy coral unit (ICP-2a).

The REY distribution of ICP-13a displayed a complex pattern that was most consistent with sediments from Gustav Creek (Fig 5.12a). This sample was taken from the basal section of sediment core 13 (Fig 5.10) and was assumed to have been mixed with early Holocene or Pleistocene alluvial (non-marine) sediments from the local region. The negative Eu anomaly present in the ICP-13a sample also matches the Gustav Creek sediment and further supports that this sample was sourced from the local Magnetic Island area.
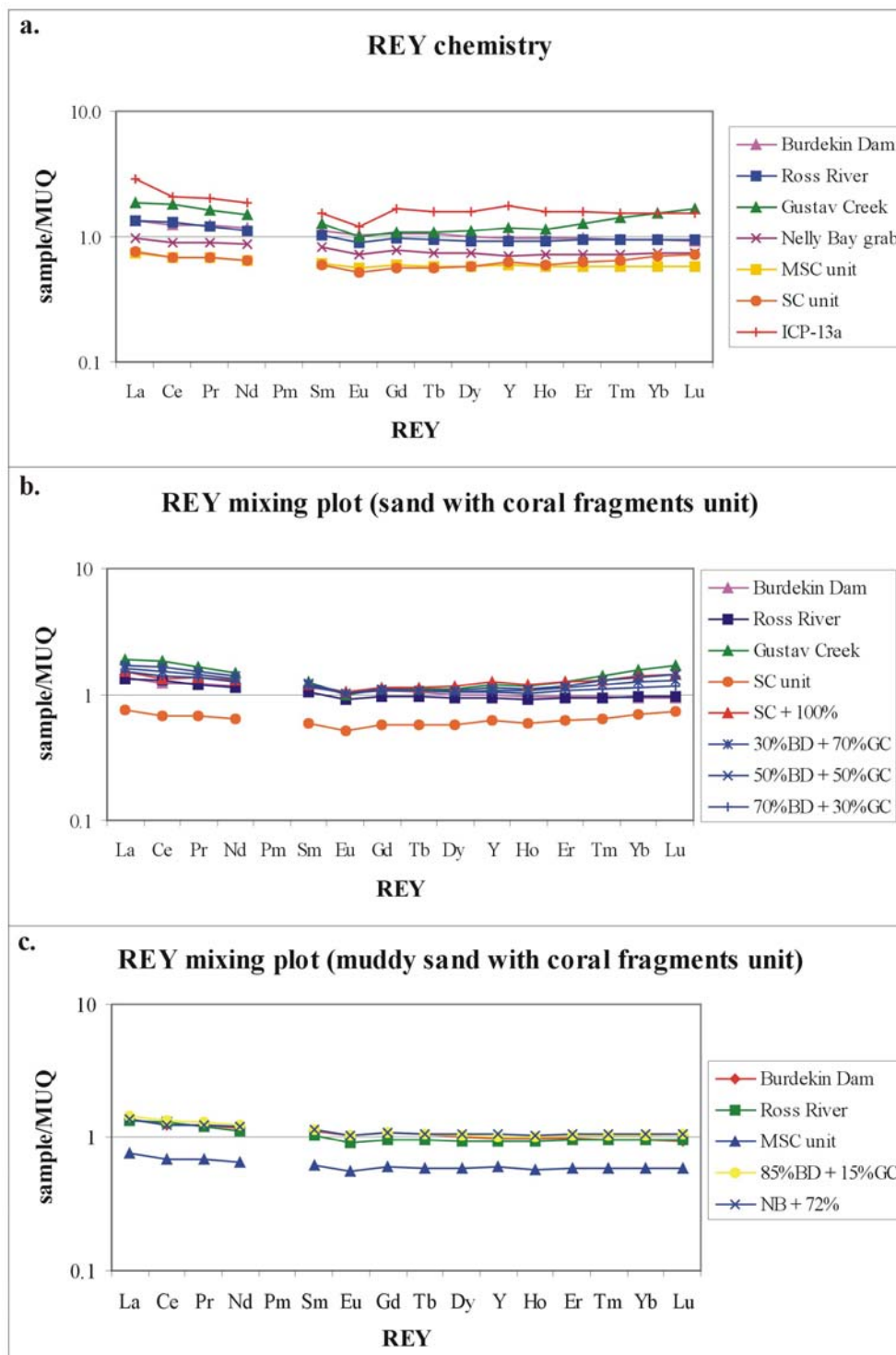
Figure 5.12 a-c. The sediments from the Burdekin (BD) and Ross Rivers (RR) and Gustav Creek (GC), the sand with coral fragments unit (SC), ICP13a and the muddy sand with coral fragments unit (MSC) all contain distinctive REY signatures (a). To investigate the major terrestrial source to the sediments in the Nelly Bay sediment cores, mixing plots were constructed for the SC and MSC units (b-c, respectively). The SC is dominantly composed of Gustav Creek sediments (b) while the MSC unit was made up of either Burdekin or Ross River sediments (c). The ICP-13a sample was thought to have been mixed with Pleistocene sediments and contains a similar REY signature to Gustav Creek (a).

5.5.10. Summary

Six sedimentary units were identified in sediment cores from Nelly Bay: sand unit, coral fragments unit, medium sand with coral fragments unit, muddy sand with coral fragments unit, sandy mud with coral fragments unit and mud with minor coral fragments unit. The sand unit is deposited along the Nelly Bay beach and was probably formed when sea level fell to its present position. The coral fragments unit was found on the reef and tidal flats in Nelly Bay and this unit has been deposited within the last 2,000 years. The medium sand with coral fragments unit has a calibrated C-14 age ranging from modern to 1,830 cal years BP and probably formed when sea level had regressed to its current elevation. The muddy sand with coral fragments unit has an age range from 2,150-6,350 cal years BP and was composed of medium to coarse sand and coral fragments (up to 7 cm long) with a variable mud component (incorporating the sandy muddy coral and mud with minor coral fragments units). The fine-grained terrigenous component of this unit was probably derived from the Burdekin River, although more data is required from the Burdekin River sediments to confirm the sediment source(s). The sandy mud with coral fragments and the mud with minor coral fragments units appear to be the stratigraphic equivalent of the muddy sand with coral fragments unit, as they are all of similar age, mineralogy and chemistry. The muddy sand with coral fragments unit may become muddier towards the bottom of the unit; however, the sediment cores failed to penetrate deep enough to observe these lower units (with the exception of core 13). These units were merged into one "muddy sand with coral fragments" layer. The sedimentary layers are similar to that documented by previous investigations (McIntyre and Associates, 1986; 1989; Golder Associates, 2000). These studies identified a "sand-coral" layer, which averaged 3 m in depth. This layer was considered the equivalent of the medium sand with coral fragments and the muddy sand with coral fragments units as these layers have a combined depth of approximately 3 m. If the mud component was removed from the muddy sand with coral fragments unit, it would probably resemble the medium sand with coral fragments unit.

5.6. Stratigraphic model of Nelly Bay

5.6.1. Overview

The topographic profiles, sediment cores and data from previous investigations were compiled to produce a stratigraphic profile of Nelly Bay. Previous studies provided information about the depths of Pleistocene sediments and the granitic bedrock. The cause of death of the fossil mid-Holocene corals can be better understood when the corals are placed within this stratigraphic profile. This stratigraphic profile was combined with the Holocene sea-level reconstruction (Fig 5.3) to produce a stratigraphic model for Nelly Bay during the Holocene.

5.6.2. Stratigraphy of Nelly Bay

The relative position of each sediment core was compiled along a standard topographic profile of Nelly Bay to develop the stratigraphy of the embayment. The stratigraphic profile also drew on previous investigations to construct both the Pleistocene and bedrock units (Fig 5.13). The depth of the Pleistocene unit was estimated from boreholes and seismic investigations in Nelly Bay (McIntyre and Associates, 1986; 1989; Golder Associates, 2000; Carter and Johnson, 1989; Sinclair Knight Merz, 1998). The Pleistocene unit is estimated to be approximately 3-5 m deep and located around 2.0-5.5 m below the surface sediments (Carter and Johnson, 1989; Sinclair Knight Mertz, 1998). The granitic bedrock unit was identified by seismic investigations ("reflector 2") around 10-13 m below the AHD (Sinclair Knight Merz, 1998). Therefore, this unit is approximately 7-10 m below the surface sediments. In addition, the bedrock unit becomes progressively closer to the surface as the profile moves landward towards Nelly Bay. This interpretation is supported by the observation that the granitic bedrock unit outcrops approximately 50 m landward of the former beach ridge in the X-base section. The maximum thickness of the sand unit was estimated to be approximately 4 m from excavation pits dug into the beach sand in Nelly Bay (McIntyre and Associates, 1989).

Schematic cross section Nelly Bay stratigraphy

VE= 10:1

Elevation (lowest astronomical tide)

600 ± 60
1830 ± 130
2150 ± 150   6330 ± 130
4220 ± 190
6080 ± 150
6350 ± 150
6300 ± 130

1100 ± 120
Modern
3530 ± 130
3990 ± 150

Distance (m)

Legend

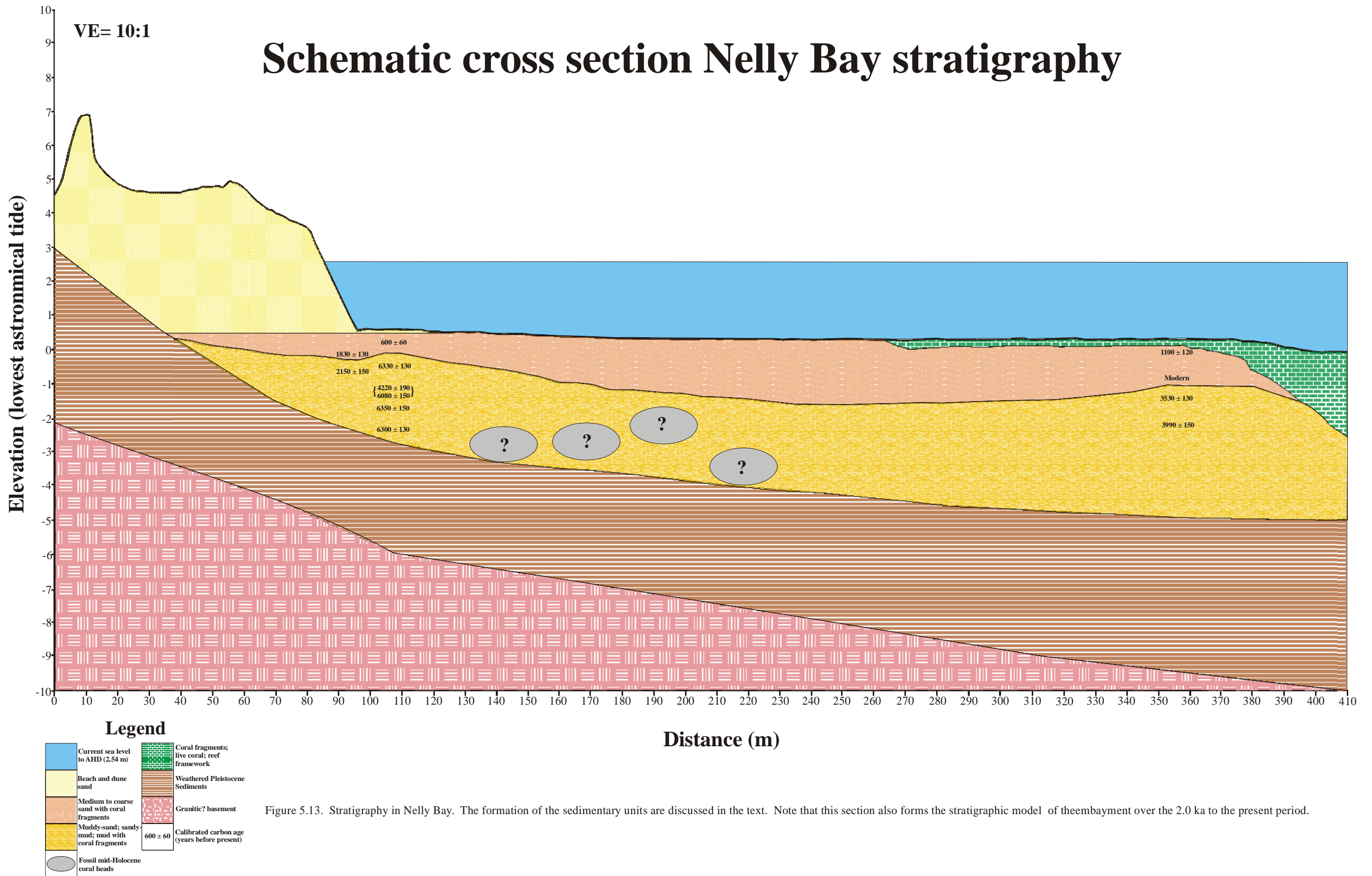|			
Current sea level to AHD (2.54 m)		Coral fragments; live coral; reef framework	
Beach and dune sand		Weathered Pleistocene Sediments	
Medium to coarse sand with coral fragments		Granitic? basement	
Muddy-sand; sandy-mud; mud with coral fragments	600 ± 60	Calibrated carbon age (years before present)	
Fossil mid-Holocene coral heads			

Figure 5.13. Stratigraphy in Nelly Bay. The formation of the sedimentary units are discussed in the text. Note that this section also forms the stratigraphic model of the embayment over the 2.0 ka to the present period.

The age range of the fossil mid-Holocene corals indicates they correspond in age to the muddy sand with coral fragments unit. The corals probably began growing on the unconsolidated Pleistocene sediments and grew as the muddy sand with coral fragments unit accumulated. This unit was interpreted as the remnants of the former reef flat. The oldest calibrated C-14 age for the muddy sand with coral fragments unit (6,350 ± 150 cal years BP) was indistinguishable from the oldest age for the fossil mid-Holocene corals (6,290 ± 110 cal years BP). However, the Holocene sea-level reconstruction (Fig 5.3) indicates that sea level reached a + 1.0-1.5 m elevation approximately 1,000 years before the growth of these corals and the formation of the muddy sand with coral fragments sedimentary package. This "age gap" is discussed further in section 5.6.3 where a stratigraphic model of Nelly Bay during the Holocene was constructed.

5.6.3. Stratigraphic model of Nelly Bay over the Holocene and the death of the fossil mid-Holocene corals

The stratigraphic model constructed for Nelly Bay over the Holocene focused on four major time periods:

1. 10.0-7.5 ka year period when sea level was rapidly rising;
2. 7.5-6.0 ka period of relative stabilisation of sea level at approximately 1.5 m above present and initiation of growth of the fossil *Porites* corals;
3. 6.0-1.5 ka period of relatively stable sea level and productive reef growth before sea level fell to its present elevation, approximately 1.0-1.5 ka. This period was also important as it encapsulates the time of the muddy sand with coral fragments unit and the death of the fossil mid-Holocene corals; and
4. 1.5 ka-present period when sea level stabilised and coincided with the formation of the current beaches and the further development of the Nelly Bay Reef.

For the purpose of this model, sea level during the 10.0-7.5 ka period was placed at -5 m based on the highest elevation of mangrove mud deposits in Cleveland Bay which provided a calibrated C-14 age of 7,590 ± 190 cal years BP (Carter et al., 1993; Table 5.2). The "beach" during this time would have stretched from the tip of Bright Point across Nelly Bay (Fig 5.14), following the modern 5 m isobath. The stratigraphic profile of this time

would have been dominated by Pleistocene and early Holocene alluvial sediments (Fig 5.15).
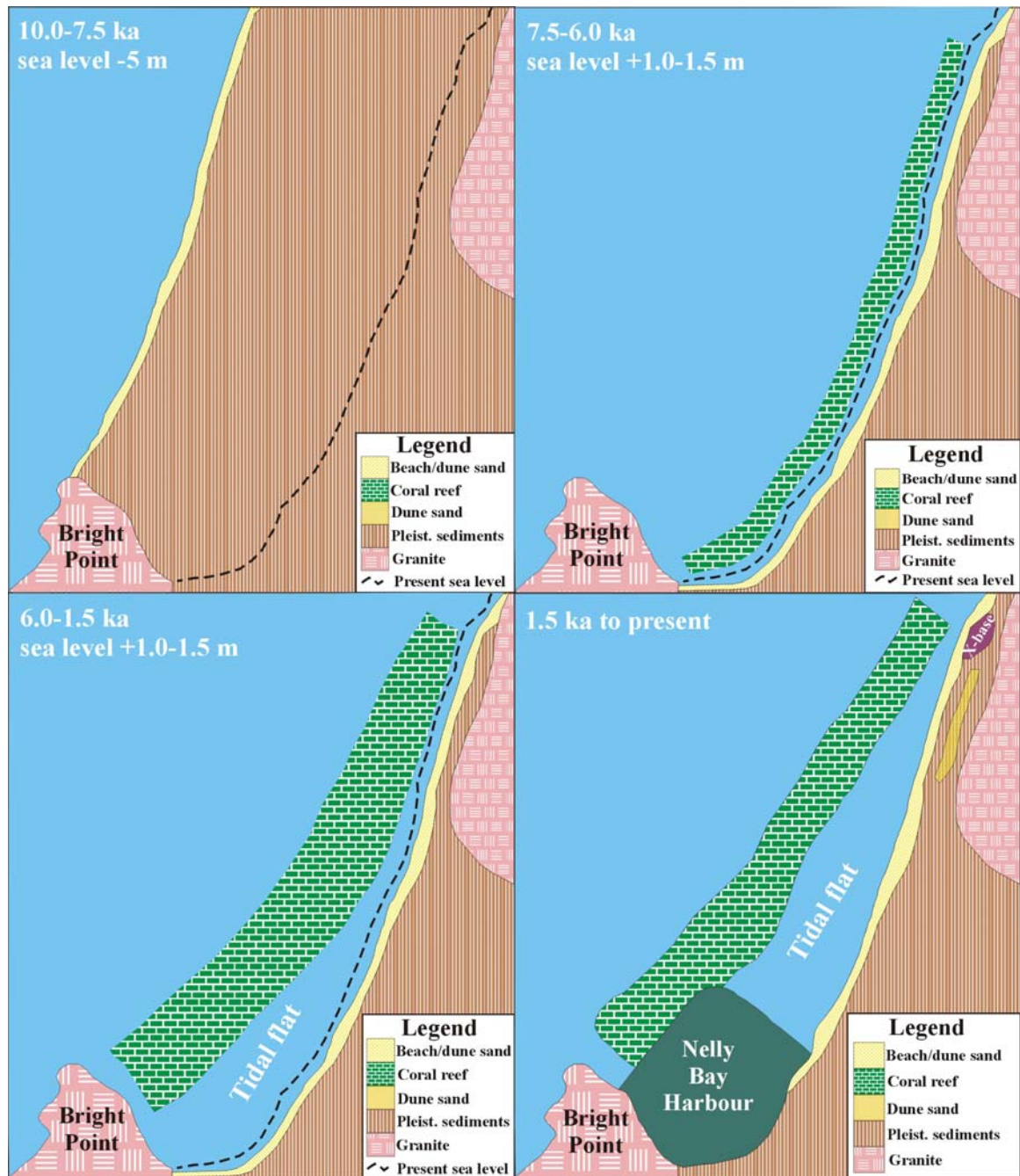
Figure 5.14. Plan views of Nelly Bay over the major Holocene time periods identified in this study. Sea level for the 10.0-7.5 ka period has been placed at -5 m and, based on the present isobaths, the "beach" at this time was located from the tip of Bright Point across the embayment. This period has been drawn as a stratigraphic profile and displayed in Fig 5.15. The 7.5-6.0 ka period was marked by relatively stable sea level, approximately 1.0-1.5 above the present elevation. The Nelly Bay reef formed near the present shoreline during this time. This period corresponds with the stratigraphic profile presented in Fig 5.16. The 6.0-1.5 ka timeframe is marked by the seaward progradation of the Nelly Bay reef (stratigraphic profile: Fig 5.17). The 1.5 ka to present time period represents sea level falling to its current position. Note the location of the Nelly Bay Harbour and X-base Backpackers. Also note the location of the former beach ridge preserved near X-base. This plan view corresponds with the current stratigraphy in the area (Fig 5.13).

Stratigraphic profile Nelly Bay 10.0-7.5 ka

VE= 10:1

Legend

- Sea level early-Holocene (~ -5 m)
- Beach and dune sand
- Weathered Pleistocene Sediments
- Granitic? basement

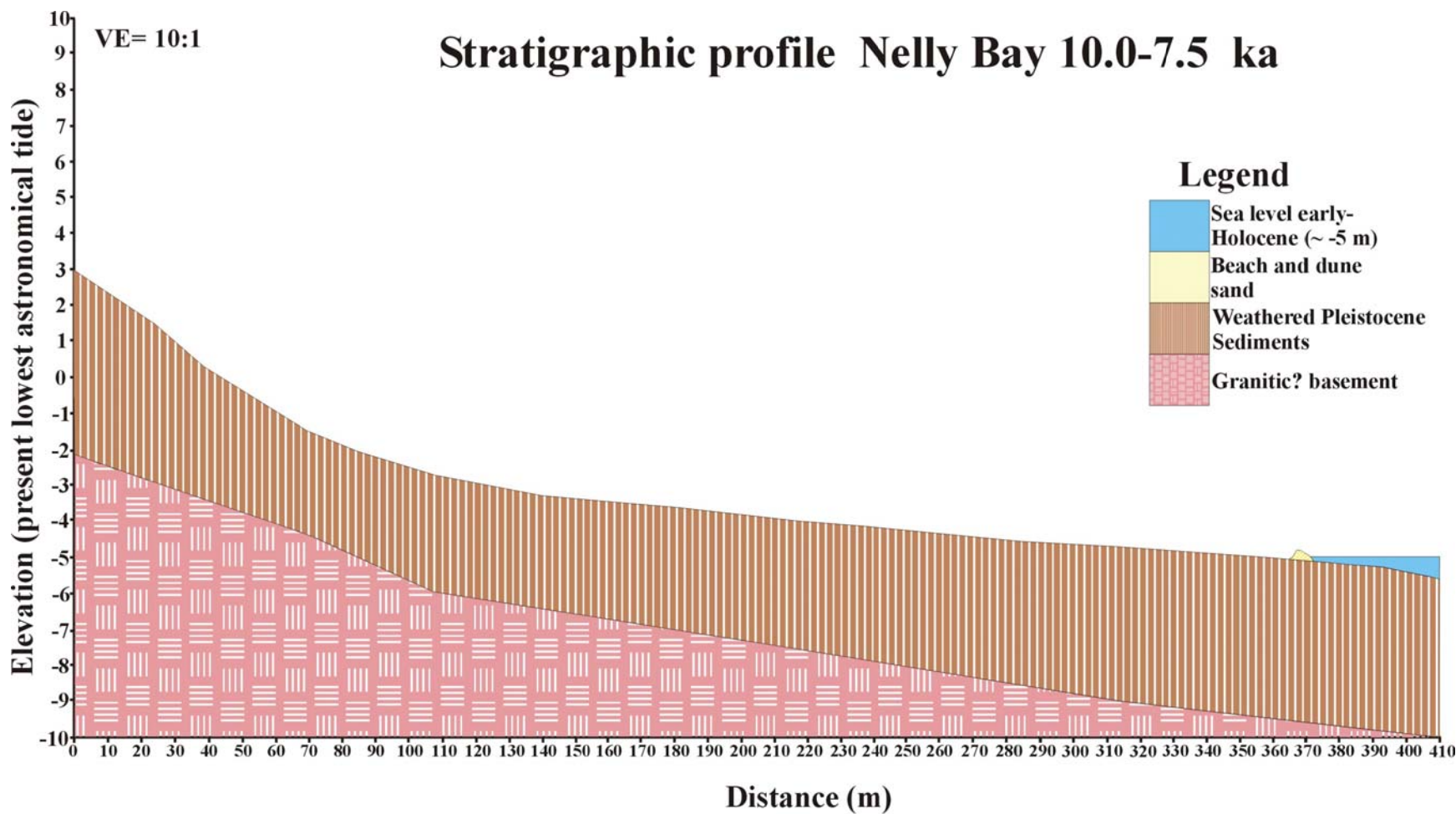Figure 5.15. Stratigraphic profile of Nelly Bay during the 10.0-7.5 ka period. The embayment would have been dominated by alluvial Pleistocene deposits and early Holocene sediments during this time.

The 7.5-6.0 ka period was an important time for the Holocene evolution of Nelly Bay (Fig 5.14). This period marked the initiation of the Nelly Bay reef complex around 6,300 cal years BP. This age was similar to the estimates of Hopley (1986) who suggested that the reef was a little over 7,000 years old. This estimate was based on the age structure of the fringing reefs of Rattlesnake and Orpheus Island (Hopley et al., 1983). The stratigraphic profile for the 7.5-6.0 ka timeframe illustrates the formation and development of the mid-Holocene beach ridge, Nelly Bay reef as well as the growth of the mid-Holocene corals and the formation of the muddy sand with coral fragments unit (Fig 5.16).

The muddy sand with coral fragments unit is thought to be a remnant of the former reef slope and/or flat. The initial reef probably formed near the present shoreline and gradually accreted and prograded seawards (Fig 5.14). The oldest ages for the muddy sand with coral fragments unit and the fossil coral heads were identical, and suggest that the Nelly Bay reef formed around this time (~6,300 cal years BP). However, the sea-level reconstruction shows that sea level reached +1.0-1.5 m approximately 7,000-7,500 cal years BP (Fig 5.3). Therefore, there is approximately a 1,000-year "gap" from when sea level stabilised to the first growth of the Nelly Bay reef. Hopley et al. (1983) suggested that coral reef growth during the early Holocene may have been restricted because of highly turbid conditions from the extensive reworking of the Pleistocene clay units. Reworking of these units may not only have generated turbid conditions, but also have prevented the formation of a stable substrate that is necessary for coral recruitment and growth. In addition, the oldest oyster bed (6,280 ± 110 cal years BP; Higley, 2000) and the oldest microatoll (6,150 ± 170 cal years BP; Chappell et al., 1983) dated from Magnetic Island may also indicate that the conditions in the embayment were unsuitable for these organisms until approximately 6,300 years BP. Alternatively, the sediment cores may have missed the early reef colonies for age-determination.

The composition of the muddy sand with coral fragments unit indicates that the Nelly Bay reef grew in conjunction with the deposition of terrigenous sand and mud particles. The sand-sized particles were probably derived from local beach sediments and deposited episodically during heavy rainfall and cyclonic events. Coarse terrigenous sediment

deposition was observed on the Nelly Bay reef flat during Tropical Cyclone Althea in 1971 (Hopley, 1986) and a regular occurrence of large storm events during the Holocene has been documented in the regional geological record (Nott and Hayne, 2001; Hayne and Chappell, 2001). The mineralogy of the sandy units, which are dominantly composed of quartz and feldspar (Table 5.3), was consistent with weathering from a local granitic source. An appreciable mud-sized fraction was observed in a sediment grab sample from the present Nelly Bay reef slope. Reef structures developing on, and in conjunction with, muddy substrates are a common occurrence on north Queensland's inshore fringing coral reefs (e.g. Johnson and Risk, 1987).

Stratigraphic profile Nelly Bay 7.5-6.0 ka

Stephen E Lewis

Environmental trends in the GBR lagoon and Burdekin River catchment during the mid-Holocene and since European settlement using Porites coral records, Magnetic Island, QLD.

VE= 10:1

Legend

- **Sea level AHD mid-Holocene (~3.5 m)**
- **Beach/dune sand**
- **Muddy-sand with coral fragments**
- **Fossil mid-Holocene coral heads**
- **Coral fragments; live coral; reef framework**
- **Weathered Pleistocene Sediments**
- **Granitic? basement**

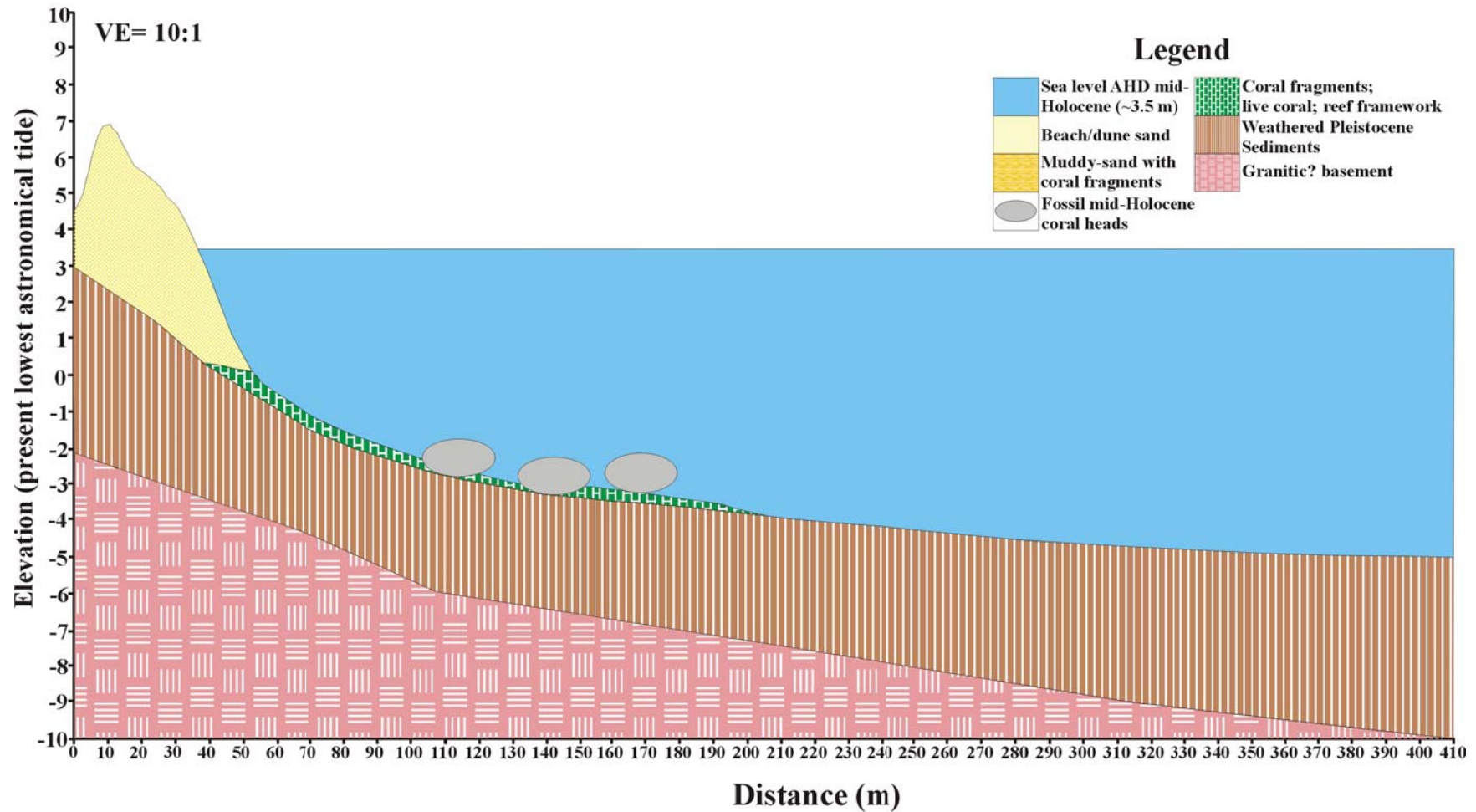**Elevation (present lowest astronomical tide)**

Distance (m)

Figure 5.16. Stratigraphic profile of Nelly Bay over the 7.5-6.0 ka timeframe. During this time the Nelly Bay reef became established and began prograding seaward. These conditions were favourable for the growth of the fossil mid-Holocence coral heads due to little competition from the faster growing corals.

The key feature over the 6.0-1.5 ka period was the seaward prograding reef flat (Figs 5.14; 5.17). Ages from the sediment cores (Fig 5.13) support a prograding reef structure which has previously been reported for the fringing reefs of Orpheus (Hopley et al., 1983) and Fantome Islands (Johnson and Risk, 1987; Fig 5.18). This period was marked by high productivity as indicated by rapid accretion and development of the reef structure (Fig 5.17). This rapid accretion of the Nelly Bay reef may have caused the death of the fossil *Porites* corals; the *Porites* corals reached their upper growth limits, died and became buried by sediments. Massive long-living *Porites* corals are commonplace in the deeper waters, but are still a short distance from the Nelly Bay reef flat (J. Tanner personal communication, 2004). Reef growth would have facilitated a considerable build up of biogenic sediment to the area, and the muddy sand with coral fragments deposit (the remnants of the reef flat) may have accumulated at a faster rate than the massive corals could grow, essentially suffocating them. The proposed model is also supported by the data of microatolls from Geoffrey Bay (Magnetic Island) which shows that the atolls become younger further out to sea (Chappell et al., 1983) as do the microatolls observed near Fantome Island (Johnson and Risk, 1987; Fig 5.18).

A change in the environmental conditions such as sea level could have resulted in a "colony turnover" where the fossil corals were overgrown by other corals by the process of "succession". Kan et al. (1997) employed this term to describe an extensive build-up of different coral communities within a channel cutting near Hayman Island (Fig 5.19).

An alternative mechanism to explain the development of the Nelly Bay reef flat has been suggested by Hopley (1986; Hopley et al., 1983). A series of jet probes from the adjacent Geoffrey Bay reef flat indicated that it may have developed on an older structure parallel to the shoreline (Hopley et al., 1983; Hopley and Partain, 1987; Fig 5.20). This structure may be the remnants of a former Pleistocene reef or of cemented Pleistocene alluvial sediments (Hopley et al., 1983); the Nelly Bay reef flat may also have developed on a similar feature. However, seismic surveys have failed to observe this structure and, therefore, the hypothesis cannot be confirmed or rejected (Carter and Johnson, 1989; Sinclair Knight Merz, 1998). Hopley (1986) suggested that once the reef became established, it continued

to grow landwards and seawards from this "structure". The landward reef growth in a lagoon-like environment may have been restricted to growth forms such as microatoll and massive coral heads, and this lagoon may have gradually in-filled with biogenic and terrigenous sediments transported during storm events (Hopley, 1986). The reworking of the muddy sand with coral fragments unit which is evident from the age reversals in core 13 (Fig 5.9) may suggest periods of intense stormy weather which, in turn, may also have contributed to the demise of the fossil corals. However, this hypothesis is unlikely as the muddy sand with coral fragments deposit is more consistent with lower energy conditions. The "lagoonal" environment could have provided favourable low energy conditions for the accumulation of the muddy sandy coral unit (Fig 5.14) and the accumulation of this sedimentary layer may have buried the fossil corals. While no obvious reef framework was identified in the sediment cores, the age structure of the embayment appears to support the former seaward prograding model.

A combination of the models of Johnson and Risk (1987) and Hopley (1986) best explain the formation of the Nelly Bay reef. The reef probably formed on consolidated Pleistocene sediments and then prograded seawards. A more sophisticated coring procedure that penetrates sediments, reef framework and bedrock (e.g. diamond drilling) would need to be performed in Nelly Bay to confirm this hypothesis.
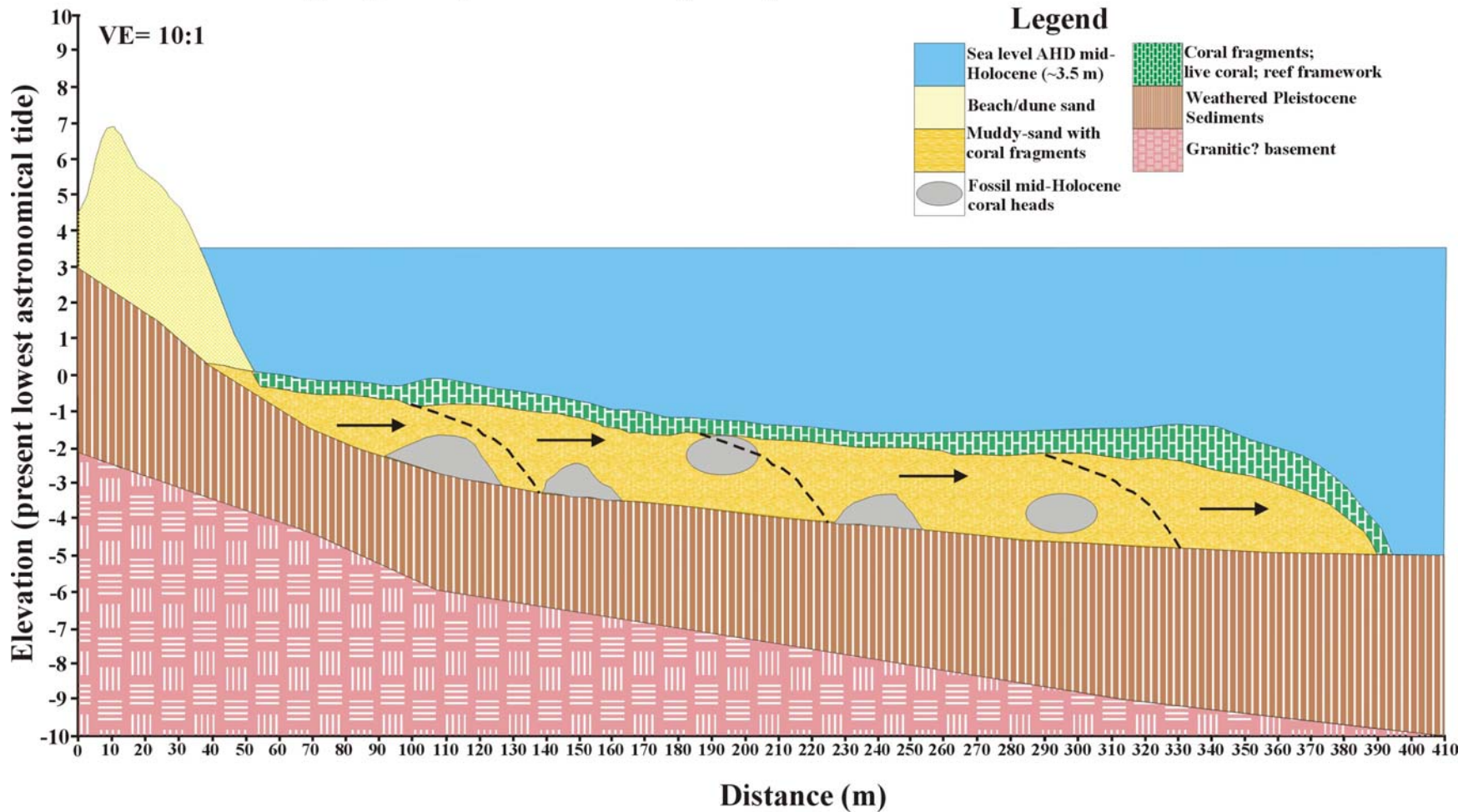
Stratigraphic profile Nelly Bay 6.0-1.5 ka

Figure 5.17. Stratigraphic profile of Nelly Bay from 6.0 to 1.5 ka. The Nelly Bay reef became better established as it prograded further seawards. The fossil mid-Holocene *Porites* corals were buried by biogenic and terrigenous sediments from the rapidly prograding reef flat. Note the dotted lines and arrows which indicate the seaward prograding Nelly Bay reef flat.
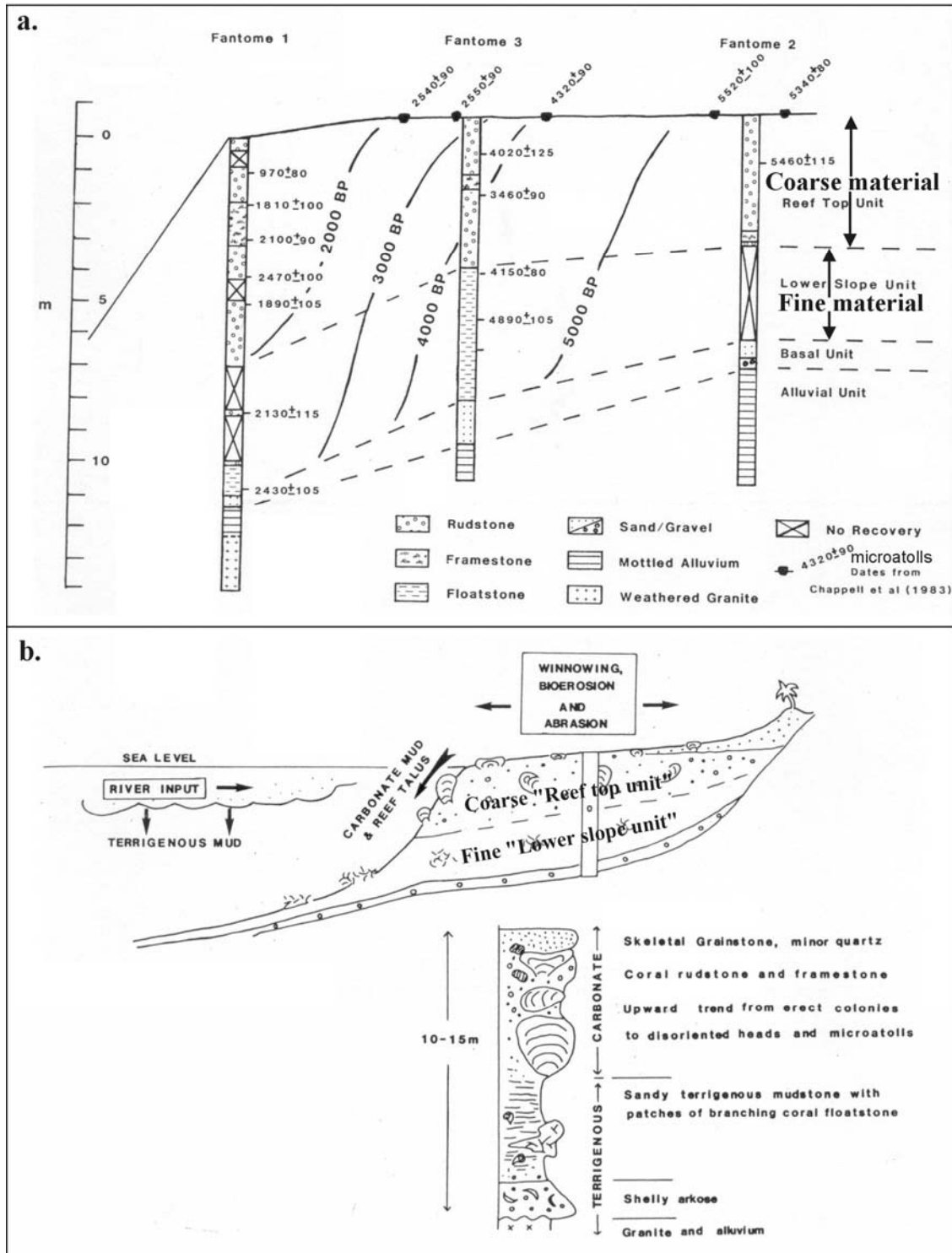
Figure 5.18 a-b. Sediment cores and C-14 ages of the Fantome Island fringing reef flat support the prograding reef model. The age structure in the Nelly Bay sediment cores also indicates that the reef flat formed near the present shoreline and prograded seawards in a similar manner to the Fantome Island reef flat (a). The model for the prograding reef flat (b) suggests that fine terrigenous sediment, derived from rivers, is deposited on the reef slope while sand-sized particles are transported from the beach and deposited on the reef flat as it extends seawards (adapted from Johnson and Risk, 1987).
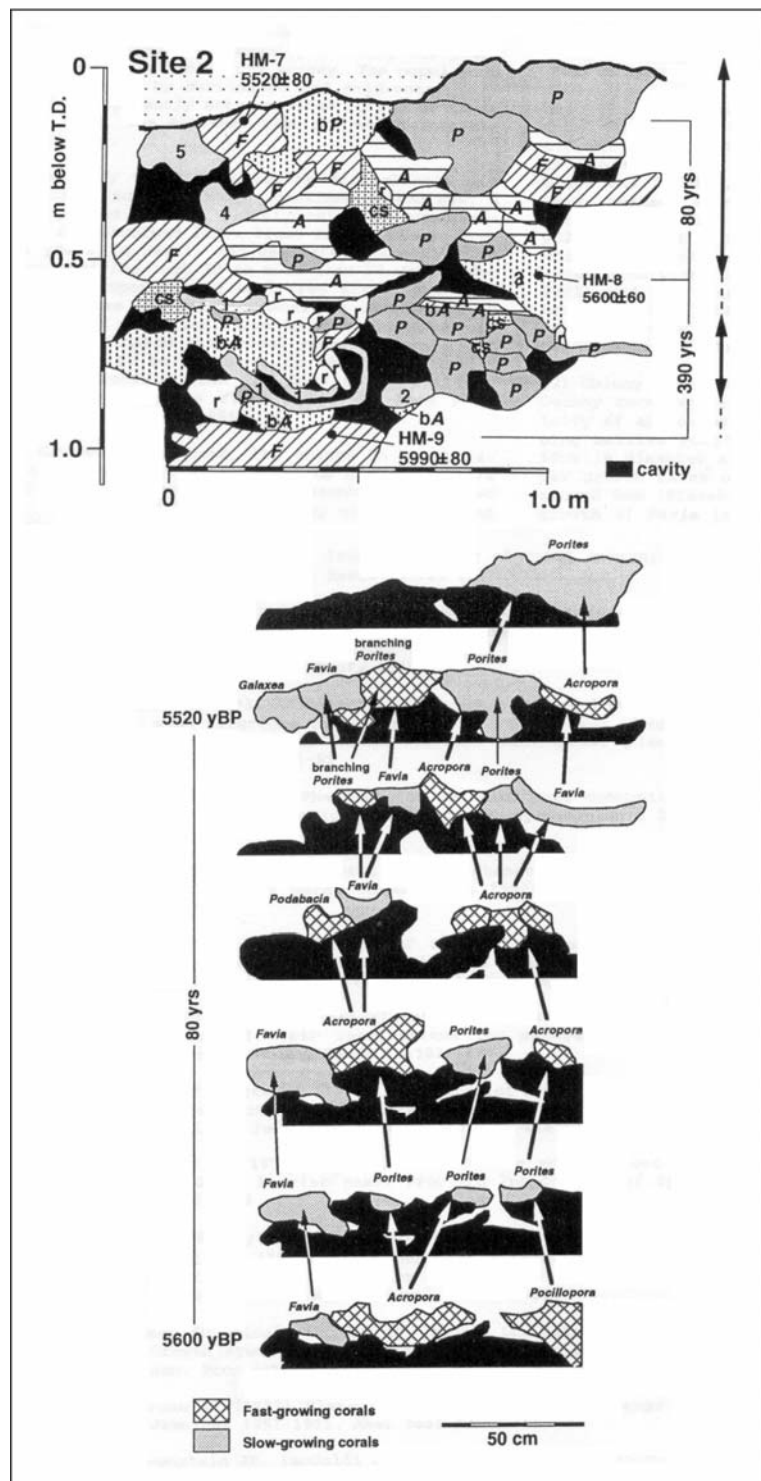
Figure 5.19. Coral framework on a fringing reef from Hayman Island (from Kan et al., 1997). This framework illustrates the competition that the fossil *Porites* (P) corals in this study may have faced with faster-growing corals, such as Acropora (A) and Favids (F), accreting over the slower growing massive corals. A change in environmental conditions such as sea level can also result in a "colony turnover" where new coral recruits grow over the old colonies. The corals from Nelly Bay would have experienced a greater terrigenous influence than this example from Hayman Island.
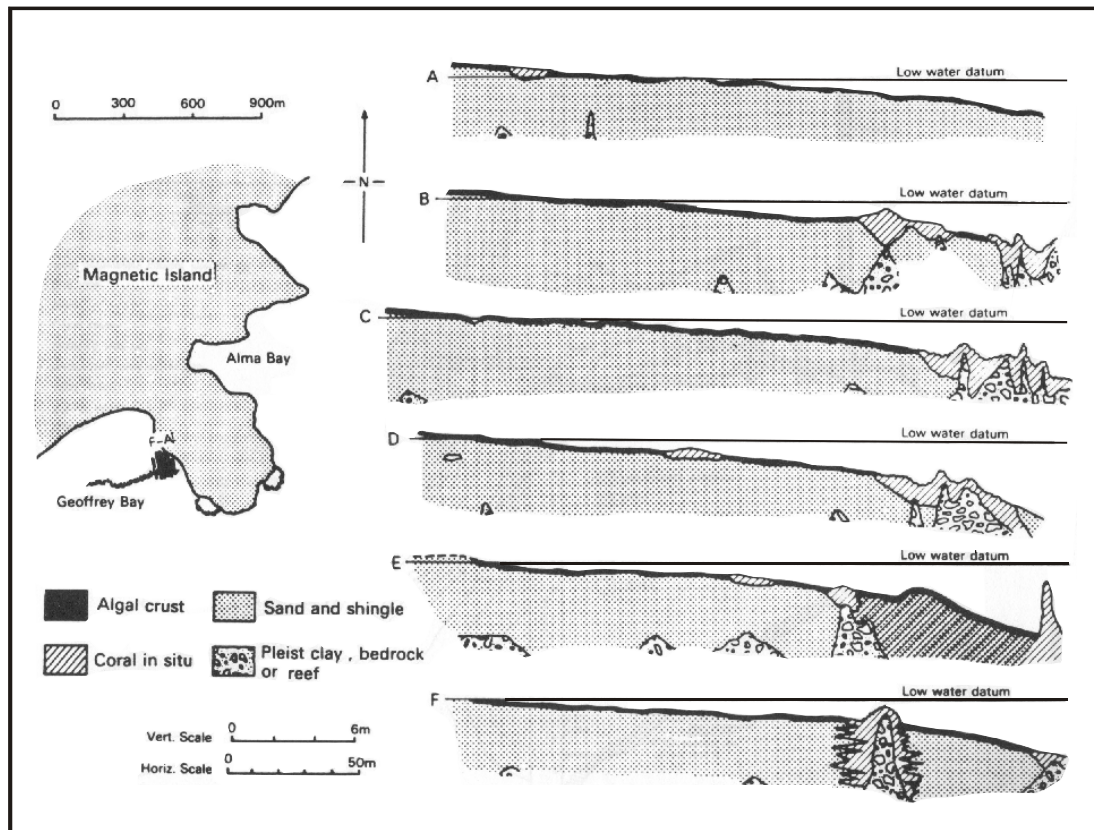
Figure 5.20. A series of jet probes in Geoffrey Bay suggested that this reef formed on consolidated Pleistocene sediments which may be either bedrock or a former reef (from Hopley and Partain, 1987). The data were used to model the growth of the reef from the early Holocene (A) to the present (F). A similar mechanism is plausible for initiation of the adjacent Nelly Bay reef.

The 1.5 ka to the present timeframe marks a period when sea level fell and remained at its current elevation. The sea-level regression would have left the mid-Holocene beach ridge in Nelly Bay stranded, a feature preserved near X-base (Fig 5.13). This regression would have caused the Nelly Bay reef flat to protrude above the mean low water springs (MLWS) elevation, and thus expose the reef flat to a higher-energy regime which, in turn, may have reworked the surface sediments and removed the mud component.

5.6.4. Summary

A stratigraphic model of Nelly Bay has been developed for four important periods during the Holocene. The first period coincided with the rapid early Holocene sea-level transgression from 10-7.5 ka. Nelly Bay, during this time, was dominated by

Pleistocene/early Holocene alluvial sediments. The second period (7.5-6.0 ka) coincided with sea-level elevations of about 1.0-1.5 m above the present level, and with the formation of the Nelly Bay reef and the growth of the fossil mid-Holocene corals. The 1,000 year gap from the sea-level highstand (~ 7.5 ka) to the formation of the reef (~ 6.5 ka) may be due to the turbid conditions that were generated by the reworking of alluvial Pleistocene sediments and the absence of a suitable substrate. From 6.0-1.5 ka, the Nelly Bay reef flat rapidly prograded seawards. It appears that the *Porites* corals were buried over time by layers of terrigenous and biogenic sediments. During 1.5 ka to the present, sea level regressed and stabilised at its current elevation. The modern reef may have experienced higher-energy conditions as sea level fell by approximately 1 m and, as a result, a coarser sedimentary unit (medium sand with coral fragments) was deposited. In addition, the sea-level regression left the former beach ridge (preserved near X-base) stranded.

5.7. Chapter summary

- Calibrated U-Th and C-14 ages for the large fossil *Porites* corals suggest they grew for a short time period between 5,790-6,290 cal years BP.
- Three of these corals (NEL03, NEL06 and NEL07) appeared to have died suddenly around 6,000-6,150 cal years BP.
- The U-Th and C-14 dates of the NEL03 coral suggest that the local C-14 reservoir correction (ΔR) for Magnetic Island is approximately 95 ± 15 years.
- Holocene sea level was reconstructed using calibrated C-14 ages of fixed biological indicators (FBIs), coral microatolls and mangrove mud. The calibrated C-14 sea-level curve indicates that sea-level transgressed rapidly during the early Holocene and stabilised around 7,000 cal years BP at a height of 1.0-1.5 m above the present elevation.
- Sea level remained more or less at this elevation (with the possible exception of 3 small-scale oscillations of 1.0-1.5 m) until 1.5-2.0 ka when it regressed to its present position.

➢ Four main morphological zones were identified in the topographic profiles including dune, beach, tidal flat and reef flat.

➢ An extensive sand body next to the Nelly Bay road may be the relict of a foredune system established during the mid-Holocene sea-level highstand.

➢ Four major laterally continuous Holocene sedimentary units were identified in the Nelly Bay sediment cores including the sand unit, the coral fragments unit, the medium sand with coral fragments unit and the muddy sand with coral fragments unit.

➢ The sand unit represents the Nelly Bay foredune and beach which probably formed when sea level fell to its present position about 1.0-1.5 ka.

➢ The coral fragments and medium sand with coral fragments units were of similar age (modern-1,830 years BP) and may have formed during higher-energy conditions when sea-level regressed to its present elevation.

➢ The muddy sand with coral fragments unit represents a combination of the muddy sand with coral fragments, sandy mud with coral fragments and mud with minor coral fragments units. The age of this unit ranged from 2,150-6,350 years BP and the convoluted age structure in core 13 suggests the unit has been reworked.

➢ The large fossil mid-Holocene *Porites* corals were overcome by terrigenous and biogenic sediment accumulation from the rapid progradation of the Nelly Bay reef flat. The fossil corals are confined to the muddy sand with the coral fragments unit which appears to be a remnant of the prograding reef flat.